الجمهورية الجزائرية الديمقراطية الشعبية

République Algérienne Démocratique et Populaire

وزارة التعليم العالي و البحث العلمي

Ministère de l'Enseignement Supérieur et de la Recherche Scientifique

Université Mohamed Khider - Biskra
Faculté des Sciences et Technologies
Département de génie civil
et hydraulique
Ref :……

جامعة محمد خيضر - بسكرة
كلية العلوم و التكنولوجيا
قسم الهندسة المدنية
و الري
المرجع :86/دكتوراه/ط ث/م ج/2025

Thèse

Présentée pour obtenir le diplôme de

Doctorat Troisième Cycle (LMD)

Domaine : Génie Civil

Spécialité : Matériaux de construction

Thème :

Comportement des Bétons à Base des Agrégats de Démolition et Sable de Dune

Par :

Kamel AKROUM

Défendu publiquement le : 12/05/2025

Devant un jury composé de :

N°	Nom et prénom	Grade	Qualité	Établissement
01	CHEBILI Rachid	Pr.	Président	Université de Biskra
02	MEZGHICHE Bouzidi	MCA	Directeur de Thèse	Université de Biskra
03	TAALLAH Bachir	Pr.	Examinateur	Université de Biskra
04	GHARIB Abderrahmane	Pr.	Examinateur	Université de Djelfa

الجمهورية الجزائرية الديمقراطية الشعبية

Democratic and Popular Republic of Algeria

وزارة التعليم العالي و البحث العلمي

Ministry of Higher Education and Scientific Research

Mohamed Khider University - Biskra
Faculty of Science and Technology
Department of Civil engineering
and hydraulics
Ref :……

جامعة محمد خيضر - بسكرة
كلية العلوم و التكنولوجيا
قسم الهندسة المدنية
و الري
المرجع : 86/دكتوراه/ط ث/م ج/2025

Thesis

Presented to obtain the degree of

Doctorate Third Cycle (LMD)

Field: Civil Engineering

Specialty: Building Materials

Theme:

Behaviour of Concrete Based on Demolition Aggregates and Dune Sand

By:

Kamel AKROUM

Publicly defended on: 05/12th/2025

In front of a jury composed of:

N°	Full name	Grade	Quality	Establishment
01	CHEBILI Rachid	Pr.	President	University of Biskra
02	MEZGHICHE Bouzidi	MCA	Thesis director	University of Biskra
03	TAALLAH Bachir	Pr.	Examiner	University of Biskra
04	GHARIB Abderrahmane	Pr.	Examiner	University of Djelfa

إهـــــداء

إلى سبب وجودي في هذه الحياة،

إلى من لهما ـ بعد الله ـ الفضل فيما وصلت إليه الآن،

إلى الذين أحباني دون مقابل،

إلى من أخلصا لي وضحّيا من أجلي،

إلى من شجعاني لخوض غمار الحياة ودعماني لتقديم أفضل ما لدي،

إلى من كانا ولا يزالان مصدر تحفيزي وإلهامي الرئيسي،

إلى "والداي الكريمين"،

إلى روح أمي الطاهرة ـ رحمها الله تعالى ـ وأدخلها فردوسه الأعلى بجوار أمنا خديجة ـ رضي الله عنها وأرضاها ـ وبجوار نبينا محمد ﷺ،

إلى إخوتي،

إلى أخواتي وأزواجهن،

إلى أبناء وبنات أخواتي واحداً واحداً دون استثناء،

إلى زملائي وزميلاتي في العمل،

إلى جميع معلمي وأساتذتي المحترمين عامة من المدرسة الابتدائية إلى الجامعة،

إلى السيدة الفاضلة "كريمة رحال" أستاذتي لمادة العلوم الطبيعية بالمتوسطة خاصة والتي لم يرضها أن أكتفي بشهادة الماستر،

إلى كل من ساعدني بأي شكل من الأشكال لإنجاز هذا العمل المتواضع،

إلى كل من آمن بي وشجعني لاقتحام ميدان الدراسات العليا بالجامعة،

إلى كل من تمنى لي مزيد التألق في رحاب العلم والمعرفة،

إلى كل من سره خبر نجاحي في مسابقة الدكتوراه بجامعة بسكرة واستقبله بابتسامة مشرقة،

إلى كل من بادلني المحبة والاحترام الصادقين،

وتعبيرا عن امتناني الأبدي،

أهدي هذه الأطروحة.

Dedication

To those who brought me into this life

To those who, after God, are responsible for where I am now.

To those who loved me unrequitedly.

To those who have been faithful and sacrificed for me.

To those who encouraged me to go through life and supported me to do my best.

To those who have been and continue to be my main source of motivation and inspiration.

To my ‘honourable parents’.

To the soul of my pure mother - may Allah have mercy on her - and may she rest in Paradise next to our mother Khadija - may Allah be pleased with her - and next to our Prophet Muhammad (peace and blessings of Allah be upon him).

To my brothers.

To my sisters and their husbands.

To my nieces and nephews, one by one, without exception.

To my colleagues and co-workers.

To all my respected teachers and professors in general, from primary school to university.

To the honourable Mrs. Karima Rahal, my teacher of natural sciences at the intermediate school in particular, who was not satisfied with my Master's degree.

To everyone who helped me in any way to realise this humble work.

To everyone who believed in me and encouraged me to enter the field of postgraduate studies at the university.

To all those who wished me more brilliance in the field of science and knowledge.

To all those who were pleased with the news of my success in the doctoral competition at the University of Biskra and received it with a bright smile.

To all those who reciprocated my sincere love and respect.

As an expression of my eternal gratitude.

I dedicate this thesis.

شكـــر وامـتـنـان

بادئ ذي بدء، أود أن أعرب عن تقديري وامتناني للدكتور الفاضل "بوزيدي مزغيش" لإشرافه على هذه الأطروحة من جهة ولرحابة صدره و مرونته في اختيار مخابر البحث المحتضنة لهذا العمل التجريبي من جهة أخرى، الأمر الذي جعلني أشعر بالارتياح طيلة السنوات التي استغرقها هذا العمل البحثي المتواضع، كما أود أن أشكر الدكاترة والأساتذة الأفاضل المؤطرين و المرافقين للتكوين في شقه النظري وكذا الطاقم الإداري بقسم الهندسة المدنية والري بجامعة محمد خيضر- بسكرة- الذين أبانوا عن احترافية في أداء مهامهم، كما لا يفوتني أن أشكر بشكل خاص الدكتور الفاضل " بشير طاع الله " رئيس لجنة التكوين في الدكتوراه على تعاونه الكبير. و لأنه ﴿"لا يشكر الله من لا يشكر الناس" -حديث شريف-﴾، فإنه من غير المسموح لي نسيان فضل كل من الدكتور الفاضل" فيصل سليماني" رئيس قسم الهندسة المدنية الأسبق بجامعة باجي مختار -عنابة- الذي قدم لي كل التسهيلات قبل و أثناء متابعة تكويني في الدكتوراه بالتوازي مع أدائي لواجباتي المهنية بالقسم، و الدكتورة الفاضلة "سعاد منادي" رئيسة القسم الحالية التي واصلت بنفس الكيفية تقديم كل التسهيلات، وكذا جميع الأساتذة و الدكاترة الأفاضل الذين قدموا لي الدعم المعنوي والتقني من خلال تشجيعاتهم و مناقشاتهم المثمرة و توجيهاتهم العلمية القيمة.

أشكر أيضا أستاذي العزيز والقامة العلمية الدكتور "شريف بن تركي" الذي أكن له كل الاحترام والتقدير والعرفان لدعمه وتشجيعه إياي على استئناف دراستي بعد انقطاع طويل وكذلك أساتذتي الكرام "كمال جغابة" و"مولود مرزود" و"زبرطعي بدرالدين " و"عاشورة جمال" و"السعيد حجاج" و" عزالدين قرين" و "الطاهر قدوار" و"حسين شابي" والأستاذ القدير "رجال بشير".

أشكركافة زملاء و زميلات العمل بالأخص خوالدي خير الدين و أسرته الكريمة.

كما لا يمكنني أن أنسى لطف وبساطة وتعاون مديري ورؤساء مصالح وموظفي مختبرات كل من:

* المدرسة الوطنية العليا للتكنولوجيا و الهندسة (م و ع ت ه) -عنابة- (المدرسة الوطنية العليا للمناجم والمعادن (م و ع م م) سابقا) وأخص بالذكر مهندسي المخابر: " سمير سكحال " و "هشام براهمية " و "مصطفى متيري "ورئيسة المصلحة "حكيمة زدوري".

* مخبر الميتالوغرافيا، وحدة البحث في المناجم والتعدين، مركز البحث في التكنولوجيات الصناعية (م ب ت ص) بعنابة ((أوراسم) سابقا).

* قسم الفيزياء بجامعة محمد خيضر- بسكرة-.

* قسم الميكانيك بجامعة باجي مختار -عنابة- وأخص بالذكر الدكتور الفاضل "ناصرالدين موقاص".

* قسمي الهندسة المدنية بكل من جامعتي 8 ماي 1945- قالمة- وباجي مختار-عنابة-.

* مخبر مراقبة جودة مواد البناء وعلى رأسه الأستاذ القدير "محمد فوزي حبيطة".

* فني الحدادة الأخ الكريم " حسين خيذر".

لا يفوتني كذلك أن أشكر زملائي وزميلاتي طلبة الدكتوراه والدكاترة الذين وفقوا في مناقشة أطروحاتهم سواء من جامعة محمد خيضر- بسكرة - أو جامعة باجي مختار- عنابة - أو جامعة محمد بوضياف - المسيلة - على الأوقات الطيبة التي قضيناها معا في رحاب العلم والمعرفة والتي جعلت التكوين في الدكتوراه تجربة ممتعة.

شكر خاص للدكتورة "أمينة حودة" على دعمها وتشجيعها لي من خلال عرض تجربتها الخاصة.

الشكر موصول أيضا لكل من الدكاترة: "سكندر حملاوي" و"أحمد خميس" و"أميرة عياط" و"إيمان سعدي" و"محمد بن زرارة" و"مروة لعقاقين" و"مهدي زايد" و"سليمة بوكور" وبشكل استثنائي صديقي العزيز طالب الدكتوراه: "نورالدين بولقصيبات".

أود أيضا أن أشكر الأساتذة الأفاضل أعضاء لجنة المناقشة الذين وافقوا على مراجعة وتقييم هذه الأطروحة من خلال ملاحظاتهم وتوجيهاتهم القيمة بلا شك والتي ستسهم بالتأكيد في جعل هذا العمل يبدو أكثر جودة.

Acknowledgments

First of all, I would like to express my appreciation and gratitude to Dr Bouzidi MEZGUICHE for his supervision of this thesis on the one hand, and for his kindness and flexibility in choosing the research laboratories to host this experimental work on the other hand, which made me feel comfortable throughout the years that this modest research work took, I would also like to thank the distinguished doctors and professors who accompanied the theoretical training and the administrative staff of the Department of Civil Engineering and Hydraulics at Mohamed KHIDER University - Biskra - who showed professionalism in the performance of their duties, and I cannot fail to thank in particular Dr Bachir TAALLAH, Chairman of the Doctoral Training Committee, for his great cooperation.

And because ﴿'He who does not thank people does not thank God'-Noble Hadith-﴾, I am not allowed to forget the virtues of Dr Faicel SLIMANI, former Head of the Department of Civil Engineering at BADJI Mokhtar University – Annaba - who provided me with all facilities before and during my doctoral training in parallel with my professional duties in the department, Dr Souad MENADI, the current head of the department who continued to provide me with all facilities, and all the distinguished professors and doctors who provided me with moral and technical support through their encouragement, fruitful discussions, and valuable scientific guidance.

I would also like to thank my dear professor Dr Cherif BEN TORKI, to whom I have the utmost respect, appreciation and gratitude for his support and encouragement to resume my studies after a long interruption, as well as my esteemed professors Kamel DJEGHABA, Mouloud MERZOUD, Badreddine ZBARTAI, Djamel ACHORA, Said HADJADJ, Azzeddine GRINE, Taher GUEDOUAR, Hocine CHABBI and the able professor Bachir REDJEL.

I would like to thank all my colleagues, especially KHOUALDI Kheireddine and his family.

I cannot forget the kindness, simplicity and co-operation of the directors, heads of departments and staff of the laboratories of:

* The Higher National School of Technology and Engineering (HNSTE) – Annaba - (formerly the Higher National School of Mines and Metals (HNSMM)), in particular the laboratory engineers: 'Samir SOUKEHAL', 'Hicham BRAHMIA', 'Moustapha METIRI' and the head of service 'Hakima ZEDOURI'.

* Metallographic Laboratory, Research Unit in Mines and Mining, Research Centre for Industrial Technologies (RUMM-RCIT) in Annaba (formerly URASM).

* Department of Physics, Mohamed KHIDER University -Biskra-.

* The Department of Mechanics at BADJI Mokhtar University -Annaba-, especially Dr Nacereddine MOKAS.

* The Civil Engineering Departments at the Universities of 8 May 1945 -Guelma- and BADJI Mokhtar -Annaba-.
* The building materials quality control laboratory, headed by Professor Mohamed Faouzi HABITA.
* The blacksmith, brother “Hussein Khaydar”.

I would also like to thank my fellow doctoral students and doctors who successfully defended their theses, whether from Mohamed KHIDER University -Biskra-, BADJI Mokhtar University -Annaba-, or Mohamed BOUDIAF University -M’sila-, for the good times we spent together in the spirit of science and knowledge, which made doctoral training an enjoyable experience.

Special thanks to Dr Amina HOUDA for her support and encouragement by sharing her own experience.

Thanks also to Drs: ‘Skander HAMLAOUI, Ahmed KHEMIS, Amira AYAT, Imane SAADI, Mohamed BENZERARA, Maroua LAGAGUINE, Mehdi ZAIED, Salima BOUKOR, and exceptionally to my dear friend and PhD student: Noureddine BOULEKSIBATE’.

I would also like to thank the honourable professors who agreed to review and evaluate this thesis through their valuable comments and guidance, which will certainly contribute to making this work look even better.

ملخص

في ظل الاستنزاف السريع للموارد الطبيعية والطلب المتزايد باستمرار على مواد البناء، يواجه قطاع البناء تحديًا كبيرًا يتمثل في كيف نلبي الحاجة المتزايدة إلى البنية التحتية مع الحفاظ على البيئة وضمان ديمومة المنشآت ؟ تزداد أهمية هذه المشكلة مع التوسع العمراني السريع المدفوع بالتقدم التكنولوجي والنمو السكاني، مما يتطلب تطوير أنسجة عمرانية ديناميكية وقابلة للتكيف. لذلك، أصبح من الضروري إعادة التفكير في طرق إنتاج المواد وتبني حلول مبتكرة ومستدامة لدعم التنمية المستدامة للمدن والبنى التحتية.

تعتمد دول العالم إلى حد كبير على الخرسانة في إنجاز مشاريعها البنائية بشكل يجعل استنفاد الموارد الطبيعية -المصدر الرئيسي للمواد التي تشكل الخرسانة- أكثر كثافة وبالتالي أكثر إثارة للقلق. بناء على ذلك، يتعين على العالم أن يبذل المزيد من الجهود في البحث عن موارد بديلة.

تعد إعادة تدوير مواد البناء المسترجعة من الأبنية "خارج الخدمة" والبنى التحتية المهدمة أومن مخلفات ورشات البناء ومصانع الخرسانة مسبقة التصنيع وكذا مصانع مواد البناء -لاستعمالها كمورد بديل- من الأفكار الواعدة، حيث تظهرصداقة بيئية ونجاعة اقتصادية ملفتة للانتباه. يضاف إلى ذلك توفر مصدر طبيعي غير تقليدي هام للرمال لا يزال بعيدا عن الاستغلال الأمثل خاصة في مجال البناء ألا وهو الكثبان الرملية الصحراوية.

إسهاما منا في بذل الجهود الرامية إلى إيجاد موارد بديلة لمواد البناء المهددة بالاستنفاد، يدرس هذا العمل إمكانية الجمع بين إعادة تدوير الخرسانة القديمة في شكل مجاميع حصى خشن واستغلال رمال الكثبان الصحراوية كبديل للرمل التقليدي لإنتاج خرسانة بيئية ذات جودة. أظهرت الخصائص الفيزيائية لهاتين المادتين البديلتين تكاملا فيما بينهما من ناحية قابلية التشغيل. كما لوحظ تحسن في مقاومة ضغط الخرسانة بنسبة سبعة في المائة مقارنة مع الخرسانة المرجعية المنتجة من مواد ذات مصدر تقليدي. أنجزت بعض اختبارات مؤشرات الاستدامة بغرض استعمالها كمبررات لجدوى توأمة هذه المواد البديلة بالإضافة إلى معاينة سلوك الخرسانة بعد إخضاعها إلى ظروف قاسية (التآكل، تجمد- ذوبان، أوساط كيميائية، حرارة مرتفعة). وقد سجلنا نتائج مرضية إجمالا.

الكلمات المفتاحية:

استنزاف الموارد الطبيعية ؛ مواد بديلة؛ إعادة تدوير الخرسانة؛ الاستدامة.

Résumé

Face à l’épuisement accéléré des ressources naturelles et à l’augmentation constante des besoins en matériaux de construction, le secteur du bâtiment est confronté à un défi majeur : comment répondre à la demande croissante en infrastructures tout en préservant l’environnement et en assurant la durabilité des ouvrages ? Cette problématique est d’autant plus pressante que l’urbanisation rapide, soutenue par les avancées technologiques et la croissance démographique, impose la création de tissus urbains dynamiques et adaptés aux évolutions de la société. Il devient ainsi indispensable de repenser les modes de production des matériaux et de privilégier des solutions innovantes et responsables pour accompagner le développement durable des villes et des infrastructures. Les pays du monde entier dépendent fortement du béton pour leurs projets de construction, ce qui rend l'épuisement des ressources naturelles - la principale source des matériaux qui composent le béton - plus intense et donc plus préoccupant. Le monde doit donc redoubler d'efforts pour trouver des ressources alternatives. Le recyclage des matériaux de construction récupérés dans les bâtiments « désaffectés » et les infrastructures démolies ou dans les ateliers de construction, les usines de béton préfabriqué et les usines de matériaux de construction - pour les utiliser comme ressource alternative - est une idée prometteuse, qui se révèle remarquablement respectueuse de l'environnement et efficace sur le plan économique. En outre, il existe une importante source naturelle non traditionnelle de sable qui est encore loin d'être exploitée de manière optimale, en particulier dans le domaine de la construction : les dunes de sable du désert. Afin de contribuer aux efforts visant à trouver des ressources alternatives pour les matériaux de construction en voie d'épuisement, ce travail étudie la possibilité de combiner le recyclage du béton ancien sous forme de gros granulats avec l'utilisation du sable des dunes du désert comme alternative au sable conventionnel pour produire un béton écologique de qualité. Les propriétés physiques de ces deux matériaux alternatifs ont montré une complémentarité en termes de maniabilité. Une amélioration de 7 % de la résistance à la compression du béton a été observée par rapport au béton de contrôle produit à partir de matériaux conventionnels. Certains tests indicateurs de durabilité ont été réalisés pour justifier la faisabilité du jumelage de ces matériaux alternatifs ainsi que le comportement du béton après l'avoir soumis à des conditions extrêmes (abrasion, gel-dégel, milieux chimiques, haute température). Des résultats globalement favorables ont été rapportés.

Mots clés :

Épuisement des ressources naturelles ; matériaux alternatifs ; recyclage de béton ; durabilité.

Abstract

Faced with the rapid depletion of natural resources and the continuously growing demand for construction materials, the building sector is confronted with a major challenge: how to meet the increasing need for infrastructure while preserving the environment and ensuring the durability of structures? This issue is made even more urgent by rapid urbanisation, driven by technological advancements and population growth, which requires the development of dynamic and adaptable urban fabrics. It is therefore essential to rethink material production methods and prioritise innovative, sustainable solutions to support the sustainable development of cities and infrastructure. Countries around the world rely heavily on concrete for their construction projects, making the depletion of natural resources - the main source of the material that makes up concrete - more intense and therefore more worrisome. Accordingly, the world needs to put more effort into finding alternative resources. Recycling building materials recovered from 'decommissioned' buildings and demolished infrastructures or from construction workshops, precast concrete plants and building materials factories - for use as an alternative resource - is a promising idea, showing remarkable eco-friendliness and economic efficiency. In addition, there is an important non-traditional natural source of sand that is still far from being optimally exploited, especially in the field of construction: the desert sand dunes. As a contribution to efforts to find alternative resources for depleting building materials, this work investigates the possibility of combining the recycling of old concrete in the form of coarse aggregates with the utilisation of desert dune sand as an alternative to conventional sand to produce eco-quality concrete. The physical properties of these two alternative materials showed complementarity in terms of workability. A seven per cent improvement in the compressive strength of the concrete was observed compared to control concrete produced from traditionally sourced materials. Some durability indicator tests were carried out to justify the feasibility of twinning these alternative materials as well as the behaviour of the concrete after subjecting it to extreme conditions (abrasion, freeze-thaw, chemical media, high temperature). Overall favourable results are reported.

Keywords:

Depletion of natural resources; alternative materials; concrete recycling; durability.

Table of Contents

إهـــــداء III
Dedication IV
شكــر وامــتنـان V
Acknowledgments VI
ملخص VIII
Résumé IX
Abstract X
Table of Contents XI
List of Figures XIX
List of Tables XXII
Symbols and Abbreviations XXIV
GENERAL INTRODUCTION 1
Circumstances and Points of Support for the Research 4
Research Objective 8
Breakdown and Organisation of the Thesis 8
CHAPTER I _ CONSTRUCTION ACTIVITY OVERVIEW 10
I.1. INTRODUCTION 10
I. 2. CONSTRUCTION ACTIVITY IN ALGERIA 10
I. 2.1. Housing 10
I. 2.2. Road Infrastructure 12
I. 2.3. Rail Infrastructure 13
I. 2.4. Bridges and Tunnels 14
I. 2.5. Airports 15
I. 2.6. Seaports 16
I. 2.7. Hydraulic Structures (Dams) 16
I. 2.8. Specific Structures 17
I. 3. CONSTRUCTION ACTIVITY WORLDWIDE 18
I. 3.1. Housing 19
I. 3.2. Road Infrastructure 21
I. 3.3. Rail Infrastructure 22
I. 3.4. Bridges and Tunnels 23
I. 3.5. Airports 25
I. 3.6. Seaports and Lock 26
I. 3.7. Hydraulic Structures 26
I. 3.8. Specific Structures 27

I. 4. CONCLUSION 29
CHAPTER II _ BIBLIOGRAPHIC SYNTHESIS 32
II. 1. INTRODUCTION 32
II. 2. AGGREGATES 32
II. 2.1. Definition 32
II. 2.2. History of the Aggregates Use in Construction 33
II. 2.3. Aggregates Importance in Concrete 33
II. 3. CONVENTIONAL AGGREGATES 33
II. 3.1. Definition 33
II. 3.2. Global Aggregates Production, Consumption and Need 33
II. 3.3. Manufacturing 34
II. 3.4. Massive Rock Manufacturing Process 35
II. 3.5. Loose Rock Manufacturing Process 36
II. 3.6. Classification 37
II. 3.6.1. Granularity 37
II. 3.6.2. Real Density 38
II. 3.6.3. Origin 38
II. 3.6.4. Preparation Method 38
II. 3.6.5. Geological Nature 38
II. 4. SAHARA DUNE SAND 39
II. 4.1. Definition 39
II. 4.2. Availability 39
II. 4.3. Dune Types 40
II. 4.3.1. Reversed Dunes 41
II. 4.3.2. Nebka Dunes 41
II. 4.3.3. Star Dunes (Stars) 41
II. 4.3.4. Half-Moon Dunes 41
II. 4.3.5. Transversal Dunes 41
II. 4.3.6. Longitudinal Dunes 41
II. 4.3.7. Barchanoid Dunes (Ridges) 42
II. 4.3.8. Dome Dunes 42
II. 4.3.9. Parabolic Dunes 42
II. 4.4. Physical Characteristics 42
II. 4.5. Origin of Granulometry 44
II. 5. DEMOLITION AGGREGATE 44
II. 5.1. Definition 44

II. 5.2. Description of Demolition Aggregates 44
II. 5.3. History of Demolition Aggregate Use in Construction 44
II. 5.4. Availability 45
II. 5.5. Demolition Aggregates Production 46
II. 5.6. Difference Between Recycling and Downcycling 47
II. 5.7. Manufacturing Process 47
II. 5.8. Classification of Demolition Aggregates 50
II. 5.9. Properties of Demolition Aggregates 51
II. 6. DEMOLITION AGGREGATE IMPROVEMENT TECHNIQUES 53
II. 6.1. Methods Separating the Adherent Mortar from the Natural Aggregate 53
II. 6.1.1. Mechanical Treatment 54
II. 6.1.2. Chemical Treatment 54
II. 6.1.3. Thermal Treatment 55
II. 6.1.4. Microwave Treatment 56
II. 6.1.5. Ultrasonic Vibration Treatment 56
II. 6.1.6. Hydrodesmolition 57
II. 6.1.7. Electro-Fragmentation 57
II. 6.1.8. Chemo-Mechanical Treatment 58
II. 6.2. Methods Reducing the Adherent Mortar Porosity 59
II. 6.2.1. Carbonation 59
II. 6.2.2. Accelerated Carbonation 59
II. 6.2.3. Bacterial Precipitation (Biocarbonation) 60
II. 6.2.4. Changing the Surface Condition (Coating of Recycled Aggregates) 61
II. 6.3. Methods Modifying the Demolition Aggregate Hydric Status 62
II. 6.3.1. Pre-Wetting 62
II. 6.3.2. Pre-Saturation 62
II. 7. CONCRETE 62
II. 7.1. Definition 62
II. 7.2. Concrete Importance 63
II. 7.3. Ordinary Concrete Constituents 63
II. 7.3.1. Cement 63
II. 7.3.2. Fine Aggregate (Sand) 63
II. 7.3.3. Coarse Aggregate (Gravel) 64
II. 7.3.4. Mixing Water 64
II. 7.3.5. Plasticizer 64
II. 7.4. Ordinary Concrete Formulation Methods 64

II. 7.4.1. Féret Method 65
II. 7.4.2. Fuller and Thompson Method 65
II. 7.4.3. Abrams' Method 65
II. 7.4.4. Bolomey Method 65
II. 7.4.5. Caquot Method 66
II. 7.4.6. Faury Method 66
II. 7.4.7. Joisel Method 67
II. 7.4.8. Dreux – Gorisse Method 67
II. 7.4.9. Baron et Lesage Method 67
II. 7.4.10. Scramtaiev Method 67
II. 8. CONCRETE BASED ON DEMOLITION AGGREGATES 69
II. 8.1. Fresh State Properties 69
II. 8.1.1. Workability 69
II. 8.1.2. Density 70
II. 8.1.3. Occluded Air 71
II. 8.2. Hardened State Properties 72
II. 8.2.1. Density 72
II. 8.2.2. Mechanical Properties 73
II. 8.2.3. Ultrasonic Pulse Velocity 75
II. 8.2.4. Water-Accessible Porosity 78
II. 8.2.5. Water Absorption 78
II. 8.2.6. Permeability 79
II. 8.2.7. Mass Evolution 79
II. 9. DEFORMABILITY 80
II. 9.1. Factors Influencing Deformability 80
II. 9.2. Principle of Deformability Under Compressive Load 81
II. 9.3. Instantaneous Deformations Under Compressive Load 81
II. 9.4. Deformability of Recycled Concrete Under Compressive Load 82
II. 9.5. Static Young's Modulus (E) 83
II. 9.6. Types of Static Young's Modulus 83
II. 9.7. Dynamic Young's Modulus 84
II. 9.8. Poisson's Ratio (ν) 85
II. 10. TRANSITION ZONE AT THE AGGREGATE/PASTE INTERFACE (ITZ) 85
II. 10.1. ITZ's Impact on the Concrete Performance 85
II. 10.2. ITZ Formation 86
II. 10.3. ITZ in Concrete Based on Demolition Aggregates 87

II. 11. CONCRETE BEHAVIOUR IN SEVERE CONDITIONS 90
II. 11.1. Abrasion 90
II. 11.2. Freeze and Thaw Cycles 91
II. 11.3. Chemical Attacks 92
II. 11.4. High Temperature 94
II. 12. ANALYSIS OF VARIANCE "ANOVA" 96
II. 13. CONCLUSION 97
CHAPTER III _ MATERIALS AND EXPERIMENTAL METHODOLOGY 99
III. 1. INTRODUCTION 99
III. 2. MATERIALS 99
III. 2.1. Cement 99
III. 2.2. Mixing Water 100
III. 2.3. Admixture 100
III. 2.4. Fine Aggregates (Sand) 101
III. 2.5. Coarse Aggregates (Gravel) 103
III. 3. EXPERIMENTAL METHODOLOGY 105
III. 3.1. Part 1: Production and Selection of Demolition Coarse Aggregates with Low-Water Absorption 106
III. 3.1.1. Parent Concretes Manufacturing 106
III. 3.1.1.1. Formulation Method 107
III. 3.1.1.2. Mixing Plan 108
III. 3.1.1.3. Preparation of Specimens 108
III. 3.1.2. Physical Characterisation of Fresh Parent Concrete 109
III. 3.1.2.1. Workability 109
III. 3.1.3. Mechanical Characterisation of Hardened Parent Concretes 110
III. 3.1.3.1. Compressive Strength 110
III. 3.1.4. Demolition Aggregates Manufacturing 110
III. 3.1.5. Physical Characterisation of Demolition Aggregates 113
III. 3.1.5.1. Water Absorption of Demolition Aggregate Subfractions 113
III. 3.1.5.2. Reconstitution of Demolition Aggregate Fractions 114
III. 3.1.5.3. Water Absorption of Demolition Aggregate Fractions 114
III. 3.1.6. Algorithm 114
III. 3.1.7. Time and Location Conditions 115
III. 3.2. Part 2: Use of Demolition Coarse Aggregates and Saharan Dune Sand in Concrete Formulation 116
III. 3.2.1. Parent Concrete Manufacturing 116
III. 3.2.2. Demolition Aggregates Manufacturing 116
III. 3.2.3. Son Concretes Manufacturing 117

III. 3.2.4. Formulation Method 117
III. 3.2.5. Aggregate Water Demand and Effective W/C Ratio 118
III. 3.2.6. Workability 119
III. 3.2.7. Density 119
III. 3.2.8. Occluded Air 120
III. 3.2.9. Concrete Composition and Physical Properties 121
III. 3.2.10. Preparation of Specimens 122
III. 3.2.11. Hardened Concrete Density 122
III. 3.2.12. Mechanical Tests 123
III. 3.2.12.1. Compressive Test 124
III. 3.2.12.2. Three Points Flexural Test 124
III. 3.2.12.3. Splitting Test 125
III. 3.2.13. Ultrasonic Pulse Velocity 126
III. 3.2.13.1. Device Description 126
III. 3.2.13.2. Results' Reading and Interpretation 127
III. 3.2.13.3. Dynamic Modulus of Elasticity 127
III. 3.2.14. Deformability 128
III. 3.2.14.1. Testing Program 128
III. 3.2.14.2. Longitudinal Deformation 128
III. 3.2.14.3. Transversal Deformation 129
III. 3.2.15. Durability Indicators Tests 130
III. 3.2.15.1. Total Absorption Test 130
III. 3.2.15.2. Absorption by Capillarity Test 130
III. 3.2.15.3. Porosity Accessible to Water (Hydrostatic Weighing) Test 131
III. 3.2.15.4. Water Permeability Test 132
III. 3.2.16. Scanning Electron Microscope (SEM) Analyses 133
III. 3.2.16.1. Working Principle 133
III. 3.2.16.2. FEI Quanta 250 FEG-SEM Description 134
III. 3.2.17. Severe Conditions Tests 135
III. 3.2.17.1. Abrasion Test 135
III. 3.2.17.2. Freeze and Thaw Test 136
III. 3.2.17.3. Chemical Attacks Test 137
III. 3.2.17.4. High Temperature Test 137
III. 4. CONCLUSION 138
CHAPTER IV _ PRESENTATION OF RESULTS AND DISCUSSION 141
IV. 1. INTRODUCTION 141

IV. 2. PRODUCTION AND SELECTION OF DEMOLITION AGGREGATES WITH LOW-WATER ABSORPTION 141
IV. 2.1. Parent Concretes Quality 141
IV. 2.1.1. Compressive Strength 141
IV. 2.2. Demolition Aggregates' Water Absorption 142
IV. 2.3. Statistical Analysis 146
IV. 2.4. Statistical Analysis Related to DA Sub-fractions (d/D) 147
IV. 2.5. Statistical Analysis Related to DA Fraction (d/D) 148
IV. 2.6. Validation 149
IV. 3. PART 2: USE OF DEMOLITION COARSE AGGREGATES AND SAHARAN DUNE SAND IN CONCRETE FORMULATION 151
IV. 3.1. Parent Concrete 151
IV. 3.1.1. Compressive strength 151
IV. 3.2. Son Concretes 151
IV. 3.2.1. Microscopy and Granulometry of Sand 151
IV. 3.2.2. Water Demand and Workability 152
IV. 3.2.3. Compressive strength 152
IV. 3.2.4. Three-Point Flexural Strength 155
IV. 3.2.5. Splitting Tensile Strength 155
IV. 3.2.6. Ultrasonic velocity 156
IV. 3.2.7. Dynamic Modulus of Elasticity 157
IV. 3.2.8. Deformability 159
IV. 3.2.8.1. Constraint Longitudinal Deflection 159
IV. 3.2.8.2. Constraint Transversal Deflection 160
IV. 3.2.8.3. Deflection Module and Elasticity Module 161
IV. 3.2.9. Durability Indicators 163
IV. 3.2.9.1. Absorption by Total Immersion 163
IV. 3.2.9.2. Water Permeability 164
IV. 3.2.9.3. Absorption by Capillarity 164
IV. 3.2.10. SEM Observations 166
IV. 3.2.11. Behaviour in Severe Conditions 167
IV. 3.2.11.1. Abrasion 167
IV. 3.2.11.2. Freeze-Thaw Cycles 168
IV. 3.2.11.3. Chemical Attacks 171
IV. 3.2.11.4. High Temperature 177
IV. 4. CONCLUSION 183
GENERAL CONCLUSION 187

PERSPECTIVES 191
APPENDIX 1 194
APPENDIX 2 195
BIBLIOGRAPHICAL REFERENCES 198
PUBLICATIONS AND COMMUNICATIONS FROM THE THESIS 226
A. PUBLICATION OF ARTICLES 226
B. INTERNATIONAL COMMUNICATIONS 226

List of Figures

GENERAL INTRODUCTION

Figure 1 : Life Cycle of Construction Material or Building [57] 7

CHAPTER I

Figure I. 1 : The City of Sidi Abdallah, Algeria [61] 11
Figure I. 2 : Situation of the Road Network in Algeria [64] 12
Figure I. 3 : Map of the Algerian Railway Network [66] 13
Figure I. 4 : Algiers Metro [68] 14
Figure I. 5 : Bridges and Tunnel in Algeria [69, 71–73] 15
Figure I. 6 : New Algiers Airport [75] 15
Figure I. 7 : Model of the Port of El Hamdania - Cherchell [76] 16
Figure I. 8 : Beni Haroun Bridge and Dam [78] 16
Figure I. 9 : Religious Structure [80] 17
Figure I. 10 : Cultural, Sporting and Touristic Structures [83, 85–87] 18
Figure I. 11: Cities Around the World [90, 93–96] 21
Figure I. 12 : Road Infrastructure in USA and China [97, 99] 22
Figure I. 13 : Rail Infrastructure Around the World [98, 100, 101, 103] 23
Figure I. 14 : Some Important Bridges in the World [98, 104] 24
Figure I. 15 : The Gotthard Base Tunnel [105] 24
Figure I. 16 : World's Largest Airports [101, 107, 112, 113] 25
Figure I. 17 : The New “Doha Seaports and Terneuzen Lock” [114, 115] 26
Figure I. 18 : Great World Dams [98, 114, 117] 27
Figure I. 19 : The Abraj Kudai [119] 28
Figure I. 20 : Cultural, Sporting and Touristic Structures Around the World [101, 120, 121] 29

CHAPTER II

Figure II. 1 : Sand and Gravel Production Worldwide in 2023, by Country and in Thousands of Tons 34
Figure II. 2 : Massive Rock Manufacturing Process [132] 35
Figure II. 3 : Manufacturing Process in Loose Rock [132] 36
Figure II. 4 : Quarries of Limestone and Silicon Sand [134–136] 37
Figure II. 5 : The Desert Card [143] 40
Figure II. 6 : Types of Dunes According to Wind Direction [144, 145] 40
Figure II. 7 : Particle Size Distribution of Desert Dune Sand (Laghouat-Algeria) [150] 43
Figure II. 8 : SEM Image and EDX Analysis of the Desert Dune Sand (Laghouat-Algeria) [150] 43
Figure II. 9 : Buildings Threatened With Ruin and Uncontrolled Dumping of Demolition Concrete (Course of the Revolution and Seybouse City, Annaba _ Algeria). 45
Figure II. 10 : Share of Recycled Aggregates in Total Aggregates Production [163] 46
Figure II. 11 : Recycling Platform and Aggregate Production [123, 149] 47
Figure II. 12 : Process Flow Diagram for a State-of-the-Art Recycling Facility [150] 49
Figure II. 13 : Typical Composition of Demolition Waste 51
Figure II. 14 : Natural and Recycled Gravel’ Los Angeles Coefficient [104] 51
Figure II. 15 : Relationship Between Mortar Content and Density [153] 52

Figure II. 16 : Relationship Between Mortar Content and Demolition Aggregate Water Absorption [153]..... 53
Figure II. 17 : Principle of Ultrasonic Vibration Treatment [177]..... 56
Figure II. 18 : Interaction Between Pressurised Water and the Treated Material [178] 57
Figure II. 19 : Mainly Calcium Carbonate Crystalline Forms [180] 59
Figure II. 20 : Accelerated Carbonation Device in the Laboratory – Treatment of Recycled Aggregates by Accelerated Carbonation [29]..... 60
Figure II. 21 : Precipitation of CaCO3 in the Pores and Microcracks of Recycled Gravel, Before and After to be Treated by Bioprecipitation [180]..... 61
Figure II. 22 : Rotary Drum Laboratory Granulator for Cement Encapsulation of Recycled Aggregates [189]..... 62
Figure II. 23 : Variation of Slump of Concretes Containing Different Types of Aggregates: a)- 100% Crushed Granite, b)- 80% Crushed Granite + 20% Recycled Aggregates, c)- 50% Recycled Granite + 50% Recycled Aggregates, d)- 100% Recycled Aggregates [212]..... 70
Figure II. 24 : Influence of Recycled Gravel Rates and Cement Types on the Air Content of Concrete [28] 71
Figure II. 25 : Percentage of Air Occluded as a Function of the Substitution Rate [167] 72
Figure II. 26 : Compressive Strength of Recycled Concrete Compared to Conventional Concrete [236] 74
Figure II. 27 : Evolution of Tensile Strength by Splitting, Over Time, as a Function of the Replacement Rates of Recycled Aggregates [237]..... 74
Figure II. 28 : Correlation Between Resistance and Ultrasonic Velocity [238]. 76
Figure II. 29 : Effect of Aggregate Type (Similar Concretes Except Aggregate Type) on the Relationship (Pulse Velocity - Compressive Strength) [243]..... 77
Figure II. 30 : Water-Accessible Porosity for Concretes at Different Substitution Rates After 90 Days of Curing in Water (BR: Reference Concrete, S30G30: 30% Substitution, G100: 100% Substitution - Given in Green: E/L) [245] 78
Figure II. 31 : Permeability as a Function of the Substitution Rate of Recycled Aggregates (BR: Reference Concrete, S30G30: 30% Substitution, G100: 100% Substitution- Given in Green: E/L) [245]..... 79
Figure II. 33 : Types of Static Young's Modulus of Elasticity of Concrete [253] 84
Figure II. 34 : Aggregate, Paste and Transition Zone in an Ordinary Concrete 85
Figure II. 35 : ATZs in Concretes or Mortars Containing Concrete Demolition Aggregates [27]..... 87
Figure II. 36 : Traditional Mixing Procedure (NMA^2) [265]..... 88
Figure II. 37 : New Mixing Technique ($TSMA^3$) [265] 88
Figure II. 38 : New ITZs seen at the SEM [265] 89
Figure II. 39 : Comparison of New ITZs Using Different RCAs Types [265]..... 90
Figure II. 40 : Chemical Reactions Causing Concrete Damage (According to Lauer, K. and Lachaud, ft. and Salomon, M.) [280]..... 93
Figure II. 41 : Variation of Mass of Concrete Subjected to Sulfate Attack [282] 94
Figure II. 42 : Evolution of the Residual Induced Permeability of Concrete as a Function of Temperature [287]... 95
Figure II. 43 : Dimensional Variation of Recycled Concrete as a Function of Temperature [208]..... 96

CHAPTER III

Figure III. 1 : Cement Packed in a Bag of 50 kg 100
Figure III. 2 : Dune Sand Extraction Site (Biskra, Algeria) 101
Figure III. 3 : Extraction Site of Siliceous Alluvial Sand (Tebessa, Algeria)..... 101
Figure III. 4 : Gradation Curves of Both Sand Types (STB and SD) 102
Figure III. 5 : Electron Microscope and Sand Microscopic Observations..... 103
Figure III. 6 : Gradation Curves of Natural Aggregates (NAs) 103
Figure III. 7 : Natural and Demolition Coarse Aggregates Used in Part 2 of the Study..... 105
Figure III. 8 : Steps in the Abrams Cone Procedure for Measuring Slump..... 109
Figure III. 9 : Concrete Broken into Pieces and Jaw Crusher..... 111

Figure III. 10 : Procedure for the Preparation of DAs and Quantification of Water Absorption..... 112
Figure III. 11 : Example Showing Sizes and Types of the Crushed DAs..... 112
Figure III. 12 : Water Absorption Test Steps..... 113
Figure III. 13 : Size Reduction of an Unreinforced Beam and Crushing Result 117
Figure III. 14 : Sand and Coarse Aggregates Combinations..... 117
Figure III. 15 : Water Absorption by Aggregate Type 118
Figure III. 16 : Total Water Demand in Concrete Formulations 118
Figure III. 17 : Result of the Slump Test Conducted on One of the Concrete Mixtures Studied 119
Figure III. 18 : Weighing of a Known Volume of Fresh Concrete..... 120
Figure III. 19 : Aerometer with Manometer 121
Figure III. 20 : Hardened Concrete Specimens..... 122
Figure III. 21 : Weighing of Hardened Concrete Specimen 123
Figure III. 22 : Hydraulic Presses for the Mechanical Tests..... 123
Figure III. 23 : Cubic Samples (10x10x10) cm3 Extracted from an Unreinforced Beam for a Compression Test. 124
Figure III. 24 : Mechanical Diagram of the Three-Points Flexion Test..... 125
Figure III. 25 : Cubic Concrete Specimen Tested by Splitting..... 126
Figure III. 26 : Ultrasonic Pulse Velocity Tester..... 126
Figure III. 27 : Deformability Measurement by Strain Gauge Frame..... 128
Figure III. 28 : Experimental Setup for Capillary Absorption Test 131
Figure III. 29 : Hydrostatic Concrete Weighing Device..... 132
Figure III. 30 : Water Permeability Meter 133
Figure III. 31 : Scanning Electron Microscope, EDAX and Sample Holder..... 134
Figure III. 32 : Compartment with Concrete Half-Cube, Steel Balls, Steel Beads and Water 136
Figure III. 33 : Concrete Specimens in the Nabertherm Muffle Furnace 138
Figure III. 34 : Crackmeter (MAGNIF 24^{x})..... 138

CHAPTER IV

Figure IV. 1 : Water Absorption Following DA Sub-Fractions for 20 Minutes (%)..... 142
Figure IV. 2 : Water Absorption Following DA Reconstituted Fractions (%) for 20 Minutes 143
Figure IV. 3 : Water Absorption Maximum, Average, and Minimum Values of DA Sub-Fractions..... 144
Figure IV. 4 : Water Absorption Maximum, Average, and Minimum Values for DA Reconstituted Fractions 144
Figure IV. 5 : DA Reconstituted Fractions' Minimum Water Absorption Values from the Same PC (Min) and Selected from All PCs (Min Selected)..... 145
Figure IV. 6 : DA Sub-Fractions' Water Absorption after 20 Minutes as a Function of DAD_{max}/NAD_{max} Ratio ... 146
Figure IV. 7 : DA Reconstituted Fractions' Water Absorption after 20 Minutes as a Function of DAD_{max}/NAD_{max} Ratio 146
Figure IV. 8 : Compressive Strength of 2-Years Parent and Sons Concretes..... 153
Figure IV. 9 : Compressive Strength of 28-Day Study Concretes..... 154
Figure IV. 10 : Compressive Strengths Evolution..... 155
Figure IV. 11 : Three-Points Flexural Strengths of 28-Day Concretes..... 155
Figure IV. 12 : Splitting Strengths of 28-Day Concretes..... 156
Figure IV. 13 : Ultrasonic Velocity of the 28-Days Concretes..... 156
Figure IV. 14 : The Concretes' Dynamic Elasticity Modulus..... 157
Figure IV. 15 : Elasto-Instantaneous Longitudinal Deflection of Concretes..... 159
Figure IV. 16 : Elasto-Instantaneous Transveral Deflection of Concretes 160
Figure IV. 17 : Deflection Module of Concretes..... 162
Figure IV. 18 : Elasticity Module of Concretes..... 162

Figure IV. 19 : Porosity of Concretes 163
Figure IV. 20 : Permeability Coefficient of Concretes 164
Figure IV. 21 : Kinetics of Capillary Absorption Coefficient (Ca_t) of the Concretes as a Function of the Square Root of Time (√t) 165
Figure IV. 22 : SEM observation of the concrete samples 166
Figure IV. 23 : Concrete Specimen After 2, 4, 6 and 8 Hours of Abrasion 167
Figure IV. 24 : Mass Evolution (left, in grams) and Mass Loss Ratio (right, %) of Concrete Samples as a Function of Abrasion Duration 168
Figure IV. 25 : The External Appearance of the Concretes Exposed to 50 Freeze-Thaw Cycles 168
Figure IV. 26 : Mass Evolution After Freeze-Thaw Cycles 169
Figure IV. 27 : Compressive Strength After Freeze-Thaw Cycles 170
Figure IV. 28 : External Appearance After 2 Years of Immersion in Chemical Media 172
Figure IV. 29 : Mass Evolution After 2 Years of Immersion in Chemical Media 173
Figure IV. 30 : Compressive Strength Evolution After 2 Years of Immersion in Chemical Media 174
Figure IV. 31 : Ultrasonic Velocity Evolution after 2 Years of Immersion in Chemical Media 175
Figure IV. 32 : Correlation Between Ultrasonic Velocity and Compressive Strength after 2 Years of Immersion in Chemical Media 176
Figure IV. 33 : Correlation Between Mass and Compressive Strength after 2 Years of Immersion in Chemical Media 177
Figure IV. 34 : Spalling of a Concrete Specimen after High Temperature Exposure 178
Figure IV. 35 : Concrete Cracking after High Temperature Exposure Seen with a Crack Meter 178
Figure IV. 36 : Mass Evolution after High Temperature Exposure 179
Figure IV. 37 : Compressive Strength Evolution after High Temperature Exposure 180
Figure IV. 38 : Ultrasonic Velocity Evolution after High Temperature Exposure 181
Figure IV. 39 : Correlation Between Ultrasonic Velocity and Compressive Strength Following High-Temperature Exposure 182
Figure IV. 40 : Correlation Between Mass and Compressive Strength Following High-Temperature Exposure ... 183

List of Tables

CHAPTER II

Table II. 1 : The Main Crushers Used [133] 36
Table II. 2 : Global C&D Waste Production in 2018 [160] 46
Table II. 3 : Advantages and Disadvantages of Different Types of Crushers [165] 50
Table II. 4 : Advantages and Disadvantages of Some Recycled Aggregates Treatment Methods [175] 58
Table II. 5 : α Values as a Function of W/C 68
Table II. 6 : General Relationship Between Concrete Quality and Impulse Velocity [239] 75
Table II. 7 : Some Proposed Correlation Models Between Compressive Strength R (MPa) and Ultrasonic Velocity V (km/s, *: m/s) [244] 77

CHAPTER III

Table III. 1 : Chemical Composition of Cement 100
Table III. 2 : Mineralogical Composition of Cement 100
Table III. 3 : Physical Characteristics of the Admixture 101
Table III. 4 : Physical Characteristics of Sands 102
Table III. 5 : Chemical Compositions of Sands 102

Table III. 6 : Grain Rate by Size 102
Table III. 7 : Particular Refusal of NA Sub-Fractions 104
Table III. 8 : Physical Characteristics of the Coarse Aggregates Used in Part 1 of the Study 104
Table III. 9 : Physical Characteristics of the Coarse Aggregates Used in Part 2 of the Study 104
Table III. 10 : Parent Concretes Composition 107
Table III. 11 : Concrete Slump Groups 109
Table III. 12 : Time and Place Conditions for the Tests 115
Table III. 13 : Aggregates Water Absorption, Water Demand and W_{eff} /C 119
Table III. 14 : Concretes Composition 121
Table III. 15 : Concretes Physical Properties in the Fresh State 121

CHAPTER IV

Table IV. 1 : Findings for the 28-Day Parent Concretes' Compressive Strength in MPa (Part 1) 142
Table IV. 2 : DA Aggregate Sub-Fractions' Water Absorption After 20 Minutes 143
Table IV. 3 : DA Reconstituted Fractions' Water Absorption After 20 Minutes 143
Table IV. 4 : ANOVA Summary: 20 Minutes-Water Absorption Linked with DA Sub-Fraction Size 147
Table IV. 5 : ANOVA Findings: Water Aborption for 20 Minutes Linked with DA Sub-Fraction Size 147
Table IV. 6 : ANOVA Summary: 20 Minutes-Water Absorption Linked with Sub-Fraction Origin 148
Table IV. 7 : ANOVA Results: 20 Minutes-Water Absorption Linked with Sub-Fraction Origin 148
Table IV. 8 : ANOVA Summary: 20 Minutes-Water Absorption Linked with DA Fraction Size 148
Table IV. 9 : ANOVA Results: 20 Minutes-Water Absorption Linked with DA Fraction Size 148
Table IV. 10 : ANOVA Summary: 20 Minutes-Water Absorption Related to DA Fraction Origin 149
Table IV. 11 : ANOVA Results: 20 Minutes-Water Absorption Related to DA Fraction Origin 149
Table IV. 12 : An overview of the water absorption measurements at 20 minutes obtained for a single test sample three times in succession using the standard method Succession 150
Table IV. 13 : An overview of the water absorption measurements at 20 minutes obtained at five different test samples using the standard method 150
Table IV. 14 : Findings from the 2-Year Parent Concrete's Compressive Strength Test (Part 2) 151
Table IV. 15 : Compressive Strengths of the Concretes 154
Table IV. 16 : Frost Strength Coefficient 170

Symbols and Abbreviations

PC	–	Parent Concrete
NASTBC	–	Concrete With Natural Coarse Aggregate and Alluvial Sand
NASDC	–	Concrete With Natural Coarse Aggregate and Dune Sand
DASTBC	–	Concrete With Demolition Coarse Aggregate and Alluvial Sand
DASDC	–	Concrete With Demolition Coarse Aggregate and Dune Sand
IWSF	–	Deposit or Burial Through Inert Waste Storage Facilities
TLF	–	Technical Landfills
STB	–	Siliceous Alluvial Sand
SD	–	Saharan Dune Sand
γ_{app}	–	Apparent Density
γ_{abs}	–	Absolute Density
FM	–	Fineness Modulus
P	–	Porosity
VSE	–	Visual Sand Equivalent
NA	–	Natural Aggregate
DA	–	Demolition Aggregate
WA	–	Water Absorption Coefficient
LA	–	Los Angelos Coefficient
MDS	–	Micro Deval Dryd Coefficient
C	–	Cement Dosage
W	–	Water Dosage
G/S	–	Gravel-to-Sand Ratio
W/C	–	Water-to-Cement Ratio
W/C_{eff}	–	Efficient Water/Cement Ratio
S	–	Slump
Oa	–	Occluded Air
γ_{cal}	–	Calculated Density
γ_{real}	–	Real Density
AFPC	–	Association Française Pour La Construction (French Construction Association)
ANOVA	–	Analysis of Variance

AFREM	–	Association Française De Recherches Et d'Essais Sur Les Matériaux Et Les Constructions (French Association for Research and Testing on Materials and Construction)
SDD_{max}	–	Maximum Diameter of Dune Sand Grains
$STBD_{max}$	–	Maximum Diameter of Siliceous Alluvial Sand Grains
$SDD_{max}/STBD_{max}$	–	The Ratio of Maximum Grains Diameters of Two Sand
FSC	–	Frost Strength Coefficient
Abs_{total}	–	Total Absorption
M_{sat}	–	Mass of the Specimen After 24 Hours of Saturation
M_{dry}	–	Mass of the Dry Specimen
Ca_t	–	Capillary Absorption Coefficient
M_t	–	Mass of the Specimen at a Given Time
M_0	–	Initial Mass of the Specimen
A	–	Section of the Specimen
K_p	–	Infiltration Coefficient
Q	–	Volume of Seepage Water
H	–	Thickness of the Specimen
F	–	Surface of the Specimen
$P_1 – P_2$	–	Pressure Difference Between the Inlet and the Outlet of the Specimen
T	–	Experiment Time
η	–	Change in Viscosity of Water as a Function of Temperature
D	–	Diameter of the Specimen
K	–	Influence of Specimen Diameter
T	–	Age Equivalent to 50 Cycles
A	–	Age of Concrete at the Start of the Test
N	–	Number of Freeze-Thaw Cycles
K_{rg}	–	Frost Resistance Coefficient
R_{rg}	–	Residual Compressive Strength
R_{sat}	–	Compressive Strength of Water-Saturated Observation Concrete
FSC	–	Frost Strenght Coefficients
CaO	–	Free Lime
$CaCO_3$	–	Calcium Carbonate or Lime Stone
$Ca(OH)_2$	–	Portlandite

CO_2	–	Carbon Dioxide
C-S-H	–	Hydrated Calcium Silicate
E/C	–	Water To Cement Weight Ratio
F_c	–	Average Compressive Strength
F_{tf}	–	Average Split Tensile Strength
C_2S	–	Bi-Calcium Silicate
C_3A	–	Tricalcium Aluminate
C_3S	–	Tricalcium Silicate
MEB	–	Scanning Electron Microscope
DRX	–	X-Ray Diffraction
G (3/8)	–	3/8 Fraction Gravel
G (8/16)	–	8/16 Fraction Gravel
G (16/25)	–	16/25 Fraction Gravel
ρ	–	Volumic Mass

GENERAL INTRODUCTION

GENERAL INTRODUCTION

In Algeria, many constructions and bridges - of which concrete is a part - have already reached the end of their pre-estimated lives or almost, especially in the country's north. Except for those with confirmed historical, cultural and economic values, these constructions and bridges will certainly be demolished. This requires serious reflection on the fate of the enormous debris quantity to be cleared accumulating with the thousands of tons from public and private construction sites [1]. Recorded natural disasters such as the earthquakes of Chlef ex "El Asnam" (1954; 1980) and Boumerdes (2003) [2–4] in turn have a significant share of waste. Many countries in the world are experiencing the same situation. In some countries, the war machine has left behind destroyed cities with almost demolished infrastructures and buildings. Logically, after the war ended, gigantic reconstruction operations will be started after clearing the debris. The idea of eliminating this debris by deposit or burial through inert waste storage facilities (IWSF) and technical landfills (TLF) is not still original [1, 5, 6]. Their saturations imply the opening of others to the detriment of the environment [7]and the legislation requires in response stricter conditions limiting the grant of authorizations. This waste type begins to be inadmissible [5, 6]. In similar cases, several countries in the world that have opened major projects for infrastructure renovation and replacement of old buildings with more modern ones are facing the same problems. Construction and reconstruction operations in the world are taking on an accelerated pace due to the obligation to follow the high pace imposed by the known development in the various areas of life (social, economic, cultural, sporting, etc.). New cities are springing up like mushrooms all over the world. The creation of artificial land extending into the seas using sand comes as a solution to the land problem for some countries [8, 9]. For all this, we will need very big building materials quantities, mainly sand and coarse aggregates (gravels) used in the concrete composition. Unfortunately, construction and reconstruction operations may not be able to keep up with the accelerated pace given the shortage of traditional natural sand and coarse aggregate resources due to the depletion, the fear of depletion or the geological nature in the vicinity of the construction sites. Transferring to import is not always better [9]. In addition to the economic impact of the mismanagement of the resources, depriving future generations of natural wealth will likely cause an intergenerational tear. This work contributes to research addressing these complex issues. The globe is 30 per cent composed of Sahara

[10]. The Algerian territory is 70 per cent Sahara, which represents a big resource of non-traditional sand. The thousands of tons of demolished concrete above mentioned can be transformed into a big reserve of aggregates. The idea of bringing together Saharan dune sand and coarse aggregates from demolished concrete to make new concrete presents a two-dimensional recovery with a multidimensional impact. According to Bouhnik, (2007) and Guettala et al., (2003) [11, 12], the use of Saharan dune sand in the sand concrete formulation made it possible to achieve compressive strengths of around 31 MPa, whereas ordinary concrete with Saharan dune sand cannot exceed 24 MPa according to Bentata, (2004) and Bouhnik, (2007) [11, 13]. Trying to reconcile these studies, we tried to improve the mechanical performance of ordinary concrete formulated with Saharan dune sand by promoting the mortar amount in the mixture, in other words, to formulate a pumpable ordinary concrete. A previous attempt to formulate a non-pumpable ordinary concrete resulted in an insufficient mortar volume compared to the volume of the coarse aggregates, which is a second reason why we opted for the choice of pumpable ordinary concrete. On the other hand, according to Hani Mokbel, (2014), Sanchez de Juan and Gutiérrez, (2009) and Zhao et al., (2015) [14–16], the water absorption capacity of the aggregates extract from old concrete increases with the decrease of their size due to the increase of old adherent mortar' amount. The finest fractions of demolished concrete aggregates then have the highest water absorption capacity compared to the largest [14, 16]. This encouraged us to abandon the (3/8) fraction in this study.

Kang et al. [17, 18] discovered a link between the rise in DAs' compressive strength and the increment in their size, which resulted from a decrease in OM content. Sánchez de Juan et al. and Hemmati Pourghashti, H. et al. [15, 19] have reported that the OM content in the 4/8 mm fraction of DAs ranges from 33% to 55%, while it ranges from 23% to 44% in the 8/16 mm fraction. To prevent excessive water absorption, it is recommended that DAs for structural concrete should not contain more than 44% OM. If the OM content exceeds this threshold, the water absorption of DAs may exceed 8%. To address this issue, researchers have explored two main approaches: mortar-gravel (OM-NA) separation techniques (mechanical, chemical, physical, thermomechanical, etc.) and specific old mortar (OM) treatments (pre-saturation, pre-wetting, accelerated carbonation, using silane-based water repellents, etc.) [20–31]. In all instances, these strategies whether they involve separating mortar from gravel or treating old mortar,

were implemented during the final stages of DAs production [32–46]. However, according to S. Braymand and Yin Jinming, these methods carry costs, require time, and pose potential health risks for certain applications [47, 48]. According to Jang, H. et al, [49] some treatments, such as hydrochloric acid (HCl) solutions, have an extreme level of aggressiveness, capable of disintegrating limestone aggregates during application. This characteristic requires meticulous attention when selecting appropriate methods because of the potential risks associated with this strong chemical. Within this research, we aimed to investigate the impact of aggregate size on concrete performance, specifically focusing on the ratio (DAD_{max}/NAD_{max}), which represents the maximum size of demolition aggregate (DAD_{max}) in relation to the maximum size of natural aggregate (NAD_{max}) used in the parent concrete. Our objective is to elucidate the correlation between this ratio and the water absorption capacity of the resulting material. Based on the findings from this initial phase, we will select coarse demolition aggregates for further analysis in the subsequent part of the study. This approach not only enhances our understanding of how aggregate size influences water absorption but also informs the selection of materials for optimizing concrete formulations. By carefully examining these relationships, we aim to contribute valuable insights that can improve the mechanical properties and sustainability of concrete made with recycled aggregates.

Gravels intended for the manufacture of concrete are generally sold on the Algerian market in fractions 3/8, 8/16 and 16/25 mm. Depending on the element to be produced (structural, decorative or other), one, two or three of these fractions are used in the concrete formulation. Which makes 7 gravel combinations possible. The latter were translated in this work into 7 types of parent concrete, among which we find binary, ternary and quaternary with granular skeletons that are continuous for some and discontinuous for others. This made it possible to study a variety of concretes. The sub-fractions chosen are based on the standardized sieves available at the laboratory level, of which there are 10. Each test was repeated 3 times and the average was calculated. Which gave a total of 210 values reduced into 70 average values. The parent concretes (PCs) were produced in a laboratory setting, and the maximum diameter of the Natural Aggregates (NAs) (NAD_{max}) was predetermined. If the PCs were not manufactured in a laboratory, we would have had to perform a visual inspection to determine their NAD_{max}. The DAs were sorted into sub-fractions based on their known maximum

diameter (DAD_{max}), and their water absorption was measured for 20 minutes, with the DAD_{max}/NAD_{max} ratio serving as a determining factor. As per Zhaoa et al. [50], there is a strong correlation between the OM content in DAs and their water absorption, with higher OM levels resulting in increased water absorption. By analyzing the water absorption data, a threshold ratio of DAD_{max}/NAD_{max} was determined to generate DAs sub-fractions containing a minimum amount of OM. The sub-fractions were reclassified into (3/8), (8/16), and (16/25) mm fractions, aligning with the particle size distribution of the NAs. The water absorption over 20 minutes was then calculated based on the dominance of each sub-fraction. Additionally, a DAD_{max}/NAD_{max} threshold ratio was defined for the (3/8), (8/16), and (16/25) mm fractions. Before the crushing process, the careful selection and management of Parent Concrete (PC) compositions, tailored to the desired DAs fraction, constitutes an insightful upstream intervention.

As the second phase of this study, we conducted compression tests on the demolished concrete (parent concrete) to assess its quality. Following this, we performed a series of physical and mechanical characterisation tests on the constituent materials. We formulated four different types of concrete by combining sand with coarse aggregates and examined their properties in both fresh and hardened states. Additionally, we conducted durability indicator tests to evaluate the performance of these concrete mixes under severe conditions.

These investigations are crucial for understanding how different aggregate compositions affect the overall mechanical properties of concrete, particularly in terms of strength and durability. The insights gained from this phase will inform future applications and optimise the use of recycled materials in concrete production, ensuring that structural integrity is maintained even under challenging environmental conditions.

Circumstances and Points of Support for the Research

This thesis research is based on a set of data that gives it usefulness and importance. Some of these are listed below:

1. <u>Great Need for Aggregates for Construction Activities:</u>

The construction of buildings and infrastructures is mainly based on concrete thanks to the various advantages it offers. Concrete is made up of around 80% aggregates. According to Thomas Martaud (2009) [51], statistics provided by Arquié et al, 1990

give approximate figures for the aggregate needed to build certain structures: 3,000 tonnes for a secondary school; 5,000 tonnes for a hospital; 12,000 tonnes for a kilometre of road and 30,000 tonnes for a kilometre of motorway. For its annual consumption, the world needs 2.2 billion tonnes of sand, 4.7 billion tonnes of gravel and 9 billion tonnes of concrete [52].

2. Shortage of Natural Aggregates (Sand and Gravel):

Suppliers of natural aggregates (sand and gravel) risk not being able to meet all the demand from the construction and public works market, given the shortage of these two vital materials due to the geological nature of certain sites, on the one hand, and to restrictions on the exploitation of deposits by the competent authorities, on the other.

3. Large Deposits of Dune Sand:

Desert sand is abundant in desert lands, which cover approximately one seventh of the Earth's surface and one third of its land area. The Sahara, the largest hot desert in the world, spans almost 8,600,000 square kilometers, featuring diverse topographical types. Stony and rocky regions account for 82% of its mineral cover, while sand deserts, including ergs, cover approximately 18%. This 18% is significant, with a total area of 1,548,000 square kilometers. The Sahara extends beyond the Red Sea, merging with the Arabian Desert to cover almost 12 million square kilometer [53, 54].

4. Large Quantities of Construction Waste:

The amount of local and global waste generated by the planned and unplanned demolition of buildings and engineering structures continues to grow. Of the 25 billion m2 of buildings in Europe, 35% are over 50 years old, 40% were built before 1960 and 75% are energy inefficient, according to European Commission statistics [52]. The construction sector in Europe produces around 40-50% of all waste produced in the world, with construction waste production corresponding to 1,725 kg per inhabitant per year, or 37.5% of total waste. According to national statistics, in 2014 Belgium produced more than 26 million tonnes of construction and demolition waste, a pile almost twice as high as the Great Pyramid of Giza. According to a study published by the Apur in February 2022, the construction of 27.5 million m^2 and the demolition of 9.5 million m^2 are planned between now and 2030 as part of the Greater Paris development projects. 220.5 million tonnes of waste produced in France by economic

activities comes from the construction and public works sector 1. According to the Regional Waste Management Plan, between 2016 and 2025, the construction and public works sector will produce around 40 million tonnes of waste per year in the Île-de-France region, over 90% of which will be non-hazardous waste and therefore potentially recoverable if it is not landfilled or incinerated [55]. In Libya, following the destruction of buildings after the revolution, the volume of construction waste was estimated at 80 million tonnes [56]. There are many reasons for demolition, which can be divided into three categories:

- Normal End-of-Life Category (Full Life Cycle):

This category is characterised by a drop in performance and a serious deterioration in the condition of buildings and engineering structures after many years of service. As a result, these structures can no longer be used in accordance with the rules of the art of construction and safety standards.

- Early End-of-Life Category (Shortened Life Cycle):

In this category, buildings and engineering structures are still performing well and have not suffered any deterioration, except that the purpose for which they were built is coming to its planned end (concrete plants, life bases, temporary buildings, etc.).

- Accidental End-of-Life Category (Interrupted Life Cycle):

In this category buildings and engineering structures come to an unforeseen end of service as a result of accidental ruin or the threat of ruin. It can be divided into two sub-categories:

- Natural Accidental End-of-Life Sub-Category:

In this sub-category the causes of ruin or threatened ruin of buildings and engineering structures are purely natural following natural disasters such as earthquakes and landslides.

- Accidental Human End-of-Life Sub-Category:

In this sub-category, man is the cause of the ruin or threat of ruin of buildings and engineering structures through errors (incidents, road accidents, etc.) or through planned or unplanned destruction (military and civil wars).

The Life cycle of construction material or building is shown in Figure 1.

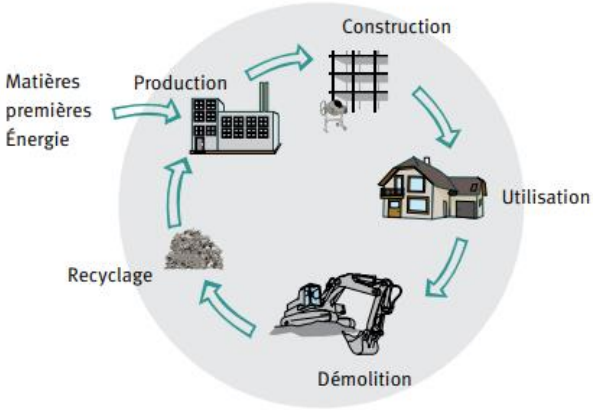

Figure 1 : Life Cycle of Construction Material or Building [57]

5. Environmental Problems

Whether at local or international level, the environment is often the victim of infringements linked to certain human activities or sometimes natural phenomena requiring human intervention.

❖ The disposal of debris by dumping or burial in inert waste storage facilities (ISDI) and technical landfill centres (CET) has become more difficult and subject to very strict conditions.

❖ The northward movement (creep) of Saharan sand and the threat of desertification have forced the Algerian state to set up anti-desertification programmes that consume a great deal of energy and effort and require large state budgets (green dam, etc.).

6. Economic Problem

The need to complete planned projects on time, faced with a shortage of aggregates, means that foreign currency imports have to be used.

7. Probable Social Problem

The deprivation of future generations of natural wealth as a result of intensive and unstudied exploitation of resources will probably cause an intergenerational rift. According to Statista Research Department (2024) [58], world sand and gravel production in 2023 will amount to 402,700 thousand tonnes, broken down as follows: USA : 130,000, China 88,000, Italy 33,000, Turkey 15,000, France 14,000, India 12,000, Netherlands 12,000, Germany 11,000, Bulgaria 8,600, Russia 7,300, Malaysia 7,000 and Spain 6,600, Poland 5,800, Australia 5,500, Canada 5,500, United Kingdom 4,200, Argentina 4,000, Indonesia 3,500, Mexico 2,700, Japan 2,000 and finally the rest of the world with a total of 25,000.

Research Objective

The aim of this research work is to contribute to efforts to tackle the problems raised by the two-dimensional upgrading of the two 'environmentally undesirable' materials in a high-performance concrete.

Breakdown and Organisation of the Thesis

The thesis work was carried out in the civil engineering research laboratory of the University of Biskra (LRGC-Biskra) and the civil engineering laboratory of the University of Annaba (LGC-Annaba) under the supervision of Dr. Bouzidi MEZGHICHE, Senior Lecturer A. This thesis consists of four chapters, preceded by a general introduction highlighting the various aspects on which we have based our approach to this subject. The first chapter deals with the Construction Activity Overview. The second chapter presents a bibliographic synthesis. The third chapter presents the characterisation of the materials used, the experimental methodology for the preparation of the concretes, the characterisation and control tests on the concretes in the fresh and hardened states, as well as some durability indicator tests. Finally, the fourth and last chapter covers the results obtained and their interpretation and sets out the conclusions of the study. The outlook, references and appendices complete this research document.

CHAPTER I

CONSTRUCTION ACTIVITY OVERVIEW

CHAPTER I _ CONSTRUCTION ACTIVITY OVERVIEW

I.1. INTRODUCTION

The construction industry is a vital component of economic and social development, influencing various sectors and contributing significantly to a nation's growth. In Algeria, as in many other countries, the construction sector is experiencing rapid expansion driven by a growing population and increasing urbanization. This chapter provides an overview of construction activities both in Algeria and globally, highlighting the key areas of focus within the industry.

In the first section, we will delve into the specifics of construction activity in Algeria, examining critical areas such as housing, road and rail infrastructure, bridges and tunnels, airports, seaports, hydraulic structures like dams, and other specific constructions. Each of these elements plays a crucial role in supporting the country's infrastructure needs and enhancing the quality of life for its citizens.

Following this, we will broaden our scope to explore construction activities worldwide. By comparing Algeria's construction landscape with global trends, we can identify similarities and differences that may inform future developments in the sector. This comparative analysis will cover various aspects of construction, including housing, transportation infrastructure, and hydraulic structures.

Through this comprehensive examination, Chapter I aims to establish a foundational understanding of the construction industry's significance in Algeria and its alignment with global practices, setting the stage for further exploration in subsequent chapters.

I. 2. CONSTRUCTION ACTIVITY IN ALGERIA

Construction activity in Algeria has continued to progress since independence and in particular over the last two decades marked by unprecedented financial ease thanks to the surge in the price of oil knowing that the national economy is mainly based on this resource. In the following some examples of the lively activity of the construction sector.

I. 2.1. Housing

Algeria has implemented ambitious housing plans to meet the needs of its population and promote urban and social development. The country's five-year plan (2005-2009) aimed to construct 1,251,209 housing units, divided into five distinct programs. These

projects, largely based on the use of concrete, demonstrate the government's commitment to meeting the housing needs of its population [1]. The government has developed a new five-year plan (2020-2024) aimed at the construction of one million housing units, including public rental housing units, subsidized promotional rents, promotional rental housing units, and aid for self-construction of rural housing. This ambitious program demonstrates the government's commitment to meeting the population's housing needs and promoting inclusive and sustainable urban development [59]. The Algerian government has announced the construction of 4.2 million housing units as part of its urban development initiatives. Additionally, the national stock of educational establishments saw a significant increase, from 28,457 to 28,839 structures in 2022, demonstrating the efforts made to strengthen the country's education system [60]. The city of Sidi Abdellah (Figure I. 1) is an example of the government's efforts to improve living conditions. Located 25 km west of Algiers, the new town benefits from excellent accessibility and plans to upgrade 400 ha of existing fabrics. The project aims to create a university, training, and advanced technology center, covering 7,000 ha, including 3,158 ha urbanized and 3,842 ha of protection zones. The expected population is 450,000 inhabitants, requiring the construction of 90,000 housing units.
To date, 93,000 housing units have been completed or are in progress, including 69,260 in rental purchase, 9,668 in LPP, and 1,000 in LPL. 43,426 housing units have been serviced, including 41,349 delivered. 70 pieces of equipment are registered, including 34 completed, 19 in progress, and 17 not launched. Additionally, 60 investment projects were affected, including 11 completed and operational, 8 in progress, 7 stopped, and 33 not launched [61].

Figure I. 1 : The City of Sidi Abdallah, Algeria [61]

I. 2.2. Road Infrastructure

According to Rabah Aicha (2022) [62], Algeria's road network is recognised as one of the densest in Africa, covering 124,107 km. The East-West motorway, with an initial length of 1,216 km, extends to 1,720 km, including ancillary roads and slip roads. The motorway features 60 interchanges, 5 tunnels, 390 engineering structures including 25 major viaducts, as well as rest areas, service stations, truck stops and maintenance centres. At present, a section of 84 km remains to be completed, as well as access roads linking the ports of Djen Djen and Béjaïa over a total distance of 741 km. The 60 km access road to the port of Mostaganem has already been completed, while the 60 km access road to Batna and the 41 km access road to Ghazaouet are under construction. In addition, the Hauts Plateaux motorway extends for 1,020 km, and a North-South motorway project, formerly the Trans-Saharan route, is currently being planned, including additional access roads. According to [63], an 84 km section of the motorway remains to be completed, as do the access roads linking the ports of Djen-Djen and Béjaïa over a total distance of 741 km. A 60 km access road leading to the port of Mostaganem is already complete. Two other access roads, 60 km to Batna and 41 km to Ghazaouet, are currently under construction. The Hauts Plateaux motorway extends over 1,020 km. In addition, a North-South motorway project, formerly known as the sub-Saharan route, including access roads, is currently in the development phase [64]. Figure I. 2 shows a number of road projects that have been completed or are under way.

Figure I. 2 : Situation of the Road Network in Algeria [64]

I. 2.3. Rail Infrastructure

❖ According to "Le chantier magazine" [65], Algeria has set itself the ambitious target of increasing its national rail network to 6,500 km by 2023. To achieve this, the country needs to build 2,300 km of new lines in just three years. In the longer term, once this initial target has been reached, Algeria plans to build a further 6,000 km of track. In this way, the Algerian rail network should reach an impressive total of 12,500 km by the target date. Figure I. 3 shows a detailed map of Algeria's current and projected rail network.

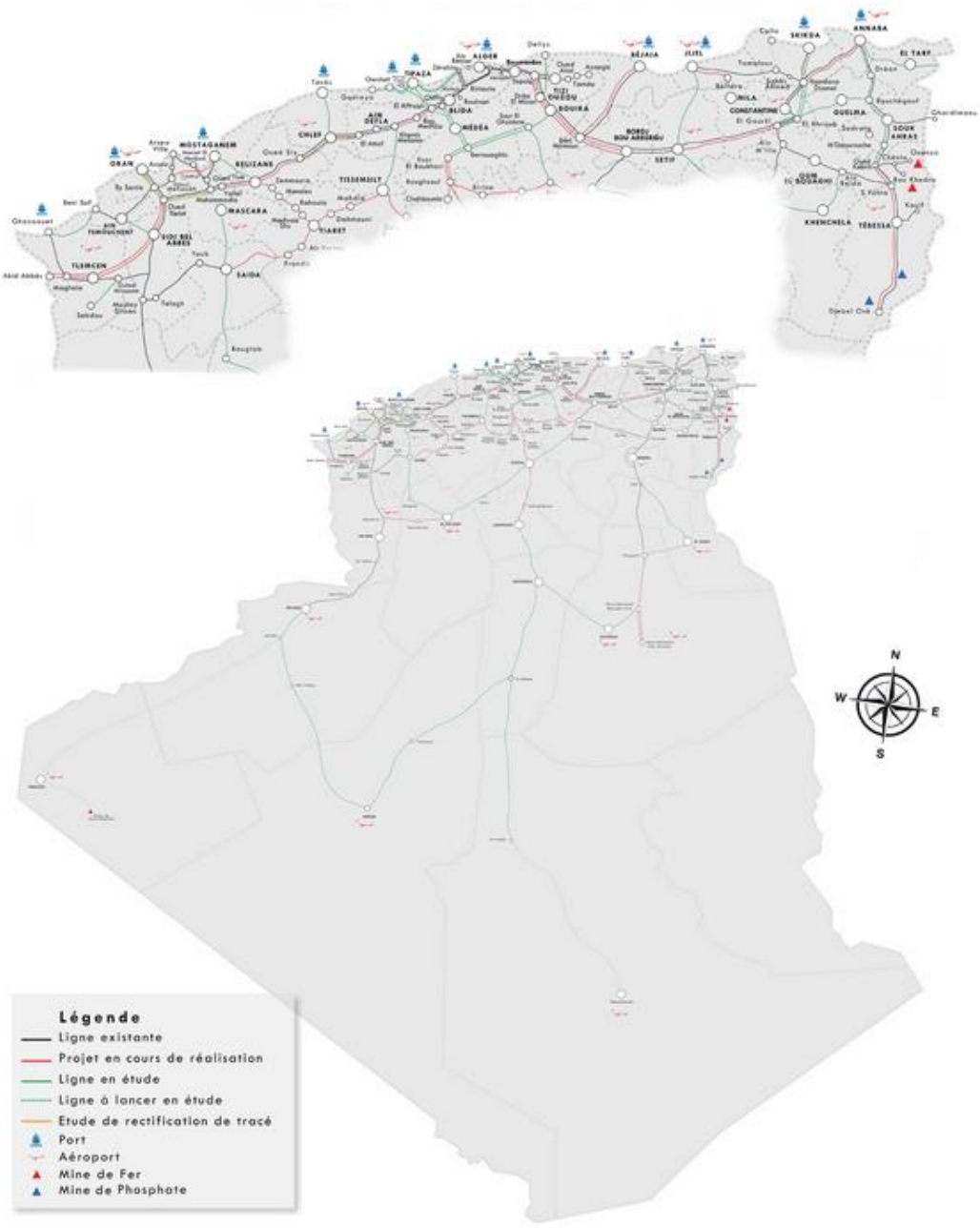

Figure I. 3 : Map of the Algerian Railway Network [66]

❖ According to information from [67], a 9.5 km extension of the Algiers Metro (Figure I. 4), linking El Harrach-centre station to Algiers airport, is due to be completed and put into service in the first quarter of 2026. This extension, comprising nine stations, is designed to improve connectivity and mobility for residents by serving major districts such as Beaulieu, Oued Smar, City 5 July, Bab Ezzouar, the El Harrach University Center, the Bab Ezzouar Business Center and Houari Boumediene University. It will also provide an interconnection with the tramway at the University of Houari Boumediene crossroads, strengthening multimodal transport options in the region.

Figure I. 4 : Algiers Metro [68]

I. 2.4. Bridges and Tunnels

Algeria has witnessed a significant increase in the number of engineering structures over the years. The art structure park has grown from 800 in 1962 to approximately 5,000 in 2007, with 742 structures built since 1999. The national engineering structure park now boasts over 10,500 road and highway engineering structures. Notably, several exceptional viaducts have been constructed, including the Trans Rhumel Viaduct, Oued Rekham Viaduct, Tlemcen Viaduct, and El Qantas Railway Tunnel. These structures represent significant engineering achievements and play a crucial role in enhancing transportation infrastructure across Algeria [62, 69–72]. These exceptional engineering structures (Figure I. 5) represent significant engineering achievements and play a crucial role in enhancing transportation infrastructure across Algeria.

Figure I. 5 : Bridges and Tunnel in Algeria [69, 71–73]

I. 2.5. Airports

Algeria is planning to build a new airport (Figure I. 6) with a capacity of over 10 million passengers a year, to complement the existing international airport (6 million passengers a year). The construction of this new terminal coincides with the renewal of the Air Algeria fleet. The new airport, which will cover an area of 20 hectares, will be equipped with state-of-the-art infrastructure: a 4,500-space car park, three aircraft parking areas, taxiways covering an area of more than 424,000 m^2, as well as 120 check-in desks and 84 control counters. The new terminal will have a capacity of 10 million passengers per year and will be able to handle 1,800 baggage items per hour [74].

Figure I. 6 : New Algiers Airport [75]

I. 2.6. Seaports

Once inaugurated, the commercial port of Cherchell, the 'Port of El Hamdania' (Figure I. 7), will become the most important port infrastructure on the African continent. In addition to the four active quarries, there are plans to open nine new quarries covering an area of 87 hectares. Construction material requirements are estimated at nearly 30 million cubic metres. These materials will be transported to the port site by at least four land routes and one sea route [76].

Figure I. 7 : Model of the Port of El Hamdania - Cherchell [76]

I. 2.7. Hydraulic Structures (Dams)

According to Lilia A. (2022) [77], Algeria currently has 75 operational dams. Furthermore, the country is set to add 5 more dams to its operational capacity in the near future. Additionally, there are 5 more dams currently under construction. Figure I. 8 illustrates the Beni Haroun Bridge and Dam in Mila.

Figure I. 8 : Beni Haroun Bridge and Dam [78]

I. 2.8. Specific Structures

In Algeria, many special projects (religious, cultural, sporting, touristic, etc.) have been completed, are under way or are planned for the coming years. Among the most famous is:

❖ The Great Mosque of Algiers, one of the largest Muslim temples in the world, welcoming 120,000 worshippers. The mosque also includes a cultural centre and a theological training institute [79]. Figure I. 9 illustrates the Great Mosque of Algiers in El-mohamadia.

Figure I. 9 : Religious Structure [80]

❖ On the sporting front, new ultra-modern stadiums have been built in Algeria to host the 2019 African Cup of Nations. One of these new gems is the Nelson Mandela stadium, located in the western suburbs of Algiers. With a capacity of 40,784, it is the fifth largest stadium in Algeria. Inaugurated in January 2023, the stadium meets FIFA standards and has notably hosted matches at the 2023 African Nations Championship (CHAN). The construction of the Nelson Mandela stadium in Algiers required a record concrete pour of 8,400 m³ for the 3 m-deep foundation platform. This exceptional pour consumed 280 tonnes of cement and 21,000 tonnes of aggregates [81].

❖ On the cultural front, the Algiers Opera House, opened in 2016, is a renowned venue for music and the performing arts. This 59,000 m^2 building was designed by Italian architect Vittorio Gregotti and can accommodate 1,400 spectators. Several performance halls, a conservatory and creative workshops are housed here [82].

❖ The Algiers International Conference Centre, located in the Club des Pins,

covers 270,000 m² and offers 230,000 m² of floor space. It includes a 6,000-seat auditorium, a banqueting hall for 3,000 people and a 15,000 m² exhibition hall. The interior design combines Islamic Moorish and modern styles, with advanced electromechanical systems. This flagship project contributes to the internationalisation of Algeria [83].

❖ An ambitious transport diversification plan has been announced by the Algerian Ministry of Transport, with the emphasis on developing the cable car network. The aim of this programme is to renovate, maintain and build new lines linking various cities in the country. Numerous renovations will be carried out on existing lines from 2024, while work in progress, such as the Constantine and Tizi Ouzou cable cars, should be completed in the first quarter [84]. Figure I. 10 shows some Cultural, sporting and touristic structures.

Figure I. 10 : Cultural, Sporting and Touristic Structures [83, 85–87]

I. 3. CONSTRUCTION ACTIVITY WORLDWIDE

Research firm Global Data forecasts average annual growth of 3.6% in the global construction industry between 2018 and 2022, reaching a global turnover of $12.9 trillion by 2022. According to the forecasts detailed in the report ‘World Construction Outlook to 2022: 3rd Quarter 2018’, this figure represents a significant increase on the $10.8 trillion recorded in 2017 [88]. The world's largest concrete projects showcase

construction industry ingenuity and advanced technology, pushing engineering boundaries. These impressive achievements highlight global concrete projects' scale and innovative use in creating large infrastructures, marking significant construction field advances.

I. 3.1. Housing

❖ Qatar

Lusail Real Estate Development spans 38 km^2, blending residential, commercial, retail, and exclusive islands, shaping Qatar's urban landscape. Doha Festival City is a dynamic entertainment hub with diverse offerings like Ikea, hotels, and a convention center, meeting the needs of visitors and residents. Healthcare facilities in Doha, including five primary healthcare centers and four hospitals at Hamad Medical City, enhance medical accessibility citywide for residents' well-being [89].

❖ China

The Tianjin Eco-City is an ambitious project designed to address the housing demands of the burgeoning middle class in major cities' outskirts while championing sustainable development. This government-backed initiative aims to create a network of eco-friendly cities that will bolster China's global image as a champion of sustainability. Situated just 150 km from Beijing, the Tianjin Eco-City is envisioned to house approximately 350,000 residents upon its scheduled completion in 2020, setting a new standard for sustainable urban living in the country 2020 [8, 90].

❖ Saudi Arabia

The Line is a visionary project for a Saudi smart city in Neom, boldly reimagining urban living without cars or streets, with a mission to achieve carbon neutrality. This groundbreaking initiative envisions a linear metropolis spanning 170 kilometers in length, 500 meters in height, and 200 meters in width, designed to welcome approximately 9 million residents. As part of Saudi Arabia's Neom initiative, "The Line" is a key component in the country's strategy to diversify its economy beyond oil, positioning itself as a major economic hub and a pioneer in sustainable urban innovation [91].

❖ Egypt

The ‘new administrative capital’ emerges majestically from the sands to the east of Cairo, covering an area of 750 km^2, the size of Singapore. Located 50 km from the city centre and Tahrir Square, this city will house the institutions of power. The authorities plan to relocate 6 million inhabitants to relieve congestion in the current capital. This pharaonic project, the New Capital, is taking shape on a 270 km^2 desert plain halfway between Cairo and Suez. It aims to create 21 residential districts and 25 business or government districts, representing an investment of 60 billion dollars. This emerging city embodies Egypt's desire to project itself into the future, by offering its citizens a modern living environment, while strengthening its international influence [92].

❖ Nigeria

Lagos, a bustling megalopolis, is Nigeria's main economic and industrial centre. With an estimated population of 20 million, it alone generates 10% of the country's GDP. Faced with numerous urban challenges, the city is investing in ambitious projects such as Eko Atlantic City, an artificial island designed to become a new ecological business district. At the same time, Lagos is establishing itself as a major technology hub in Africa, home to a number of innovative start-ups. Despite infrastructure problems, particularly in terms of internet connectivity, the city is attracting more and more investors and entrepreneurs, contributing to its rapid transformation. Lagos embodies the emergence of a modern and dynamic Africa [93]. Figure I. 11 illustrates some cities around the world.

Figure I. 11: Cities Around the World [90, 93–96]

I. 3.2. Road Infrastructure

❖ USA' LBJ Express Project

The LBJ Express project aims to alleviate congestion on 13 miles of I-635 (LBJ Freeway) and I-35E in Dallas. The project involves reconstructing main lanes and frontage roads along I-635 and adding six managed lanes from I-35E to US 75. Six elevated managed lanes will be constructed along I-35E from Loop 12 to the I-35E/I-635 interchange. The project's total cost is $2,645 million [97].

- China Highway

China's motorway network has grown exponentially since 2008, expanding from zero to 60,000 kilometers. This rapid development has positioned China as the second-largest motorway network in the world, after the United States. By 2020, the goal is to reach 100,000 kilometers, aiming to connect remote areas and promote balanced development across the country. This infrastructure modernization is part of a broader vision to enhance connectivity, facilitate economic exchanges, and improve living conditions for local residents [98]. The Chongqing Elevated Road, a key component of

Qingdao's "three vertical and four horizontal" expressway network, is a prime example of this effort. Spanning from Shandong Road to Xianshan Road, it plays a crucial role in easing congestion and improving connectivity between the city's north and south regions [99]. Figure I. 12 illustrates some road infrastructures around the world.

Figure I. 12 : Road Infrastructure in USA and China [97, 99]

I. 3.3. Rail Infrastructure

- L.G.V Bordeaux - Tours

The Tours-Bordeaux High-Speed Rail project, also known as the South Europe Atlantic high-speed rail, is a significant infrastructure development in France. Completed in 2017, this €7.8 billion project involved constructing a 302 km high-speed link between Tours and Bordeaux, reducing travel time between Paris and Bordeaux by an hour and benefiting 20 million passengers annually [100].

- London Crossrail

The Crossrail project, one of Europe's largest construction sites, is building 42 km of tunnels beneath London to create a new high-frequency rail network. Set for completion in 2022, the £19 billion project will enhance connectivity, reduce journey times, and accommodate over 200 million passengers annually [101].

❖ Riyadh Metro

In just 5 years, Saudi Arabia is building the world's largest public transport system - 85 stations, 176km of rail, and 6 metro lines across Riyadh, at a cost of $27 billion. This landmark project will establish the Kingdom's first comprehensive urban transit network, modernizing mobility and sustainability [102].

- China’s TGV

China's high-speed rail network, launched in 2007, has become the world's largest, with plans for 13,000 km in 2019 and 16,000 km by 2020. Operated by CRH, the network uses trains from global manufacturers like Bombardier and Siemens. While facing challenges like a 2011 collision and weather-related damage, the network continues expanding, with some lines limited to 300 km/h. Recently, CSR unveiled the experimental 500 km/h CRH500, built with lightweight materials, though not surpassing the French speed record. This ambitious project showcases China's commitment to developing a world-class high-speed rail infrastructure [98]. Figure I. 13 illustrates some rail infrastructures around the world.

Figure I. 13 : Rail Infrastructure Around the World [98, 100, 101, 103]

I. 3.4. Bridges and Tunnels

❖ The Hong Kong-Zhuhai-Macao Bridge

It is a series of bridges and tunnels in China's Pearl River Delta, linking the cities of Hong Kong, Zhuhai and Macao. Created in 2009, the gigantic project became the world's longest maritime bridge when it was inaugurated in 2018. It comprises a 22.9

km bridge, a 6.7 km underwater tunnel and 4 artificial islands. The bridge is designed to withstand earthquakes, typhoons and ship strikes for 120 years. With a daily waiting capacity of 40,000 vehicles, it will considerably reduce journey times between these major economic centres [98, 101].

❖ The Atlantic Bridge

It is a remarkable work of art linking the North and South American continents over the Panama Canal, built by VINCI Construction Grands Projets. This cable-stayed bridge, 4.6 km long, with 3.1 km of remarkable engineering structures, is the longest cable-stayed concrete bridge in the world. It has a central span of 530 metres and an air draught of 75 metres, making it suitable for the largest commercial vessels [104].
Figure I. 14 shows some important bridges in the world.

Figure I. 14 : Some Important Bridges in the World [98, 104]

- The Gotthard Base Tunnel in Switzerland

This tunnel (Figure I. 15), stretching 57 kilometers from Erstfeld to Bodio, is the world's longest tunnel. It connects industrial centers in Belgium, Italy, Germany, the Netherlands, and Switzerland. Opened in 2016, the tunnel consists of two tubes, each nearly 8 meters in diameter [105].

Figure I. 15 : The Gotthard Base Tunnel [105]

I. 3.5. Airports

Beijing, Dubai, Istanbul and Saudi Arabia are aiming to become the world's largest airports [106, 107] (Figure I. 16).

- China

China is planning to build 240 airports by 2020 to cope with the growth in air traffic. Beijing increased its airport capacity to 80 million passengers after the 2008 Olympic Games, but saturation was reached earlier than expected. Daxing airport, designed by ADP Ingénierie, will become one of the world's largest with 100 million passengers on 700,000 m² and 6 runways [106, 108–110].

❖ United Arab Emirates

Dubai plans to increase the capacity of its Al Maktoum airport from 5 to 160 million passengers by 2025, as part of the $30 billion 'Dubai World Central' project [111].

❖ Turkey

In Istanbul, a new 150-million-passenger airport will open in 2018 at a cost of €7 billion [111].

❖ Saudi Arabia

Saudi Arabia is also inaugurating its ultra-modern Red Sea airport in 2021, with a capacity of several million passengers [107].

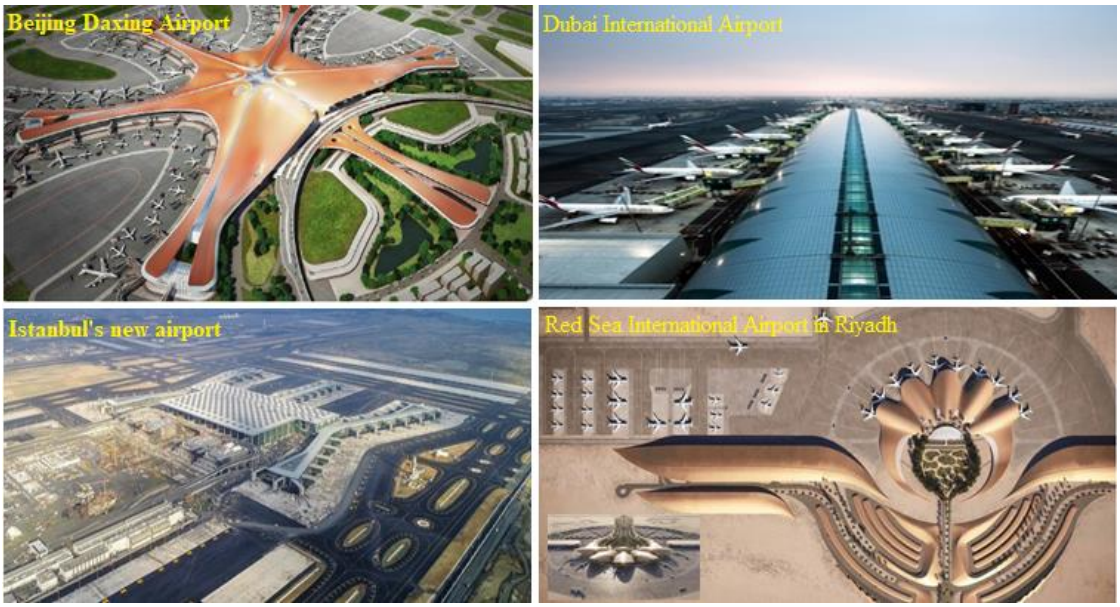

Figure I. 16 : World's Largest Airports [101, 107, 112, 113]

I. 3.6. Seaports and Lock

The New Doha Port Development Project, also known as Hamad Port, is a groundbreaking initiative that has transformed Qatar's maritime landscape. Spanning 26.5 km2, it is one of the largest and most advanced seaports in the Middle East. Located to the south of Doha, the port has an annual capacity to accommodate over 12 million twenty-foot equivalent units [114].

❖ The New Terneuzen Lock in the Netherlands, one of the world's largest locks, connects Rotterdam and Paris via a vital shipping route. By 2023, the lock will measure 427 meters long, 55 meters wide, and 16.4 meters deep, accommodating larger vessels. Construction requires 60,000 tonnes of steel, 32,000 tonnes of concrete reinforcement bars, 325,000 m³ of concrete, and the dredging of 9,500,000 m³ of soil. The lock complex must serve four key purposes: flood prevention, water release, shipping trade support, and continuous road traffic flow. By carefully considering these functions and utilizing available resources, the New Terneuzen Lock will improve the region's flood control and transportation systems [115]. Figure I. 17 shows the New “Doha Seaports and Terneuzen Lock”.

Figure I. 17 : The New “Doha Seaports and Terneuzen Lock” [114, 115]

I. 3.7. Hydraulic Structures

- China Dams

China has launched an ambitious plan to increase hydropower production, with the aim of achieving 50% more than at present. Over 70% of China's energy needs are met by coal, which will gradually be replaced by hydroelectric power. The commissioning of the Three Gorges dam in 1999 already illustrates this strategy. Despite international concerns about the impact on people and the environment, China is continuing to implement its plan by building new dams. The first of these new projects, the Xiaowan dam on the Mekong, has a capacity to generate 4,200 MW of electricity [98].

- The Great Ethiopian Renaissance Dam

The Grand Ethiopian Renaissance Dam, also known as the Millennium Dam, harnesses the Blue Nile River's power in Ethiopia. Construction began in 2011, with a significant milestone reached in February 2022 as it started generating 375MW of electricity for the national grid. Once the reservoir fills over the next 7 years, the dam's capacity will increase to 5.15 gigawatts, marking a substantial growth from its current output. This project signifies Ethiopia's commitment to utilizing renewable energy sources for economic development and energy security [88].

- The Çetin Dam and Hydroelectric Power Plant

The Çetin Dam and Hydroelectric Power Plant located in Şirvan and Pervari districts of Siirt, construction began in July 2017 by Limak İnşaat. With an installed capacity of 420 MW, it will annually generate 1.174 billion kWh of energy. This project features the largest RCC dam in Turkey and Europe, standing at 165 meters with a volume of 4.726.527 m^3 [116]. Figure I. 18 shows some great dams in the world.

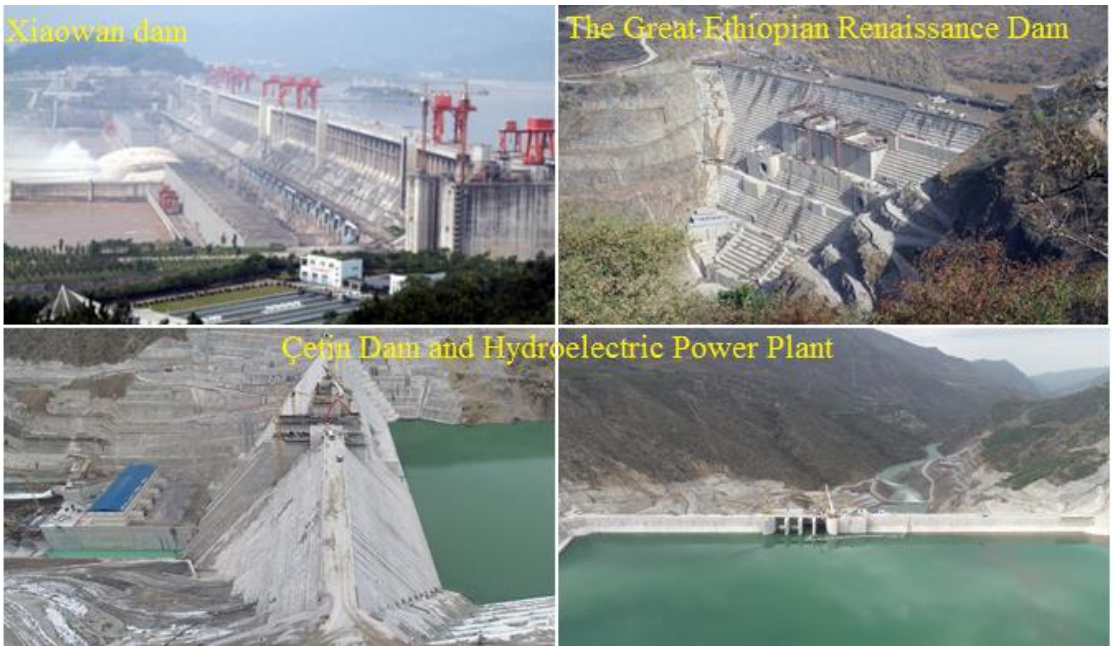

Figure I. 18 : Great World Dams [98, 114, 117]

I. 3.8. Specific Structures

- Abraj Kudai

Abraj Kudai (Figure I. 19) set to become the world's largest hotel upon completion, will boast an impressive 10,000 rooms, with a unique design featuring a ring of 12 45-storey

towers, including 10 4-star and 2 5-star hotel towers, as well as 70 restaurants and helipads for convenient helicopter and light aircraft access [118].

Figure I. 19 : The Abraj Kudai [119]

- The Great Egyptian Museum

Located in Cairo, the Great Egyptian Museum aims to become one of the largest museums in the world, the largest in the country and the largest establishment devoted to Egyptian civilisation. With a surface area of over 490,000 m² and more than 100,000 exhibits, this museum will be a veritable temple of Egyptian culture. The budget for this pharaonic project is estimated at nearly 1 billion dollars, reflecting the importance of this project for the conservation and promotion of Egyptian culture [101].

- Mercedes-Benz Stadium

Mercedes-Benz Stadium is a football and American football stadium located in Atlanta, Georgia, United States. It opened in August 2017 and has a capacity of 71,000, which can be increased to 83,000 for certain events. The stadium is owned by the State of Georgia and operated by the AMB Group, parent organisation of the Falcons and Atlanta United. The total cost of construction is estimated at around 1.6 billion dollars [101].

- Allegiant Stadium in Las Vegas (Nevada, United States)

Allegiant Stadium is one of the most modern and functional stadiums in the world. With a capacity of 65,000, extendable to 72,000 for cultural events, Allegiant Stadium has a unique system of grandiose French windows over 60 metres wide, overlooking the famous Las Vegas [95].

- The Jeddah Tower

The Jeddah Tower set to become the world's tallest, will soar over 1000 meters with 167 habitable floors in Saudi Arabia. Initiated by Prince Al-Walid and designed by

Adrian Smith, it will feature flats, offices, and a luxury hotel. The massive structure requires over 80,000 tonnes of steel, six times the size of the Eiffel Tower, and is expected to be completed in 2020 at a cost of over $1 billion [101].

- The Resort World Casino in Las Vegas

The Resort World casino will be the largest in the world, proposed by the Malaysian casino giant Genting Group. The resort will feature over 3,100 hotel rooms across 14,000 square meters, along with a 4,000-seat cinema, ice rink, aquarium, Chinese garden, and panda enclosure. The theme is centered around Chinese culture, with thousands of machines and hundreds of table games to attract visitors globally [101].

- The Palm Jumeirah

Visible from afar in the Persian Gulf; the Palm Jumeirah is a massive artificial island shaped like a palm tree, featuring a five-kilometer-long trunk and 17 palm fronds. This exclusive leisure and holiday center is home to numerous apartments, villas, luxury hotels, leisure parks, shopping centres, and marinas, along with a 120-kilometer-long sandy beach. The palm fronds are even visible from space. Figure 20. I illustrates cultural, sporting and touristic structures around the world.

Figure I. 20 : Cultural, Sporting and Touristic Structures Around the World [101, 120, 121]

I. 4. CONCLUSION

Based on the overview of construction activity in Algeria and globally, it is evident that the construction sector plays a vital role in economic development and infrastructure enhancement. In Algeria, significant investments in housing, road and rail infrastructure, bridges, tunnels, airports, seaports, and hydraulic structures demonstrate

a commitment to improving living standards and connectivity. Globally, similar trends are observed, with a focus on developing robust infrastructure to support growing populations and economies. The emphasis on specific structures further highlights the need for innovative solutions tailored to unique challenges faced in various regions. In conclusion, the construction activity landscape reflects the critical importance of infrastructure development in both Algeria and worldwide. Continued investment and strategic planning are essential to address current needs and future demands, ensuring sustainable growth and improved quality of life for communities.

CHAPTER II

BIBLIOGRAPHIC SYNTHESIS

CHAPTER II _ BIBLIOGRAPHIC SYNTHESIS

II. 1. INTRODUCTION

The second chapter of this thesis presents a comprehensive bibliographic synthesis focused on the critical components of construction materials, particularly aggregates and concrete. Understanding the properties, production methods, and applications of various types of aggregates is essential for improving concrete performance and sustainability.

This chapter begins with an exploration of aggregates, defining their role in construction and tracing their historical use. It highlights the importance of both conventional aggregates and innovative alternatives, such as Sahara dune sand and demolition aggregates, which are gaining prominence in modern construction practices. The synthesis further delves into the manufacturing processes, classification, and physical characteristics of these materials. It examines the significance of aggregate properties on concrete formulation and performance, including fresh and hardened state characteristics.

Additionally, the chapter addresses advanced topics such as the transition zone at the aggregate/paste interface (ITZ), deformability under load, and the methodologies for conducting multiscale investigations into material properties. Statistical analyses will also be discussed to validate findings and support conclusions drawn from the literature. By synthesizing existing research and insights on aggregates and concrete, this chapter aims to provide a solid foundation for understanding their roles in construction and paving the way for future innovations in material science.

II. 2. AGGREGATES

II. 2.1. Definition

Aggregates consist of a set of mineral grains that, depending on their size (ranging from 0 to 125 mm), fall into one of seven categories: fillers, sandblastings, sands, gravels, pebbles, ballast, or rip-rap. These aggregates are obtained by exploiting deposits of alluvial or marine sands and gravels, by crushing solid rocks (limestone or igneous), or through the recycling of products such as demolition materials. Their nature, shape, and characteristics vary depending on the deposits and production techniques used [122].

II. 2.2. History of the Aggregates Use in Construction

For centuries, structures and monuments have been erected using hard stones like sandstone, granite, and limestone. For instance, aggregates were used, among other resources, in the construction of the extensive road and aqueduct network of the Roman Empire. Often, these stones were taken out of quarries that were distant from the locations where they were utilized. The need for aggregates expanded significantly in the 19th century with the advent of cement and concrete. The rise in the building industry has led to an increase in the usage of stone-based raw materials [123].

II. 2.3. Aggregates Importance in Concrete

Aggregates play a crucial role in concrete by serving as fillers, reducing the volume of cement needed and thus offering economic and ecological benefits. Additionally, aggregates form the concrete skeleton, providing structural integrity and limiting dimensional variations due to their greater rigidity compared to cement paste. This technical advantage ensures a more stable and durable concrete structure.

II. 3. CONVENTIONAL AGGREGATES

II. 3.1. Definition

Conventional aggregates are the most commonly used aggregates in concrete production, typically composed of natural sand, gravel, or crushed stone that meet industry standards.

II. 3.2. Global Aggregates Production, Consumption and Need

Global aggregates production, consumption and need are critical issues that require urgent attention. According to Statista [58], global production of sand and gravel in 2023 amounted to 402,700,000 tons, with the United States leading production at an estimated 130 million tones (Figure II. 1). However, a lack of gravel and sand is a widespread problem impacting many areas of the world [124].

An estimated 40 to 50 billion tons of sand are used annually, with China consuming the most at 60% of the world's output. To meet construction demands, countries like the United Arab Emirates, especially Dubai, import sand, with projects like the Burj Kalifa requiring 45,700 tons of Australian sand. Dubai's artificial islands, such as the Palm Islands and "The World" project, consumed massive amounts of sand, with the Palm

Islands using approximately 150 million tons and "The World" requiring more than 500 million tons [125].

China's cement consumption is also alarming, as it consumed the same volume in two years that the United States would have consumed in a century. One volume of cement is generally associated with between 2 and 3 volumes of sand in mortar and with 2 volumes of sand and between 3 and 4 volumes of gravel in concrete [126–128].

A recent study published in the journal One Earth highlights the urgent need to address the growing demand for aggregates, particularly sand, which is set to explode over the next few decades. Projections indicate that demand will double by 2060, reaching 55 gigatons per year, posing significant environmental and social risks [129]. Scientists warn that this increased demand could lead to irreversible damage to ecosystems and trigger conflicts over the scarcity of this resource [130].

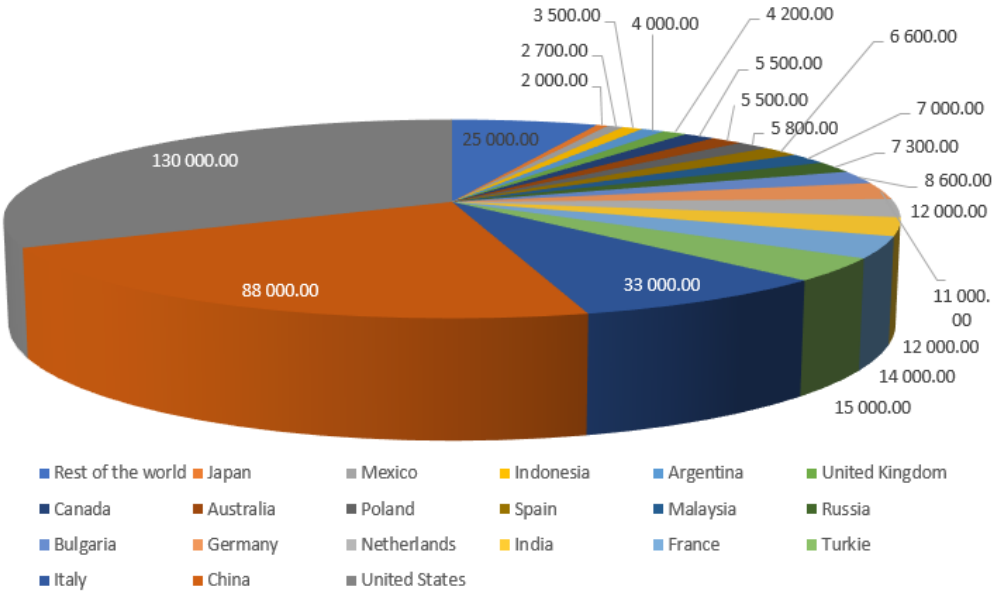

Figure II. 1 : Sand and Gravel Production Worldwide in 2023, by Country and in Thousands of Tons

II. 3.3. Manufacturing

The two main stages of aggregate processing are (1) basic processing, which involves crushing, screening, and washing to achieve the right gradation and cleanliness, and (2) beneficiation, which involves using techniques like heavy media separation, jigging, rising-current classification, and crushing to improve quality [131]. Aggregates can be made from solid rock, loose rock, or recycling materials.

II. 3.4. Massive Rock Manufacturing Process

Production in solid rock (Figure II. 2) begins with an extraction phase, using explosives. This is called blasting. The extracted material is then washed, crushed and screened to obtain the desired granularity. The largest fractions of rock are rejected during screening, to undergo further crushing [132]. Table II.1 shows the main types of crushers used in quarrying and respectively the phenomenon allowing crushing [133].

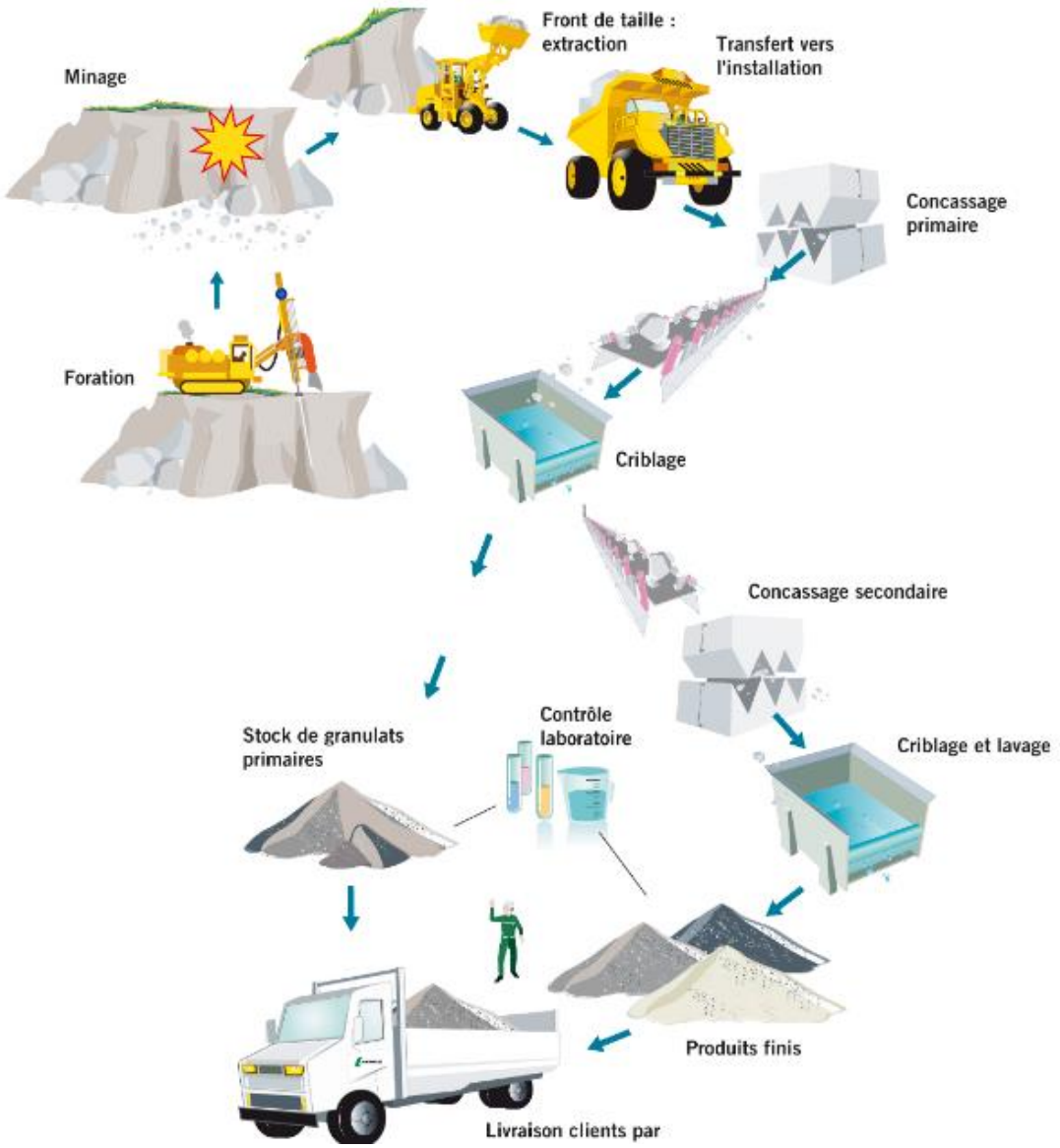

Figure II. 2 : Massive Rock Manufacturing Process [132]

Table II. 1 : The Main Crushers Used [133]

Crusher type	Jaw crusher	Gyratory crusher	Roller crusher	Impact crusher
Phenomenon	Compression	Compression	Crushing	Projection
Intervention stages	Primary - - -	primary secondary ternary -	- Secondary Ternary Quaternary	- Secondary Ternary Quaternary
Illustration		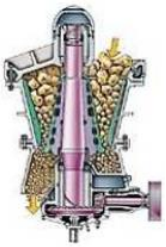		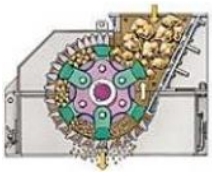

II. 3.5. Loose Rock Manufacturing Process

The production of loose rock (Figure II. 3) is simpler because extraction does not require the rock to be split: it is mined directly in the quarry, before being washed and sorted, with little or no crushing. Washing is, however, an important stage in removing the clay that coats the sand or gravel [132].

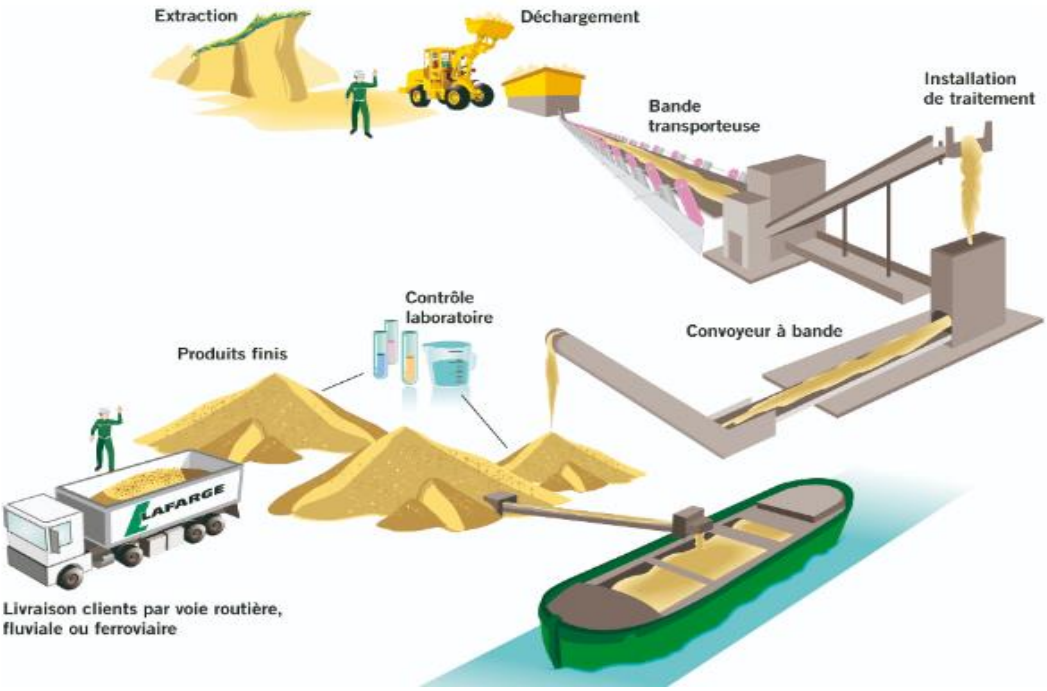

Figure II. 3 : Manufacturing Process in Loose Rock [132]

Examples of limestone and silicon sand quarries are shown in Figure II. 4.

Figure II. 4 : Quarries of Limestone and Silicon Sand [134–136]

II. 3.6. Classification

The classification of aggregates is a means of distinguishing between different types according to well-defined criteria. According to F. MAUBERT (1989) [137], The classification criteria for aggregates are mainly: granularity, density, origin and method of preparation.

II. 3.6.1. Granularity

Granularity is the dimensional distribution of the grains making up an aggregate. The diameters of these grains are between two minimum values ‘d’ and maximum values ‘D’ by which this aggregate is designated. On the basis of this designation, the latter is assigned one of the conventional names specified by standard NF EN 933-2 [138] in the following increasing order of granularity:

- Fillers 0/D where D < 2 mm with at least 70% passing 0.063 mm
- Sablons s 0/D where D < 1 mm with less than 70% passing 0.063 mm
- Sands 0/D where 1 < D < 6.3 mm
- Bass 0/D where D > 6.3 mm
- Gravel d/D where d > l et D < 125 mm
- Ballasts d/D where d > 25 mm and D < 50 mm

II. 3.6.2. Real Density

According to the standards (NF P 18-309; NFP 18-554 and NF P 18-555) [139–141] aggregates can be classified into three classes according to the actual density of the grain:

- Light when it is less than 2 gr/cm^3
- Medium when it is between 2 and 3 gr/cm^3
- Heavy when it is greater than 3 gr/cm^3

II. 3.6.3. Origin

Aggregates can be classified according to origin into two categories:

- Natural when they have only undergone a mechanical transformation operation;
- Artificial when they have undergone other processing operations.

II. 3.6.4. Preparation Method

The preparation of natural aggregates is done by a succession of mechanical operations: crushing, screening, washing, etc…

For artificial aggregates, the method of preparation must be specified in its designation (expanded clay, granulated slag, crystallized slag, etc…).

II. 3.6.5. Geological Nature

Natural aggregates are extracted from deposits of loose detrital formations or massive rock formations.

- Loose Detrital Formations

For materials from detrital rocks, a simple washing is enough to get rid of the fines, screening ensures particle size sorting and crushing to reduce the size of large elements. Materials can be rolled, crushed or rolled-crushed as needed. To have fine elements the sand can be crushed.

- Alluvium From Water courses

The deposition of alluvial materials in river beds occurs thanks to the phenomena of erosion and transport by water. Alluvium constitutes the main source of supply of aggregates. Generally, they are classified into 3 categories:

- Siliceous gravel
- Sand-lime gravel
- Gravel limestone

- Sedimentary Formations of Marine and Continental Origin

Most of its sands are fine to medium granularity with very large quartz dominance.

- Dunes and Coastal Strips

They can be found in lenses of fine sand, or in the form of sea pebble beaches.

- Arenas

On-site weathering residues of magmatic and metamorphic rocks. Arenas of granite origin are the most exploited.

- Moraines

Very heterogeneous unusable deposits. If they are taken up by a watercourse and deposited downstream, they can be assimilated to coarse alluvial deposits. Moraines contain all the huge blocks and fine silty or clayey sands.

- Slope Scree

The majority of scree slopes (eluvions, colluvions sometimes locally called groise, grouine, etc.) are due to the effects of freezing and especially the alternation of freezing and thawing. Only limestone scree can be exploited as aggregates, depending on the mechanical characteristics of the original rocks.

II. 4. SAHARA DUNE SAND

II. 4.1. Definition

A dune is defined by the Larousse dictionary as a sandy mound created by the wind on coastlines and in deserts. This sand formation is often referred to as a ‘sand pile’ shaped by wind forces [142].

II. 4.2. Availability

The world's major hot deserts are primarily located on the western coasts of continents between latitudes 15° and 30° N and S. These deserts include the Sahara Desert (over 9,064,958 square km), the Great Australian Desert, the Arabian Desert, the Iranian Desert, the Thar Desert, the Kalahari Desert, and the Namib Desert. The North American desert stretches from Mexico to the United States, known by different names such as the Mohave, Sonoran, California, and Mexican deserts. Figure II. 5 shows the distribution of deserts around the world.

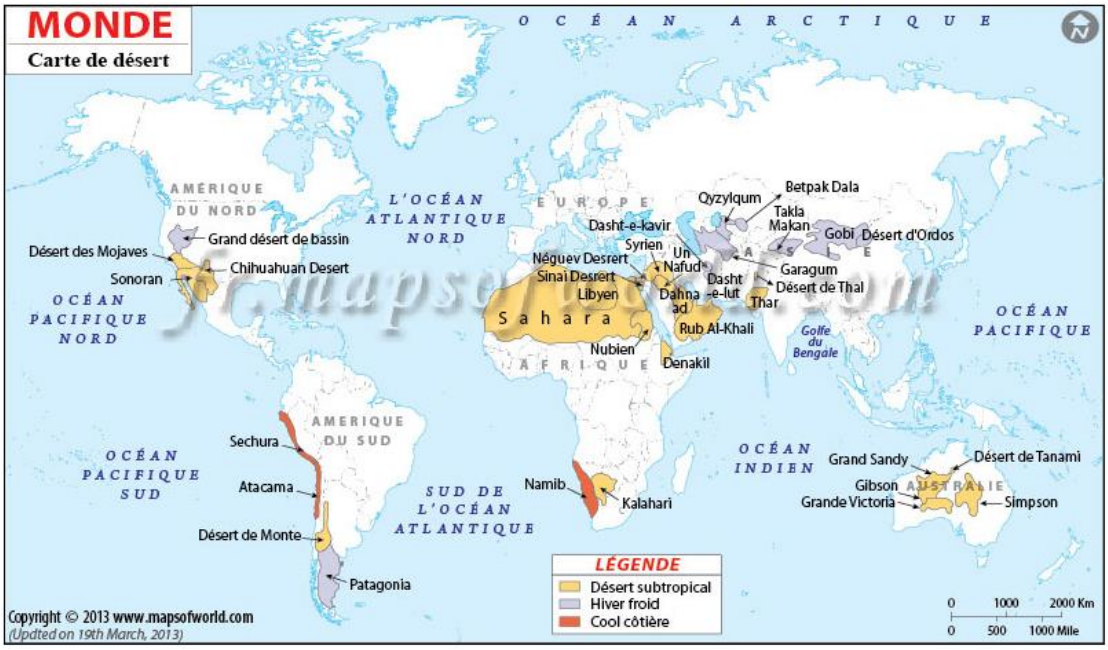

Figure II. 5 : The Desert Card [143]

II. 4.3. Dune Types

Sand dunes are mounds formed by grains of sand that are blown apart and brought together by the wind. Wind speed, turbulence and direction determine the types of dunes that form. Figure II. 6 show the different shapes of dunes created by winds.

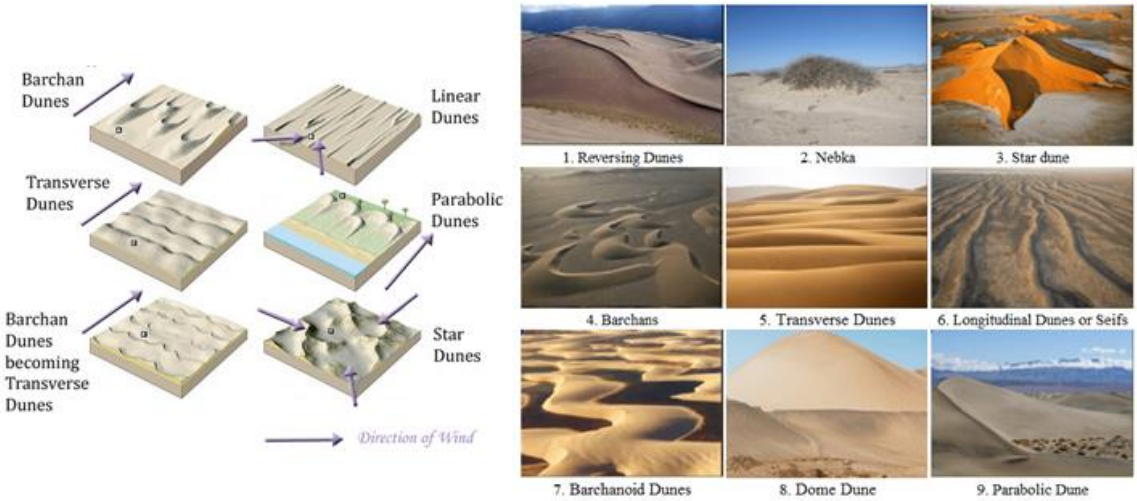

Figure II. 6 : Types of Dunes According to Wind Direction [144, 145]

The amount of sand available plays an important role in the formation of sand dunes. Dunes are generally classified according to their shapes, as highlighted by Omondi (2018) [146]. The main types of sand dunes include parabolic dunes, linear dunes and aeolian dunes.

II. 4.3.1. Reversed Dunes

These are dune wings at different heights with a parabolic shape resulting from the change in the usual wind direction, which leads to a reversal of the orientation of the dunes in relation to their initial orientation.

II. 4.3.2. Nebka Dunes

Accumulation of sand generally forming around a clump of vegetation in a desert. In the outwash beds of wadis where sand and silt are more abundant, vegetation is more vigorous, and elongated mounds called nebka in the Sahara, can rise several metres around the trunks of tamarisk trees, for example [147].

II. 4.3.3. Star Dunes (Stars)

Winds blowing in opposite directions as a result of seasonal changes or secondary wind currents give rise to this type of dune. They are the most voluminous, with a maximum height of a few hundred metres and long arms extending in several directions in the shape of a starfish, hence their name. Their arms can be several kilometres long.

II. 4.3.4. Half-Moon Dunes

Also known as ‘Barchanes’, which means ‘moving dunes’ in Turkish. When the wind blows in one direction throughout the year, crescent-shaped dunes appear, ranging in height from 1 to 50 metres and in length and width from 15 to 500 metres. The horns point in the direction of the wind.

II. 4.3.5. Transversal Dunes

They are elongated and lie perpendicular to the direction of the prevailing wind. They originate where there is an abundant source of sand and extend for several kilometres, sometimes reaching a height of several hundred metres.

II. 4.3.6. Longitudinal Dunes

Also known as “linear dunes” or “Seif dunes”. They appear when the wind blows regularly throughout the year in two different directions. They occur where the sand supply is average. They run parallel to the prevailing wind direction, creating parallel ridges of dunes. They are longer than they are wide. The ridges can be straight or slightly sinuous. They can reach 400 km in length, 600 m in width and 40 m in height.

II. 4.3.7. Barchanoid Dunes (Ridges)

Plan view of an asymmetrically wavy dune crest with parallel rows of consolidated barchans, or linked crescents. It migrates forward and is positioned transverse to the direction of the main wind. Its leeward slopes dip sharply (32–34°) and its windward slopes softly dip. Broad, inter-dune corridors usually divide barchanoid ridges. Fulje are interdune depressions found between closely spaced barchanoid ridges (Glenn 1979). Compared to the very slightly curved transverse ridges, their individual segments exhibit larger curvature (Breed and Grow 1979; Thomas 1989, p. 248 and references therein). While transverse ridges feature mostly horizontal strata, they exhibit curved strata in cross sections parallel to the crest. Two alternating... patterns are seen in Barchanoid ridges.

II. 4.3.8. Dome Dunes

They have a portion missing from the side and are shaped like an oval or circle. They are uncommon and only appear on the edges of arid deserts. At modest wind speeds, they can form. Domed dunes can change into several types of dunes. In dunes that are too tiny for barchan growth, where the horns and slide faces cannot develop, domes can also exist [148].

II. 4.3.9. Parabolic Dunes

Parabolic dunes, also known as blowout dunes, are breathtaking geological formations that can stretch up to 12 kilometers in length. These U-shaped wonders are formed when vegetation grows at the extremities of a cluster, while the central part continues to advance under the relentless force of a prevailing unidirectional wind. The unique shape of these dunes, with their tips pointing towards the direction of the wind, is a testament to the relentless power of erosion and deflation [149].

II. 4.4. Physical Characteristics

The dune sands of the Sahara Desert, particularly in the Grand Erg Oriental, exhibit distinct physical characteristics. The grain size distribution of these sands is bimodal, with modal classes in the fine sand size range 2 φ and 2.64 φ (φ is a logarithmic scale used in sedimentology to describe grain size. The phi scale is calculated as: $\varphi = -\log_2(d)$ where d is the diameter of the grain in millimeter. A smaller φ value indicates larger grain sizes, while a larger φ value indicates finer grains). The well-sorted nature of the

sands is evident from their sorting values, which are less than 0.5, indicating a high degree of sorting. The grain size distribution is positively skewed, suggesting an excess of fine grains compared to a normal distribution. Furthermore, the sands are very platykurtic, with kurtosis values indicating a high textural maturity. Finally, the dune sands are dominated by rounded and well-rounded grains, reflecting the extensive abrasion and rounding processes that have occurred during their transport and deposition [54]. The dune sand utilized in the study by Benharzallah Krobba et al. [150] was sourced from the Algerian desert, specifically in the northern region near the city of Laghouat, located 400 km south of Algiers. This sand has a fineness modulus of 0.84 and a granular size range of 0 to 0.5 mm. The grading curve for the dune sand is illustrated in Figure II. 7. Scanning Electron Microscopy (SEM) investigations reveal that the grains are predominantly rounded, although some irregular and angular grains are also present, as shown in Figure II. 8. Additionally, Energy Dispersive X-ray (EDX) analysis confirms the primarily siliceous composition of the dune sand.

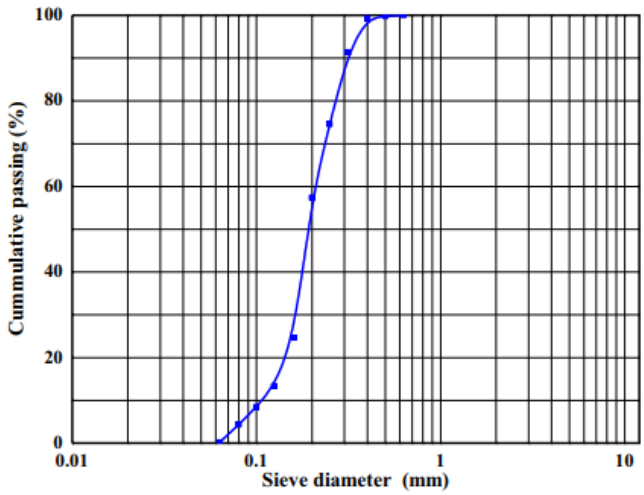

Figure II. 7 : Particle Size Distribution of Desert Dune Sand (Laghouat-Algeria) [150]

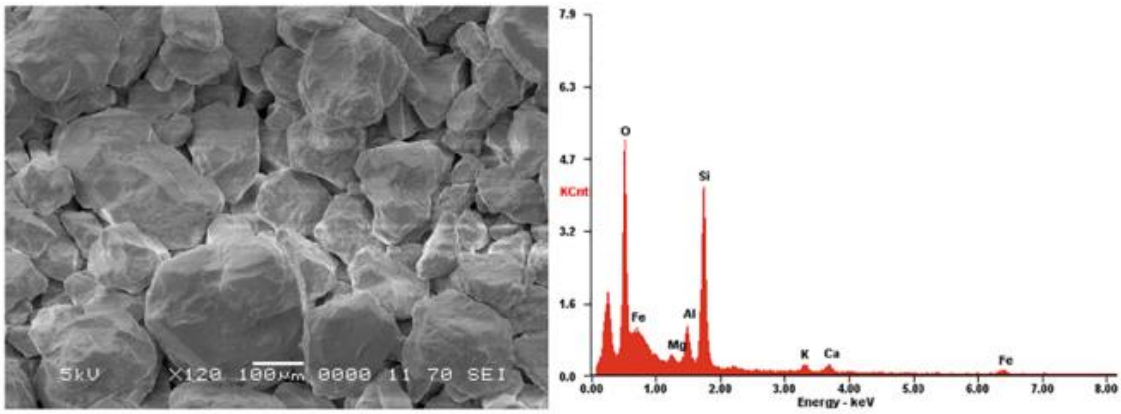

Figure II. 8 : SEM Image and EDX Analysis of the Desert Dune Sand (Laghouat-Algeria) [150]

II. 4.5. Origin of Granulometry

Strong winds, often exceeding 100 km/h, are the driving force behind the formation of desert dunes. These powerful gusts suspend the grains of sand, with the turbulent air flow strong enough to counterbalance gravity, preventing the grains from falling back to the ground. This allows the sand to be transported over vast distances. The lightest and smallest grains can be carried for thousands of kilometers, while the heaviest and largest grains remain on the beaches due to their weight. This selective transportation process results in desert dunes being composed of fine sands with grains typically ranging from 0.1 mm to 0.3 mm in size [151].

II. 5. DEMOLITION AGGREGATE

II. 5.1. Definition

Demolition aggregate (recycled) is defined by article 2 of decree n°. 84-378 of December 15, 1984 [152] as inert waste from demolition work. It does not undergo any physical, chemical or biological modification during its landfill.

II. 5.2. Description of Demolition Aggregates

Concrete demolition aggregates differ significantly from natural aggregates in their composition, consisting of two bodies of different nature: the natural aggregate and the cement mortar attached to it. This cement mortar is the primary cause of the decline in the characteristics of recycled aggregates. The water absorption coefficient of recycled aggregates is much higher than that of natural aggregates. The precise value of the water absorption of recycled aggregates depends on the parent concrete and the amount of residual mortar on the aggregates. According to Juan et al (2009) [153], the quantity of mortar varies according to the concrete crushing process and is directly related to the grain size. In addition, several studies have been carried out to define this mortar [154]. It has also been observed that the properties of the mortar are influenced by the performance of the initial concrete [155].

II. 5.3. History of Demolition Aggregate Use in Construction

The idea of waste recycling emerged immediately after World War II, with research published around the world. In 1947, a dissertation at Cornell University investigated the possibility of recycling waste, inspired by Ploger's 1946 work, read by the Russian

academic Gluthge. In Germany, in 1948, RAC used concrete produced from recycled rubble. In the mid-1970s, the introduction of CCR made concrete research a solution to problems created by environmental requirements and strict restrictions on waste disposal. Most developed countries are ahead in waste recycling, recognizing the importance and necessity of this process. New Zealand and Denmark are pioneers in this area [156, 157].

II. 5.4. Availability

In Algeria, the production of inert waste is constantly increasing due to demographic expansion and the need for new housing. Construction sites are increasing rapidly, generating large quantities of inert waste. In 2016, the annual production of inert waste represented around 11 million tonnes, mainly from the building and public works sector (construction and demolition waste). Building and public works (BTP) companies are major producers of inert waste, including concrete, bricks, tiles, concrete coated with adhesives, plaster, glass, bitumen, earth and pebbles, insulation materials, floor coverings, and so on. It is estimated that inert waste production will reach over 13 million tonnes by 2020 [158]. Figure II. 9 shows Buildings threatened with ruin and uncontrolled dumping of demolition concrete.

Figure II. 9 : Buildings Threatened With Ruin and Uncontrolled Dumping of Demolition Concrete (Course of the Revolution and Seybouse City, Annaba _ Algeria).

2012 World Bank research estimates that 1.3 billion tonnes of solid garbage are produced annually worldwide. By 2025, this volume is anticipated to rise to 2.2 billion tonnes annually. Around the world, half of the solid waste produced annually is made up of building materials [159] which represents a significant source of demolition aggregates worldwide. Table II. 2 shows global C&D waste production in 2018 [160].

Table II. 2 : Global C&D Waste Production in 2018 [160]

N°	Country	C&D Waste Generation (Million tons)
1	Hong Kong	18.12
2	India	112 to 700
3	Europe	500
4	Autralia	20.4
5	Netherlands	22
6	Italy	39
7	UK	58
8	France	65
9	Germany	86
10	United States	534
11	China	1 130

In 2012, France produced 246 million tonnes of waste from the building and public works (BTP) sector. In 2022, almost 19% of construction and public works waste will be generated in the building sector. The recovery rate for construction waste varies between 48% and 64%. ADEME ratios are used to quantify and qualify the production of waste (or demolition products) depending on the type of deconstruction operation (rehabilitation or demolition) at the building scale until 2024 and beyond. The demolition data directory recently established by Apur has identified around 16 million tonnes of construction waste from construction projects by 2030 [161, 162].

II. 5.5. Demolition Aggregates Production

Although recycled aggregates still account for only a small proportion of overall aggregates production, there has been encouraging year-on-year growth (Figure II. 10).

Figure II. 10 : Share of Recycled Aggregates in Total Aggregates Production [163]

This growth is due to regulations on the use of recycling aggregates, environmental targets set by governments and improvements in recycling techniques.

II. 5.6. Difference Between Recycling and Downcycling

Recycling involves preserving the intrinsic value of a product, allowing it to be reused in the production of the same or similar products. This process is known as sustainable material flow or loop recycling. In contrast, downcycling occurs when a recycled product loses some of its value due to its use in a lower-quality application [57]. According to recent studies, the rehabilitation of the E411/A4 highway between Daussoulx and Thorembais is being carried out on a new site, enabling the recycling of materials on site and significantly reducing CO_2 emissions [149]. The Ostin area, near Namur, has been transformed into a 5-hectare site featuring a mobile asphalt mixing plant, a mobile concrete mixing plant, and a processing center for materials resulting from the demolition of the site. Figure II .11 shows an example of recycling platform and aggregate production.

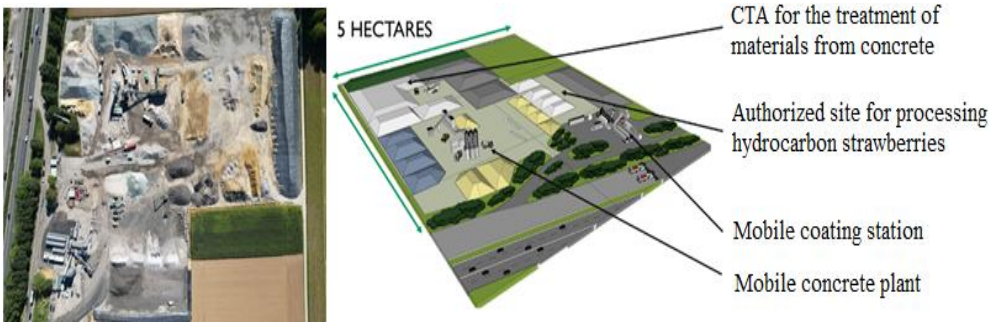

Figure II. 11 : Recycling Platform and Aggregate Production [123, 149]

II. 5.7. Manufacturing Process

Mobile equipment placed on location or in a warehouse, as well as sizable crushing plants, are two methods for producing recycled aggregates. In most cases, the recycling process must be followed through on the following stages in order to generate excellent aggregates:

- ✓ Control of Debris

It is best to stockpile debris in a deliberate manner. For instance, high-quality concrete trash (precast concrete, road concrete) is heaped up separately and given different care. Regardless, it is challenging to convert excessively contaminated concrete flows into high-quality concrete aggregates without employing a variety of cleaning methods.

- ✓ Debris Fragmentation and Pre-Screening

These steps remove sand, organic matter, and dirt that may attach to the debris and facilitate a smooth crushing operation.

- ✓ Crushing Debris

A variety of crusher types can be used to accomplish this:

- Utilising Magnetos to Disperse the Fragments
- Air Separators (Light Particle Ejection)
- By Hand Sorting
- Combined Cleaning
- Trash Being Screened and Divided into Halves.
- Aggregate Storage.
- Separating the Waste by Fraction by Screening.
- Group Storage.

Figure II. 12 presents the process flow diagram for a state-of-the-art recycling facility. The diagram illustrates the various stages involved in efficiently processing and recycling construction and demolition waste to recover valuable materials like aggregates [150].

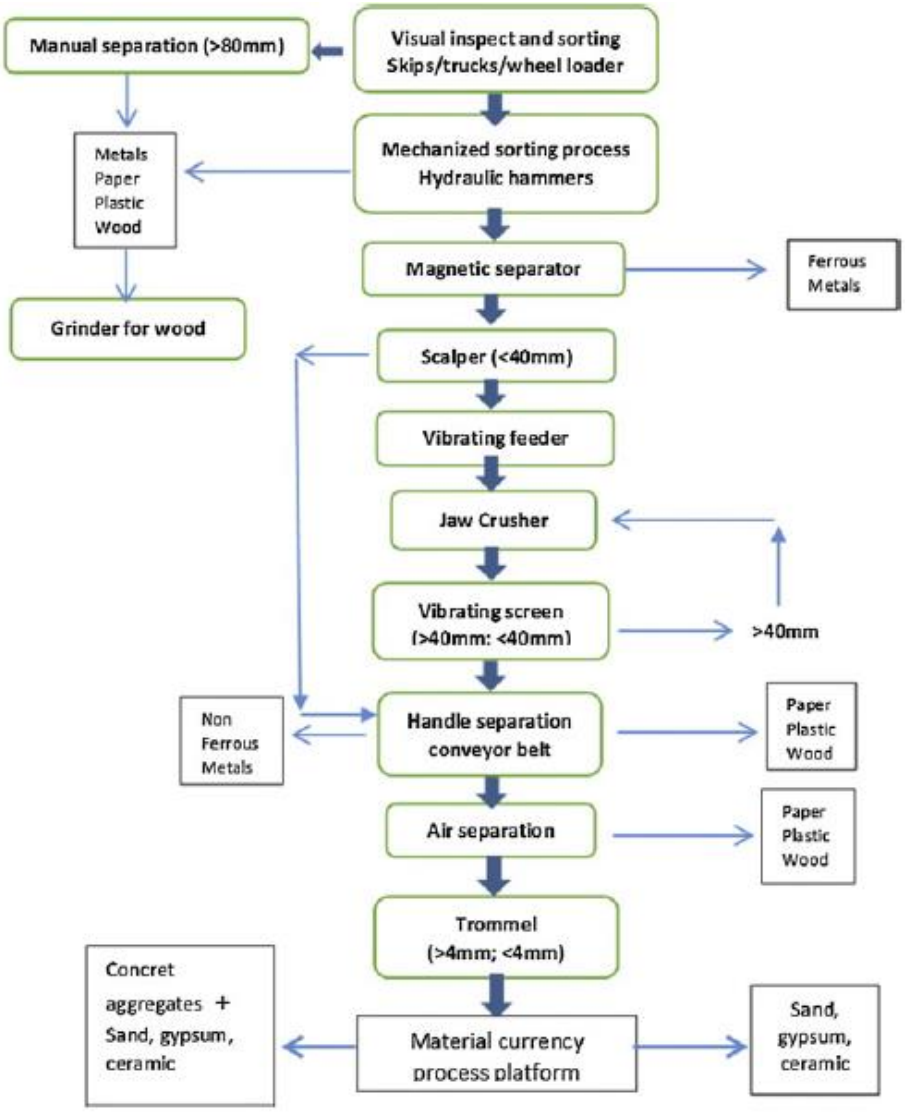

Figure II. 12 : Process Flow Diagram for a State-of-the-Art Recycling Facility [150]

Thus, a waste processing facility consists of a set of equipment or a mix of equipment that generates high-grade recycled aggregates. Generally, either mobile or stationary systems are used for the manufacturing of aggregates based on demolition and construction debris [164]. It is important to remember that mobile installations are less effective than fixed installations since their bulk is restricted to make them movable. In order to obtain granules, there are two main steps in the recycling process for building and demolition waste: crushing and screening. The goal of crushing is to reduce waste size. This step's goal is to reduce waste to particles with a certain average size. Three different types of crushers are frequently used to do this: impact crushers, jaw crushers and cone crushers [165]. Table II. 3 below lists the advantages and disadvantages of the three different crusher types

Table II. 3 : Advantages and Disadvantages of Different Types of Crushers [165]

Crusher type	Advantages	Disadvantages
Impact crusher	* Large reduction factor (relationship between incoming and outgoing particle size) * Produces aggregates with good geometry and good strength	* Produces more clean particles * Produces a wider particle size range
Jaw crusher	* Allows you to process large pieces of reinforced concrete * Produces aggregates in a narrower size range	* Produces aggregates with poor geometry and strength
Cone crusher	* Produces fewer clean particles * Produces aggregates in a narrower size range * Good compromise between the factor reduction and production of fine particles	* Produces aggregates with poor geometry and strength

II. 5.8. Classification of Demolition Aggregates

Demolition aggregates can be classified into different types based on their constituents:

- Rc: concrete, concrete products, mortar, concrete masonry units
- Ru: unbound aggregates, natural stone, aggregates treated with hydraulic binders
- Rg: glass
- Ra: bituminous materials
- Rb: baked clay elements, non-floating aerated concrete
- X: clays, soils, metals, wood, plastics, plaster

This classification system helps in identifying the composition of the recycled aggregates and ensures their proper utilization in construction projects. Figure II. 13 shows the usual distribution of demolition waste according to the nature of the materials [166].

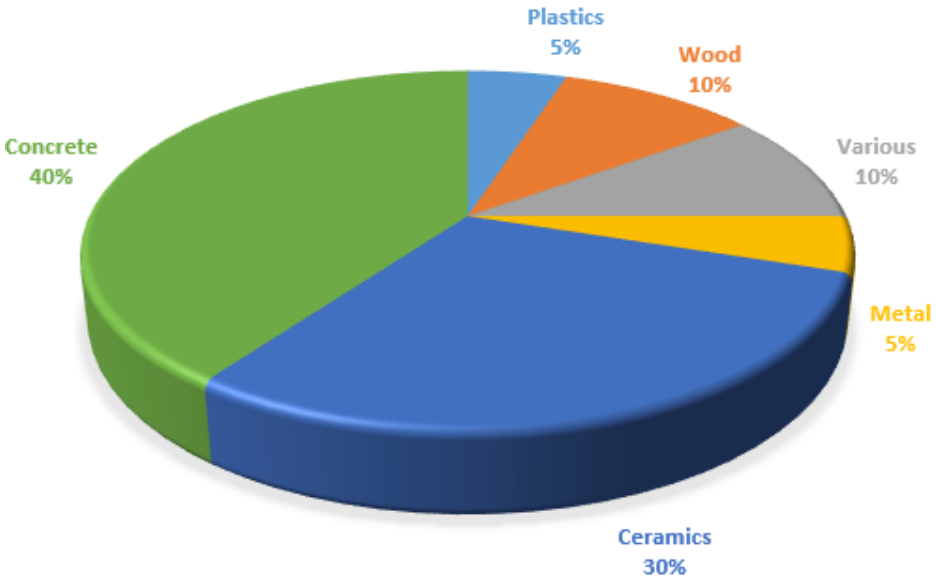

Figure II. 13 : Typical Composition of Demolition Waste

II. 5.9. Properties of Demolition Aggregates

II. 5.9.1. Mechanical Properties

- Resistance to Shock and Attrition

In general, recycled aggregates have slightly weaker mechanical characteristics than natural aggregates. The Los Angeles (LA) and Micro-Deval (MDE) coefficients are higher, which suggests lower resistance to shock and attrition. Impact resistance is decreased when mortar is present [167] (Figure II. 14).

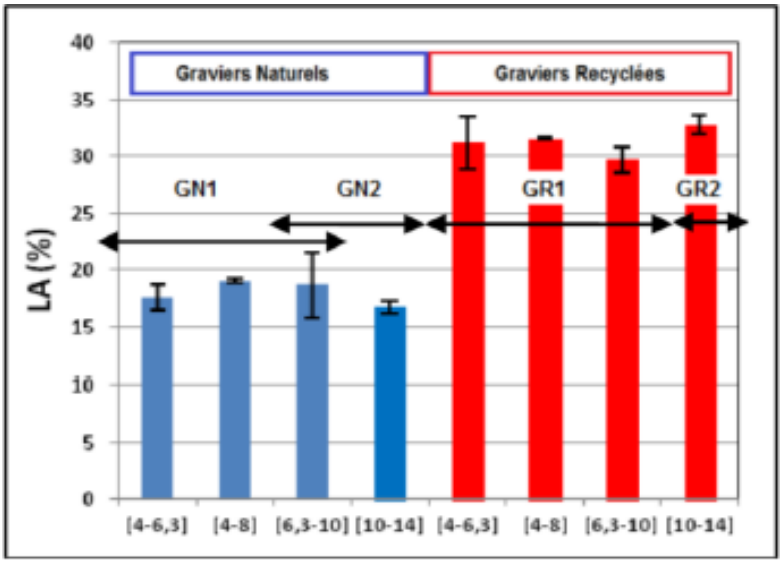

Figure II. 14 : Natural and Recycled Gravel' Los Angeles Coefficient [104]

Nevertheless, their mechanical characteristics remain acceptable for numerous uses in the field of building and public works [168].

II. 5.9.2. Physical Properties

- Density

The density of recycled aggregates is generally lower than that of natural aggregates, due to the presence of adhesive mortar. Numerous parameters, including as mortar type, grain size, water-cement ratio, and admixture addition, affect the connection between mortar content and density in a demolition aggregate:

- Type of Mortar: The type of mortar used affects the density and composition of the mortar. For instance, compared to a high-density mortar, a light mortar will have a higher density and a lower mortar content.
- Granulometry: The density and composition of mortar are influenced by the granulometry of recycled aggregates. Compared to coarser aggregates, finer aggregates are less dense and contain more mortar [168].
- Water-to-Cement Ratio: This factor influences the density and composition of mortar. Higher mortar content and reduced density are the results of increasing the water-to-cement ratio.
- Admixtures: Adding admixtures can change the density and composition of mortar. For instance, adding organic or mineral plasticizers can lower density and raise mortar content.

  Figure II. 15 shows the relationship between attached mortar content and bulk specific density.

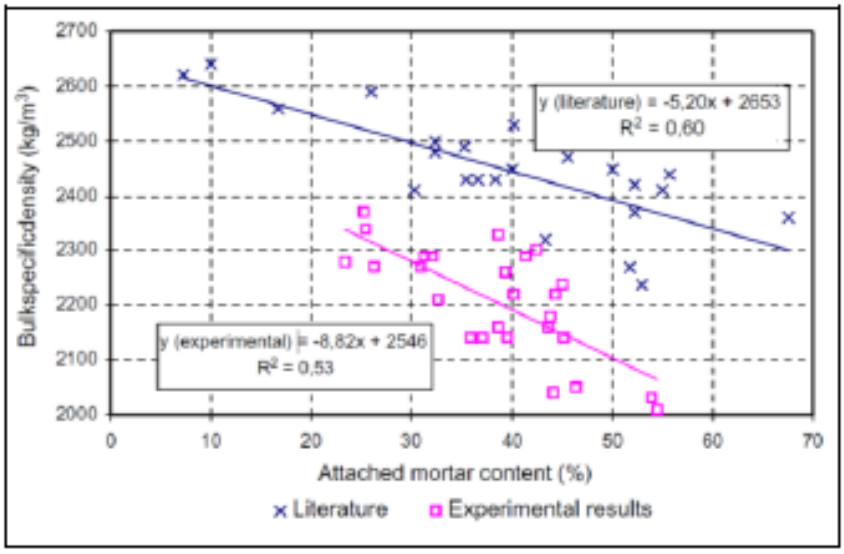

Figure II. 15 : Relationship Between Mortar Content and Density [153]

- Water Absorption

The water absorption of demolition aggregate is typically between 3 and 12%, compared to 0.5 to 3% for natural aggregates. Their granularity depends on the crushing

process used [169]. Research [153] has shown that the increase in water absorption is directly linked to the increase in the fraction of mortar attached to these aggregates. The more porous the mortar, the greater the ability of the aggregate to absorb water (Figure II. 16).

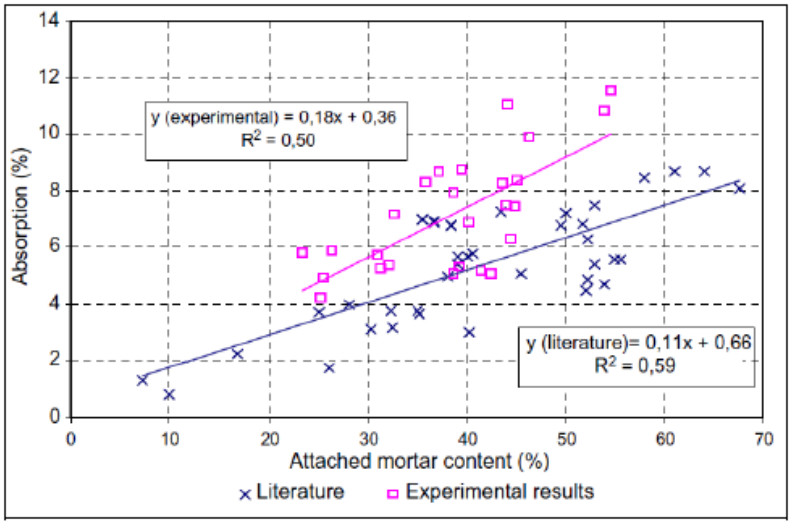

Figure II. 16 : Relationship Between Mortar Content and Demolition Aggregate Water Absorption [153]

II. 6. DEMOLITION AGGREGATE IMPROVEMENT TECHNIQUES

To enable demolition aggregates to be used without risk in the formulation of structural concretes, as a replacement for conventional aggregates, several methods and combinations of methods are used acting on one of the following three axes:

- Separation of Adherent Mortar from Natural Aggregate
- Reducing the Porosity of the Adherent Mortar
- Modification of the Hydric Status of the Demolition Aggregate

These different approaches are based on the differences in properties between conventional aggregates and the old adherent mortar, as well as on the highly porous interfacial transition zone between these two elements [170]. The following are some of the techniques used:

II. 6.1. Methods Separating the Adherent Mortar from the Natural Aggregate

Methods for separating mortar and natural aggregates are based on the differences in physical and chemical properties between these two components. They include mechanical, chemical and thermal treatments aimed at selectively weakening the mortar to facilitate its separation from the aggregates.

II. 6.1.1. Mechanical Treatment

Based on standardised Los Angeles and Micro-Deval tests [171, 172], the mechanical treatments of aggregates enable mortar-aggregate separation by shocks (impact separation method) or by abrasion (Micro-Deval test method). By removing the attached cement paste from the recycled aggregates' surface, these procedures hope to enhance the aggregates' physical characteristics and make them more compatible with the new cement paste when used to formulate concrete.

a) Impact Separation Method

It is based on the Los Angeles test, which aims to assess the strength of aggregates by fragmenting them inside a cylinder containing steel balls. The effectiveness of this method is influenced by a number of factors, including the quantity of aggregate treated, the number of balls used, the rotation speed of the cylinder and the duration of the treatment. To improve separation, it is recommended that the treatment time be increased. However, it is important to note that this method is considered to be very energy-intensive [173].

b) Abrasion Separation Method

The abrasion separation method is based on the micro-Deval test. This test involves measuring the abrasion of aggregates by placing them in a container filled with water and steel balls. The container is then rotated, which has the effect of abrading the material being tested. This method depends on the treatment time, but is less effective than impact separation. However, it does have the advantage of keeping the natural aggregates unfragmented. Separation by abrasion is an interesting technique because it preserves the integrity of the aggregates while measuring their resistance to abrasion. Although less effective than impact separation, it remains an option to be considered in certain contexts [15].

II. 6.1.2. Chemical Treatment

The chemical method for treating recycled aggregates is based on the difference in acid resistance between cement paste and natural aggregates. The process involves immersing the crushed concrete aggregates in an acid solution to dissolve the cement paste through an acid-base reaction, while preserving the aggregates. After rinsing to remove the residual acid, the aggregates treated in this way have a slightly rough surface, improving their adhesion to binders. However, the choice of acid must take

into account the nature of the natural aggregates, as limestone risks being attacked by an acid that is too strong [174]. The use of salicylic acid is therefore recommended for this type of aggregate. This chemical surface treatment cleans and prepares demolition aggregates, eliminating oxides and impurities while creating a controlled roughness that is beneficial for reuse in the production of new building materials.

II. 6.1.3. Thermal Treatment

a) High Temperature Method

The high-temperature processing method entails heating the grains to cause three phenomena that allow the separation of the natural aggregates and the spice paste [175]. These three phenomena are as follows:

- ✓ Equilibrium by Thermal Gradient: The surface temperature of the recycled concrete aggregates is high, while their core is lower, resulting in temperature differences within the recycled aggregates. These constraints lead to the cracking of the recycled concrete granules.
- ✓ Chipping by Internal Pressure: As a result of the temperature increase, the water in the recycled granules' pores takes on a gaseous shape. A portion of this water vapour, unable to escape, builds up pressure and causes internal pressures that break the cement paste.
- ✓ Loss of the Cement Paste's Mechanical Properties: At high temperatures, cement paste degrades and loses its mechanical properties, releasing natural aggregates.

b) Low Temperature Method

Low-temperature treatment of recycled aggregates is based on freeze-thaw cycles [175], which involve two main phenomena:

- ✓ Thermal Gradient Spalling:

During freezing, the aggregate surface cools faster than the core, creating internal stresses that crack the aggregate.

- ✓ Increase in Water Volume:

When the aggregate becomes solid, the water in its pores freezes and increases in volume. This volumetric expansion, confined within the pore space, generates internal stresses that degrade the cement paste. Recycled aggregates, previously saturated with water, are exposed to numerous freeze-thaw cycles. The thermal and hydric stresses induced cause the cement paste to crack and shatter, freeing the natural aggregates. This

low-temperature treatment, which is more economical and environmentally friendly than chemical or thermal methods, means that concrete aggregates can be recycled and reused in the production of new building materials.

II. 6.1.4. Microwave Treatment

Microwave treatment is considered a pre-treatment before traditional crushing. It is based on the difference in sensitivity to microwaves between cement paste and natural aggregates. Microwaves create temperature gradients in the recycled aggregates, generating stresses and micro-cracks in the cement paste. If water is present in the pores, its vaporisation under the effect of heat also generates additional stresses.

Compared with conventional heat treatment, the advantage of this method is that it degrades the natural aggregates less, thanks to the lower treatment time and temperature. However, this microwave pre-treatment is more effective on coarse recycled aggregates than on fine aggregates, making it easier to separate them from the cement paste during subsequent crushing. [175, 176].

II. 6.1.5. Ultrasonic Vibration Treatment

The ultrasonic vibration treatment relies on high-frequency sound waves propagating and interferences formed at the natural stone particles' surface and the cement paste [175]. At this transitional zone's level, the reflective surfaces create interferences that lead to constraints, fracturing the cement paste and enabling its removal (Figure II. 17). It is advised to regularly distribute the waves around the grains in order to maximise the effectiveness of this method and minimise the degradation of the natural grains. Although this approach is more efficient than traditional crushing, it still requires a significant amount of energy, and its effectiveness is heavily dependent on the granulometry of the treated grains [177].

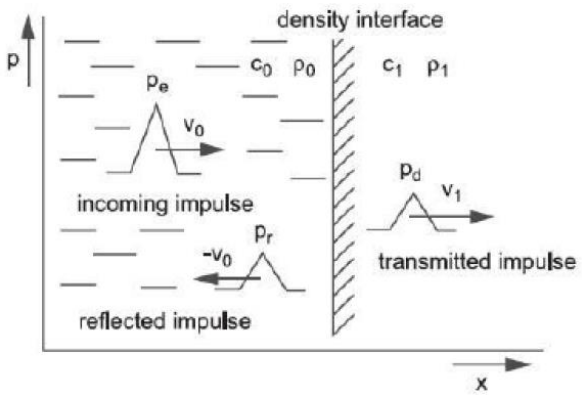

Figure II. 17 : Principle of Ultrasonic Vibration Treatment [177]

II. 6.1.6. Hydrodesmolition

The hydrodesmolition method, which uses a pressurised water jet to separate the concrete from the steel reinforcements of the reinforced concrete, is the foundation of the hydroaulic treatment (Figure II. 18). Normal range for the water jet's pressure is between 200 and 3000 bars [175]. This technique is based on two principles:

a) Effect when water under extreme pressure comes into touch with materials, a significant amount of energy is released into a small area. Significant constraints are imposed on disintegrating materials by this energy.

b) Pressure in pores :

When the treated material is porous, water under pressure seeps into the pores and causes restrictions inside it. These restrictions will cause the material to be destroyed. This treatment is dependent upon the applied pressure and the distance between the treated material and the buse. If there is too much energy to disperse, these parameters must be carefully adjusted to avoid damaging the natural aggregates.

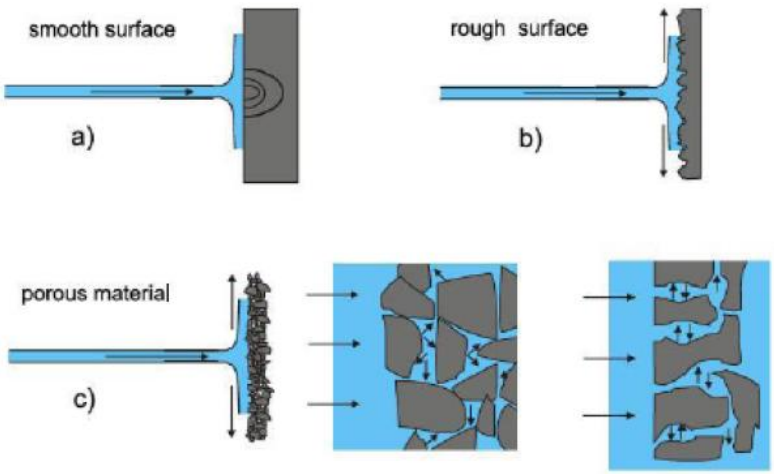

Figure II. 18 : Interaction Between Pressurised Water and the Treated Material [178]

II. 6.1.7. Electro-Fragmentation

The process of electro-fragmentation involves introducing an electrical current into a multiphasic material. As the electrical current flows through the material, it polarises the various components. Polarisation is based on the characteristics of the constituents. At the contact between natural aggregate and cement paste, an imbalance between positive and negative charges results, creating local plasma formation. This plasma creation is accompanied by a thermal dilatation that releases the natural cement paste aggregate and creates a radial wave of choc [178].

II. 6.1.8. Chemo-Mechanical Treatment

The goal of the chimio-mechanical treatment of recycled cement aggregates (RA) is to improve their properties by removing the adhesive cement paste. It combines chemical treatments with mechanical methods including fracturing and skewing.

The mechanical methods enable the granule surface cation paste to be mechanically broken down and separated. Chemical treatments, such as the use of acids, breakdown and remove this adhesive paste. This combined approach reduces the water absorption of RA by decreasing their porosity. This enhances their compatibility with the new cement paste when GR is recycled for concrete production. Although this chimio-mechanical technology is more efficient than solely mechanical methods, it is still energy-intensive and can produce pollutants, necessitating the optimisation of treatment parameters.

Abbas et al. (2008) [179] have chosen to use chemical degradation in conjunction with the exposure of recycled grains to a sodium sulphate solution and the creation of constraints that lead to a gel and decomposition action in the grains to separate the mortar from the natural aggregates. However, the main goals of this study were to quantify the mortar in order to use it in the classification of recycled aggregates. The method is not suitable for large-scale recycled aggregate manufacturing.

According to Heriberto Martinez Hernandez (2022) [180], although mechanical, chemical and thermal techniques make it possible to remove a significant amount of residual mortar from recycled aggregates, they consume a lot of energy, increasing costs and making them uneconomic on a large scale. In addition, these treatments can generate contaminants and further damage the properties of the aggregates, for example by causing them to crack. Table II. 4 shows Advantages and disadvantages of some recycled aggregates treatment methods.

Table II. 4 : Advantages and Disadvantages of Some Recycled Aggregates Treatment Methods [175]

Treatment	Ease of use	Energy consumption	Max efficiency (% mass loss)	Difficulties
Mechanical	Easy	LA: 2 kWh/ton	60	Shocks LA: aggregate damage
Ultra sound	Specific equipment for industrial use	12 kWh/ton	70	Health
High temperature	Easy, similar to cement fabrication	250 kWh/ton	20	Aggregates damage
Low temperature	Specific equipment for industrial use	-	-	Obtaining a very low temperature
Microwave	Specific equipment for industrial use	-	71	Health
Chemical	Not possible at industrial scale	No	100	Health, waste issued from treatment
Thermal-mechanical	Easy (hot)	Close to thermal	45	Aggregates damage

II. 6.2. Methods Reducing the Adherent Mortar Porosity

Studies are also being conducted on additional options, such as biocarbonation, rapid carbonation, and natural carbonation, to identify more affordable and environmentally responsible ways to raise the quality of recycled concrete aggregates.

II. 6.2.1. Carbonation

Carbonation is a complex physico-chemical reaction between carbon dioxide (CO_2), water and alkaline compounds present in a specific environment. This phenomenon occurs when humidity exceeds 70% and the environment is highly alkaline. According to the CO_2 dissolution and speciation equations, CO_2 dissolved in water is transformed into carbonate ions (CO_3^{2-}) under these conditions. These carbonate ions then interact with other ions present in the environment, such as calcium ions (Ca^{2+}) from the dissolution of alkaline compounds such as portlandite ($Ca(OH)_2$) or hydrated calcium silicates (C-S-H). Stable minerals are formed by the precipitation of carbonate and calcium ions, mainly calcium carbonate ($CaCO_3$) in various crystalline forms (calcite, aragonite, vaterite) (Figure II. 19). Natural carbonation has a significant effect on the longevity of cementitious materials, by altering their mechanical characteristics and microstructural structure.

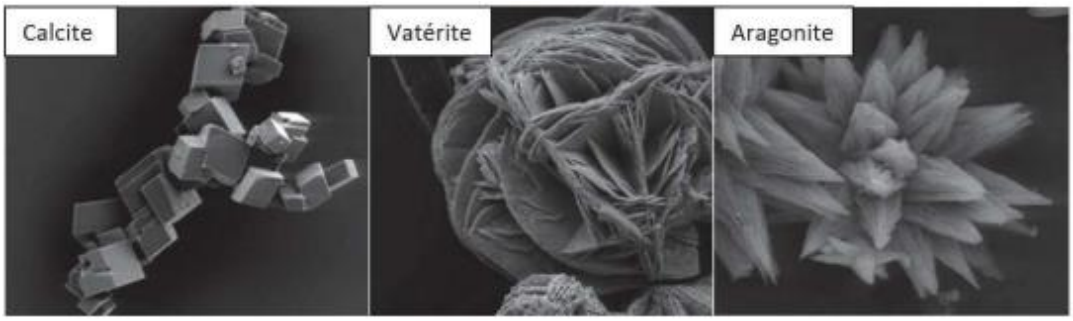

Figure II. 19 : Mainly Calcium Carbonate Crystalline Forms [180]

II. 6.2.2. Accelerated Carbonation

Concrete naturally undergoes a carbonation process during its use in construction. Accelerated carbonation treatment is possible for concrete crushed from recycled aggregates (RA) after deconstruction. This process is based on an in-depth analysis of the factors that influence the carbonation process, making it possible to calculate and assess the level of CO_2 that could be stored by these RAs. In addition to storing carbon, accelerating carbonation also reduces the porosity of aggregates. Indeed, when carbonation reactions occur, calcium carbonates ($CaCO_3$) fill the pores of the RA,

which improves their physical characteristics and makes them more suitable for reuse in new concrete. This accelerated carbonation treatment of RAs therefore has a dual benefit: on the one hand, it enables the captured CO_2 to be recovered, and on the other, it improves the characteristics of the recycled aggregates, making them easier to incorporate into the production of sustainable concrete. RAs are treated by accelerated carbonation by placing them in a hermetic enclosure to promote homogeneous diffusion of CO_2. Accelerated carbonation of RA is caused by the transfer of CO_2 across their surface, over a period ranging from 1 hour to 7 days for exposure to 100% CO_2 (Figure II. 20). The efficacy of this method has been demonstrated in the literature [181–184]. However, most tests are carried out in laboratory conditions, and further studies are essential to improve the carbonation parameters and assess the long-term effect on the performance of recycled concrete.

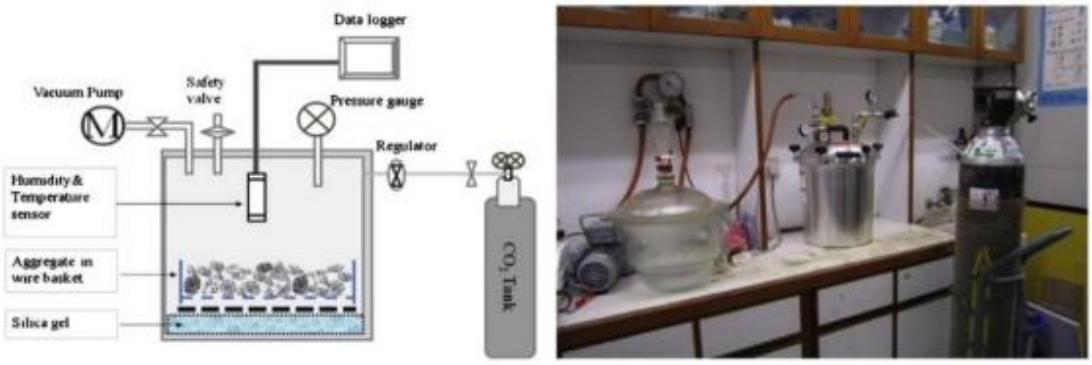

Figure II. 20 : Accelerated Carbonation Device in the Laboratory – Treatment of Recycled Aggregates by Accelerated Carbonation [29]

II. 6.2.3. Bacterial Precipitation (Biocarbonation)

The precipitation of calcium carbonates is a mechanism frequently encountered in the living world, used by many organisms to form their skeleton. This phenomenon is not specific to multicellular organisms, as unicellular organisms such as Coccolithophoridae can also precipitate carbonates to form a protective layer around their cells. The most remarkable formations are stromatolites, dating back 3.5 billion years and responsible for trapping CO_2 in the primitive atmosphere. This natural process of carbonate precipitation under the action of prokaryotic microorganisms is still present today and is the subject of studies for innovative applications, such as the surface treatment of recycled concrete aggregates [180]. The surface treatment of recycled concrete aggregates by bio-precipitation, studied by Heriberto Martinez Hernandez in 2022 [180], involves forming a layer of $CaCO_3$ around the aggregates

over a period of a few days, thereby limiting their water absorption. Non-pathogenic bacteria capable of producing $CaCO_3$ have been identified, selected and adapted to the alkaline environment of the aggregates. The optimum conditions for homogeneous bacterial growth and uniform production of $CaCO_3$ on the surface were determined. The processes developed, applied to mortar discs, confirmed a significant reduction in water absorption after just one month, thanks to the essential homogeneity of this surface treatment. Figure II. 21 shows the precipitation of $CaCO_3$ in the pores and microcracks of recycled gravel, before and after to be treated by bioprecipitation [180].

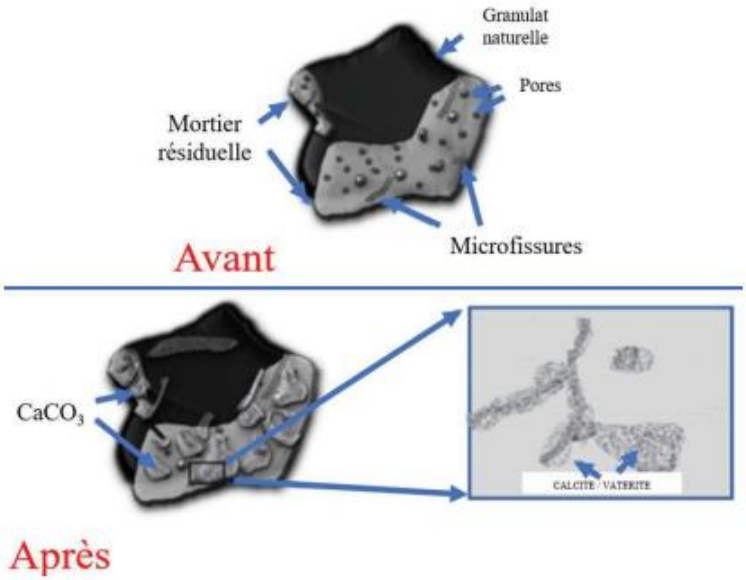

Figure II. 21 : Precipitation of CaCO3 in the Pores and Microcracks of Recycled Gravel, Before and After to be Treated by Bioprecipitation [180]

II. 6.2.4. Changing the Surface Condition (Coating of Recycled Aggregates)

Compared to natural aggregates, recycled aggregates (RA) have a lower quality due to increased porosity and a rougher surface. This can affect their ability to bind cement and provide the concrete with a robust structure [185].

Several surface treatment techniques have been developed to improve the quality of RA. Coating is one of the effective methods. It consists of covering the RA grains with a thin layer of material (such as cement, mineral powders or polymers) leading to the improvement of their surface condition and mitigating the negative effects of the RA characteristics [34, 185–188].

Figure II. 22 shows the device intended for the encapsulation of the recycled aggregate with cement. It is a 45 cm diameter laboratory granulator with a rotating drum.

Figure II. 22 : Rotary Drum Laboratory Granulator for Cement Encapsulation of Recycled Aggregates [189]

II. 6.3. Methods Modifying the Demolition Aggregate Hydric Status

Changing the hydric status of the demolition aggregate can help to better control its interaction with the cement paste. This change is achieved by:

II. 6.3.1. Pre-Wetting

Pre-wetting recycled aggregates with water is a process which consists of humidifying recycled aggregates before their use in the manufacture of concrete. This helps reduce excessive water absorption by recycled aggregates, which can affect the rheological behaviour of fresh concrete and its long-term durability [190, 191].

II. 6.3.2. Pre-Saturation

Pre-saturation of recycled aggregates consists of pre-wetting them for a minimum period of 24 hours, which makes it possible to reach a point of water saturation beyond which water absorption is so low that it can be considered negligible [28, 192].

II. 7. CONCRETE

II. 7.1. Definition

Concrete is a common building material that has transformed civil engineering and modern architecture. It is made up of coarse and fine aggregates (gravel and sand), cement, water, and occasionally additives. After it dries, concrete may take on intricate shapes because it is so easy to work with when it is raw. Although it has a good

compressive strength, steel, cables, or fibres must be used for reinforcing because it is weak in tension. The high volumetric mass of the material can be decreased by utilising light aggregates, which account for around 80% of the total volume.

II. 7.2. Concrete Importance

Construction materials such as concrete are essential; they are used to build three-quarters of single-family homes and more than 90% of multi-family homes. Based on the most recent data from the French Union of the cement industry (FUCI), concrete continues to dominate the building industry. More and more French people are concerned about their home's thermal comfort, isolation, and fire resistance. Concrete construction provides an excellent solution to these concerns. In fact, concrete is a strong and durable material that may be used to create long-lasting structures [193].

Many people choose concrete for building projects due to its sturdy and resilient properties, enabling the completion of long-lasting structures. Concrete's resistance makes it suitable for large-scale works, and cementitious concrete walls are stronger yet lighter. For even greater resistance, armored concrete walls with a metal armature can be used, providing both strength and stability.

In addition to its structural benefits, concrete also has good thermal capacities, allowing for proper insulation and humidity control, resulting in improved comfort within the building [194].

II. 7.3. Ordinary Concrete Constituents

Concrete is a composite material composed of various key ingredients (constituents) that combine to form a strong and adaptable building material [195]. The principal constituents consist of:

II. 7.3.1. Cement

The binding agent, typically Portland cement, which undergoes a chemical reaction with water to harden and set, providing the concrete with its cohesive properties [196].

II. 7.3.2. Fine Aggregate (Sand)

Fine aggregate, also known as sand, is a type of aggregate material that is typically composed of small particles ranging in size from 0 mm to 6.3 mm [138]. It is used in concrete mixtures to provide a smooth surface and improve workability.

II. 7.3.3. Coarse Aggregate (Gravel)

Coarse aggregate, also known as gravel, is a type of aggregate material that is typically composed of larger particles ranging in size from 1 to 125 mm or larger [138]. It is used in concrete mixtures to provide strength and stability.

II. 7.3.4. Mixing Water

Mixing water is the water used to mix with the cement and aggregate to form a concrete mixture. It is essential for the chemical reaction between the cement and water, which hardens the concrete over time [197].

II. 7.3.5. Plasticizer

A plasticizer is an additive used in concrete mixtures to improve workability and reduce the amount of water needed. It helps to create a more fluid mixture that is easier to pour and shape [198].

II. 7.4. Ordinary Concrete Formulation Methods

The different techniques used to figure out how much cement, water, aggregates, and other admixtures to put in a concrete mixture to get the right qualities are referred to as concrete formulation methods. The methods for calculating concrete composition are numerous, and no single method is universally recognized as the best [195]. Historically, the principles governing concrete formulation began to be rationalized in the late 19th century. The composition of concrete typically results from a compromise among various often conflicting requirements. A concrete formulation can be deemed satisfactory if it meets several key criteria: it must exhibit adequate compressive strength after curing, allow for easy workability during application with standard construction methods, demonstrate minimal shrinkage and low creep, and maintain cost-effectiveness. Several typical techniques for formulating concrete have emerged over time, each addressing these criteria in different ways. These methods reflect the evolving understanding of material properties and the practical needs of construction, ensuring that concrete can perform effectively in a variety of applications while balancing performance and economic considerations.

II. 7.4.1. Féret Method

In 1892, Féret [199] conducted pioneering research on concrete formulation, focusing on the principle of optimal compactness. Initially, he determined the compactness of a ternary sand mix before incorporating a cement matrix. However, this method produced mortar with a discontinuous grain size distribution and did not yield the most compact material in its hardened state. Through equation (II. 1), Féret established a relationship between compressive strength and volumetric proportions, particularly using the volumetric ratio of cement to aggregate (E/C).

$$\boldsymbol{fc = K_{Féret} + \left(\frac{1}{(1+(e+v)/c}\right)} \qquad \textit{II. 1}$$

II. 7.4.2. Fuller and Thompson Method

In 1907, Fuller and Thompson proposed a method based on achieving maximum compactness through a continuous grading of aggregates. Their innovative approach incorporated not only the cement but also the extreme dimensions of the grains, specifically the smallest (d) and largest (D) sizes, as outlined in formula (II. 2). However, it is important to note that the shape of the grains was not considered in their method. This foundational work laid the groundwork for subsequent developments in concrete formulation techniques, emphasizing the importance of grain size distribution and material properties in achieving optimal concrete performance.

$$P_{Fuller\ T\ bom\ pson} = 100 \text{ x } \sqrt[5]{d/_D} \qquad \textit{II. 2}$$

II. 7.4.3. Abrams' Method

In 1918, Abrams [199] empirically defined a method where the cement dosage and the maximum aggregate size are the primary parameters influencing concrete composition (formula II. 3). He introduced the Abrams coefficient (an improved version of the Féret coefficient) to account for the nature and shape of the aggregates.

$$fc = K_{Abrams} \text{ x} \left(\frac{1}{7.5^{(1.5E/C)}}\right) \qquad \textit{II. 3}$$

II. 7.4.4. Bolomey Method

In 1925, Bolomey [195] proposed a continuous grading curve that includes cement and is described by the following formula (II. 4).

$$P_{Bolomey} = A_{Bolomey} + (100 - A_{Bolomey}) \text{ x} \sqrt{d/D} \qquad \text{II. 4}$$

The distinction from the Fuller and Thompson equation lies in the term $A\ Bolomey$, which depends on both the shape of the aggregates and the consistency of the concrete. Bolomey's equation for compressive strength, expressed in equation (II. 5), serves as a variant of Féret's law.

$$fc = K_{Bolomey} + \left(\frac{C}{E+V} - 0.5\right) \qquad \text{II. 5}$$

II. 7.4.5. Caquot Method

In 1937, Caquot [195] expanded the search for maximum compactness to an infinite number of granular classes, based on the void index curve of a mixture of two aggregates of different sizes. He experimentally defined a relationship predicated on the principle that the volume of voids primarily depends on the diameters d (smallest dimension) and D (largest dimension) (formula II. 6). This led to the concept of infinite optimal grading. However, in practice, grain dimensions are limited, necessitating adjustments to the proportions of the smallest and largest aggregates. Additionally, he introduced the wall effect caused by larger aggregates, further influencing the overall concrete composition.

$$V = V_0 \text{ x } \sqrt[5]{d/D} \qquad \text{II. 6}$$

II. 7.4.6. Faury Method

In 1944, J. Faury [195] proposed a new continuous grading law for concrete formulation following a comprehensive study of concrete properties. He drew inspiration from Caquot's theory regarding the compactness of uniformly sized aggregates corresponding to an average packing density. Faury utilized a horizontal axis scaled in $\sqrt[5]{D}$ to achieve a linear curvature and established a breakpoint to differentiate between fine and coarse aggregates. This breakpoint is defined at D/2, with the corresponding ordinate value Y calculated using the following formula (II. 7):

$$Y = A + 17\sqrt[5]{D} + \frac{B}{\frac{R}{D} - 0.75} \qquad \text{II. 7}$$

where B represents a constant reflecting the significance of concrete packing, varying between 1 and 1.5; R is the mean radius of the mold calculated as R=Surface/Perimeter; and A is a constant indicating the workability of the concrete. The ratio R/D accounts for the wall effect caused by larger aggregates.

II. 7.4.7. Joisel Method

In 1952, Joisel [195] expanded upon the work of Caquot and Bolomey, introducing a more generalized method. He posited that the grading law leading to maximum compactness is a function of $\sqrt[m]{D}$, where m varies according to the packing density of uniformly sized aggregates, ranging from 3 to 10. Joisel employed a linear reference curve, $\sqrt[m]{D}$, for the horizontal axis and established a reference line that considers cement, water, voids, grain size, and the compactness of granular classes.

II. 7.4.8. Dreux – Gorisse Method

By 1970, Dreux and Gorisse [195] implemented a method based on granular optimization that remains widely used for ordinary concrete. This empirical approach utilizes a reference grading curve comprising two straight segments in a semi-logarithmic diagram. Unlike Faury's method, cement is excluded from the reference curve; its mass C is determined separately. This comprehensive method accounts for numerous parameters (equation II. 8), including the geometry of the cast piece, the type and dosage of cement, the fineness, shape, quality, and dimensions of aggregates, as well as the consistency and strength of the concrete.

$$\boldsymbol{f_{cm} = G_{Dreux} \text{ x } \sigma_c \left(\frac{C}{E} - 0.5\right)} \qquad \textit{II. 8}$$

II. 7.4.9. Baron et Lesage Method

In 1976, Baron and Lesage [200] introduced a technique for optimizing the granular skeleton of concrete using a workability meter. This method involves determining the proportions of inert solid constituents that yield the fastest flow in the workability meter through successive approximations. After establishing these proportions, the water dosage is adjusted until the desired flow is achieved.

II. 7.4.10. Scramtaiev Method

The Scramtaiev [201] method is a concrete mix design approach that emphasizes finding the optimal cement content and water-cement ratio to meet a specified compressive strength. This method takes into account the characteristics of both the cement and aggregates used, as well as the desired workability of the concrete [202, 203]. It is based on the principle that heavily compacted concrete, when in its fresh state, approaches absolute density. This means that the total absolute volume of the constituent materials in one cubic meter equals the volume of the compacted concrete

mix [201, 204]. Initially, the composition of the concrete is determined through approximate calculations, which is then refined using experimental mixing trials to optimize the concrete formulation. The following formulas (II. 9-12) are utilised to determine the proportions of the constituent materials in the concrete mix:

$$\boldsymbol{W}\left(\frac{kg}{m^3}\right) = \frac{W}{C} \text{ x } \boldsymbol{C} \qquad \textit{II. 9}$$

$$\boldsymbol{S}\left(\frac{kg}{m^3}\right) = \left[\mathbf{1000} - \left(\frac{C}{\rho_C} + \frac{W}{\rho_W} + \frac{CS(Gr)}{\rho_{CS(Gr)}}\right)\right] \text{ x } \boldsymbol{\rho_s} \qquad \textit{II. 10}$$

$$\boldsymbol{CS(Gr)}\left(\frac{kg}{m^3}\right) = \frac{\mathbf{1000}}{V_{cav\ CS(Gr)} \text{ x } \left(\frac{\alpha}{\gamma_{vol(Gr)}} + \frac{1}{\rho_{CS(Gr)}}\right)} \qquad \textit{II. 11}$$

$$\boldsymbol{V_{cav\ CS(Gr)}} = \mathbf{1} - \frac{\alpha}{\gamma} \qquad \textit{II. 12}$$

Where:

- S is the sand content (kg/m³)
- W is the water content (kg/m³)
- C is the cement content (kg/m³)
- CS (Gr) is the crushed stone or gravel content (kg/m³)
- $V_{cav\ CS\ (Gr)}$ is the porosity of the crushed stone or gravel in loose state (substituted in the formula as a relative value)
- α is the coefficient of spacing of crushed stone particles (or excess mortar) (assumed to be 1.05 to 1.10 for dry mixes and 1.2 to 1.4 or more for fluid mixes) (Table II. 5)
- $\gamma_{vol\ CS(Gr)}$ is the bulk density of the crushed stone or gravel (kg/L)
- ρ_S, ρ_C, ρ_W and $\rho_{CS(Gr)}$ are the specific gravities (kg/m³) of sand, cement, water and crushed stone or gravel respectively (kg/L)
- W/C is the water-cement ratio

Table II. 5 : α Values as a Function of W/C

α values as a function of W/C						Quantity of cement (kg/m³)
0.8	0.7	0.6	0.5	0.4	0.3	
1.3	1.32	1.26	-	-	-	250
-	1.42	1.38	1.30	-	-	300
-	-	1.44	1.38	1.32	-	350
-	-	-	1.46	1.40	1.31	400
-	-	-	1.56	1.52	1.44	500

-	-	-	-	1.56	1.52	600

II. 8. CONCRETE BASED ON DEMOLITION AGGREGATES

We can identify concrete in two phases, the first in the fresh state and the second hardened, and therefore distinguish the types of properties according to the two states of the concrete.

II. 8.1. Fresh State Properties

When the concrete has not yet completed its curing and hardening processes, it is considered fresh. During the mixing process, water is the element that will allow the compact skeleton formed by the insertion of solid grains to flow freely. This means that water will eventually disperse the compact skeleton to allow the grains to move sufficiently to enable the desired implementation.

II. 8.1.1. Workability

Suitability for employment is also known as mixture consistency or workability. The simplicity with which the concrete may be applied to ensure proper formwork filling and reinforcing coating is known as workability, according to Dreux and Festa (1998) [205]. It describes the concrete's fluidity prior to the material hardening.

Several studies have shown that, for the same water content, the workability of concrete made with recycled aggregates is lower than that of standard concrete. This inferiority is particularly noticeable when the percentage of substitution exceeds 50% [206]. The difference between the workability of concrete made from recycled aggregates and natural aggregates is attributed to the greater porosity of the former. To improve this situation, studies were carried out to vary the conditions under which the aggregates were prepared. The results showed that adding water corresponding to the water absorption of the aggregates tested significantly improves the workability of fresh concrete [207].

Numerous factors affect workability, including the type and amount of cement used, the aggregates' shape, the amount of water used, and the usage of adjuvants. Slump test with Abrams’s cone makes it simple to measure. The slump of concrete containing recycled aggregates should be lower than that of conventional concrete due to the higher water absorption capacity of recycled aggregates compared to natural aggregates. The

surface texture and angularity of recycled aggregates significantly influence the workability of the concrete [208].

Numerous studies have reported reduced workability in concrete with recycled aggregates, necessitating the addition of extra water to achieve desired consistency [209–211].

To address the increased water absorption of recycled aggregates, various methods have been tested to improve workability. For instance, Poon et al. [212] explored several pre-wetting techniques for recycled aggregates before mixing them into the concrete. Their findings indicated that the loss of slump is closely related to the moisture condition of the recycled aggregates. Figure II. 23 illustrates the variations in slump for concrete mixtures containing different types of aggregates, highlighting the importance of managing the moisture content to optimise workability.

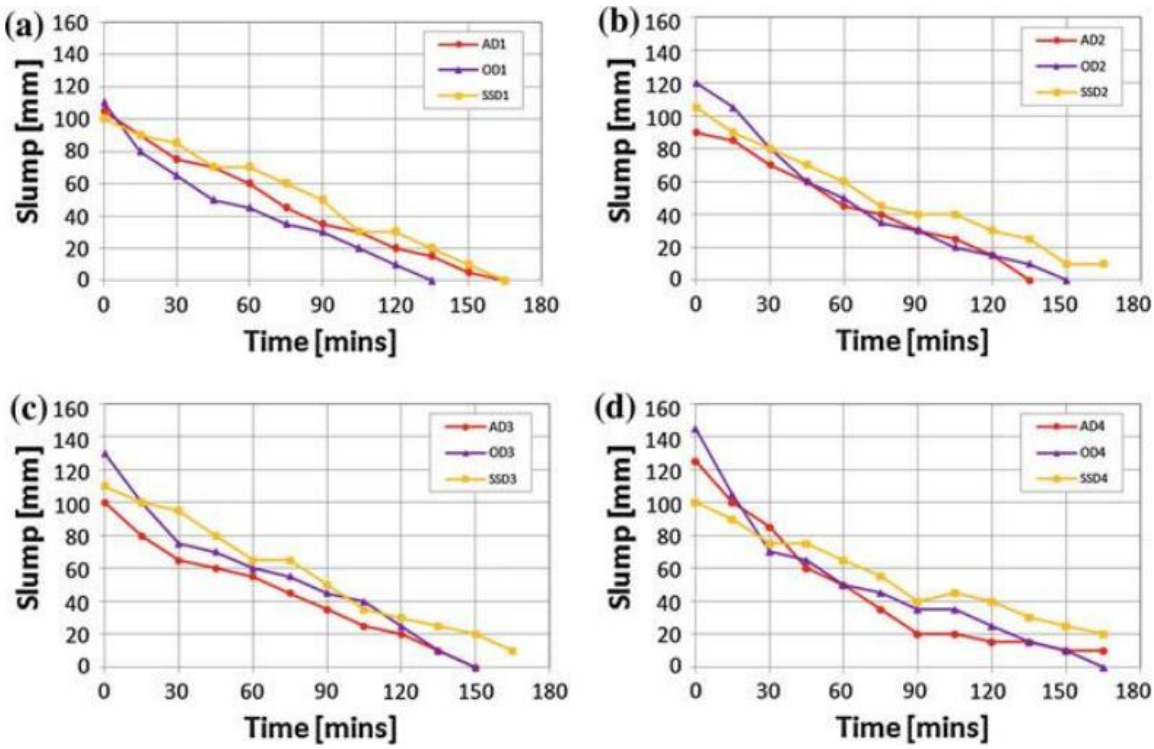

Figure II. 23 : Variation of Slump of Concretes Containing Different Types of Aggregates: a)- 100% Crushed Granite, b)- 80% Crushed Granite + 20% Recycled Aggregates, c)- 50% Recycled Granite + 50% Recycled Aggregates, d)- 100% Recycled Aggregates [212]

II. 8.1.2. Density

The density of fresh concrete containing recycled aggregates is slightly lower than that of a mixture containing natural aggregates, as the density of recycled aggregates is

lower than that of natural aggregates. The presence of residual cement mortar attached to the aggregate is the main factor contributing to the decrease in density. Katz [213] observed no significant difference in the density of concretes containing RCA prepared from old concrete of three different ages (1, 7, and 28 days), suggesting that the amount of adhered mortar in the different concrete aggregates was similar regardless of their crushing age. Soutsos et al. [214] observed a slightly lower fresh density in concrete containing RCA compared to concrete containing limestone aggregate due to volumetric substitution rather than on a weight basis of the aggregate. They reported that variations in RCA properties have little effect on the resulting concrete density. They observed a reduction of approximately 5% in the density of the concrete mix when all-natural aggregate was replaced by RCA. The reported values are generally between 2000 and 2200 kg/m^3 [28].

II. 8.1.3. Occluded Air

The entrained air content does not seem to differ significantly compared to conventional concrete. The shape and roughness of recycled aggregates can make it more difficult to extract air bubbles from the concrete during vibration. Some authors have observed slightly higher levels of entrapped air, on average, in concrete made with recycled aggregates, with a difference of around 0.6% compared with conventional concrete [215, 216]. Figure II. 24 shows Influence of recycled gravel rates and cement types on the air content of concrete.

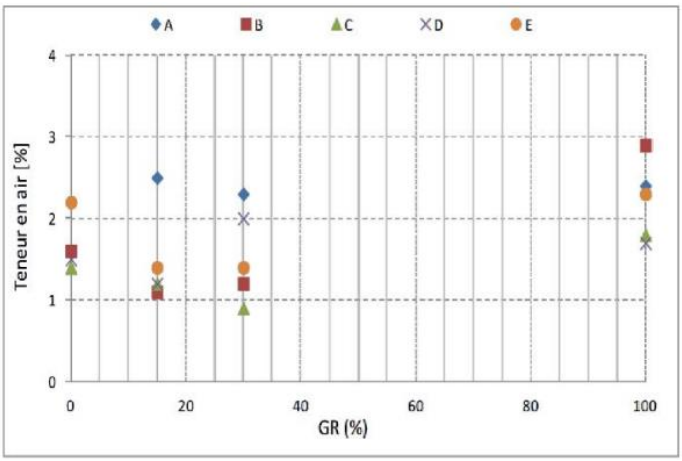

A : CEM I 52.5 R CE CP 2 ; B : CEM I 52.5 R CE ; C : CEM I 52.5 N CE CP 2 ; D : CEM I 52.5 N SR 3 CE PM CP2 ; E : CEM I 52.5 N CE ES CP2.

Figure II. 24 : Influence of Recycled Gravel Rates and Cement Types on the Air Content of Concrete [28]

The greater porosity of recycled aggregates compared to natural aggregates is responsible for the slight increase in the percentage of air trapped in recycled concrete. Indeed, with a substitution rate of 100%, the percentage of occluded air is slightly higher, varying from 4 to 5% [167]. Figure II. 25 shows the percentage of air occluded as a function of the substitution rate.

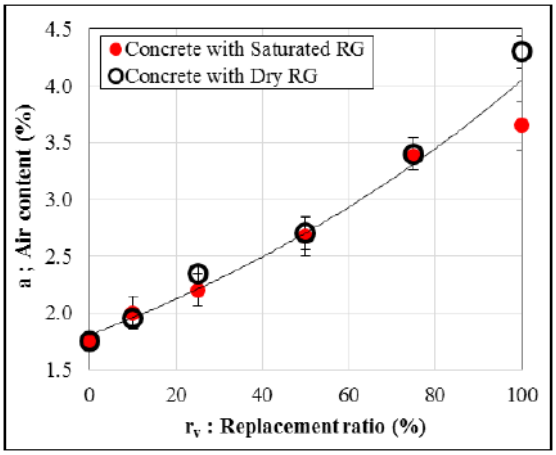

Figure II. 25 : Percentage of Air Occluded as a Function of the Substitution Rate [167]

II. 8.2. Hardened State Properties

Concrete is considered hardened when it has developed sufficient strength and stability to support loads and resist deformation. This typically occurs after a curing period, which can vary based on factors such as cement type, environmental conditions, and additives. While concrete reaches its initial set within hours, it is commonly regarded as "hardened" after 28 days of curing, achieving about 70-90% of its ultimate compressive strength. For practical purposes, concrete can be deemed hardened when it can withstand handling without significant deformation, usually a few hours after placement, though full structural capabilities are confirmed through longer-term testing.

II. 8.2.1. Density

When analysing the results of compression tests, knowing the specimens' mass is a useful indicator. In fact, we can infer a variable density of the concrete tested if the weighing results are widely scattered, which will cause the results of the compression tests to be scattered. Following demolding, it appears that the effects of temperature changes during specimen storage are more closely related to humidity levels.

According to Thomas J. et al. [217], Pedro and de Brito [218] highlighted the challenges associated with the loss of workability and the decrease in density of concrete when natural aggregates are substituted with recycled concrete aggregates (RCA). McNeil and Kang [219] noted that the density of RCA is lower than that of natural aggregates due to the presence of adhered mortar on the recycled aggregates, leading to a corresponding reduction in the density of RCA concrete compared to the control mix. Furthermore, Rao et al. [220] established a linear relationship between the compressive strength and density of RCA concrete, indicating that as density decreases, compressive strength may also be affected.

II. 8.2.2. Mechanical Properties

The mechanical properties of recycled concrete aggregate (RCA) concrete, including compressive strength, splitting tensile strength, flexural strength, and modulus of elasticity, tend to decrease as the replacement level of natural aggregates increases [221–227]. However, these properties can be enhanced by carefully selecting the recycled aggregates prior to concrete production [222–225, 227, 228]. Verma and Ashish [229] found that while compressive and flexural strengths improved slightly at lower replacement levels, significant deterioration occurred when more than 50% of natural aggregates were replaced. Hamad and Dawi [230] reported an average reduction of 10% in mechanical properties for concrete made with RCA derived from both normal and high-strength concrete. Saha and Rajasekaran [231] observed substantial decreases in compressive, splitting tensile, and flexural strengths with the addition of RCA. Conversely, Tabsh and Abdelfatah [232] indicated that high-grade RCA concrete (around 50 MPa) maintained strength despite aggregate replacement, while ordinary concrete exhibited significant strength loss. Exteberria et al. [233] noted that concrete with 100% RCA had a 20–25% lower 28-day strength compared to conventional mixes, although medium-strength concrete with 25% RCA showed no adverse effects on mechanical properties when maintaining consistent cement content and effective water-cement ratios. Rahal [234] found only a 3% reduction in the modulus of elasticity for RCA-containing concrete, while Limbachiya et al. [235] reported that the flexural strength and modulus of elasticity of RCA concrete were comparable to those of natural aggregate concrete. Figure II. 26 illustrates the compressive strength of recycled

concrete in comparison to conventional concrete, as presented in the study by González-Fonteboa et al. [236].

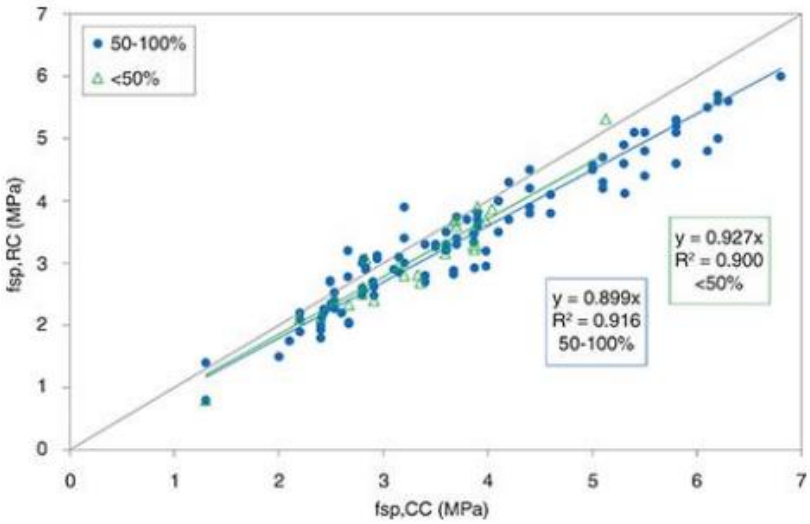

Figure II. 26 : Compressive Strength of Recycled Concrete Compared to Conventional Concrete [236]

Several studies have reported that the splitting tensile strength of recycled aggregate concrete is significantly enhanced when curing durations are extended. In some cases, the tensile strength of concrete with recycled aggregates even exceeds that of conventional concrete. Kou et al. (2008) [237] noted that the improvement in the microstructure of the interfacial transition zone (ITZ) and the resulting increase in the bond strength between the new cement paste and the old aggregates could be a contributing factor to the observed enhancement in splitting tensile strength. Notably, improvements have been observed in recycled aggregate concrete after five years of curing, with tensile strengths sometimes surpassing those of natural aggregate concrete [237] (See Figure II. 27).

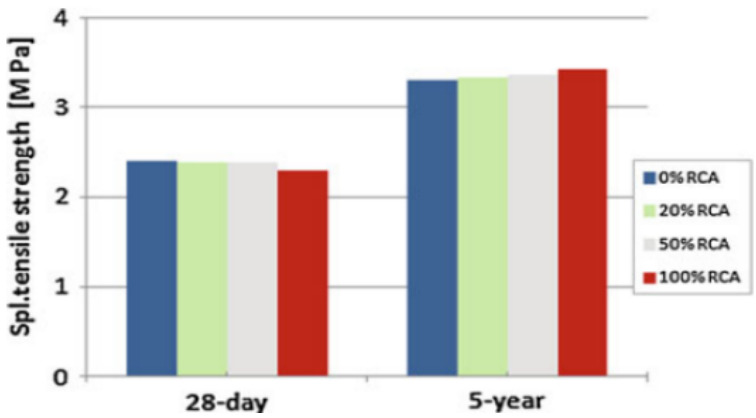

Figure II. 27 : Evolution of Tensile Strength by Splitting, Over Time, as a Function of the Replacement Rates of Recycled Aggregates [237]

II. 8.2.3. Ultrasonic Pulse Velocity

The ultrasonic pulse velocity (UPV) method has been successfully employed for over 60 years to assess concrete quality. This technique determines the homogeneity of concrete, identifies the presence of cracks or voids, monitors changes in properties over time, and evaluates physical and dynamic characteristics. Additionally, it allows for estimating concrete strength both in the laboratory and on-site. This method is truly non-destructive, as it relies on ultrasonic waves that do not damage the concrete element being examined. A specimen can be tested multiple times at the same location, making it useful for monitoring structural changes within the concrete over an extended period [238]. Generally, a high pulse propagation velocity indicates good quality concrete [239, 240] (See table II. 6).

Table II. 6 : General Relationship Between Concrete Quality and Impulse Velocity [239]

Impulse propagation speed (m/s)	Concrete quality
Greater than 4500	Excellent
3500-4500	Good
3000-3500	Average
Less than 3000	Doubtful

Evangelista et al. (2007) [187] assessed how much attached mortar affected the RAC's ultrasonic pulse velocity (UPV). They discovered that the UPV dropped linearly as the ratio of recycled aggregates to natural aggregates climbed 1.

Khatib (2005) [241] investigated how high temperatures affected RAC's UPV. The findings demonstrated that the UPV dropped as the curing temperature rose. At all temperatures, RAC showed lower UPV values than standard concrete 2.

Kou et al. (2012) [242] looked into the quality assessment of fly ash-containing RAC using UPV. According to their findings, the UPV dropped as the recycled aggregate replacement ratio increased. Nonetheless, the UPV of RAC was enhanced by the addition of fly ash.

The ultrasonic pulse velocity method can provide a means to estimate the in-situ and precast concrete strength, although there is no physical relationship between strength and velocity. Strength can be estimated from the pulse velocity using a pre-established graphical correlation between the two parameters (Figure II. 28).

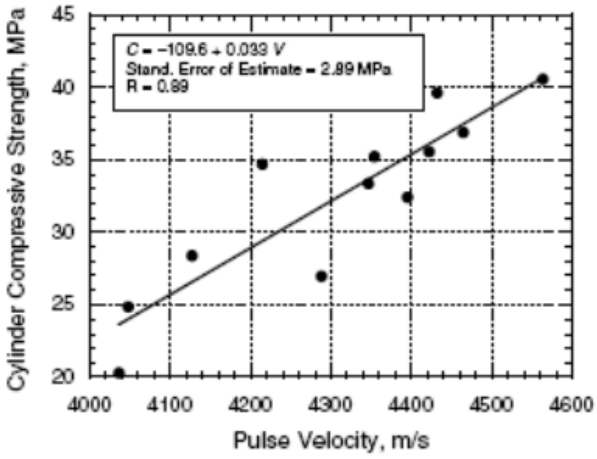

Figure II. 28 : Correlation Between Resistance and Ultrasonic Velocity [238].

The relationship between strength and pulse velocity is not unique and is affected by several factors, such as the size, type, and quantity of aggregates, the type and dosage of cement, the water/cement ratio, and the moisture content. The effect of each factor has been studied by various researchers. They have clearly stated that no attempt should be made to estimate the compressive strength of concrete from the pulse velocity unless similar correlations have been previously established for the type of concrete under study [238].

Many researchers have found that pulse velocity is significantly influenced by the type and quantity of aggregates used. Generally, the pulse velocity in the cement paste is lower than that in the aggregates. Jones [243] reported that for the same concrete mix and compressive strength, concrete with rolled gravel exhibited the lowest pulse velocity, while concrete with crushed limestone produced the highest velocity. In contrast, an intermediate pulse velocity was observed in concrete made with crushed granite. The effect of aggregate type on the relationship between pulse velocity and compressive strength is illustrated in Figure II. 29.

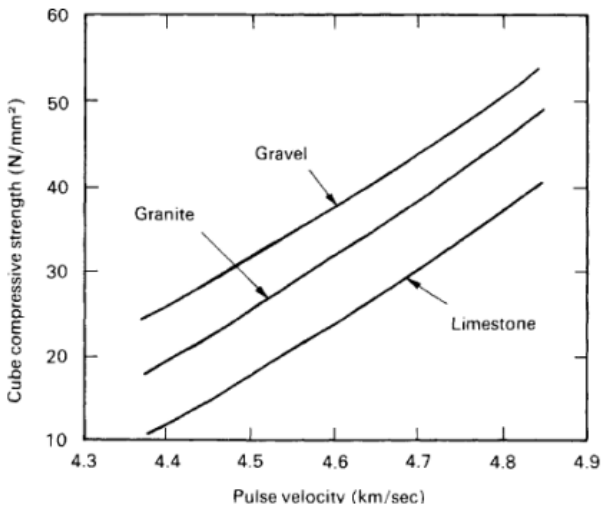

Figure II. 29 : Effect of Aggregate Type (Similar Concretes Except Aggregate Type) on the Relationship (Pulse Velocity - Compressive Strength) [243]

Several correlation models have been proposed by different authors between compressive strength R (MPa) and ultrasonic velocity V (km/s or m/s) as shown in Table II. 7.

Table II. 7 : Some Proposed Correlation Models Between Compressive Strength R (MPa) and Ultrasonic Velocity V (km/s, *: m/s) [244]

Auteurs	Fonctions de régression	Plage de Résistance	Spécimens	Granulats	Réf.
Ravindrajah et al. (1988)	$R = 0.060 \exp(1.44 V)$	15.0 à 75.0	Cube 100mm	granite D_{max}=20mm	[20]
Almeida (1993)	$R = 0.0133 V^{5.543}$ $R = 0.011 V^{5.654}$	40.1 à 120.3	Cube 150mm	Granite D_{max}=25mm	[20]
Gonçalves* (1995)	$R = 0.02 V - 65.4$	18.0 à 42.0	Carotte 70mmx70mm	/	[20]
Pascale et al* (2000)	$R = 10^{-28} V^{8.1272}$	30.0 à 150.0	Cube 150mm	Calcaire D_{max}=15mm	[20]
Qasrawi (2000)	$R = 36.72 V - 129.077$	6.0 à 42.0	Cube 150mm	variable	[23]
Soshiroda et Voraput (1999)	$R_{28} = 44.52 V_1 - 126.83$ $R_{28} = 54.18 V_{28} - 206.27$	20.0 à 65.0	Cube 150mm	gravier	[20]
Soshiroda et al. (2006)	$R_{28} = 1.941 \exp(0.815 V_1)$ $R_{28} = 0.356 \exp(1.110 V_3)$ $R_{28} = 0.131 \exp(1.293 V_7)$ $R_{28} = 0.043 \exp(1.498 V_{28})$	12.45 à 96.2	Cube 150mm	gravier	[37]
Phoon et al (1999)	$R = 124.4 V - 587.0 + \varepsilon$	35.0, 55.0 et 75.0	Cube 150mm	granite D_{max}=20mm	[20]
Hobbs et Kebir (2007)	$R=2.289V^2 -48.024V+24.271$	20.0 à 49.0	Cube 150mm	gravier D_{max}=20mm	[38]
Elvery et Ibrahim (1976)	$R = 0.012 \exp(2.27 V) \pm 6.4$	15.0 à 60.0	Cube 100mm	Gravier D_{max}=19mm	[20]
Yun et al (1988)	$R = 0.329 V - 1065$	5.0 à 30.0	Carotte 150mmx300mm	gravier D_{max}=25mm D_{max}=40mm	[20]

II. 8.2.4. Water-Accessible Porosity

According to Sereng et al. [29], the porosity of recycled concrete aggregates (RCA) is influenced by the porosity of the natural aggregates (NA), which is, in turn, affected by the amount of attached mortar. Additionally, during the production and crushing of natural aggregates, they may develop cracks that damage their surfaces. The high porosity and the presence of micro-cracks in RCA facilitate the penetration of water between the aggregates and the cement paste. Consequently, incorporating RCA leads to an increase in the porosity of the recycled concrete aggregates (RCA)[245].

Figure II. 30 from the National RecyBéton Project illustrates the results of water-accessible porosity for three classes of concrete at varying substitution rates. The figure shows a consistent increase in the porosity of RCA across all classes, with RCA containing the maximum substitution rate of G100 exhibiting the highest porosity values. Specifically, a 30% substitution of natural aggregates with RCA increases porosity by 16% to 22%, while a complete substitution (100% RCA) results in an increase in porosity ranging from 38% to 44%.

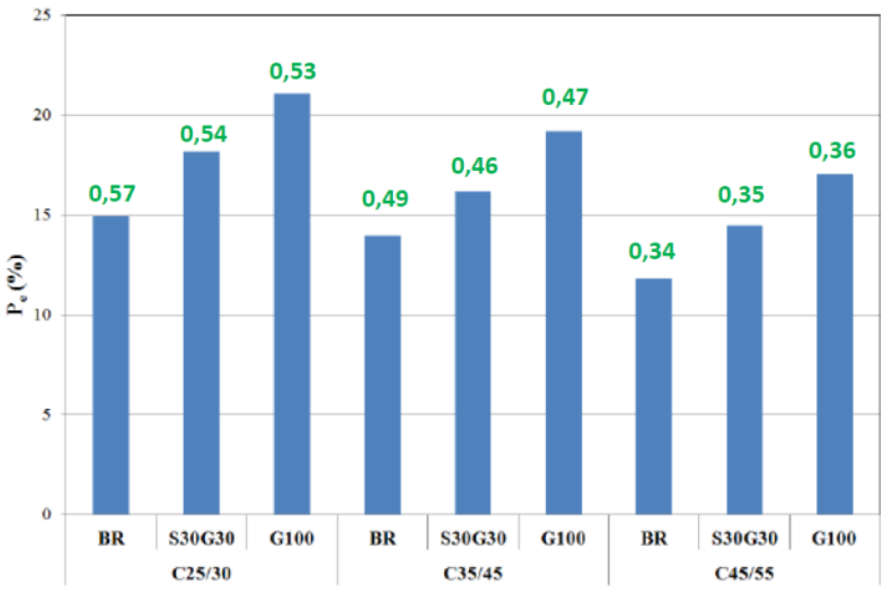

Figure II. 30 : Water-Accessible Porosity for Concretes at Different Substitution Rates After 90 Days of Curing in Water (BR: Reference Concrete, S30G30: 30% Substitution, G100: 100% Substitution - Given in Green: E/L) [245]

II. 8.2.5. Water Absorption

Concretes based on recycled aggregates have significantly higher water absorptions, by immersion or capillarity, than conventional concretes. This difference is particularly marked for absorption by capillarity, due to the greater quantity of capillary pores in

recycled concrete, due to the presence of the old mortar adhering to the aggregates [246–248].

II. 8.2.6. Permeability

According to Rasheeduzafar, Khan (1984) [249], when the water/cement (W/C) ratio exceeds 0.55, the inclusion of recycled aggregates does not significantly affect the permeability of the concrete. Conversely, at lower W/C ratios, the permeability of recycled concrete is higher than that of conventional concrete.

According to Sereng et al. [29], the permeability of recycled concrete aggregates increases with the incorporation rate of recycled aggregates due to greater pore connectivity (Figure II. 31). This effect is most pronounced at higher substitution rates (G100) and in lower strength concrete classes (C25/30). The E/L ratio also influences permeability, with lower ratios minimizing the impact of RA on more dense, higher strength mixes (C35/45 and C45/55). Reducing the E/L ratio and RA content can improve permeability and density of RAC.

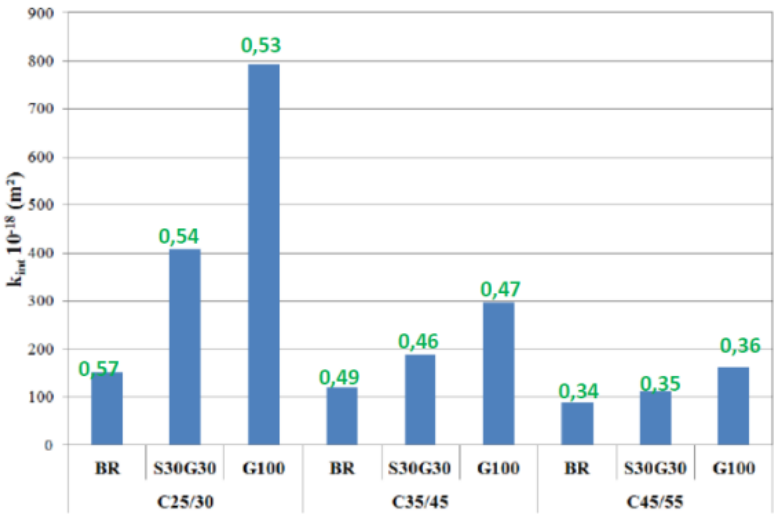

Figure II. 31 : Permeability as a Function of the Substitution Rate of Recycled Aggregates (BR: Reference Concrete, S30G30: 30% Substitution, G100: 100% Substitution- Given in Green: E/L) [245]

II. 8.2.7. Mass Evolution

The mass of concrete changes over time in response to environmental circumstances. Normal conditions cause the cement to hydrate, which causes the concrete to increase in mass during the taking and drying phases. However, under extremely dry or gel circumstances, the concrete may lose bulk due to water evaporation or surface escalation caused by freezing and thawing. The mass evolution measurement allows

one to monitor the saturation state of the concrete and identify potential disorders such as carbonation or sulphate attacks, which manifest as changes in the characteristics of the mass [203].

II. 9. DEFORMABILITY

Under load, concrete can bend in both elastic and plastic ways. The modulus of elasticity, also known as the instantaneous modulus of elasticity, is the primary quantity that characterises the deformability of concrete. According to the study, concrete deforms differently under compression than it does under tensile bending.

Concrete has notable plastic deformations under compression, which start to appear at 20% of the breaking stress. As the plastic deformations rise, the total modulus of deformation decreases. Concrete has very little plastic deformations under tensile bending, and these deformations do not appear until the concrete fails.

Porous aggregate concrete exhibits significantly less plastic deformation than heavyweight concrete. For a given concrete, the compressive modulus of elasticity is often greater than the tensile modulus. The deflection and cracking behavior of reinforced concrete structures can be greatly impacted by this variation in elastic characteristics. Rather of depending solely on compression testing, the elastic characteristics of concrete can also be estimated using the relationship between the tensile and compressive moduli of elasticity using simpler tensile bending experiments [250–253].

II. 9.1. Factors Influencing Deformability

Several factors influence the deformability of concrete, including:

Composition: The type and proportions of aggregates, cement, and water significantly affect the mechanical properties and, consequently, the deformability of concrete.

Age: Concrete gains strength and stiffness over time as it cures, which impacts its deformability under load.

Moisture Content: The presence of moisture can affect the microstructure of concrete, influencing its compressive strength and deformability.

Loading Rate: The rate at which the load is applied can also affect the deformability, with faster loading rates typically leading to lower deformability.

Understanding the deformability of concrete is essential for engineers and architects when designing structures, ensuring they can withstand applied loads and environmental conditions while maintaining safety and functionality.

II. 9.2. Principle of Deformability Under Compressive Load

The principle of deformability in concrete is primarily governed by its elastic and plastic behaviour. Under low levels of stress, concrete behaves elastically, meaning that it will return to its original shape once the load is removed. The relationship between stress and strain in this elastic region is linear and is described by well-known Hooke's Law (II. 13) where stress is proportional to strain. It's expressed as:

$$\boldsymbol{\sigma = E \times \varepsilon} \qquad \textit{II. 13}$$

In this equation, σ represents the applied stress, E is the modulus of elasticity, and ε denotes the strain. The modulus of elasticity (E) quantifies this relationship, providing a measure of the stiffness of the concrete. As the compressive load increases and approaches the material's ultimate strength, concrete begins to exhibit plastic behaviour. In this phase, the material undergoes permanent deformation, and micro-cracking may occur. The ability of concrete to deform plastically before failure is essential for energy absorption and redistribution of stresses within a structure.

II. 9.3. Instantaneous Deformations Under Compressive Load

When subjected to relatively low loads, concrete experiences nearly instantaneous elastic and reversible deformation, adhering to the Hooke's Law. In this equation, σ represents the applied stress, E is the modulus of elasticity, and ε denotes the strain. Understanding these properties is essential for ensuring the long-term performance of concrete in various applications. Beyond a certain load, a plastic zone develops; resulting in permanent deformation after the load is removed. When the load is applied over time, the high viscosity of concrete leads to creep behaviour, causing it to act as an elasto-visco-plastic material [254]. The following figure shows the stress-strain curve obtained by recording F_{bc} - ε_{bc} during a compression test on a (16×32) cm^3 specimen (Figure II. 42), providing valuable insights into the instantaneous deformations of concrete under compressive loading.

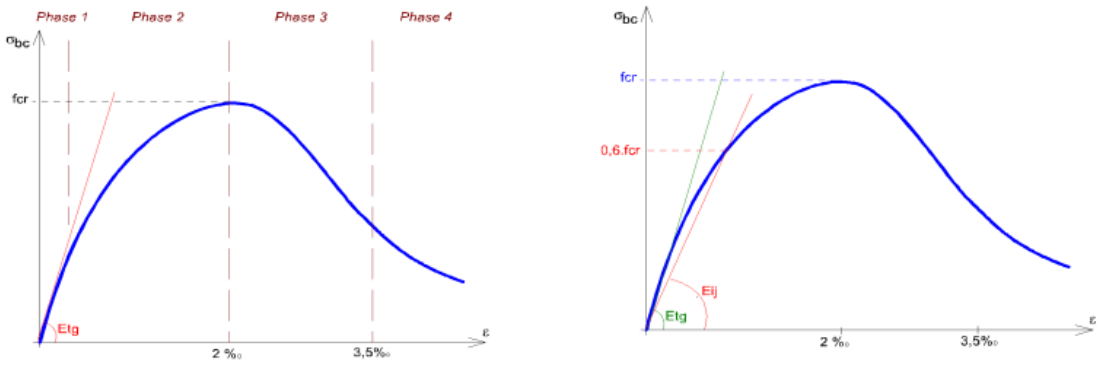

Figure II. 42 : The Experimental Stress-Strain Curve During a Compression Test on a Cylindrical Specimen (16×32) cm^3 [254]

The stress in the concrete at 'j' days is given by the following relationships:

$$\begin{cases} f_{cj} = \dfrac{j}{4.76+0.83\times j}\, f_{c28} & \text{for : } f_{c28} \leq 60 \text{ Mpa} \quad \text{at age of} \quad j \leq 28 \text{ days.} \\ f_{cj} = 1.1\, f_{c28} & \text{for : } f_{c28} \leq 60 \text{ Mpa} \quad \text{at age of} \quad j > 60 \text{ days.} \end{cases}$$

$$\begin{cases} f_{cj} = \dfrac{j}{1.40+0.95\times j}\, f_{c28} & \text{for : } f_{c28} > 60 \text{ Mpa} \quad \text{at age of} \quad j \leq 28 \text{ days.} \\ f_{cj} = f_{c28} & \text{for : } f_{c28} > 60 \text{ Mpa} \quad \text{at age of} \quad j > 60 \text{ days.} \end{cases}$$

For a short-term stress (t < 24 h), a concrete age (j > 60 days) and a compressive strength ($f_{c28} \leq 60$ MPa), the secant instantaneous strain modulus E_{ij} is defined as follows (II. 14,15) [255]:

$$\boldsymbol{E_{ij} = 11000\, \sqrt[3]{f_{cj}}} \qquad \textit{II. 14}$$

and

$$\boldsymbol{f_{cj} = 1.1\, f_{c28}} \qquad \textit{II. 15}$$

II. 9.4. Deformability of Recycled Concrete Under Compressive Load

The deformability of concrete under compressive load refers to its ability to undergo deformation when subjected to external forces. This property is critical in assessing the performance and safety of concrete structures, as it influences how the material behaves under load and how it can absorb energy during events such as earthquakes. According to Minh-Duc Nguyen et al. [256], for the same class of compressive strength, the introduction of recycled aggregates leads to a decrease in tensile strength and the modulus of elasticity. The peak deformation and ultimate deformation increase with a higher substitution rate of recycled aggregates. In recycled concrete, the presence of recycled aggregates contributes to a more dissipative behaviour, likely due to more

progressive and diffuse damage resulting from the nature of the gravels and the presence of increased porosity. Furthermore, the modulus of elasticity decreases with the substitution rate of aggregates. Minh-Duc Nguyen et al.'s study found that a 100% substitution rate of gravel results in a 23.85% reduction in the modulus of elasticity for concrete classified as C25/30 [256].

Two essential characteristics of materials that characterise their elastic behaviour under different kinds of stress are Young's modulus (E) and Poisson's ratio (v).

II. 9.5. Static Young's Modulus (E)

The modulus of elasticity or Young's modulus, so named in honour of Thomas Young, quantifies a material's stiffness. It is the primary measure of elasticity, defined as the ratio of stress to corresponding strain below the proportional limit, according to ASTM Designation E 6-66. Stated otherwise, it is the elastic region's slope of the stress-strain curve. Young's modulus is commonly expressed in gigapascals (GPa) or Pascal (Pa).

II. 9.6. Types of Static Young's Modulus

For materials like concrete with a curvilinear stress-strain relationship, four terms can describe the modulus of elasticity (see Figure II. 43):

Initial Tangent Modulus: Slope at the origin of the stress-strain curve.

Tangent Modulus: Slope at any specified stress or strain.

Secant Modulus: Slope of the secant line from the origin to a specified point on the curve.

Chord Modulus: Slope between any two specified points on the curve.

These definitions refer to the static modulus of elasticity, which can be measured in compression, tension, or shear. Young's modulus (E) refers to tension or compression, while the shear modulus (G) relates to rigidity. The ASTM standard for determining static elastic constants of concrete is ASTM C 469-65, which defines the chord modulus between two points on the stress-strain curve. The lower point corresponds to a strain of 50 microinches/inch (0.05 μmm/mm), and the upper point corresponds to 40% of the concrete's strength at loading, ensuring an average modulus throughout the working stress range. Specimens should be loaded at least twice, with calculations based on the average of subsequent loadings.

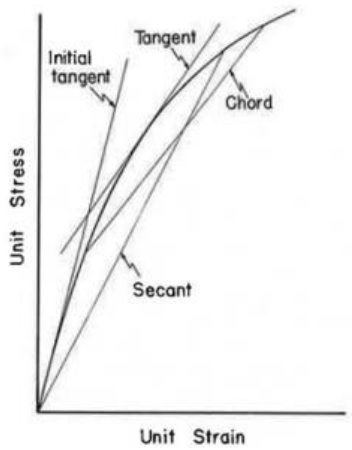

Figure II. 32 : Types of Static Young's Modulus of Elasticity of Concrete [253]

II. 9.7. Dynamic Young's Modulus

The modulus of elasticity of concrete is influenced by several key factors, with the type of coarse aggregate being the most significant. Other important factors include the compressive strength, water-cement ratio, and the method of concrete curing. These elements collectively determine the overall stiffness and performance of concrete in structural applications [257].

The modulus of elasticity of concrete containing recycled construction and demolition waste as aggregates is generally lower than that of concrete with natural aggregates. This decline in modulus of elasticity increases with a higher replacement rate of natural aggregates by recycled aggregates. In some cases, the reduction in modulus of elasticity for recycled aggregate concrete can reach up to 50% compared to conventional concrete made with natural aggregates. This significant decrease highlights the impact of aggregate type on the mechanical properties of concrete [258]

In the study conducted by PAVLŮ T. et al. (2014) [259], concrete mixtures were formulated using recycled aggregates of types A, B, and C, with coarse natural aggregate replacement levels of 31%, 50%, and 62%. Specifically, mixtures containing type C aggregates included 62% and 70% total replacement, with 100% of the coarse fraction substituted and 30% of the natural sand replaced. All mixtures were designed to achieve a C30/37 strength class, maintaining consistent cement content and water-cement ratios. The findings revealed that recycled aggregate concrete exhibited a lower modulus of elasticity compared to conventional concrete. Furthermore, both dynamic and static modulus values were adversely affected by the quantity and quality of the

recycled aggregates, which also influenced the correlation between these two modulus types.

II. 9.8. Poisson's Ratio (ν)

Siméon Poisson, a French mathematician, is credited for naming Poisson's ratio, which quantifies the lateral strain a material experiences under compressive or longitudinal tensile stress. The definition of it is the lateral strain divided by the longitudinal strain. Poisson's ratio has an arbitrary unit that usually falls between 0 and 0.5. The Poisson's ratio for regular concrete is usually between 0.15 and 0.20, meaning that when longitudinal force is applied, the material will flex somewhat. The Poisson's ratio can already be expressed as follows (II. 16):

$$v = \frac{E}{2G} - 1 \qquad II.\ 16$$

where:

ν is the Poisson's ratio,

E is the Young's modulus of elasticity,

G is the shear modulus (modulus of rigidity or torsional modulus).

II. 10. TRANSITION ZONE AT THE AGGREGATE/PASTE INTERFACE (ITZ)

II. 10.1. ITZ's Impact on the Concrete Performance

The coarse aggregate, the mortar matrix holding the fine aggregate and cement paste, and the transition zone at the aggregate-paste contact make up the three phases of the concrete system. This zone is found surrounding all of the coarse particles despite being quite fine (Figure II. 36).

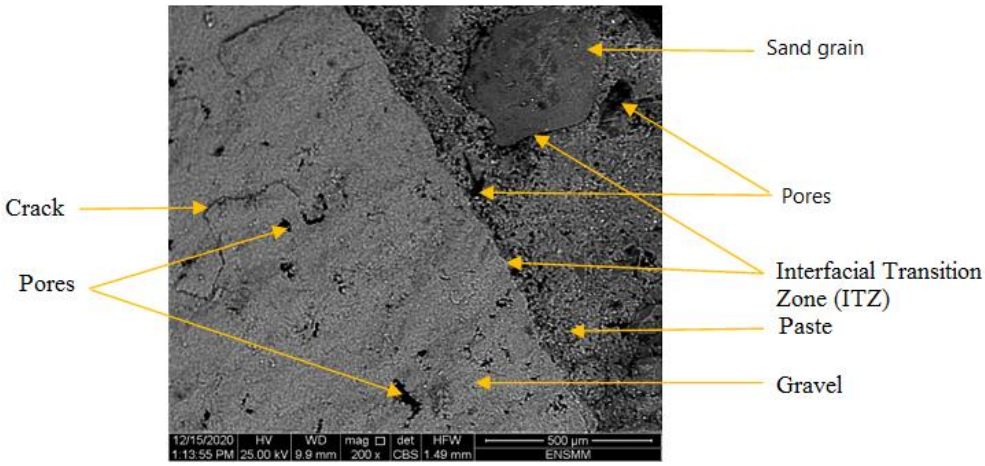

Figure II. 33 : Aggregate, Paste and Transition Zone in an Ordinary Concrete

Ultimately, it makes up to 45% of the concrete's volume [170]. Serving as a connection between the two main components of concrete, the mortar matrix and the coarse aggregate, this transition zone has a significant impact on the mechanical characteristics of the material. Defects in the transition zone might cause the strength of the concrete to be low even in cases where the strength of these two components is high. When the W/C ratio is high, there are more of these. In this instance, the growth of portlandite ($Ca(OH)_2$) in the transition zone is aided by the preferred presence of large capillary holes that are somewhat saturated with water beneath or close to the big aggregates. There are gaps in the transition zone caused by these crystals' easy leaching out and lackluster strength addition to the concrete. Subsequently, the transition zone becomes weaker and loses its ability to transmit the pressures applied to the concrete [260]. Therefore, while evaluating the mechanical strength and longevity of concrete, it is vital to take the aggregate-paste interface into account. It is now understood that high-performance concrete will be weakened by its big aggregates, while ordinary concrete will fracture along the transition zone. The transition zone is what limits the strength of the concrete because most concretes have conventional strengths, which are less than 35 MPa at 28 days [260].

II. 10.2. ITZ Formation

The formation of the interfacial transition zone (ITZ) in concrete is primarily due to the presence of a water layer surrounding the aggregates in fresh concrete. The distribution of water in the cement paste around the aggregates is heterogeneous, with a higher water-to-cement ratio (w/c) near the aggregates. This effect can be attributed to two main phenomena during the contact between fresh cement paste and aggregates: the wall effect and micro-bleeding. The wall effect corresponds to a less dense packing of cement grains around the aggregate compared to the cement paste in the bulk. Micro-bleeding is caused by a local accumulation of water under the aggregates during concrete placement. In addition to these two mechanisms, the "lateral growth" effect and the transport of hydrates during hydration also contribute to the formation of the ITZ. During hydration, near the aggregates, the hydrates develop in a single direction towards the cement matrix, leading to an increase in porosity in the zone closest to the aggregates (lateral growth effect). This heterogeneous distribution of hydration products and the higher w/c ratio in the ITZ result in a weaker and more porous zone

compared to the bulk cement paste, which can affect the overall mechanical properties of concrete [27].

II. 10.3. ITZ in Concrete Based on Demolition Aggregates

Recycled concrete aggregates consist of a close mixture of natural aggregates and hardened cement paste. Consequently, in concrete made with recycled concrete aggregates, three types of interfacial transition zones (ITZ) can be identified: an old ITZ between the original cement paste and natural aggregates, a new ITZ between the new paste and the old paste, and an ITZ between the natural aggregate and the new cement paste (see Figure II. 37).

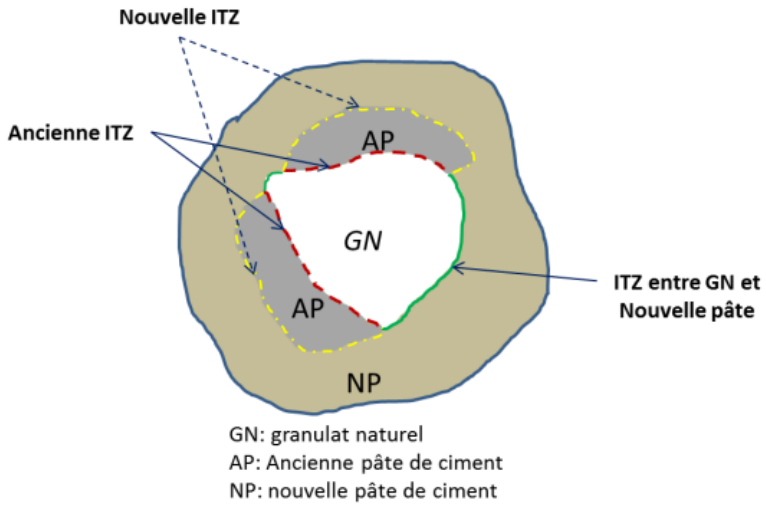

Figure II. 34 : ATZs in Concretes or Mortars Containing Concrete Demolition Aggregates [27]

According to the authors, the weakest part in recycled aggregate concrete (RAC) can be located in different areas. This weak zone may correspond to the new interfacial transition zone (ITZ) between the recycled concrete aggregate and the new cement paste. Du et al. [261] showed through indentation tests that the strength of the old cement paste in the recycled concrete aggregate is higher than that of the old ITZ, but the weakest point in RAC is the new ITZ. Rasheeduzzafar and Khan and Xiao et al. [262, 263] concluded that the weakest point in RAC depends on the relative strength between the old and new mortar or the relative quality between the old and new ITZs. If the strength of the new ITZ is lower than that of the old paste, the first cracks appear in the new ITZ. Conversely, if the strength of the new ITZ is higher than that of the old paste, cracks mainly appear in the old ITZ. Understanding the location and characteristics of the weakest zones in RAC is crucial for optimizing the use of recycled

materials and improving the overall performance of concrete made with recycled aggregates.

According to studies, the weakest point in concrete or mortar containing recycled concrete aggregates (RCAs) is often the adhered mortar, which tends to be highly porous and filled with microcracks. However, Nagataki et al. [264] demonstrated that the quality of the adhered mortar is not the primary factor in determining the quality of the RCAs. The crushing process also significantly influences the quality of the RCAs, with properties at level 1 being superior to those at level 3 in the production process. By using aggregates in different saturation states, the new interfacial transition zone (ITZ) can be modified. According to Tam et al. [265], the quality of the new ITZ improves when using aggregates in a wet state, achieved by pre-wetting the aggregates with half the total water amount for 60 seconds before adding the cement (Figures II. 38 and II. 39).

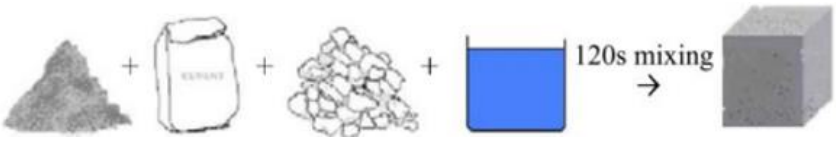

Figure II. 35 : Traditional Mixing Procedure (NMA[2]) [265]

Figure II. 36 : New Mixing Technique (TSMA[3]) [265]

Figure II. 40 illustrates a comparison between two new ITZs produced using different methods, showing that the new ITZ formed with wet aggregates exhibits lower porosity than that formed with dry aggregates.

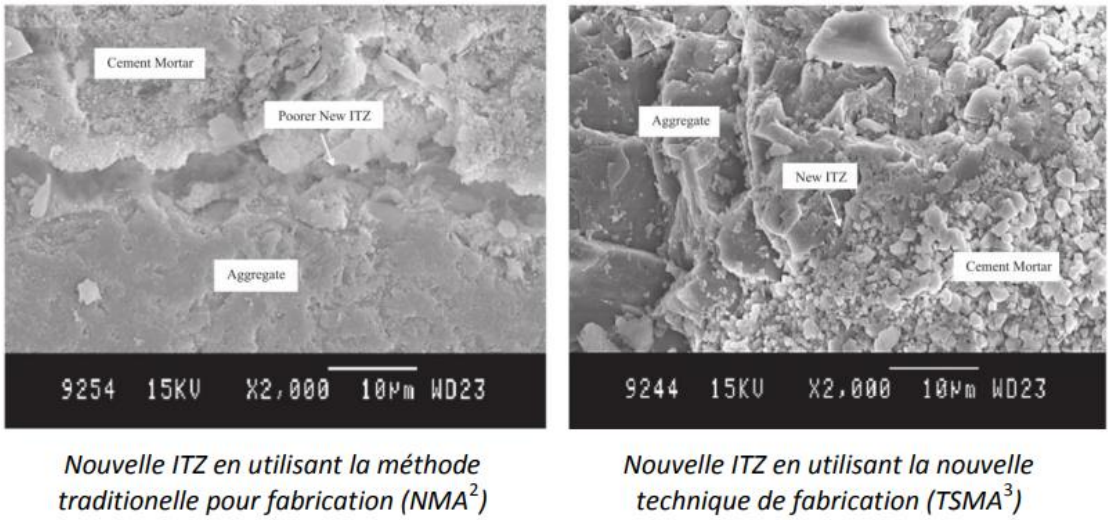

Nouvelle ITZ en utilisant la méthode traditionelle pour fabrication (NMA[2])

Nouvelle ITZ en utilisant la nouvelle technique de fabrication (TSMA[3])

Figure II. 37 : New ITZs seen at the SEM [265]

Recently, a comparison of the ITZs in two mortars with sands used in two moisture states (dry and saturated-surface-dry) with the same effective water-to-cement ratio (E_{eff}/C) was conducted by Zhao. The new ITZ in the case of saturated-surface-dry aggregate mortar is visible, unlike in the case of dry aggregate mortar. The properties of the ITZ are improved by the absorption water of the aggregates. Thus, the compressive strength of mortars based on dry recycled sand is higher than that of mortars based on saturated-surface-dry recycled sand due to a lower quality transition zone in the case of saturated-surface-dry recycled sand mortar.

In a specific case, Poon et al. [266] compared the influence of different types of recycled concrete aggregates (RCAs) on the microstructure of the ITZ. They used an ordinary recycled concrete aggregate (NC) and a high-performance recycled concrete aggregate manufactured with silica fume (HPC). The water absorption coefficients are WA_{24h}(NC)=8.8% and 7.9% and WA_{24h}(HPC)=6.8% and 6.5% for particle sizes of 10 mm and 20 mm, respectively. By comparing the two ITZs (Figure II. 41), a highly porous zone can be observed in the case of ordinary recycled concrete aggregate compared to that of high-performance recycled concrete aggregate. The old cement paste in the case of ordinary concrete is more porous and absorbent than that of high-performance concrete, leading to a higher initial E_{eff}/C ratio in the case of concrete containing ordinary recycled concrete aggregates. The ITZ in this case is therefore more porous.

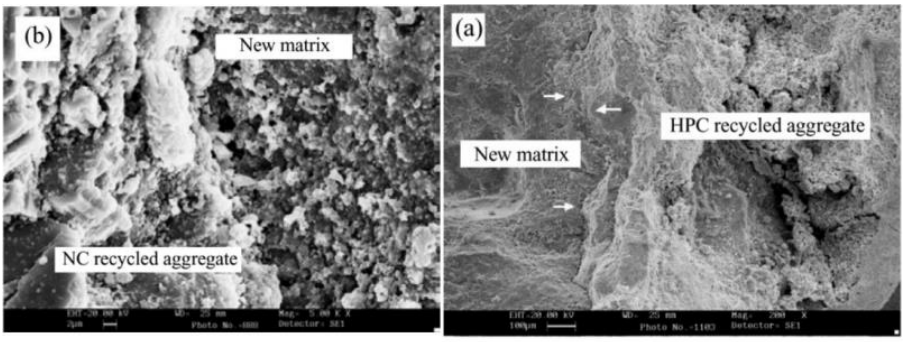

ITZ entre GBR béton ordinaire et nouvelle pâte de ciment (NC : normal-strength)

ITZ entre GBR béton haut performance et nouvelle pâte de ciment (HPC : high performance concrete)

Figure II. 38 : Comparison of New ITZs Using Different RCAs Types [265]

Overall, the influence of interfacial transition zone (ITZ) properties on the characteristics of concrete or mortar is well-documented in the literature. While the microstructure of concrete and mortars containing recycled concrete aggregates (RCAs) has been studied, most research remains largely qualitative. Furthermore, previous studies have not clearly specified the saturation state of the RCAs, which appears to play a significant role in the microstructure of the ITZ. Addressing this gap could enhance our understanding of how RCA saturation affects the performance and durability of concrete and mortar.

II. 11. CONCRETE BEHAVIOUR IN SEVERE CONDITIONS

II. 11.1. Abrasion

According to Jorge de Brito (2010) [267], the abrasion resistance of concrete containing recycled aggregates (RAs) is at least comparable to that of conventional concrete without RAs. The variation in abrasion resistance of concrete made with RAs, as the incorporation rate of these aggregates increases, is influenced not only by the origin of the RAs but also by other factors, such as curing conditions. According to Dhir et al. (1991) [268], the abrasion resistance of concrete is influenced by several factors, including the water/cement ratio (W/C), curing conditions, workability, maximum aggregate size, and the materials used in the mix. Laplante et al. (1991) [269] concluded that while silica fume can provide a slight improvement in the abrasion resistance of concrete, the type of coarse aggregate plays a more crucial role. They observed that when the water/cement (W/C) ratio is maintained at around 0.30, the abrasion resistance of the concrete closely aligns with that of the coarse aggregate source rock. Furthermore, in high-strength concretes with very low W/C ratios, the abrasion

resistance is predominantly influenced by the properties of the coarse aggregate. Olorunsogo (1999) [270], who utilized coarse recycled aggregates (RAs) from crushed concrete, noted that no definitive relationship could be established between the abrasion resistance of recycled aggregate concrete (RAC) and the proportion of RA incorporated into the mixes. Similarly, Limbachiya et al. (2000) [235], also using coarse RAs from crushed concrete, found that the differences in abrasion depth between concrete made with only natural aggregates (NAs) and that with 100% coarse recycled aggregates at design strengths of 50 and 60 N/mm² were just 0.03 mm and 0.04 mm, respectively. This indicates that, at a given design strength, RAC mixes exhibit abrasion resistance comparable to that of concrete made with natural aggregates, regardless of the RA proportion used. Sagoe-Crentsil et al. (2001) [271] observed that the abrasion loss of recycled concrete aggregates (RCA) produced with ordinary Portland cement increased by approximately 12% compared to conventional concrete without coarse RA. They also concluded that the properties of fresh and hardened RCA could be improved by using industrially produced aggregates instead of those derived from laboratory-crushed concrete, due to the enhanced grading and quality achievable through plant crushing operations.

II. 11.2. Freeze and Thaw Cycles

Most studies report that the freeze-thaw resistance of recycled concrete is lower than that of conventional concrete, and this resistance depends particularly on the degree of water saturation of the material [272–275]. According to J. Lavado et al. (2020) [276], as quoted by J. Bao et al. (2015) [277], recycled aggregate concrete (RAC) exhibits a high water absorption rate due to the presence of numerous micro-pores and micro-cracks in recycled coarse aggregate. This characteristic makes RAC susceptible to reaching the critical water saturation level that can lead to freeze-thaw damage, resulting in poor frost resistance. However, with appropriate technical measures, RAC can still meet specified performance requirements.

To enhance the durability of recycled aggregate concrete (RAC), several strategies are recommended, including reducing the water-cement ratio, incorporating mineral admixtures such as fly ash and slag, carefully selecting the particle size of recycled aggregates, and improving the quality of recycled coarse aggregate. Implementing these measures can significantly boost the performance of RAC in various construction applications [277]. Additionally, researchers have discovered that incorporating an air-

entraining agent can make concrete produced from recycled aggregates as durable against freeze-thaw cycles as that made from natural aggregates [278]. Air-entraining agents improve the freeze-thaw resistance of recycled concrete by creating microscopic air bubbles within the mix, which serve as pressure-relief chambers during freeze-thaw cycles. This helps to mitigate the internal stresses caused by water expansion when it freezes, thereby reducing the risk of cracking and damage. As a result, the use of air-entraining agents can enhance the long-term durability and reliability of RAC in environments subject to harsh weather conditions.

II. 11.3. Chemical Attacks

According to Holcim [277], sulfate-rich waters (or selenite waters) and sulfate-rich soils pose a significant threat to hardened concrete. When sulfate ions from these environments interact with tricalcium aluminate (either hydrated or anhydrous) in the hardened cement paste, they can form expansive compounds such as ettringite (or Candlot salt). Concrete is generally considered to be in a potentially aggressive environment if it comes into contact with groundwater containing more than 600 mg/L of sulfates or soil layers with over 3,000 mg/kg of sulfates, classified as environments EA2 or EA3.

According to Hermann Kurt (1992, 1995) [279, 280], a well-composed, well installed, and properly treated concrete can withstand a wide range of chemical combinations. Its resistance to some others, however, is limited. A survey conducted by the OECD (Organization for Economic Co-operation and Development) revealed that the main causes of degradation observed on 800.000 bridges worldwide are chloride contamination and sulfate attack [281]. Numerous acids also attack concrete, however many inoffensive combinations of neutral inorganic or organic substances as well as certain mildly basic solutions are not. It's important to remember that many combinations only turn toxic when water or aqueous solutions are present. The severity of the damage depends on a number of other factors, such as temperature, the duration of the noxious compounds' effect, and their concentration. The composition of the concrete, its water-to-cement ratio, its permeability, etc., all play a significant role. Figure II. 32 represents the substances exerting a chemical action on concrete.

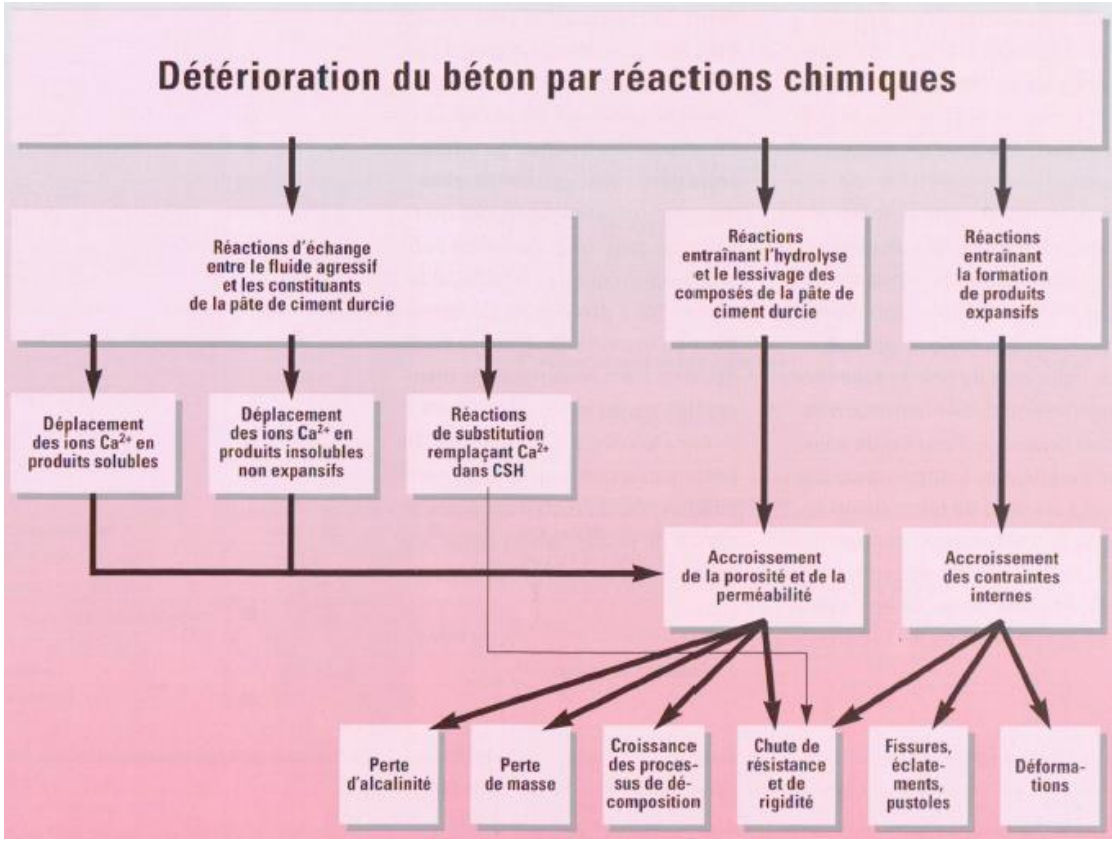

Figure II. 39 : Chemical Reactions Causing Concrete Damage (According to Lauer, K. and Lachaud, ft. and Salomon, M.) [280]

According to Hongru Zhang et al. [277], the failure mechanism of RAC under external sulfate attack is more complex compared to normal aggregate concrete (NAC) due to the presence of more diverse material phases on the micro/meso scales . The porous ITZ and the quality of recycled aggregates play a crucial role in the sulfate resistance of RAC. To mitigate sulfate attack, concrete mixes should be designed with low permeability, using sulfate-resistant cements, supplementary cementitious materials, and admixtures. Proper curing and protection of concrete from sulfate-bearing environments is also essential for ensuring long-term durability.

According to the study by Qianyun Wu et al. (2021)[282], the mass loss of concrete subjected to sulfate attack initially increases with time before eventually decreasing (Figure II. 33). This phenomenon occurs as sulfate ions interact with the hydration products in the concrete, leading to changes in the internal microstructure. The reaction produces expansive crystals, such as ettringite and gypsum, which can initially cause mass loss. Notably, concrete containing 10% fly ash demonstrated an increase in mass by 2.17% compared to uncorroded concrete.

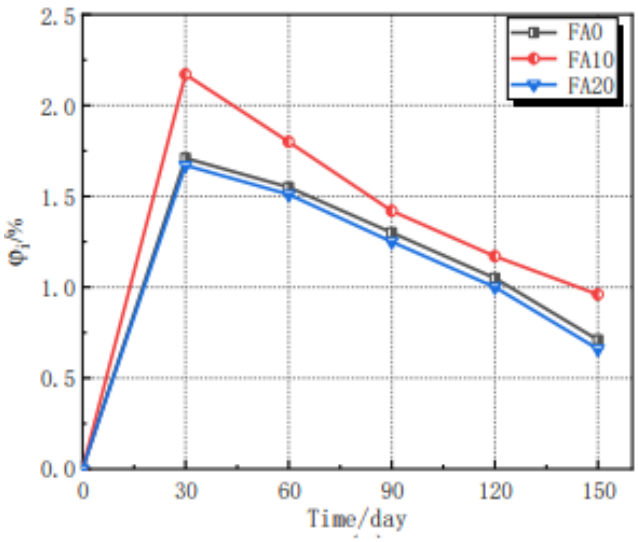

Figure II. 40 : Variation of Mass of Concrete Subjected to Sulfate Attack [282]

Santillán et al. explained the controversy, proposing that although the high porosity of ITZ and old residual mortar in RAC leads to faster sulfate penetration compared to NAC, these pores can also provide sufficient space for the precipitation and growth of expansive products, thereby retarding expansion failure. Some researchers also suggest that the high water absorption of RA (3-10 times higher than NA [44,45]) can make the new paste denser, helping RAC resist sulfate erosion better.

Bulatovic et al. proved that the sulfate resistance of RAC is significantly influenced by the water-to-cement (w/c) ratio; a lower w/c tends to reduce concrete expansion under external sulfate attacks, consistent with findings reported by Gao et al.

II. 11.4. High Temperature

Concrete's mechanical qualities are greatly impacted by high temperature exposure. Numerous investigations have been carried out to comprehend this phenomenon. High-strength concrete (HSC) specimens heated to 600°C have had their compressive strength, modulus of elasticity, and internal pore pressure accumulation evaluated as part of the NIST experimental program. Compared to normal-strength concrete, HSC shows a more pronounced drop in compressive strength, up to 40% of its room-temperature strength, in the 100°C to 400°C temperature range [283, 284]. Due to HSC's limited permeability, which prevents the discharge of internal pressure building from vaporised water, high temperatures can cause explosive spalling. Concrete behaves differently at high temperatures depending on the kind and characteristics of the aggregates used in it, which might cause different responses in terms of compressive

strength [284, 285]. When HSC is subjected to high temperatures, the risk of explosive spalling can be reduced with the addition of polypropylene fibers. Researchers have also looked into concrete's repeated impact reaction after exposure to high temperatures, which is crucial for determining the structural integrity of the material following a fire incident.

According to Hachemi (2014) [286], the porosity of cement paste is significantly altered by temperature. Alarcon-Ruiz et al. (2002) reported that porosity increases from 22% in an unheated sample to 40% in a sample heated to 600°C. A synthesis of results from various studies indicates that total porosity of concrete rises with temperature.

According to Hachemi (2014) [286], experimental results from Kanema et al. (2005) [287], as well as other researchers, indicate that the permeability of concrete significantly increases when temperatures exceed 100°C. Figure II. 34 illustrates the variation in residual intrinsic permeability of concrete with temperature, as reported by Kanema et al. (2005). They found that permeability decreases at 150°C due to the presence of liquid water in the pores, but then increases exponentially at higher temperatures. The rise in permeability between 150°C and 300°C is attributed to the widening of capillary pores, while the increase from 300°C to 450°C results from deterioration of the cement matrix.

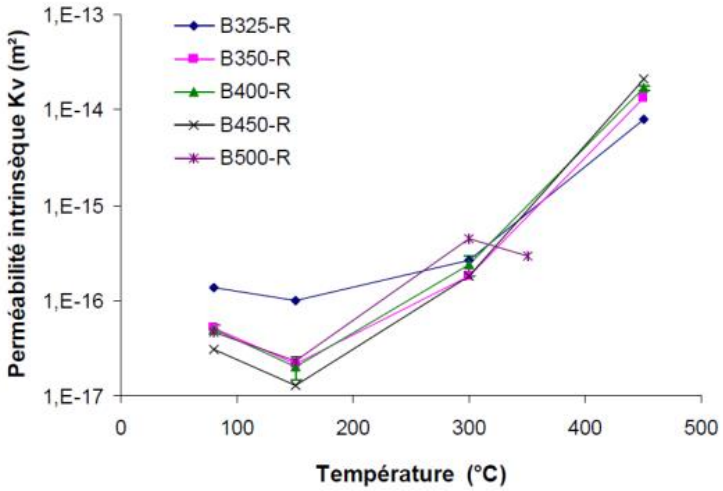

Figure II. 41 : Evolution of the Residual Induced Permeability of Concrete as a Function of Temperature [287]

According to Meftah et al. [208], the thermal expansion coefficient of concrete primarily depends on the thermal expansion of the aggregates used [288, 289]. It is generally accepted that concretes made with high-silica aggregates exhibit greater thermal expansion compared to those made with aggregates low in silica, such as

limestone. Figure II. 35 illustrates the dimensional changes of concrete specimens as a function of heating temperature.

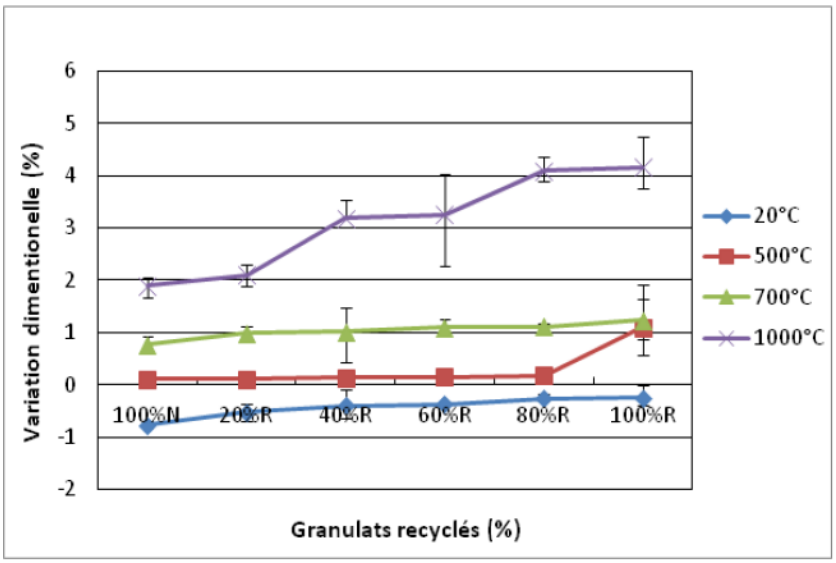

Figure II. 42 : Dimensional Variation of Recycled Concrete as a Function of Temperature [208]

II. 12. ANALYSIS OF VARIANCE "ANOVA"

ANOVA (Analysis of Variance) is a statistical method used to analyse the behaviour of a quantitative variable based on one or more qualitative variables. By comparing means, it is important to specify which groups exhibit differences. ANOVA partitions the total variation in an experiment into components attributable to controlled factors and the errors generated. The statistical significance of quadratic prediction models is evaluated using the P-value and F-value from ANOVA. In the ANOVA table, the P-value indicates the probability (ranging from 0 to 1) that the observed results (or more extreme outcomes) occurred by chance:

- If P > 0.05, the parameter is considered insignificant.
- If P < 0.05, the parameter is significant.

The first step in ANOVA involves measuring the total dispersion of data using the Total Sum of Squares (SS), calculated as follows:

$$SC_f = \frac{N}{N_{nf}} \sum_{i=1}^{N_{nf}} (\bar{y}_i - \bar{y})^2 \qquad II.\ 17$$

where $\bar{y}$ is the overall mean response. ANOVA compares variance between groups to variance within groups by calculating the F-statistic, which is the ratio of mean squares between groups (MST) to mean squares within groups (MSE). These values are derived by dividing their respective sums of squares by their degrees of freedom, typically presented in an ANOVA table. The mean square (MS) is estimated as:

$$MC_i = \frac{SS_i}{df_e} \qquad II.\ 18$$

To assess model adequacy, the Fisher F-value is used, where calculated F-values should exceed those from the F-table:

$$F_i = \frac{MC_i}{MC_e} \qquad II.\ 19$$

The last column in the ANOVA table (Contribution %) shows each factor's contribution to total variation, indicating its influence on the outcome:

$$\boldsymbol{Cont}\% = \frac{SC_f}{SC_T}\ \mathbf{x\ 100} \qquad II.\ 20$$

II. 13. CONCLUSION

Chapter II provides a comprehensive bibliographic synthesis on aggregates and their critical role in concrete production. It begins with an overview of aggregates, detailing their definitions, historical usage, and significance in construction. The section on conventional aggregates explores global production and manufacturing processes, highlighting classification methods based on various criteria. The discussion then shifts to specific types of aggregates, including Sahara dune sand and demolition aggregates, examining their availability, properties, and production techniques. Improvement methods for demolition aggregates are also outlined, showcasing innovative techniques for enhancing their quality. Finally, the chapter addresses the various concrete types, including self-compacting and fiber-reinforced concrete, emphasizing their constituents and formulation methods. This synthesis underscores the importance of selecting appropriate aggregates to optimize concrete performance while promoting sustainable construction practices. Overall, the insights presented in this chapter lay a solid foundation for understanding the complexities of aggregate use in modern concrete applications.

CHAPTER III

MATERIALS AND EXPERIMENTAL METHODOLOGY

CHAPTER III _ MATERIALS AND EXPERIMENTAL METHODOLOGY

III. 1. INTRODUCTION

The materials and experimental techniques used in this study are the main topics of Chapter III. This chapter, which describes the precise elements used in the composition of concrete and the methodical procedures used to assess their qualities, is crucial for laying the groundwork for the investigation.

The essential components are listed in the first part and include cement, admixtures, mixing water, fine aggregates (sand), and coarse aggregates (gravel). A thorough grasp of each material's functions in reaching intended performance results is provided by discussing its properties and importance in the concrete mix.

The chapter dives into the experimental approach after the materials section. The creation and selection of demolition coarse aggregates, as well as their application in conjunction with Saharan dune sand in the formulation of concrete, are the two primary aspects of this section. To guarantee openness and reproducibility, thorough explanations of the production procedures, physical characterisation techniques, and mechanical testing procedures are given.

Furthermore, a number of tests are described to evaluate the workability, compressive strength, durability indicators, and resilience to extreme circumstances of both fresh and hardened concrete. In order to examine the materials and tangible objects at various scales, the chapter also discusses a variety of investigation methods, including macroscopic, mesoscopic, and microscopic methods.

Chapter III attempts to give readers the background information they need to comprehend the experimental framework of this thesis by providing a comprehensive summary of the materials and procedures. Subsequent discussions of the findings and their significance for the advancement of construction materials science knowledge will be supported by this foundation.

III. 2. MATERIALS

III. 2.1. Cement

A CEM II/A-M (S-L) 42.5 N grade Portland cement sourced from the Hadjar-Soud cement plant in Annaba- Algeria, served as the binding agent within the study concrete formulations including that of the parent concretes (PCs) of the first part of this work.

This hydraulic binder (Figure III. 1) comprises around 12% limestone and 74% clinker [290]. Its chemical and mineralogical compositions are represented in the tables III. 1 and III. 2 respectively.

Figure III. 1 : Cement Packed in a Bag of 50 kg

Table III. 1 : Chemical Composition of Cement

Element	SiO_2	CaO	MgO	Fe_2O_3	Al_2O_3	SO_3	PF	K_2O
Rate (%)	22-28	55-65	1-2	3-3.6	5-6	1.8-2.5	1-2	0.3-0.6

Table III. 2 : Mineralogical Composition of Cement

Mineral	C_3S	C_2S	C_3A	C_4AF
Rate (%)	55-65	10-25	8-12	9-13

The appendix (1) contains a technical data sheet that contains more information about the product.

III. 2.2. Mixing Water

For cement hydration purposes, tap water distributed in the municipality of Sidi Amar, Annaba- Algeria is used according the standard NF EN 1008 (2003) [197].

III. 2.3. Admixture

The admixture used was Sika® ViscoCrete®-3045. It is a brown liquid that is ready to use and is a non-chlorinated water-reducing plasticizer based on modified polycarboxylates (NF EN 934-2 [198], Tables II. 3). It is ideal for usage on-site and in the ready-mixed concrete industry due to its long rheology holding duration (>1H30). Concretes that are plastic to fluid, low W/C concretes with or without silica fume, and concretes that are pumped over long distances can all be produced with Sika® ViscoCrete®-3045. It increases stability, lowers the chance of segregation, and lessens

the formula's sensitivity to changes in water and ingredient levels in fluid concretes. Table III. 3 shows its physical characteristics.

Table III. 3 : Physical Characteristics of the Admixture

Characteristic	Designation
Form	Liquid
Colour	Green Brown
PH	5 ± 1
Rate of cl^- ions	≤ 0.1 %
Rate of eq Na_2O	≤ 2.5 %
Dry Extract	36.4 ± 1.8 %
Recommended Dosage	0.25 à 2.5 %
Usual Dosage	0.3 à 0.6 %

The appendix (2) contains a technical data sheet that contains more information about the product.

III. 2.4. Fine Aggregates (Sand)

Near this study, two types of sand were used as fine aggregates: siliceous alluvial sand (STB) from El Houidjbette near Tebessa, in the northeast, and dune sand (SD) from Biskra, in eastern Algeria. While both STB and SD sands were utilised in the second half of the investigation, only STB sand was used in the first. These sands' extraction locations are shown in Figures III. 2 and III. 3.

Figure III. 2 : Dune Sand Extraction Site (Biskra, Algeria)

Figure III. 3 : Extraction Site of Siliceous Alluvial Sand (Tebessa, Algeria)

Tables III. 4 and III. 5 show the physical characteristics and chemical compositions of the two sands [291–295].

Table III. 4 : Physical Characteristics of Sands

Sand	γ_{app} (t/m^3)	γ_{abs} (t/m^3)	Mf -	Compacity (%)	Porosity (%)	VSE (%)	PSE (%)
SD	1.477	2.55	1.34	57.92	42.08	85	80
STB	1.346	2.47	1.96	54.49	45.51	85	80

Table III. 5 : Chemical Compositions of Sands

Sand	Chemical components (%)					
	Iron	CaO	SiO_2	Al_2O_3	MnO_4	PF
SD	0.55	15.90	57.48	1.27	traces	12.75
STB	0.57	0.85	77.80	0.61	traces	1.24

The proportion by grain size of both sand types is shown in Table III. 6. The gradation curves are displayed in Figure III. 4 [296, 297].

Table III. 6 : Grain Rate by Size

Sand	Rate of grains (%)		
	< 100 µm	0.250 to 0.500 µm	> 2000 µm
SD	0.45	19.44	0.00
STB	5.70	26.87	2.25

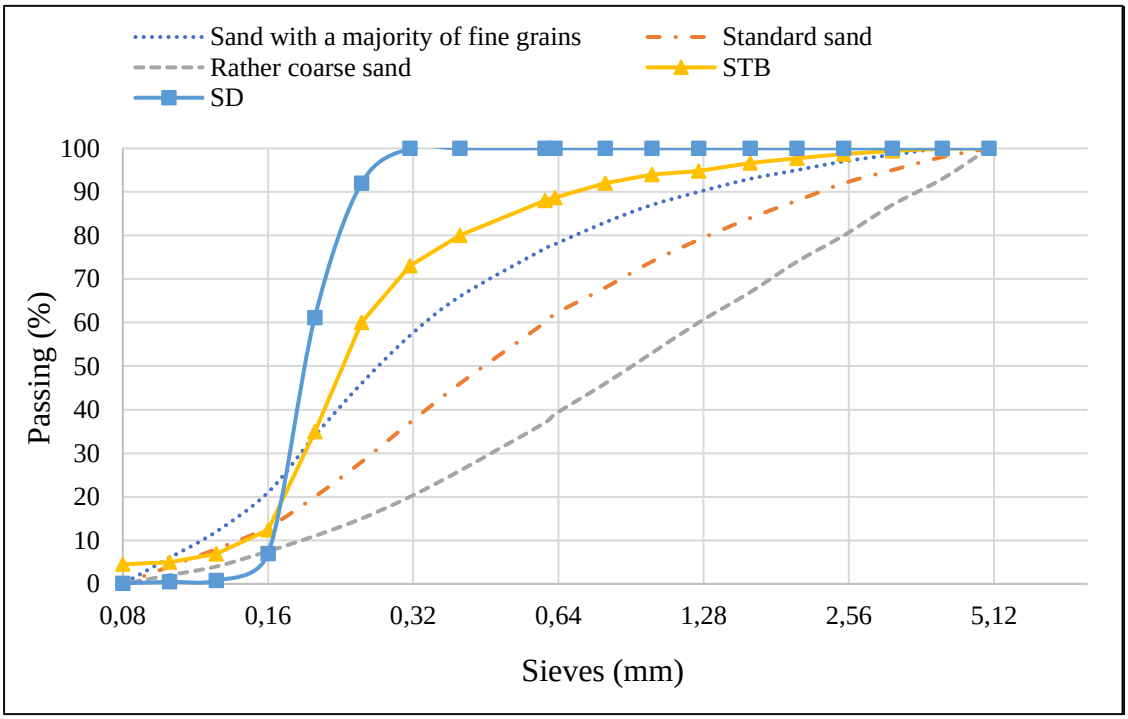

Figure III. 4 : Gradation Curves of Both Sand Types (STB and SD)

Electron microscope and sand microscopic observations are shown in Figure III. 5.

Figure III. 5 : Electron Microscope and Sand Microscopic Observations

III. 2.5. Coarse Aggregates (Gravel)

In this investigation, two different kinds of coarse aggregates were used: demolition coarse aggregates (DAs) and natural coarse aggregates (NAs). The limestone rocks from the Ain Abid quarry in Guelma, northern Algeria, were the source of the Natural Coarse Aggregates. Three different size fractions were identified from these aggregates: 3/8 mm, 8/16 mm, and 16/25 mm. Their gradation curves, which display the distribution of particle sizes within each fraction, are shown in Figure III. 6..

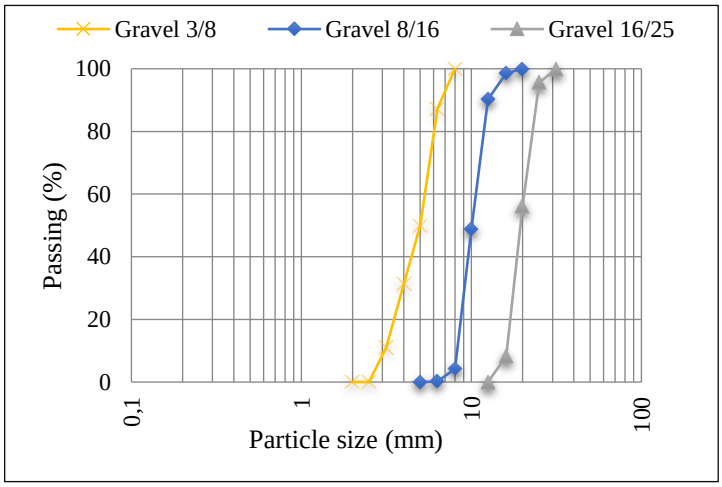

Figure III. 6 : Gradation Curves of Natural Aggregates (NAs)

Table III. 7 shows the particular refusal in percent obtained from the NA gradation analysis.

Table III. 7 : Particular Refusal of NA Sub-Fractions

(d/D)	Refusal particular a_i (%)		
	(3/8)	(8/16)	(16/25)
(2/3.15)	9.39	5.44	6.85
(3.15/4)	10.93		
(4/5)	20.40		
(5/6.3)	18.46		
(6.3/8)	37.41	0.18	
(8/10)	3.41	4.11	
(10/12.5)		44.42	
(12.5/16)		41.59	8.23
(16/20)		8.30	47.79
(20/25)		1.40	43.98

For this investigation, two types of regular parent concretes (PCs) were used to obtain demolition coarse aggregates (DAs). DAs were obtained from a 28-day ordinary concrete manufactured in a laboratory for part 1, and from a 2-year ordinary concrete created in a laboratory for part 2. Following a comprehensive examination, the physical characteristics of the coarse aggregates employed in sections 1 and 2 of the study are shown in Tables III. 8 and III. 9, respectively. These tables offer thorough information on the DAs' attributes [139, 140, 201, 298].

Table III. 8 : Physical Characteristics of the Coarse Aggregates Used in Part 1 of the Study

Characteristic	Unit	NAs	DAs
Absolute density	(t/m^3)	[2.60 - 2.65]	[2.28 - 2.40]
Apparent density	(t/m^3)	[1.60 - 1.70]	[1.14 - 1.40]
Water Absorption Coefficient	(%)	[1.12 - 1.40]	[1.30 - 8.70]
LA Coefficient	-	[22.5- 23]	[28 - 36]

Table III. 9 : Physical Characteristics of the Coarse Aggregates Used in Part 2 of the Study

Characteristic	Unity	NA 8/16	NA 16/25	DA 8/16	DA 16/25
Absolute density	(t/m^3)	2.6	2.6	2.4	2.3
Apparent density	(t/m^3)	1.7	1.6	1.4	1.35
Water Rate	(%)	1.0	1.0	1.0	1.0
Water Absorption Coefficient	(%)	4.20	1.12	6.22	4.16

LA Coefficient	-	23.0	22.5	30.0	32.0
MDE Coefficient	-	15.0	14.0	18.0	19.0
MDS Coefficient	-	20.0	21.0	23.0	24.0
Volumetric Coefficient	-	0.15	0.64	0.17	0.31

Figure III. 7 shows natural and demolition coarse aggregates used in part 2 of the study.

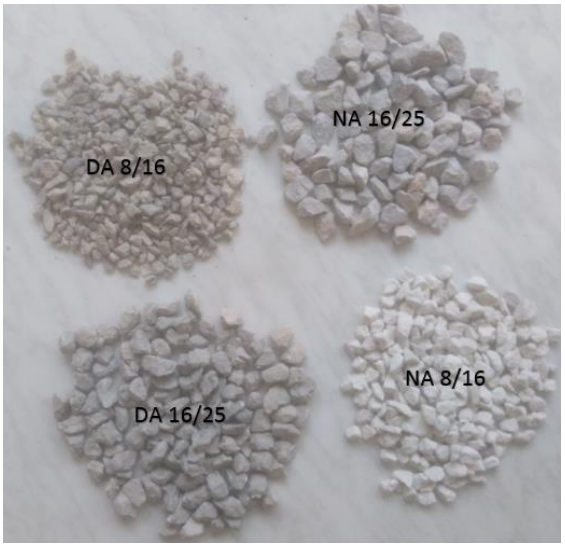

Figure III. 7 : Natural and Demolition Coarse Aggregates Used in Part 2 of the Study

III. 3. EXPERIMENTAL METHODOLOGY

The experimental investigation is divided into two primary sections, as stated in this chapter's introduction:

First Part: Production and Selection of Demolition Coarse Aggregates

Based on the size ratio of the demolition aggregates to the natural aggregates from the original concrete, this section focusses on choosing the best-quality demolition aggregates. Starting with the manufacture of parent concretes and then breaking them up into sub-fractions of different sizes, the experimental program mainly evaluates the demolition aggregates' ability to absorb water. To replicate the particle size distribution of the natural aggregates utilised in the original concrete formulation, fractions of 3/8 mm, 8/16 mm, and 16/25 mm were then rebuilt. It was possible to identify the demolition aggregate fractions with lower absorption rates, suggesting superior quality, thanks to the final evaluation of their water absorption ability.

Second Part: Use of Demolition Coarse Aggregates and Saharan Dune Sand in Concrete Formulation

The results from the first section are partially expanded upon in this section, especially with relation to the calibre of the demolition aggregates chosen for additional study. This section's experimental program examines how concrete mixtures containing replacement materials—specifically, demolition gravel and Saharan dune sand from Biskra—behave. The performance of these concrete mixtures is assessed in the study under extreme circumstances, such as high temperatures, chemical exposure, freeze-thaw cycles, and abrasion. This section attempts to improve knowledge of the durability and mechanical qualities of concrete made from recycled resources by investigating the interactions between the chosen aggregates and the environmental stresses.

III. 3.1. Part 1: Production and Selection of Demolition Coarse Aggregates with Low-Water Absorption

The maximum size of the natural aggregates that comprised the original concrete and the maximum size of the demolition aggregates that were produced after crushing the original concrete are the two parameters that are monitored in this section as it examines the absorption of demolition aggregates. The goal is to create demolition aggregates that can absorb less water without the need for special treatments. This will enable the selection of appropriate demolition aggregates for concrete formulation.

III. 3.1.1. Parent Concretes Manufacturing

Seven types of regular concrete are prepared in a lab to act as parent concretes once they cure, which is the first step in the creation of Demolition Coarse Aggregates (DAs). These parent concretes are necessary to produce DAs of superior grade. These concrete mixes are made as part of the experimental procedure, and after they have had time to solidify, they are crushed and broken apart. The different sizes of DAs that are produced by this fragmentation are then evaluated for their physical characteristics, with an emphasis on their ability to absorb water. The objective is to choose the DAs with the least amount of water absorption because this property is essential to guaranteeing the functionality and longevity of the finished concrete. Researchers can determine which aggregates are best suited for usage in novel concrete formulations by examining the DAs' size distribution and water absorption. By lowering dependency on natural aggregates, this strategy not only encourages the recycling of building materials but also supports sustainable building practices. In order to maximise the quality of the recycled aggregates and, eventually, improve the performance of the concrete made

from these materials, it is essential to carefully choose parent concrete compositions that are suited to the desired DAs fractions.

III. 3.1.1.1. Formulation Method

The DREUX-GORISSE mixing method was used in the lab to create regular concrete specimens (PCs) [195]. The ideal combination of aggregates, cement, and water content must be carefully chosen in order to produce concrete with the required workability and strength. The analysis was predicated on certain data, such as the sand's fineness modulus, cement class, workability, maximum aggregate size, density of different aggregates, compactness, clamping intensity, and average compressive strength after 28 days. A schematic granular reference curve was created in order to define the proportions of aggregates in absolute volume. Weight doses may be computed if the aggregates' density was determined. The concrete was then put through tests, and the recipe was altered as needed for the experiments. One, two, or three fractions of natural aggregates (NAs) with sizes of 3/8 mm, 8/16 mm, and 16/25 mm were used to create a total of seven different types of concrete. These were one quaternary mixture (PC7), three ternary mixtures (PC4, PC5, and PC6), and three binary mixtures (PC1, PC2, and PC3). The final concrete's quality was on par with that of the majority of Algerian-made concretes and historic structures that were in danger of being demolished [299, 300]. Interestingly, the granular skeleton of PC1, PC4, and PC7 was continuous, but the granular skeleton of the other mixes was discontinuous. This wide variety of concrete formulas made it possible to thoroughly assess each one's mechanical characteristics and performance in a range of scenarios. Table III. 10 provides a summary of the composition, density, and water-to-cement ratio (W/C) of the parent concretes (PCs).

Table III. 10 : Parent Concretes Composition

Designation	Unit	Proportioning of components in parent concrete						
		PC1	PC2	PC3	PC4	PC5	PC6	PC7
Cement	kg/m^3	400.000	398.310	360.290	398.310	360.290	360.290	360.290
Water	liter/m^3	200.000	207.120	194.560	207.120	194.560	194.560	194.560
Silicious Sand	kg/m^3	503.250	605.071	650.072	466.770	527.085	579.790	456.807
NA 3/8	kg/m^3	1221.220	-	-	269.690	383.720	-	219.270
NA 8/16	kg/m^3	-	1168.652	-	1042.800	-	383.720	292.360
NA 16/25	kg/m^3	-		1151.150	-	895.342	840.520	840.520

W/C	-	0.50	0.52	0.54	0.52	0.54	0.54	0.54
Density	kg/m^3	2324.470	2379.153	2356.072	2384.690	2360.997	2358.880	2363.807

III. 3.1.1.2. Mixing Plan

The dry aggregates and cement were put one after the other to a 35-liter concrete mixer after the proportions of the various components of the concrete had been determined and weighed. After that, the components were dry mixed for two minutes to guarantee even distribution. After that, all of the mixing water was added without stopping the mixer, and wet mixing went on for two more minutes, for a total of four minutes of mixing time. Then, right away, the new concrete was poured into cubic moulds that were 10 cm across. To remove air pockets and guarantee adequate compaction, the moulds were filled in two layers, each of which was vibrated for 30 seconds. controlled laboratory setting at 22 C° and 75% relative humidity. The samples were demolded, labelled, and then stored in water tanks for 27 days following a 24-hour exposure to the open air, as per standard NF P 18-405 [301]. In order to accurately analyse the concrete specimens' mechanical qualities later in the study, this meticulous process guarantees that they reach their ideal strength and durability. The hydration process and the overall quality of the concrete are greatly influenced by the controlled curing environment.

III. 3.1.1.3. Preparation of Specimens

According to the European standard NF EN 12390-1 and the French standard NF P18-404, 105 parent concrete (PC) samples, each 10 x 10 x 10 centimetres, were produced and allowed to cure under regulated conditions [302, 303]. Specimens are created and dried in a manner that ensures dependability in terms of both performance and quality. The samples underwent a standard curing process to guarantee optimal moisture and strength increase. Comparing different formulas and aggregate types used in later stages of the research is made easier by this methodical approach, which enables reliable testing and evaluation of the concrete's mechanical properties. By adhering to these predetermined criteria, the research aims to produce concrete that either matches or exceeds the performance characteristics typical of regular concrete used in construction.

III. 3.1.2. Physical Characterisation of Fresh Parent Concrete

III. 3.1.2.1. Workability

According to EN 12350-2 standard, the slump test is used to assess the workability of fresh concrete [304]. Three equal levels of concrete are added to a typical Abrams cone as part of the test. Each layer is condensed by striking it 25 times with a metal tamping rod. The top surface of the concrete is then levelled by passing the tamping rod across the top of the cone. The cone is then elevated vertically to allow the concrete to settle on its own. The concrete's workability and flexibility are directly correlated with the amount of settling, or slump. A higher slump indicates a more workable, more pliable concrete composition. To measure the slump, an inverted cone is placed near the slumped concrete. A ruler is used to measure the vertical distance between the top of the cone and the highest point on the surface of the drooping concrete. In centimetres, this is the reported slump value. Figure III. 8 illustrates the key steps in the slump test procedure. The slump test is a simple and reliable way to assess the workability of fresh concrete. It enables the concrete to be compacted and set securely inside the formwork. The test is widely used in the construction industry to evaluate the consistency and calibre of concrete.

Figure III. 8 : Steps in the Abrams Cone Procedure for Measuring Slump

The NF EN 206-5 standard classifies concrete slump into five groups (Table III. 11).

Table III. 11 : Concrete Slump Groups

Class	Slump (mm)	Property of fresh concrete
S1	10 – 40	Firm, very dry and poorly workable
S2	50 – 90	Plastic, medium moisture and medium workability
S3	100 – 150	Very plastic, very wet and high workability

S4	160 – 210	Fluid, very wet and high workability
S5	≥ 220	Very fluid, very wet and high workability

All PC types were kept at a 7±2 cm slump, in accordance with industry standards [304].

III. 3.1.3. Mechanical Characterisation of Hardened Parent Concretes

The concrete specimens were put through a mechanical test to determine their compressive strength. This test revealed information on the parent concrete mixtures' ability to support loads.

III. 3.1.3.1. Compressive Strength

The EN 12390-3 standard [305] was followed for conducting the compressive strength measurements. Specimens were tested when they were 28 days old to make sure they had uniform surface features and good flatness.

Test Principle: The specimen is put through a series of increasing loads until it fails. The ratio of the specimen's failure load (F) to cross-sectional area (S), given in megapascals (MPa), is used to compute the compressive stress (σc):

$$\sigma_c = \frac{F}{S} \qquad III.\ 1$$

Where:

S is the specimen's cross-sectional area (in mm2), F is the failure load (in N), and σc is the compressive stress (in MPa).

The average of the findings from six specimens is used to calculate the compressive strength. After a 28-day curing period, 10×10×10 cm^3 cubic specimens of the parent concrete were evaluated to assess their quality. Studies show that the performance of concrete created using aggregates taken from parent concrete is highly dependent on the quality of the parent concrete [15, 264, 306]. In particular, a bigger influence from the parent material's quality is correlated with higher performance requirements for the final concrete. Results of tests on 42 specimens showed compressive strengths ranging from 25.41 to 42.38 MPa. These results highlight how crucial it is to formulate recycled concrete mixtures with high-quality parent concrete.

III. 3.1.4. Demolition Aggregates Manufacturing

The parent concrete samples that had cured for 28 days were taken out of the water and left to air dry in order to prepare the Demolition Coarse Aggregates (DAs). A metal mass was used to break up the concrete into smaller bits once the surface moisture had

evaporated. As illustrated in Figure III. 9, the resulting pieces were sized to pass through a jaw crusher's input opening, with the distance between the crusher jaws being modified in accordance with the maximum aggregate size intended for production.

Figure III. 9 : Concrete Broken into Pieces and Jaw Crusher

Crushed materials were sent through a succession of designated sieves by hand shaking. Using the standardised screening method demonstrated in our experiment, these materials were passed through sieves arranged from largest to smallest in descending order of mesh size (detailed in Figure III. 10). DAs larger than 25 mm in diameter were crushed and then sieved once more. DAs that were less than two mm in diameter were discarded. The remaining particle matter was collected separately after going through each sieve and dried in an oven until a uniform bulk was achieved. This process was done to collect adequate dry DA sub-fractions (2/3.15), (3.15/4), (4/5), (5/6.3), (6.3/8), (8/10), (10/12.5), (12.5/16), (16/20), and (20/25) mm for the subsequent water absorption test. Figure III. 11 provides examples of the types and sizes of crushed DAs that were collected. This careful fractionation allowed for a comprehensive analysis of the water absorption characteristics across a range of particle sizes, providing valuable data for many commercial and scientific applications. To be compatible with the original NA samples, three new fractions (3/8), (8/16), and (16/25) mm were rebuilt with the same particle size distribution.

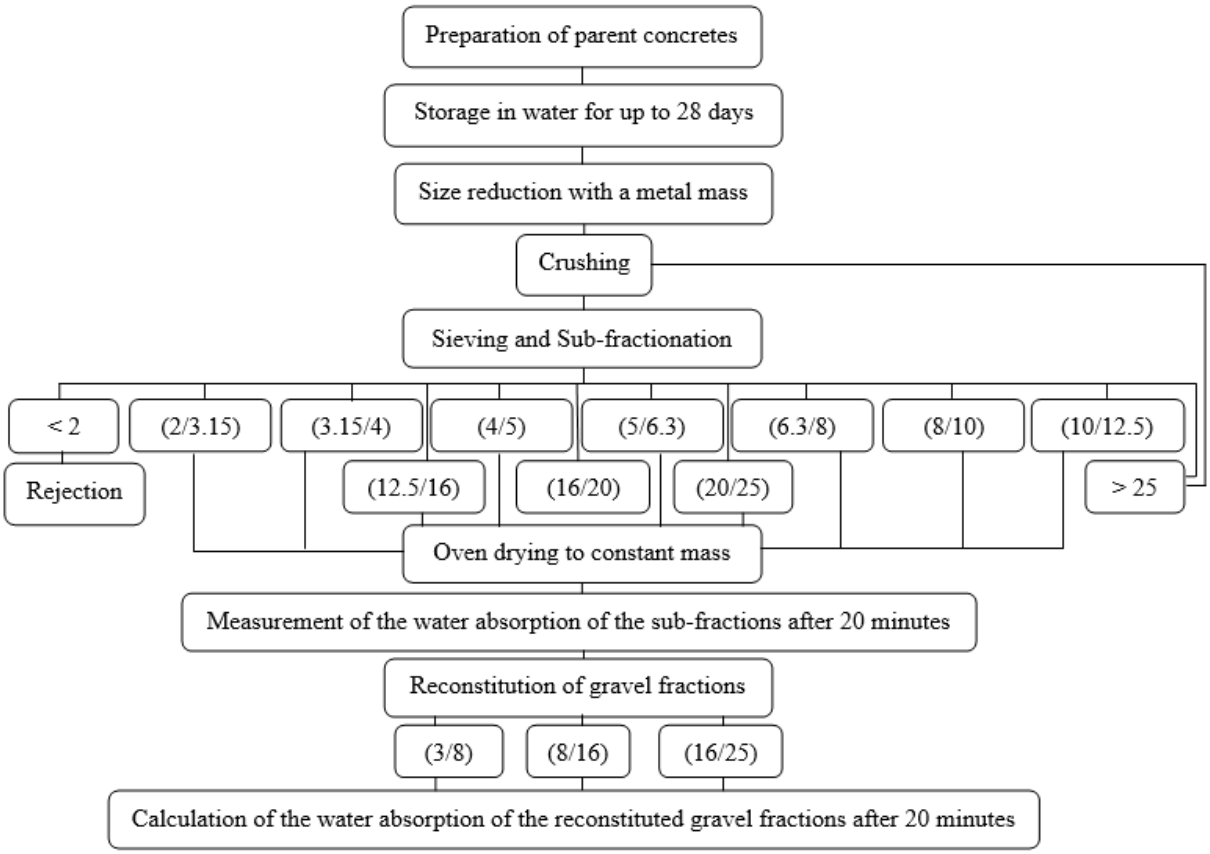

Figure III. 10 : Procedure for the Preparation of DAs and Quantification of Water Absorption

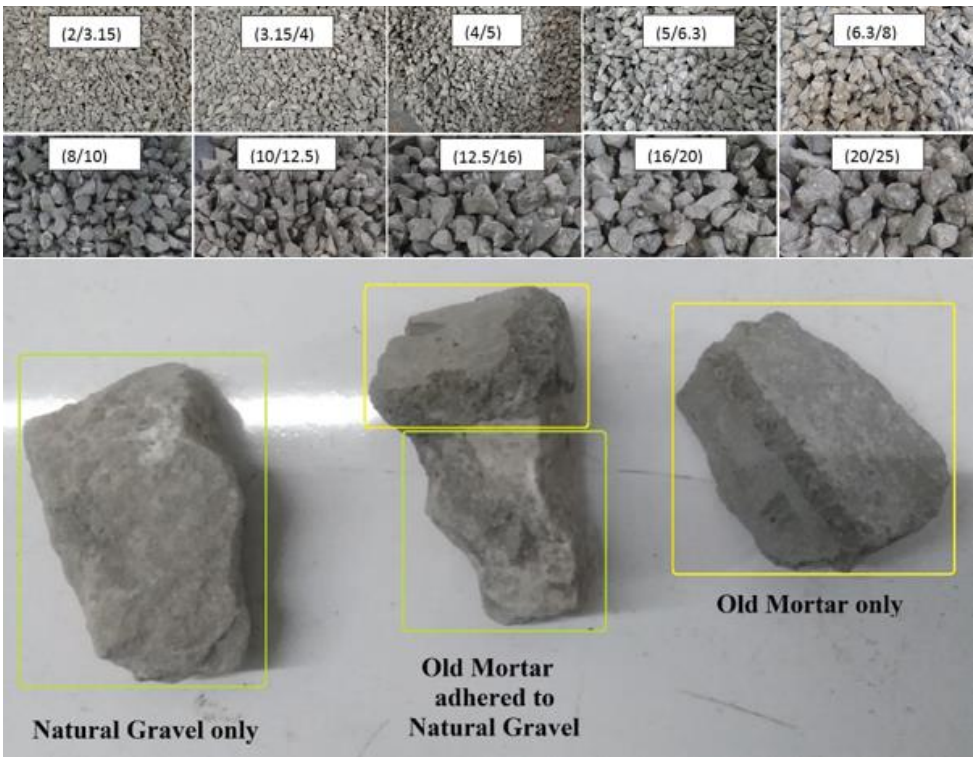

Figure III. 11 : Example Showing Sizes and Types of the Crushed DAs

III. 3.1.5. Physical Characterisation of Demolition Aggregates

The most important aspect affected is concrete's workability, which is greatly influenced by DAs' high water absorption [307]. According to Y. L. Kun Liang et al. [308], the water absorption of DAs increases rapidly in the early stages. The first 10 minutes are when the DAs reach about 90% of their water-absorbing capability. After then, but more slowly, DAs continue to absorb water until they reach saturation. Zhenhua Duan A. et al. [309] found a connection between water absorption during the first 24 hours and water absorption for the entire 24-hour period. It is possible to forecast water absorption throughout a 24-hour period from the early phase and vice versa. Due to the large number of samples, this experiment was limited to water absorption after 20 minutes only in order to save time.

III. 3.1.5.1. Water Absorption of Demolition Aggregate Subfractions

After being weighed, the DA subfractions were dried in an oven at 110 ± 5 °C until they reached a constant mass, and then they were immersed in tap water at 20 ± 2 °C. After 20 minutes, they were taken out of the water, patted dry with a cloth, and weighed once more. These stages are illustrated in Figure II. 12.

Figure III. 12 : Water Absorption Test Steps

According to NF EN 1097-6, three specimens from each of the 70 DA sub-fractions underwent the water absorption test [310]. Equation (III. 2) was used to calculate the water absorption:

$$abs_i = 100 \text{ x } \frac{m_h - m_d}{m_d} \qquad III.\ 2$$

where "m_h" is the sample's mass following immersion, "abs_i" is the percentage of water absorbed, and "m_d" is the sample's original mass before drying. The mean values of the results were shown.

III. 3.1.5.2. Reconstitution of Demolition Aggregate Fractions

Three fractions, (3/8), (8/16), and (16/25) mm, having the same particle size distribution as the NA fractions, were created by combining the DA sub-fractions. The intended mass (m) of the DA fraction may be multiplied by the factor (a_i) divided by 100 to find the mass (m_i) of each DA sub-fraction. The specific rejection expressed as a percentage of the comparable NA sub-fraction is the "a_i" factor. It is possible to compute the mass (m_i) of each DA sub-fraction using equation (III. 3).

$$m_i = \frac{m \text{ x } a_i}{100} \qquad III.\ 3$$

where "m_i" stands for the mass of the DA sub-fraction, "m" for the required mass of the DA fraction, and "a_i" for the specific rejection expressed as a percentage of the corresponding NA sub-fraction.

III. 3.1.5.3. Water Absorption of Demolition Aggregate Fractions

Equation (III. 4) was used to directly compute the DA fraction's water absorption.

$$abs = \frac{1}{100} \text{ x} \sum (abs_i \text{ x } a_i) \qquad III.\ 4$$

where "abs" stands for the DA fraction's water absorption, "abs_i" for the DA sub-fraction's water absorption, and "a_i" for the specific rejection expressed in percentage of the comparable NA sub-fraction previously shown in Table III. 7 below.

III. 3.1.6. Algorithm

The following is the search algorithm for the part 1 of the study:

- Parent concrete preparation
- Holding for up to 28 days in water
- Reduction of size using a mass of metal
- Crushing.

• (2/3.15), (3.15/4), (4/5), (5/6.3), (6.3/8), (8/10), (10/12.5), (12.5/16), (16/20) and (20/25) mm are the sieving and sub-fractionation dimensions
• Rejecting agglomerates that are less than 2 mm
• Repeating the earlier procedures (beginning with crushing) for particles bigger than 25 mm
• Drying in the oven at a steady mass
• After 20 minutes, the subfractions' water absorption is measured
• The gravel fractions' reconstitution is as follows: (3/8), (8/16), and (16/25) mm
• The reconstituted gravel fractions' water absorption after 20 minutes is calculated

III. 3.1.7. Time and Location Conditions

Table III. 12 summarises the conditions at the time and place.

Table III. 12 : Time and Place Conditions for the Tests

Operation	Time	Temperature	Location	Device/Tool	Standards
PC manufacturing	14 hours	20±2 °C	Laboratory setting	35-liter concrete mixer	NF P18-405
Curing	28 days	20±2 °C	Laboratory setting	Water tank	NF P18-404
Size reduction	4 hours	20±2 °C	Laboratory setting	Metal mass	-
Crushing	3 hours	20±2 °C	Laboratory setting	Jaw crusher	-
Fractionation	7 days	20±2 °C	Laboratory setting	Sieves	-
Oven drying	48 hours	105±5 °C	Laboratory setting	Oven	-
Dry weighing	10 seconds	20±2 °C	Laboratory setting	Precision Scale 0.1 gr	NF EN 1097-6
Water immersion	20 minutes	20±2 °C	Laboratory setting	water container	NF EN 1097-6
Dewatering	10 seconds	20±2 °C	Laboratory setting	Sieve	NF EN 1097-6
Surface drying	20 seconds	20±2 °C	Laboratory setting	Dry cloth	NF EN 1097-6
Wet weighing	10 seconds	20±2 °C	Laboratory setting	Precision Scale 0.1 gr	NF EN 1097-6

Through the ratio between the maximum diameters of the two aggregates (DAD_{max}/NAD_{max}), where DAD_{max} represents the maximum diameter of demolition aggregates (DAs) and NAD_{max} that of natural aggregates (NAs), the results of the water absorption tests were analysed to look for a potential relationship between the size of the natural aggregates (NAs) composing the parent concrete (PC) and that of the demolition aggregates (DAs) recovered. The analysis's goal is to identify the threshold ratio that, when met, permits the production of demolition aggregate sub-fractions (DAs) with a minimum adherent mortar (OM) content, or a minimum capacity to absorb

water. This, in turn, yields DA fractions with a minimum capacity to absorb water. The latter is similar to that of natural aggregates in this sense.

III. 3.2. Part 2: Use of Demolition Coarse Aggregates and Saharan Dune Sand in Concrete Formulation

This section investigates whether coarse demolition aggregates and dune sand from the Sahara (Biskra) can be combined to make regular concrete. The objective is to evaluate the possible advantages of this combination and ascertain whether it is feasible to use these materials together to create concrete of a suitable quality.

III. 3.2.1. Parent Concrete Manufacturing

Unlike Part 1 of this investigation, Part 2 used regular concrete that was two years old and had been made by another PhD student as the parent material. Regretfully, there are no details available about the concrete formulation and material characterisation of this parent concrete. A visual inspection was carried out to determine the maximum diameter of the natural aggregates employed, and the results showed that the maximum aggregate size was 25 mm. This strategy emphasises the need for observational approaches in the absence of comprehensive material data, allowing the study to proceed while recognising the limitations of the information at hand.

III. 3.2.2. Demolition Aggregates Manufacturing

The second part of this study was manufactured using the same procedures that were set up in the first component. The two-year-old regular concrete was transformed into unreinforced beams that measured 15x20x120 cm^3 and cubic specimens that were 10 cm on each side. Using a metal sledgehammer, this reduction was first done by hand. A jaw crusher was then used to crush the material (Figure III. 13). The jaws were spaced apart to create the maximum aggregate size that was required, and the concrete pieces were sized to fit through the jaw crusher's input hole. (8/16) mm and (16/25) mm were among the retained granular fractions, guaranteeing that the aggregates fulfilled the requirements for later concrete compositions. Because of the methodology's uniformity, the results from the two parts of the study may be reliably compared.

Figure III. 13 : Size Reduction of an Unreinforced Beam and Crushing Result

The largest aggregate size that could be produced dictated the jaws' spacing, and the jaw crusher's entry mouth was made to fit the size of the concrete particles. Both the (8/16) and (16/25) granular fractions are retained.

III. 3.2.3. Son Concretes Manufacturing

Combinations of sand and gravel (Figure II. 14) have allowed us to create four different kinds of common concrete, which are as follows:

• Tebessa (NASTBC) alluvial sand and natural gravel in concrete acting as a control

• Concrete made using Biskra dune sand and natural gravel (NASDC)

• Biskra dune sand and concrete with demolition gravel (DASDC)

• Concrete with alluvial sand from Tebessa and demolition gravel (DASTBC)

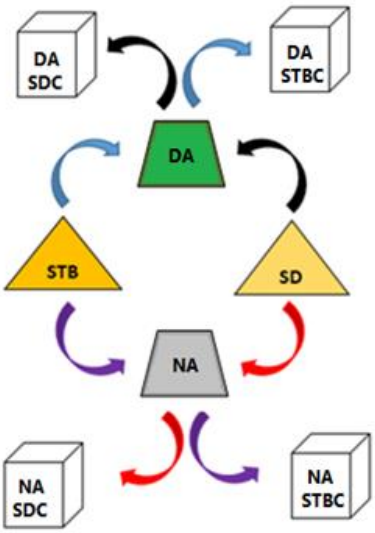

Figure III. 14 : Sand and Coarse Aggregates Combinations

III. 3.2.4. Formulation Method

The formulation approach that B. Scramtaïev suggested was used. This method's basic idea is explained in section II.7.5. Concrete formulation approaches. Calculations are used to initially estimate the composition of concrete, which includes the amounts of

cement, water, sand, and gravel. Experimental mix design techniques are then used to refine the composition.

III. 3.2.5. Aggregate Water Demand and Effective W/C Ratio

The water absorption rates by aggregate type are shown in Figure III. 15, and the total water consumption for different concrete formulations is shown in Figure III. 16. Furthermore, the aggregates' water absorption levels, matching water demands, and effective water-to-cement (W/C) ratios are compiled in Table III. 13. This thorough analysis provides important insights for improving concrete formulations by highlighting the connection between the type of aggregate used and its effect on the total water requirements of the concrete mixtures.

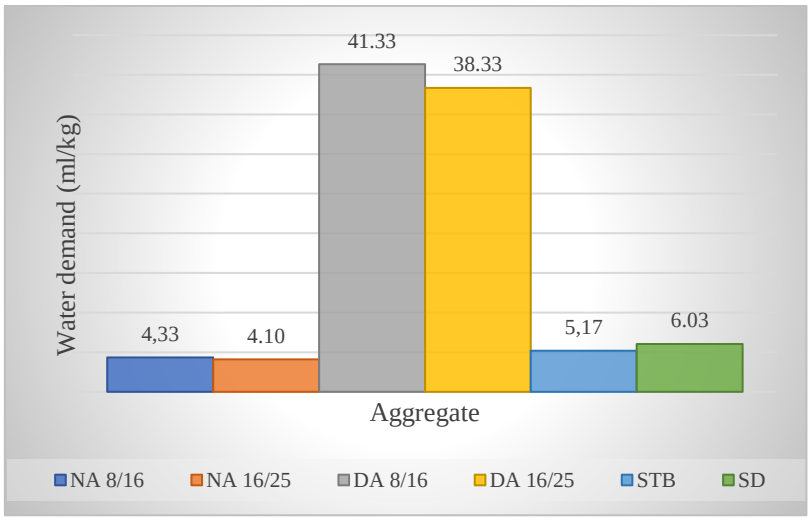

Figure III. 15 : Water Absorption by Aggregate Type

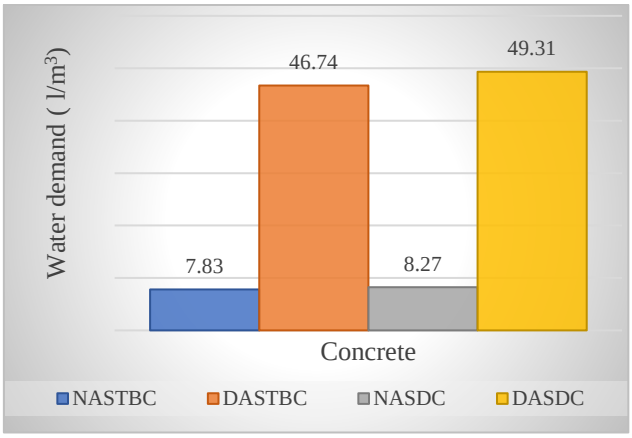

Figure III. 16 : Total Water Demand in Concrete Formulations

Table III. 13 : Aggregates Water Absorption, Water Demand and W_{eff} /C

Designation	Concrete				
	Unit	NASTBC	DASTBC	NASDC	DASDC
Aggregates water absorption	l/m^3	7.83	46.74	8.27	49.31
Total water	l/m^3	210	210	175	210
Effective water	l/m^3	202.17	163.26	166.73	160.69
Cement dosage	Kg/m^3	350	350	350	350
W_{eff} /C	-	0.58	0.47	0.48	0.46
W/C	-	0.6	0.6	0.5	0.6

III. 3.2.6. Workability

The Abrams cone test was used to evaluate the concrete's workability in accordance with standard EN 12350-2 [304], as explained in section II. 8.1.1. Workability. The target slump for all types of concrete was kept at 7±2 cm. The results of the slump test performed on one of the concrete mixtures under study are shown in Figure III. 17. This measurement is essential for making sure the concrete can be compacted and put readily during construction, which will eventually impact the finished structure's durability and overall performance.

Figure III. 17 : Result of the Slump Test Conducted on One of the Concrete Mixtures Studied

III. 3.2.7. Density

A standardised 8-liter hydrometer base and a balance that could measure the mass of fresh concrete to the closest 0.1 g were used to precisely and consistently measure the density of fresh concrete. A representative quantity of concrete can be held in the hydrometer base, which is a suitable container. In order to remove trapped air bubbles

and guarantee adequate compaction, the concrete is placed in two layers and vibrated for 30 seconds on a vibrating table during the filling process. To guarantee that the volume of concrete precisely fits the interior of the container, the upper sides are levelled with a metal ruler after filling [311]. Weighing a known volume of fresh concrete is shown in Figure III. 18 using equation (III. 5).

$$\rho_{fc} = \frac{m - m_0}{V} \qquad III.\ 5$$

Where:

ρ_{fc} is the fresh concrete density (kg/m^3)

m_0 is the empty container mass (kg)

m is the mass of container filled with fresh concrete (kg)

V : Container internal volume (m^3)

Figure III. 18 : Weighing of a Known Volume of Fresh Concrete

III. 3.2.8. Occluded Air

Air is the only compressible component in fresh concrete, under the specifications of standard NF EN 12350-7 [312]. This test's objective is to measure the amount of entrained air to confirm that, in the event of frost, the standard's minimal amount is actually reached. The air content of plastic concrete can be determined using a variety of techniques, such as the gravimetric, volumetric, and pressure methods. Using a pressure air meter for concrete and the pressure method, the entrained air content (Oa) was measured (Figure III. 19). Entrained air concentrations range from 0.8% to 1.25 percent, according to the measurement results.

Figure III. 19 : Aerometer with Manometer

III. 3.2.9. Concrete Composition and Physical Properties

The compositions of the different concrete types and their physical properties in the fresh state are gathered in Tables III. 14 and III. 15 consecutively.

Table III. 14 : Concretes Composition

Dosage	NASTBC	DASTBC	NASDC	DASDC
C (kg/m^3)	350	350	350	350
W (liter)	210	210	175	210
STB (kg/m^3)	619.961	626.866	-	-
SD (kg/m^3)	-	-	488.735	571.742
NA 8/16 (kg/m^3)	300.837	-	258.057	-
NA 16/25 (kg/m^3)	811.327	-	1024.333	-
DA 8/16 (kg/m^3)	-	351.193	-	382.653
DA 16/25 (kg/m^3)	-	756.066	-	783.730
Plasticizer (%)	-	0.25	-	-

Table III. 15 : Concretes Physical Properties in the Fresh State

Property	NASTBC	DASTBC	NASDC	DASDC
G/S (-)	1.79	1.77	2.62	2.04
W/C (-)	0.6	0.6	0.5	0.6
S (cm)	7.0	8.0	6.5	7.0
Oa (%)	1.0	1.25	0.8	1.2
γcal (kg/m^3)	2292.125	2294.125	2296.125	2298.125
γr (kg/m^3)	2291.125	2290.00	2400.125	2373.938

III. 3.2.10. Preparation of Specimens

Until the day of testing, specimens that were cubic (10x10x10) cm^3, prismatic (10x10x40) cm^3, and cylindrical (11x22) cm^3 were created and kept in water [204, 301, 303]. Hardened concrete specimens are displayed in Figure III. 20.

Figure III. 20 : Hardened Concrete Specimens

III. 3.2.11. Hardened Concrete Density

Weighing a hardened concrete specimen (Figure III. 21) and dividing its mass by its volume - which is computed based on the specimen's dimensions (see equation III. 6) - will yield the density of hardened concrete, which is commonly expressed in kilogrammes per cubic meter (kg/m³) in accordance with standard ISO 1920-5 [313]. This approach offers a simple and trustworthy way to evaluate hardened concrete's density, a crucial determinant of its quality and possible performance traits.

$$\rho_{hc} = \frac{m}{V} \qquad III.\ 6$$

Where:

P_{hc} is the hardened concrete density (kg/m^3)

m is the mass of hardened concrete specimen (kg)

V is the volume of hardened concrete specimen (m^3)

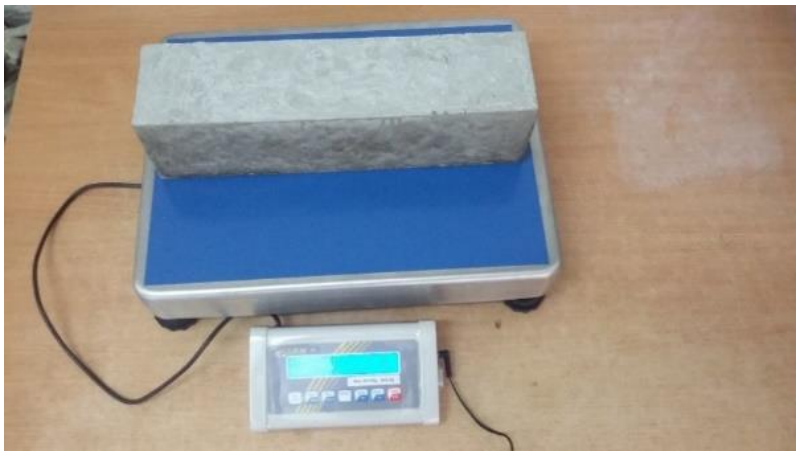

Figure III. 21 : Weighing of Hardened Concrete Specimen

III. 3.2.12. Mechanical Tests

Two indirect tensile tests (splitting and three-point flexural tests) and a compression test were performed. Two generations of regular concrete—a two-year-old parent concrete and four varieties of second-generation concrete, or son concretes—were subjected to the compression test. The son concretes were the specific focus of the two indirect tensile tests. For these testing, hydraulic presses with the required add-ons were used (Figure III. 22).

Figure III. 22 : Hydraulic Presses for the Mechanical Tests

III. 3.2.12.1. Compressive Test

Two generations of regular concrete were subjected to the compression test in accordance with the previously established testing methodology (III. 3.1.3.1. Compressive strength).

❖ Compressive Test of Parent Concretes

Compression testing was used to evaluate the quality of 10x10x10 cm³ cubic specimens of the parent concrete [305]. To guarantee consistent geometric shape and dimensions across all specimens, half (6) of the twelve specimens that were evaluated were removed from unreinforced beams using a concrete saw (Figure III. 23). This method eliminates the requirement for correction coefficients and ensures a fair comparison of performance across the various types of concrete [314–316].

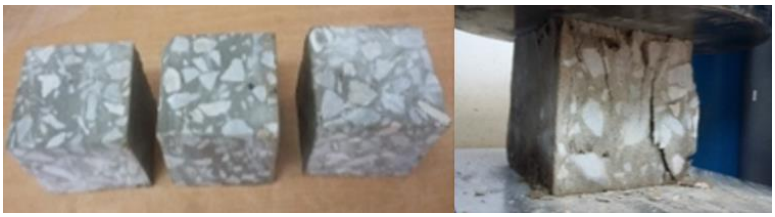

Figure III. 23 : Cubic Samples (10x10x10) cm3 Extracted from an Unreinforced Beam for a Compression Test

❖ Compressive Test of Son Concretes

To make comparisons between the control concrete and those that included substitute materials easier, cubic specimens of the same size (10x10x10 cm³) were tested in compression for each type of son concrete. Accurate and dependable testing of these specimens was made possible by the employment of hydraulic presses outfitted with the required attachments, which yielded important information on the mechanical characteristics of the parent and son concretes. This thorough testing approach is necessary to assess how well various materials work in concrete mixtures.

III. 3.2.12.2. Three Points Flexural Test

In accordance with NF P 18-407 guidelines [317], this destructive test is carried out on prismatic specimens that are 10×10×40 cm³. Finding the specimen's three-point flexural strength under a centred force applied with a hydraulic press is the goal. The average of the findings from three specimens is used to determine the tensile strength in megapascals (MPa). The test's mechanical diagram is displayed in Figure III. 24. The following relationship (III. 7) represents the flexural tensile stress:

$$\sigma_{fl} = \frac{3FL}{2b^3} \qquad III.\ 7$$

Where:

- σ_{fl} is the flexural tensile stress,
- F is the applied load,
- L is the span length between the supports,
- b is the width or the depth of the specimen (the width = the depth).

For assessing the structural integrity of concrete in a variety of applications, this method offers a trustworthy evaluation of the material's performance under bending stresses.

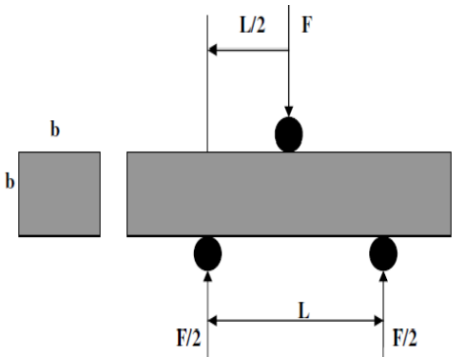

Figure III. 24 : Mechanical Diagram of the Three-Points Flexion Test

III. 3.2.12.3. Splitting Test

The NF EN 12390-6 standard [318] states that cubic specimens with dimensions of 10x10x10 cm³ are used to calculate the mechanical tensile strength by splitting (Figure III. 25). After 28 days of cure, the splitting test is carried out with a loading rate of 0.05 MPa/s. The formula III. 8 is used to determine the splitting tensile strength:

$$\sigma_{spl} = \frac{2F}{\pi l D} \qquad III.\ 8$$

Where:

σ_{spl} is the splitting resistance (MPa),

F is the maximum rupture load (N),

l is the length of the specimen (mm),

D is the lateral dimension of the specimen (mm).

For the purpose of evaluating the concrete's performance and longevity in structural applications, this test offers a trustworthy measurement of the material's tensile strength.

Figure III. 25 : Cubic Concrete Specimen Tested by Splitting

III. 3.2.13. Ultrasonic Pulse Velocity

Non-destructive ultrasonic pulse velocity testing can be used to assess the quality of concrete without inflicting any harm to the material. The measurement of the ultrasonic wave's propagation time through the concrete test specimen forms the basis of this method. It gives an estimate of the dynamic elastic module, mechanical resistance, and porosity of the material. Testing was done on cubic test specimens that measured 10x10x10 cm³ and cylindrical test specimens that measured 11x22 cm³ in accordance with standard NF P 18-418 [319]. The ultrasonic pulse velocity tester utilised is depicted in Figure III. 26.

Figure III. 26 : Ultrasonic Pulse Velocity Tester

III. 3.2.13.1. Device Description

The capacity to modify the ultrasonic pulse amplitude from 250 to 1000 V and a measurement range of 0 to 3000 µs with a resolution of ±0.1 µs are important features.

Up to 30,000 samples of test data can be collected, processed, and stored by the device, which can also measure the amount of time needed for the ultrasonic pulse to pass through the substance being examined. To guarantee the best possible sound wave transmission, it comes with two 55 kHz probes, connecting cables, a calibrating cylinder with a time constant of 42.5 µs, and contact paste.

III. 3.2.13.2. Results' Reading and Interpretation

The travel time (t) of an ultrasonic pulse through concrete is computed and displayed digitally. The faster the concrete spreads, the denser and more resistant it gets. Conversely, a lower speed indicates a larger porosity and a smaller mechanical performance. Consequently, this non-destructive method allows for quick and precise information on concrete quality without compromising the material's properties. The obtained data allows for continuous monitoring of the evolution of concrete characteristics and successfully completes the conventional destructive tests. The equation (III. 9) provides the ultrasonic wave's propagation speed.

$$V = \frac{L}{T} \qquad \textit{III. 9}$$

Where:

- L is the separation between the two sides of the concrete test specimen in contact with the two transducers
- V is the wave propagation speed (km/s)
- T is the ultrasonic wave propagation duration in seconds

III. 3.2.13.3. Dynamic Modulus of Elasticity

Using the following connection (III. 10), the dynamic modulus of elasticity (Ed) may be determined from the speed at which ultrasonic waves propagate:

$$E_d = \left(\frac{(1+\upsilon)(1-2\upsilon)}{(1-\upsilon)}\right)\rho . {V_m}^2 \qquad \textit{III. 10}$$

Where:

- E_d stands for dynamic elastic module (MPa)
- υ for non-damaged concrete's Poisson's coefficient (υ = 0.20)
- ρ for concrete density (kg/m^3)
- V_m is the mean wave propagation speed (km/s)

III. 3.2.14. Deformability

III. 3.2.14.1. Testing Program

Four varieties of concrete that were 28 days old (NASDC, DASTBC, DASDC, and NASTBC) were tested in order to determine how aggregate type affected the deformability of hardened concrete. Twelve examples of regular concrete, each measuring 11 by 22 cm³, were assessed for deformability using the methodology described by Mezghiche, B. (1996) [320]. As stated in section III.3.1.3.1 (Compressive Strength), Formula III.1 was used to determine the specimens' cylindrical strength. The behaviour of the material under stress was then evaluated by measuring both longitudinal and transverse deformations. A strain gauge frame is used to test deformability, as shown in Figure III. 27.

Figure III. 27 : Deformability Measurement by Strain Gauge Frame

III. 3.2.14.2. Longitudinal Deformation

Dial indicators that show microns were used to measure the longitudinal deformation. They were mounted in the centre of the concrete specimen using two suitable flat iron hoops. By tightening eight threaded pins (four per hoop) positioned such that each pair of adjacent pins is 90° apart and each pair of opposing pins is 110 mm apart, these hoops are brought into contact with the specimen's exterior face. The distance between the four higher pins and the bottom pins, measured longitudinally, is 140 mm. Through properly drilled and threaded holes in the hoops, the pins can move inward for tightening and outward for loosening (Figure II. 27). The stress-strain curves were used to calculate the modulus of elasticity values. Equation III. 11 states that the pair ($\sigma 1$; $\varepsilon 1el$) determines the modulus of elasticity.

$$E_{el} = \sigma_1 . \varepsilon_{1el} \qquad III.\ 11$$

where $\varepsilon_1$el is the strain brought on by the destructive stress, and σ_1 is the stress equal to 30% of the destructive stress. Equations III. 12 and III. 13 are used to derive σ_1 and $\varepsilon_1$el, respectively.

$$\sigma_1 = P_1 . S \qquad III.\ 12$$

where S is the specimen's cross-sectional area and P_1 is the load equal to 30% of the destructive load.

Equation III. 13 calculates the arithmetic average of the indicators on either side of the cylinder to estimate the increase in deformations.

where:

The specimens' absolute increase in longitudinal deformation in response to an increase in stresses is denoted by Δl_1.

$$\varepsilon_{1el} = \frac{\Delta l_1}{l_1} \qquad III.\ 13$$

The fixed base for calculating the specimens' longitudinal deformation is l_1. Formula III.14 provides the initial modulus of elasticity in compression.

$$E = \frac{\Sigma \Delta \sigma}{\Sigma \Delta \varepsilon} \qquad III.\ 14$$

where the total increase in stress at each degree from 0.05 to 0.3 Pc is represented by $\Sigma\Delta\sigma$. For every degree in the same range, $\Sigma\Delta\varepsilon$ is the total of the increases in instantaneous elastic longitudinal relative deformation.

This thorough testing method, which makes use of dial indicators and stress-strain curves, offers important insights into the deformability properties of concrete that contains different alternative components. One of the most important factors in determining the stiffness and load-bearing capability of the concrete sample is the modulus of elasticity.

III. 3.2.14.3. Transversal Deformation

Two extra dial indicators that were calibrated in microns and firmly mounted on opposing sides of the hydraulic press frame were used to assess the transverse deformation. These indicators were made to detect any movement on the order of micrometres, and they do so by placing their pistons in touch with the centre of the concrete specimen. The total of the data from both indicators is used to determine the concrete specimen's increase in transverse distortion. The elastic modulus and Poisson's

ratio are then determined using the specimens' average longitudinal and transverse deformations.

III. 3.2.15. Durability Indicators Tests

Durability is associated with the capacity to withstand the mechanical stresses of the structure as well as the physical and chemical stressors of the surrounding environment, such as moisture, the sea environment, frost, air pollution, etc. Concrete durability may be estimated by measuring the concrete's porosity, permeability, and compressive strength both before and after it is exposed to harsh circumstances [321, 322]. In cementitious materials, inverse connections between permeability and durability, porosity and compressive strength, and a direct link between compressive strength and durability have been identified. Tests for total absorption, water permeability, capillarity, and resistance to freezing and thawing were thus conducted. Test bodies (half-cylinders (11x15) cm^3) made by cutting cylindrical samples (11x22) cm^3) and cubic specimens (10x10x10) cm^3 were employed.

III. 3.2.15.1. Total Absorption Test

Equation III. 15 was used to calculate the total absorption on cylindrical test specimens (11x22) cm^3 in accordance with the guidelines provided by AFPC-AFREM [323].

$$abs_{total} = \frac{(m_{sat} - m_{dry})}{m_{dry}} \qquad III.\ 15$$

where:

The total absorption (%) is abs_{total}

m_{sat} is the specimen's mass (kg) following a 24-hour saturation period

The mass of the dry specimen is denoted by m_{dry} (kg)

III. 3.2.15.2. Absorption by Capillarity Test

Concrete's porosity is a crucial characteristic that affects all other attributes, such as durability markers and compressive strength. Concrete's pore network is evaluated by measuring capillary water absorption, which is fuelled by surface tension in the pores. The test, which observes the saturation and capillary rise of a dry sample's bottom face in contact with water, complies with AFPCAFREM guidelines [323]. The samples are discs that are 50 mm thick and were cut from 11x22 cm^3 concrete pieces. Prior to testing, the discs are kept in airtight bags following the curing time and any further treatments. After that, they are dried at 80±2°C in a ventilated oven until their mass

remains constant. To stop evaporation, sticky aluminium foil is then placed across the lateral surface. The samples are immersed in water up to 3±1 mm, and the container is closed to reduce evaporation and let the upper surface "breathe." The samples are taken out, cleaned, weighed, and put back in the container at certain intervals (0.25, 0.5, 1, 2, 4, 8, and 24 hours). The test ends after 24 hours. The experimental setup for the capillary absorption test is shown in Figure III.28.

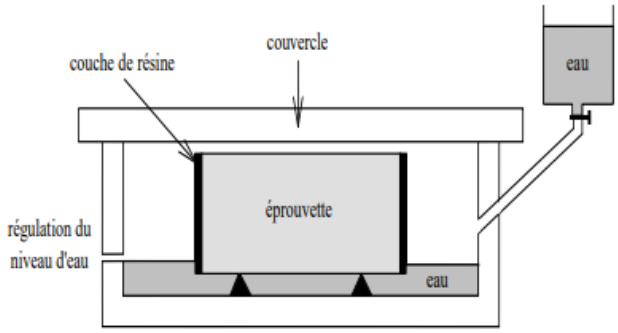

Figure III. 28 : Experimental Setup for Capillary Absorption Test

Equation III. 16 was used to get the capillary absorption coefficient (C_{at}), which is quantifiable in kg/m^2.

$$Ca_t = \frac{(m_t - m_0)}{a} \qquad III.\ 16$$

where m_t is the specimen's mass at a certain moment (kg), and Cat is the capillary absorption coefficient (kg/m^2).

The specimen's starting mass (m_0) is expressed in kilogrammes, and its section (a) is expressed in meters squared.

III. 3.2.15.3. Porosity Accessible to Water (Hydrostatic Weighing) Test

The water saturation under vacuum technique is one way to measure the porosity of concrete. Tests were carried out in compliance with NF EN 18-459. Before testing, the samples are actually kept in sealed bags and baked at 105 ± 5°C until the dry weight remains constant. The samples go through vacuum saturation once they are totally dry, and then they are submerged in water until they attain full saturation.

Following saturation, the sample is weighed in its saturated condition and then hydrostatically weighed with an accuracy of 0.01% of its mass. The following formula is used to determine the porosity P, which is given as a volumetric percentage (III. 17).

$$P_{water} = \frac{(m_{air} - m_{dry})}{(m_{air} - m_{water})} \text{ x } 100 \qquad III.\ 17$$

Where:

M_{air} is the mass of the soaked sample, m_{dry} is the mass of the sample following baking at 105°C, and P_{water} is the porosity accessible to water (%).

The mass of the sample submerged in water is denoted by m_{water}. The hydrostatic concrete weighing apparatus is shown in Figure III. 29.

Figure III. 29 : Hydrostatic Concrete Weighing Device

III. 3.2.15.4. Water Permeability Test

Under pressures of 1, 2, 3, 4, 5, 6, and 7 bar, the test measures the change in volume of water that only penetrates the top of test bodies (11 x 15 cm^3). According to ISO, each pressure lasts for one hour [324]. Using equation III. 18, the permeability coefficient was determined.

$$Kp = \frac{(Q.H)}{[F.(P_1 - P_2).\tau].\eta.k} \qquad III.\ 18$$

where Q is the amount of water that has penetrated (m^3)

Kp is the infiltration coefficient (m/s)

H represents the specimen's thickness (m)

F its surface (m^2), P_2 - P_1 the pressure differential between the specimen's inlet and outlet (Pa)

τ the experiment time (s)

η the change in water viscosity as a function of temperature (unitless)

D the specimen's diameter (m)

K is the specimen diameter (unitless) effect

[H=15 cm; $P_1 - P_2$ = 7 bar; τ = 8 hours; F = 95.033 cm²; k=1.064; η=0.89; Q = (0.0375, 0.025, 0.030 and 0.0375 litre) for NASTBC, DASTBC, NASDC and DASDC consecutively].

The employed water permeability meter is seen in Figure III. 30.

Figure III. 30 : Water Permeability Meter

III. 3.2.16. Scanning Electron Microscope (SEM) Analyses

III. 3.2.16.1. Working Principle

The FEI Quanta 250 FEG-SEM with Schottky field emission gun and Everhart-Thornley secondary electron detector (Figure III. 32) offers ultrahigh resolution imaging at 30 kV for 1.2 nm. It is made up of a broad field secondary electron detector for low vacuum operation and a backscattered electron detector for high vacuum mode. At 30 kV, it achieves a resolution of 3.0 nm. This microscope is perfect for applications in nanotechnology, materials science, biology, and compositional and microstructural imaging and analysis because of its smooth interaction with EDAX detectors. The Quanta 250 is a flexible instrument that provides in-depth understanding of the molecular makeup and shape of several materials at the nanoscale.

Figure III. 31 : Scanning Electron Microscope, EDAX and Sample Holder

III. 3.2.16.2. FEI Quanta 250 FEG-SEM Description

The Quanta FEG Scanning Electron Microscope (SEM), which enables high-quality digital imaging and magnifications of over 100,000×, produces bigger images of a variety of items. This important and widely used analytical tool may be utilised with X-ray microanalysis, has a superb field of view, and requires minimum specimen preparation. There are four fundamental components to the microscope:

• Electron source: The electron beam is emitted within a limited spatial container, with a specific energy and a small angular spread.

• Lens system: Before hitting the specimen's surface, the beam enters and travels through a network of several electromagnetic lenses.

•The scan unit: The scan generator signal is sent to the deflection mechanisms, which move the beam over the specimen region in a raster pattern. The electrical voltage changes during the scan, giving serial information about the surface of the object. The onscreen picture is produced by modulating this signal with the detecting system signal.

• The detecting device When electrons hit the specimen's surface, they react with it to create three primary types of signals: backscattered electrons, secondary electrons, and

X-rays. The detecting system picks up these signals, amplifies them, and sends the electrical signal to the control PC so that it may be seen on the monitor.

III. 3.2.17. Severe Conditions Tests

This study examines how concrete composed of beach sand and demolition coarse aggregates responds to four extreme scenarios: exposure to high temperatures, chemical assaults, freeze-thaw cycles, and abrasion. These circumstances were chosen in order to evaluate the endurance and performance of substitute concrete materials in demanding settings. The behaviour of the concrete under each circumstance was evaluated using a battery of exacting tests, with an emphasis on structural integrity and mechanical qualities. The results show that although concrete with beach sand and demolition materials shows different levels of durability to these harsh circumstances, it is a good choice for environmentally friendly building methods. This study offers important new information on how recycled materials may be used to increase the resilience of concrete structures in the face of severe environmental pressures.

III. 3.2.17.1. Abrasion Test

The study by Setti et al. (2012) [325] served as the basis for the testing regimen that follows. To get the best cement hydration, the concrete examples were formed in metal moulds that measured 10x10x10 cm^3, demolded after 24 hours, and then kept in water tanks for 27 days. In order to prepare the hardened concrete cubes for abrasion testing, they were cut into half-cubes of almost similar size using a concrete saw after 28 days. A Micro Deval device was used to abrasively treat the half-cubes. One half-cube of concrete, three stainless steel spherical balls (D = 47 ± 1 mm, P = 420 to 445 g), 1.5 kg of smaller stainless steel spherical beads (D = 10 ± 0.5 mm), and 2.5 litres of water were all included in each compartment of the apparatus (Figure III. 33). The Micro Deval was configured to run for 12,000 rotations over two hours at an average speed of 100 ± 5 rpm after the compartments were sealed and repositioned. Using the same samples, this process was carried out four times. The samples were cleaned, their exterior surfaces were wiped with a cloth, and their mass was measured after 2, 4, 6, and 8 hours of abrasion. The compartments were opened after each run. Weight loss was used to assess abrasion resistance using the following formula (III. 19).

$$ml_{ih} = 100\text{x}\frac{m_{0h}-m_{ih}}{m_{0h}} \qquad III.\ 19$$

Where:

The mass loss at i hour is denoted by ml_{ih}

The mass at 0 hour by m_{0h}

The mass at i hour by m_{ih}

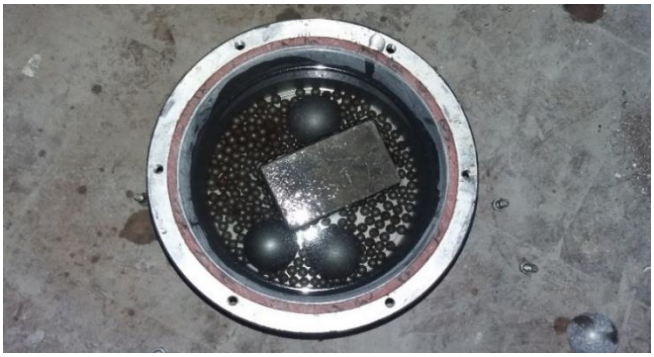

Figure III. 32 : Compartment with Concrete Half-Cube, Steel Balls, Steel Beads and Water

III. 3.2.17.2. Freeze and Thaw Test

Rapid freeze-thaw cycles were used to cubic specimens (10x10x10) cm^3 of the research concretes at 90 days of age [326]. A 6+6-hour routine guarantees two freeze-thaw cycles daily. Thus, 12.5 days were needed to complete 25 cycles, and 25 days were needed for 50. Every cycle entails thawing in water at ambient temperature up to +16°C after freezing in the air at -16°C. At 25 and 50 cycles, visual inspections and mass measurements in the saturated surface-dry state (SSD) were performed. Ultimately, compression tests were performed. A 6+6-hour routine guarantees two freeze-thaw cycles daily. Thus, 12.5 days were needed to complete 25 cycles, and 25 days were needed for 50. Every cycle entails thawing in water at ambient temperature up to +16°C after freezing in the air at -16°C. At 25 and 50 cycles, visual inspections and mass measurements in the saturated surface-dry state (SSD) were performed. Ultimately, compression tests were performed. Using equation III. 20, observation specimens (10x10x10) cm^3 that had been submerged in tap water at room temperature (20°C) were also evaluated at the age equal to 50 cycles (102.5 days).:

$$T = a + 0.25n \qquad III.\ 20$$

where:

A is the age of the concrete at the beginning of the test (day)

T is the age equal to 50 cycles (day)

n is the number of freeze-thaw cycles.

Concrete is considered frost resistant if its resistance coefficient to freezing is more than or equal to 0.75, its mass loss from freeze-thaw cycles does not exceed 5%, and its compressive strength (if any) decreases by no more than 20%. Equation III. 21 was used to determine the latter.

$$K_{rg} = \frac{R_{rg}}{R_{sat}} \qquad III.\ 21$$

Where:

K_{rg} is the frost resistance coefficient (unitless),

R_{rg} is the residual compressive strength (MPa),

R_{sat} is the water-saturated observation concrete's compressive strength (MPa).

III. 3.2.17.3. Chemical Attacks Test

After 28 days of curing, the 10x10x10 cm³ concrete specimens from the four kinds were submerged in four different liquid environments: a 5% NaOH solution with a pH of 12.64, demineralised water with a pH of 7.05, and sea water with a pH of 10.30. Simultaneously, control specimens were maintained in 7.25 pH tap water. The aggressiveness of these liquid habitats was continually maintained by their monthly renewal, which made sure that their pH levels stayed different from the concrete's. Visual examinations, weight measurements, and evaluations of ultrasonic velocity were performed both before to and after immersion to track any changes in the specimens. Finally, to assess the specimens' remaining strength following two years of exposure, unconfined compressive strength testing was performed.

III. 3.2.17.4. High Temperature Test

Three samples of each type of concrete were analysed. These specimens were subjected to temperatures of 150, 300, 450, 600, 750, and 900 °C following a year of curing. Figure III. 34 shows the concrete specimens used in this experiment within the Nabertherm muffle furnace. During the tests, the specimens' mass evolution, ultrasonic velocity, residual strength, and appearance were all evaluated.

This thorough testing process provides crucial information on the material's durability and structural soundness under challenging conditions, enabling a thorough

understanding of how exposure to high temperatures affects the concrete's performance characteristics.

Figure III. 33 : Concrete Specimens in the Nabertherm Muffle Furnace

Because it allows hostile substances to enter, cracking can reduce the durability of concrete. Cracking can result from any thermal stress, thus it's critical to comprehend the type and severity of these fractures. A crack gauge with a micrometric lens -which allows for accurate measurement of crack openings with a precision of one tenth of a millimetre for convenient reading- was used in this investigation to track cracking. The crack meter utilised is shown in Figure III. 35.

Figure III. 34 : Crackmeter (MAGNIF 24^{x})

III. 4. CONCLUSION

A thorough analysis of the materials and experimental techniques used in this study is given in Chapter III. Through methodical examination of crucial elements including cement, aggregates, and admixtures, we have determined their crucial functions in the creation and functionality of concrete. With an emphasis on their potential as environmentally friendly building materials, the chapter describes the procedures for creating and choosing demolition coarse aggregates and adding Saharan dune sand.

Additionally, the methods for mechanical testing and physical characterisation are explained in detail, guaranteeing a strong foundation for assessing the qualities of concrete. This chapter establishes the foundation for comprehending the interactions

between various components in concrete mixes through macroscopic, mesoscopic, and microscopic examinations. The knowledge acquired will be essential for interpreting findings in later chapters and expanding our understanding of building materials.

All things considered, Chapter III provides a strong framework for investigating creative concrete solutions, emphasising the value of material selection and thorough testing in reaching good-performance building results.

CHAPTRE IV

PRESENTATION OF RESULTS AND DISCUSSION

CHAPTER IV _ PRESENTATION OF RESULTS AND DISCUSSION

IV. 1. INTRODUCTION

The findings of the experimental studies carried out throughout this study are presented in Chapter IV, together with a thorough analysis of their implications. The facts pertaining to the manufacturing and selection of demolition aggregates, especially those with low water absorption, and their use in concrete compositions are clearly and methodically analysed in this chapter.

The mechanical strength of parent concretes and the demolition aggregates' capacity to absorb water are the main topics of the first part.

To verify the findings and evaluate the performance of various aggregate sub-fractions, statistical studies are used. The goal of this thorough analysis is to demonstrate a robust relationship between aggregate characteristics and concrete performance.

The chapter's second section is on concrete formulas that include Sahara dune sand and demolition materials. Important topics are covered in detail, including workability, water demand, granulometry, microscopy, and other mechanical testing. Tests that measure absorption, permeability, abrasion resistance, and durability against chemical assaults, high temperatures, and freeze-thaw cycles are also used to evaluate sustainability indicators.

Chapter IV seeks to offer important insights into the feasibility of employing recycled resources in the manufacturing of concrete by presenting and debating these findings. The results will help us better understand how these materials may improve concrete's sustainability and mechanical qualities, which will eventually promote improvements in building techniques.

IV. 2. PRODUCTION AND SELECTION OF DEMOLITION AGGREGATES WITH LOW-WATER ABSORPTION

IV. 2.1. Parent Concretes Quality

Compression testing was one crucial mechanical indicator that was used in order to assess the quality of the parent concrete.

IV. 2.1.1. Compressive Strength

The parent concrete samples are classified as normal concretes since their average strengths, as measured by compression testing, vary from 27.911 MPa to 38.678 MPa.

The results of the compressive strength tests performed on the parent concrete samples are shown in Table IV.1.

Table IV. 1 : Findings for the 28-Day Parent Concretes' Compressive Strength in MPa (Part 1)

Sample	Parent concretes of part 1 / (Values in MPa)						
	PC1	PC2	PC3	PC4	PC5	PC6	PC7
01	42.382	36.166	37.390	28.094	34.431	29.923	29.174
02	38. 212	33.818	33.140	31.248	33.767	30.491	27.466
03	33.852	34.000	36.890	27.321	32.888	28.096	27.453
04	40.562	31.475.	30.517	36.368	34.047	29.335	.26.711
05	39.094	33.487.	27.129	32.954	33.964	28.414	.27.275
06	37.967	35.774	38.152	32.906	33.005	25.412	29.386
Average	38.678	34.120	33.870	31.482	33.684	28.612	27.911

IV. 2.2. Demolition Aggregates' Water Absorption

Water absorption rises as the size of the Demolition Aggregates (DAs) falls, which is consistent with Kim Jeonghyun's findings [327]. Figures IV. 1 and IV. 2, which show the water absorption of the DA's sub-fractions and reconstituted fractions after 20 minutes, respectively, graphically illustrate this pattern.

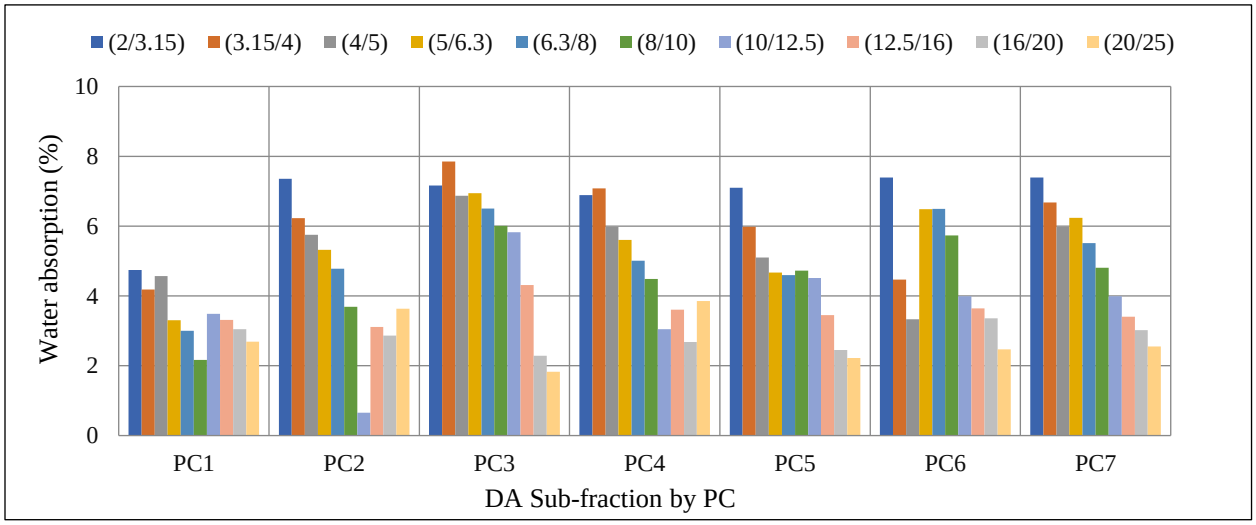

Figure IV. 1 : Water Absorption Following DA Sub-Fractions for 20 Minutes (%)

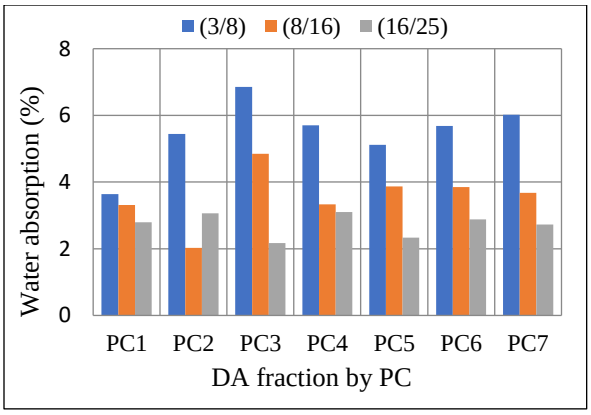

Figure IV. 2 : Water Absorption Following DA Reconstituted Fractions (%) for 20 Minutes

As seen in Tables IV. 2 and IV. 3, the water absorption of the DA fraction's constituent DA subfractions affects the DA fraction's total water absorption. Each DA subfraction has a different effect based on how dominant it is over all of its component DA subfractions. As previously mentioned, the latter is based on the specific rejection of the comparable NA sub-fraction.

Table IV. 2 : DA Aggregate Sub-Fractions' Water Absorption After 20 Minutes

(d/D)	Parent concretes						
	Water absorption after 20 minutes (%)						
	PC1	PC2	PC3	PC4	PC5	PC6	PC7
(2/3.15)	4.74	7.36	7.16	6.89	7.10	7.39	7.39
(3.15/4)	4.18	6.23	7.85	7.08	5.98	4.47	6.68
(4/5)	4.57	5.75	6.87	5.98	5.10	3.33	5.98
(5/6.3)	3.30	5.32	6.94	5.60	4.67	6.48	6.24
(6.3/8)	3.00	4.78	6.50	5.01	4.60	6.49	5.51
(8/10)	2.17	3.69	6.01	4.49	4.72	5.73	4.81
(10/12.5)	3.49	0.65	5.82	3.05	4.51	3.99	3.99
(12.5/16)	3.31	3.11	4.31	3.61	3.45	3.64	3.40
(16/20)	3.05	2.86	2.29	2.68	2.45	3.36	3.02
(20/25)	2.69	3.63	1.83	3.85	2.22	2.47	2.55

Table IV. 3 : DA Reconstituted Fractions' Water Absorption After 20 Minutes

(d/D)	Parent concretes						
	Water absorption after 20 minutes (%)						
	PC1	PC2	PC3	PC4	PC5	PC6	PC7
(3/8)	3.64	5.44	6.85	5.7	5.12	5.68	6.02
(8/16)	3.31	2.02	4.86	3.31	3.88	3.86	3.69

(16/25)	2.91	3.22	2.25	3.27	2.43	2.99	2.84

In terms of size and water absorption, the reconstitution of DA fractions from the DA sub-fractions has an inverse connection. The DA sub-fractions' maximum water absorption values vary from [3.36%; 7.85%], mean values range from [2.75%; 6.86%], and lowest values range from [0.65%; 4.74%]. Minimum values are between 12% and 82% below mean values and between 28% and 89% below maximum values. The maximum, average, and lowest water absorption values for DA sub-fractions that correspond to their parent concretes (PCs) are shown in Figure IV. 3.

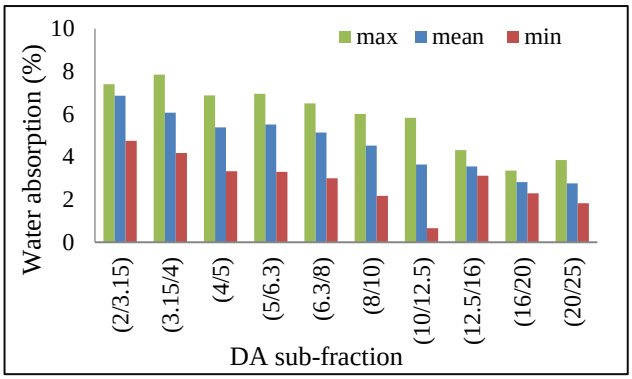

Figure IV. 3 : Water Absorption Maximum, Average, and Minimum Values of DA Sub-Fractions

Maximum water absorption values ranged from [3.27%; 6.85%], average values ranged from [2.84%; 5.49%], and minimal values ranged from [2.02%; 3.64%] when DA fractions were reconstituted using their respective DA sub-fractions from the same parent concrete (PC). The lowest values are between 31% and 58% below the maximum values and between 21% and 43% below the average values. The maximum, average, and lowest water absorption values for reconstituted DA fractions that correspond to their parent concretes (PCs) are shown in Figure IV. 4.

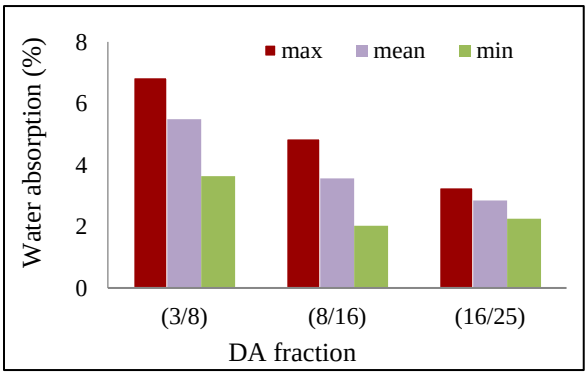

Figure IV. 4 : Water Absorption Maximum, Average, and Minimum Values for DA Reconstituted Fractions

The minimal water absorption values that were obtained while choosing the least absorbent DA sub-fractions without taking the parent concrete (PC) into consideration were between [1.89% and 3.39%]. These values were 4% to 7% lower than the minimum values obtained from DA sub-fractions of the same parent concrete (PC). The difference between the DA reconstituted fractions' lowest water absorption values when the DA sub-fractions come from the same PC (min) and when they come from different PCs (min chosen) is shown in Figure 10. Without taking into account the parent concrete (PC), the DA sub-fractions with the lowest water absorption values are (2/3.15), (3.15/4), (5/6.3), and (6.3/8) from PC1, (4/5) from PC6, (10/12.5) and (12.5/16) from PC2, and (16/20) and (20/25) from PC3. The difference between the reconstituted DA fractions' minimum water absorption values when the DA sub-fractions come from the same parent concrete (PC) (min) and when they are chosen from different PCs (min selected) is shown in Figure IV. 5.

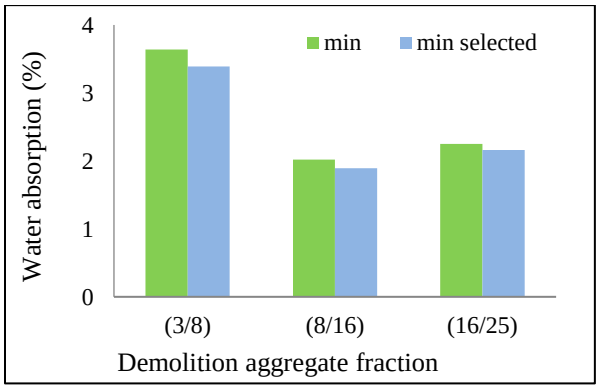

Figure IV. 5 : DA Reconstituted Fractions' Minimum Water Absorption Values from the Same PC (Min) and Selected from All PCs (Min Selected)

Based on the DAD_{max}/NAD_{max} ratio, it was simple to distinguish between the most and least absorbent DA sub-fractions thanks to the connection between the maximum diameter of the DA sub-fraction (DAD_{max}) and the maximum diameter of the parent concrete's NA fraction (NAD_{max}). After 20 minutes, the water absorption of DA sub-fractions and reconstituted DA fractions is shown as a function of the DAD_{max}/NAD_{max} ratio in Figures IV. 6 and IV. 7. When the DAD_{max}/NAD_{max} ratio is higher than 0.8 for DA sub-fractions and larger than 1 for DA reconstituted fractions, water absorption is less than 4%. Water absorption reduces when the DAD_{max}/NAD_{max} ratio rises at lower levels of the ratio.

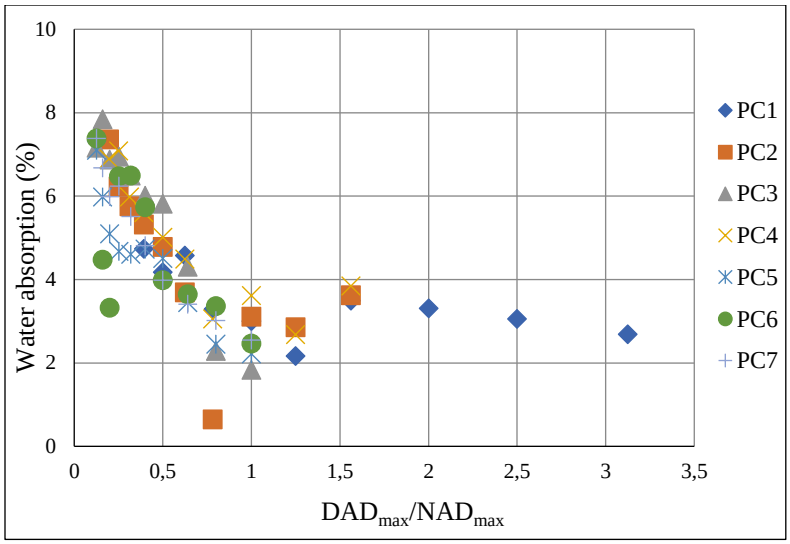

Figure IV. 6 : DA Sub-Fractions' Water Absorption after 20 Minutes as a Function of DAD_{max}/NAD_{max} Ratio

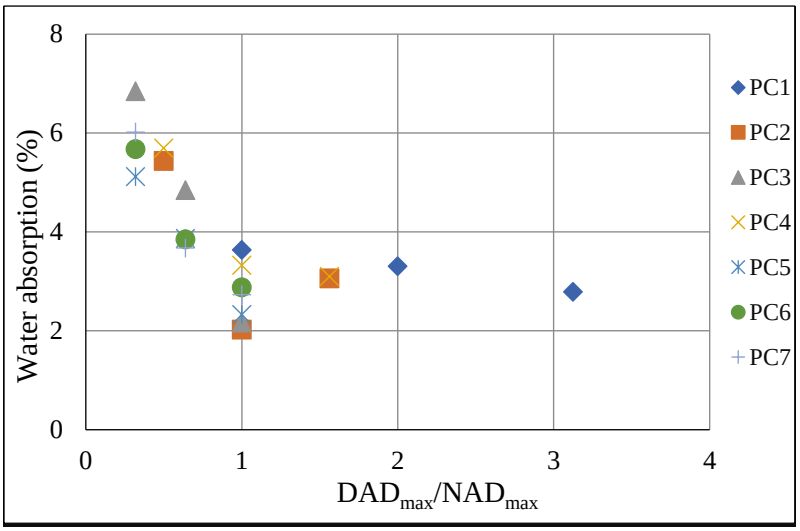

Figure IV. 7 : DA Reconstituted Fractions' Water Absorption after 20 Minutes as a Function of DAD_{max}/NAD_{max} Ratio

IV. 2.3. Statistical Analysis

To determine how each of the two variables -"DA size" and "DA origin (parent concrete)"- affected the water absorption of DA during a 20-minute period, they were examined separately. To determine if each variable significantly affected the water absorption over the course of 20 minutes and to determine the main contributions of each variable to the overall variance, Analysis of Variance (ANOVA) statistics [328] were utilised. Importantly, a factor was considered statistically meaningful if its significance level was less than or equal to 5% ($p < 0.05$).

IV. 2.4. Statistical Analysis Related to DA Sub-fractions (d/D)

The findings of the ANOVA single test for 20-minute water absorption with the independent variable "DA sub-fraction size" are summarised in Tables IV. 4 and IV. 5. In this instance, the test results are extremely significant (F = 11.38 > Fcrit = 2.04 and P-value = 3.71 E-10 < 0.05). Therefore, it may be said that the "DA sub-fraction size (d/D)" distinguishes demolition aggregate sub-fractions in terms of water absorption during a 20-minute period. The population of findings stays closely grouped around the average, as seen by the very tiny standard deviation values around each mean.

Table IV. 4 : ANOVA Summary: 20 Minutes-Water Absorption Linked with DA Sub-Fraction Size

Summary	Count	Sum	Average	Variance	SD
(2/3.15)	7	48.03	6.86	0.91	0.95
(3.15/4)	7	42.47	6.07	1.79	1.34
(4/5)	7	37.58	5.37	1.34	1.16
(5/6.3)	7	38.55	5.51	1.53	1.24
(6.3/8)	7	35.89	5.13	1.47	1.21
(8/10)	7	31.62	4.52	1.67	1.29
(10/12.5)	7	25.5	3.64	2.51	1.58
(12.5/16)	7	24.83	3.55	0.15	0.38
(16/20)	7	19.71	2.82	0.14	0.37
(20/25)	7	19.24	2.75	0.54	0.73

Table IV. 5 : ANOVA Findings: Water Aborption for 20 Minutes Linked with DA Sub-Fraction Size

Variation Source	SS	df	MS	F	P-value	F crit
Between Groups	123,18	9	13,69	11,38	3,71E-10	2,04
Within Groups	72,19	60	1,20			
Total	195,37	69				

Tables IV. 6 and IV. 7 summarise the findings of the ANOVA single test for water absorption over a 20-minute period using the independent variable "DA sub-fraction origin." In this instance, the test results are not significant (F = 1.55 < Fcrit = 2.25 and P-value = 0.176 > 0.05). Accordingly, it can be said that the "origin (PC)" does not substantially alter the sub-fractions of demolition aggregate in terms of water absorption after 20 minutes.

Table IV. 6 : ANOVA Summary: 20 Minutes-Water Absorption Linked with Sub-Fraction Origin

Summary	Count	Sum	Average	Variance	SD
PC1	10	34.50	3.45	0.67	0.95
PC2	10	43.38	4.34	3.79	1.34
PC3	10	55.58	5.56	4.31	1.16
PC4	10	48.24	4.82	2.40	1.24
PC5	10	44.80	4.48	2.21	1.21
PC6	10	47.35	4.73	2.78	1.29
PC7	10	49.57	4.96	2.76	1.58

Table IV. 7 : ANOVA Results: 20 Minutes-Water Absorption Linked with Sub-Fraction Origin

Source of Variation	SS	df	MS	F	P-value	F crit
Between Groups	25,16	6	4,19	1,55	0,18	2,25
Within Groups	170,20	63	2,70			
Total	195,37	69				

IV. 2.5. Statistical Analysis Related to DA Fraction (d/D)

Tables IV. 8 and IV. 9 provide a summary of the results of the ANOVA single test for water absorption during a 20-minute period with the independent variable "DA fraction size". The test findings in this case are very significant (P-value = 9.64 E-06 < 0.05 and F = 23.48 > Fcrit = 3.55). Consequently, it can be said that the "DA fraction size" separates the various fractions of demolition aggregate based on how much water they absorb over a 20-minute period. The extremely small standard deviation values surrounding each mean show that the population of findings remains tightly clustered around the average.

Table IV. 8 : ANOVA Summary: 20 Minutes-Water Absorption Linked with DA Fraction Size

Summary	Count	Sum	Average	Variance	SD
(3/8)	7	38.45	5.49	0.96	0.98
(8/16)	7	24.92	3.56	0.72	0.85
(16/25)	7	19.06	2.72	0.12	0.35

Table IV. 9 : ANOVA Results: 20 Minutes-Water Absorption Linked with DA Fraction Size

Source of Variation	SS	df	MS	F	P-value	F crit
Between Groups	28.25	2	14.13	23.48	9.64 E-06	3.55
Within Groups	10.83	18	0.60			

Total	39.09	20

The findings of the ANOVA single test for 20-minute water absorption with the independent variable "DA fraction origin (PC)" are summarised in Tables IV. 10 and IV. 11. In this instance, the test results are not significant (F = 0.25 < Fcrit = 2.85 and P-value = 0.95 > 0.05). Therefore, it can be said that the "DA fraction parent concrete" does not considerably alter the 20-minute water absorption of demolition aggregate fractions.

Table IV. 10 : ANOVA Summary: 20 Minutes-Water Absorption Related to DA Fraction Origin

Summary	Count	Sum	Average	Variance	SD
PC1	3	9.74	3.25	0.18	0.95
PC2	3	10.53	3.51	3.06	1.34
PC3	3	13.87	4.62	5.51	1.16
PC4	3	12.13	4.04	2.07	1.24
PC5	3	11.32	3.77	1.95	1.21
PC6	3	12.41	4.14	2.02	1.29
PC7	3	12.43	4.14	2.87	1.58

Table IV. 11 : ANOVA Results: 20 Minutes-Water Absorption Related to DA Fraction Origin

Source of Variation	SS	df	MS	F	P-value	F crit
Between Groups	3.75	6	0.62	0.25	0.95	2.85
Within Groups	35.34	14	2.52			
Total	39.09	20				

IV. 2.6. Validation

❖ Calibration of Scale

In accordance with the manufacturer's instructions and the ASTM E898-20 standard [329], the balance was calibrated using high accuracy standard weights while working normally and spanning its whole measurement range. By contrasting the values of the standard weights with those that could be read on the balance screen, the tolerance of the device was ascertained. The balance has been visually inspected on a regular basis. No visible physical damage or other problems that could impair its functionality have been found.

❖ Laboratory Testing

The pace at which old mortar (OM) adheres to the natural aggregate (NA) determines how much water a demolition aggregate (DA) absorbs. Depending on the DA granular sub-fraction, it may differ. Under identical settings, repeatability was tested on three chosen DA sub-fractions: one of small size (2/3.15), one of medium size (8/10), and one of big size (16/20) [330, 331]. Two methods were used to conduct the tests:

- three consecutive times for the three selected DAs sub-fractions on the same test sample.
- once for each of the three selected DAs sub-fractions on five distinct test samples.

Tables IV. 12 and IV. 13 display the standard deviation (SD) and the relative standard deviation (RSD).

Table IV. 12 : An overview of the water absorption measurements at 20 minutes obtained for a single test sample three times in succession using the standard method Succession

DA Sub-fraction	Tests number	20-minutes water absorption	SD	RSD
(2/3.15)	3	8.64%	0.92%	10.68%
(8/10)	3	5.34%	1.41%	26.50%
(16/20)	3	3.67%	0.57%	15.45%

The findings indicate a considerable degree of dispersion around the average water absorption, with an RSD ranging from 10.68% to 26.50%.

Table IV. 13 : An overview of the water absorption measurements at 20 minutes obtained at five different test samples using the standard method

DA Sub-fraction	Tests number	20-minutes water absorption	SD	RSD
(2/3.15)	5	5.83%	1.79%	30.68%
(8/10)	5	3.86%	1.01%	26.19%
(16/20)	5	3.46%	1.05%	30.32%

Relative standard deviation (RSD) ranges from 26.19% to 30.68%, indicating a considerable degree of dispersion around the mean water absorption. The relative standard deviation for both tiny and big DA subfractions increases noticeably when different samples are analysed. The average subfraction, however, showed no discernible alterations.

IV. 3. PART 2: USE OF DEMOLITION COARSE AGGREGATES AND SAHARAN DUNE SAND IN CONCRETE FORMULATION

IV. 3.1. Parent Concrete

IV. 3.1.1. Compressive strength

The parent concrete samples' average strength, according to the findings of the compressive strength tests (Table IV. 14), is 25.116 MPa. This figure indicates that the concrete satisfies the requirements for regular concrete, which normally fall between 20 and 40 MPa. The material's quality and capacity to bear applied stresses are reflected in its average compressive strength, which shows that it is appropriate for a range of structural uses.

Table IV. 14 : Findings from the 2-Year Parent Concrete's Compressive Strength Test (Part 2)

Sample	Parent concretes
	PC1
01	8.327
02	13.771
03	15.842
04	31.096
05	36.056
06	54.086
07	40.827
08	31.823
Average	25.116

IV. 3.2. Son Concretes

Concrete's performance qualities, such as its fitness for usage, mechanical strength, and durability under both normal and extreme situations, are largely dictated by the quality of its component components.

IV. 3.2.1. Microscopy and Granulometry of Sand

The size difference between the grains of the two types of sand is evident from microscopic examinations. It is possible to predict the maximum diameters ratio ($SDD_{max}/STBD_{max}$) of grains to be a fourth (1/4). SD grains feature smooth surfaces, somewhat rounded edges, and a distorted oval shape that can occasionally be spherical. STB grains have rougher surfaces, more elongated grains, and angles that are rather

sharp. The comments given after the microscopic observations are supported by the granulometric examination of both types of sand. The SD-specific surface is larger because the $SDD_{max}/STBD_{max}$ ratio is slightly bigger than a quarter (≈1/4). Both forms of sand fall within the fine sand range, among other factors. The overall water demand of concrete is determined by the properties of the sand, namely the granulometric curve, the fines content, and the grain shape [332]. SD is devoid of grains over 2 mm, abundant in medium grains (0.250 to 0.500 mm), and includes fewer than 5% of grains under 100 µm. STB has a very low grain content of more over 2 mm, is richer in medium grains (0.250 to 0.500 mm), and slightly surpasses 5% of grains under 100 µm. This makes both sand types good for concrete [333].

IV. 3.2.2. Water Demand and Workability

Without a few changes, it was impossible to unify the fresh state of all the research concretes. First, we chose pumpable forms of concrete since the lack of mortar required us to increase the amount of sand in the mixes [195]. Therefore, it was essential to add a tiny amount of plasticiser for DASTBC and decrease the amount of mixing water for NASDC in order to maintain a slump of 7 ± 2 cm. No changes have been made to the formulas for NASTBC and DASDC. The demolition aggregates' water absorption can be limited by selecting a minimum diameter of 8 mm; nevertheless, the lack of the granular fraction 5/8 results in a discontinuity in the overall granular extent. This has been noted for DASTBC and can impact the workability of new concrete [195], which is why a plasticiser is required. The workability of NASDC was much improved by substituting SD for STB; the absorption capacity of SD is mostly determined by the morphology and grain size of its constituents, surpassing by about 3% that of STB [334]. Since NASDC was discovered to be very plastic, 16.76% less mixing water was required in order to get the desired slump. The plastic aspect of DASDC has been maintained by the combination of SD and DA. The stiffness caused by the granular discontinuity dampened the significant flexibility brought about by the shape and granulometry of SD grains. Thus, DASDC was in a fresh, balanced condition. Both NASTBC and the desired slump were attained without any changes.

IV. 3.2.3. Compressive strength

In addition to being prepared, cured, and conserved under same conditions, two distinct concretes must be of the same age in order to be fairly compared. The compressive

strength at 2 years of age may be estimated from that recorded at 28 days of age, and vice versa, depending on the kind of cement, temperature, and hardening circumstances [335]. The compressive strengths over a two-year period were measured in this investigation. Rather of assessing the parent concrete's compressive strength at 28 days, it was decided to compare the PC's and its son's compressive strengths at 2 years of age. Figure IV. 8 displays the findings. Three measurements are averaged to produce each value. After two years, the concrete's compressive strength increased by 22.16% for DASDC and 26.89% for DASTBC due to the use of demolition coarse aggregates instead of natural coarse aggregates in the formulation. All of the 28-day fresh concretes' compressive strengths are displayed in Figure IV. 9. Additionally, each statistic represents the mean of three measurements. In general, all of the others surpass NASTBC's. The compressive strength of NASDC is 44.98% greater. This could be because to the significant effect of the water-to-cement ratio (W/C) [334, 336, 337]. The compressive strength of DASTBC is 27.66% greater. This could be because the plasticiser has made it better [338]. The compressive strength of DASDC is 7% more than that of NASTBC when the W/C is the same and no plasticiser is used. This can be because SD has better compactness because of its grain size. G/S levels are larger and sand doses are less significant for DATBC and DASDC. The compressive strengths increase as a result. A G/S ratio of 2.62 was found to be best (see Table III.15), which supports the findings acknowledged in Neville, (2011) [203]. The research concretes, however, are still within the typical concrete range.

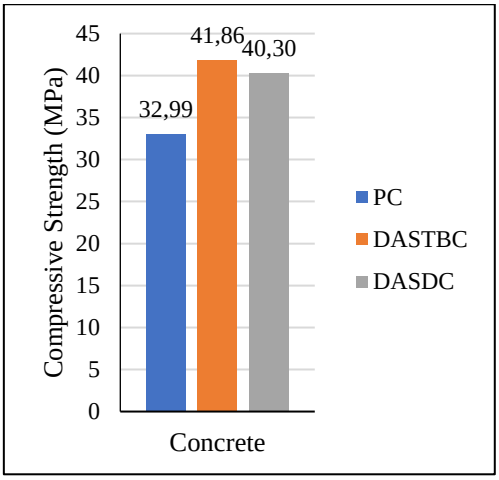

Figure IV. 8 : Compressive Strength of 2-Years Parent and Sons Concretes

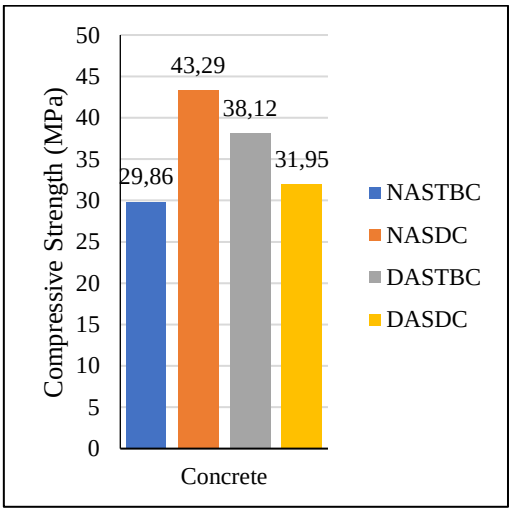

Figure IV. 9 : Compressive Strength of 28-Day Study Concretes

The son concretes' compressive strengths at various ages are displayed in Table IV. 15. Three measurements are averaged to produce each value.

Table IV. 15 : Compressive Strengths of the Concretes

Concrete	Concrete age (day)			
	7	14	28	730
NASTBC	20.571	20.988	29.863	42.781
DASTBC	37.020	38.305	43.287	49.571
NASDC	25.965	30.605	38.120	41.861
DASDC	26.720	28.580	31.946	40.301

Figure VI. 10 illustrates how the average compressive strengths of the concretes changed with age. It progresses similarly to every other concrete that was examined. Up until the seventh day, it is growing considerably at a young age. The same is true for DASDC and DASTBC. With the exception of DASTBC, where a little slope is noted, it is nearly consistent between days seven and fourteen. The compressive strengths restart increasing and the disparities between them diminish between the fourteenth and the twenty-eighth day. The compressive strengths reappear on the 730th day (2 years) and reach about 40 MPa, with the exception of NASDC, which reaches 50 MPa. Because of its lower W/C (45-47), this could be the case.

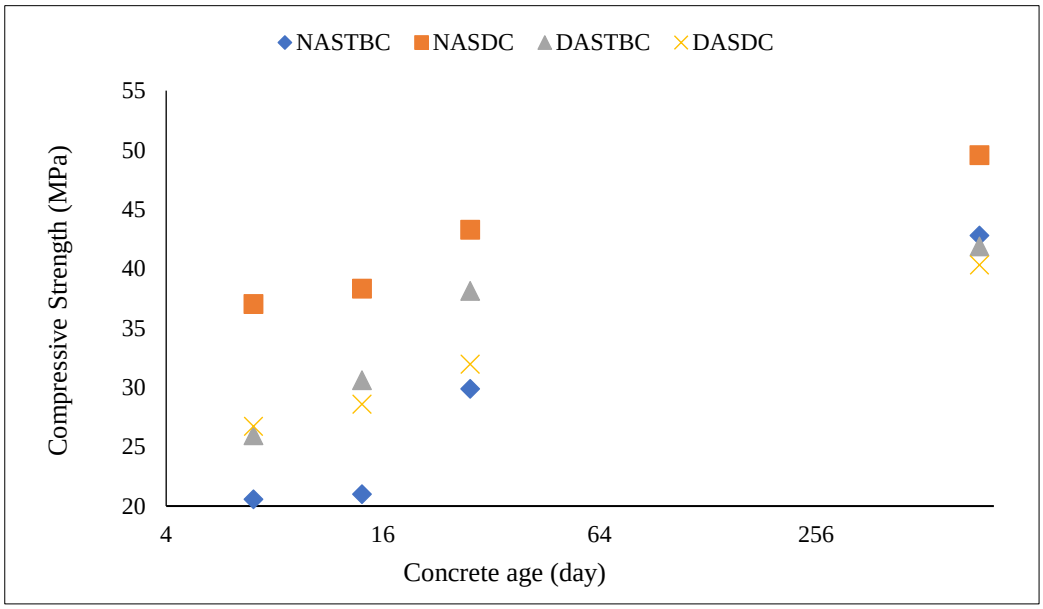

Figure IV. 10 : Compressive Strengths Evolution

IV. 3.2.4. Three-Point Flexural Strength

The outcomes of the 28-day new concretes' three-point flexural testing are displayed in Figure IV. 11. Three values are averaged to create each one. The outcomes follow the same sequence. DASTBC surpasses NASTBC by 19% and NASDC by 9%. This could be because the first one had less W/C [334, 336, 337], while the second one had plasticiser [338]. A little decline of 1.6% is noted for DASDC.

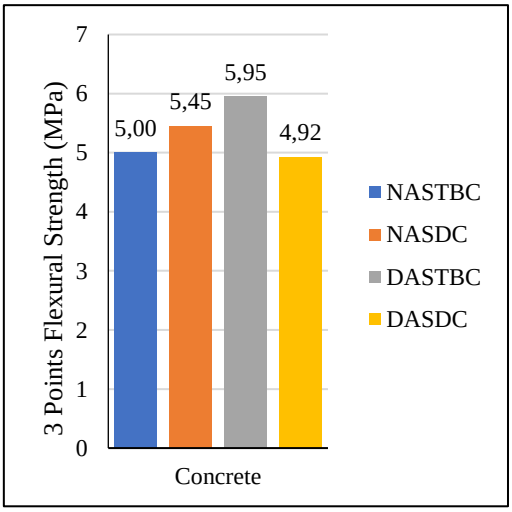

Figure IV. 11 : Three-Points Flexural Strengths of 28-Day Concretes

IV. 3.2.5. Splitting Tensile Strength

The splitting tensile test results for the 28-day fresh concretes are displayed in Figure IV. 12. Three values are averaged to create each one. The outcomes follow the same sequence. The inclusion of plasticiser may be the cause of the DASTBC concrete's

6.44% increase above the NASTBC control concrete [338]. It is possible that the smooth surface of the dune sand grains, which influences the adherence of sand-cement paste, is the cause of the 13.37% drop for the DASDC concrete [191]. Despite the presence of dune sand, NASDC concrete shows a little decline of around 1%, possibly because of the lower water-to-cement ratio (W/C), which prevents an even larger reduction [334, 336, 337].

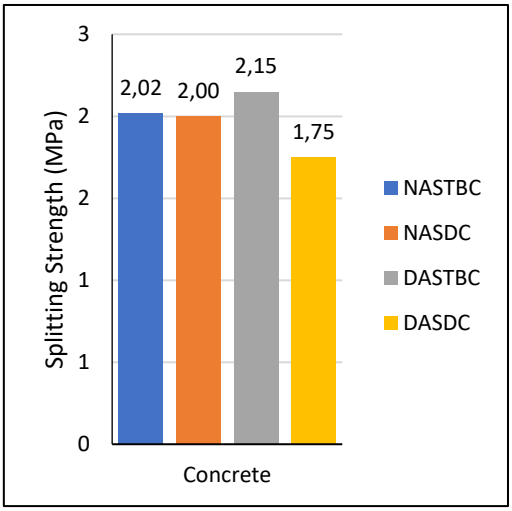

Figure IV. 12 : Splitting Strengths of 28-Day Concretes

IV. 3.2.6. Ultrasonic velocity

Using an ultrasonic instrument, the time it takes for the wave to pass through concrete samples (10x10x10 cm³) is used to determine the ultrasonic wave propagation velocity (see III. 3.2.13.2. Results' Reading and Interpretation). The wave propagation velocity in different kinds of concrete at 28 days of age is shown in Figure IV. 13.

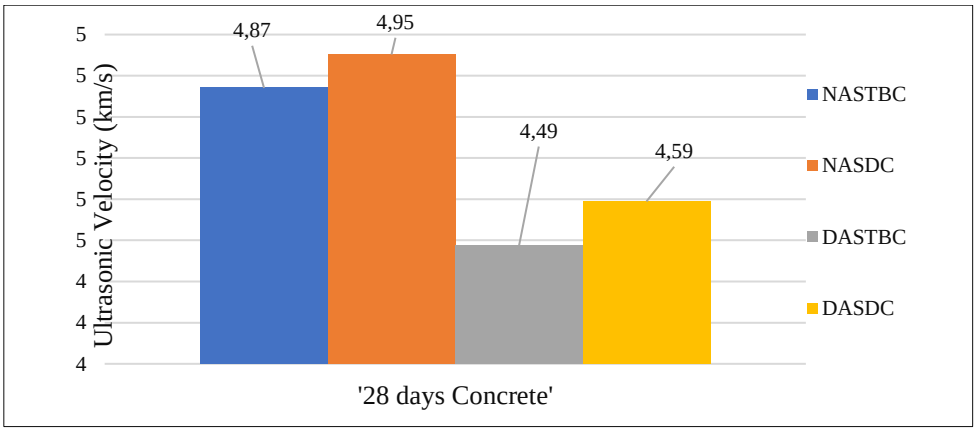

Figure IV. 13 : Ultrasonic Velocity of the 28-Days Concretes

For the 28-day concrete specimens NASTBC, NASDC, DASTBC, and DASDC, the corresponding ultrasonic velocity readings were 4.87 km/s, 4.95 km/s, 4.49 km/s, and

4.59 km/s. At 4.95 km/s, NASDC has the fastest velocity, demonstrating its higher density and structural soundness. This implies stronger matrix bonding and fewer voids, which are associated with higher-quality concrete. A high velocity of 4.87 km/s is also displayed by NASTBC, indicating strong performance traits. DASTBC and DASDC, on the other hand, had lower velocities of 4.49 and 4.59 km/s, respectively, which may indicate increased porosity or less successful bonding. Higher ultrasonic velocities in NASTBC and NASDC often signify improved durability in a range of environmental circumstances.

IV. 3.2.7. Dynamic Modulus of Elasticity

The dynamic modulus of elasticity, as determined by equation III.10 (see III.3.2.13.3 for details), is shown in Figure IV. 14. The following are the figures for the various concrete mixes: DASTBC at 42.39 GPa, NASDC at 52.06 GPa, DASDC at 42.64 GPa, and NASTBC at 50.76 GPa. While both DASTBC and DASDC show decreases of roughly 16.43% and 16.00%, respectively, indicating their reduced stiffness and greater vulnerability to deformation under load conditions, NASDC shows an increase of 2.54% in dynamic modulus compared to NASTBC, indicating enhanced elastic properties. These results highlight how aggregate type significantly affects concrete's mechanical qualities, highlighting the significance of material selection in structural applications where performance and durability are crucial.

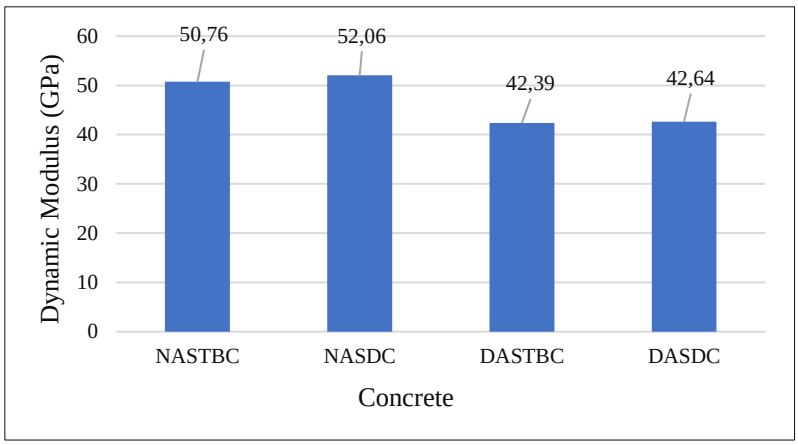

Figure IV. 14 : The Concretes' Dynamic Elasticity Modulus

The dynamic modulus of elasticity of concrete is one of the most crucial markers of its stiffness and elastic behaviour under dynamic loading conditions. The results show that the natural aggregate-using NASTBC and NASDC have significantly higher dynamic moduli than the demolition aggregate mixes. Specifically, NASDC has the greatest

modulus at 52.06 GPa, while NASTBC comes in second with 50.76 GPa. The 2.4% improvement in elasticity for NASDC over NASTBC indicates that it has superior elastic properties and is more resistant to deformation under dynamic stresses.

TBC, these findings reveal a loss of around 16.5% and 16.0%, respectively, in stiffness and deformation susceptibility under similar loading conditions. The close findings for DASTBC and DASDC suggest that compositional modifications have not significantly impacted their elastic behaviour. All things considered; these findings demonstrate how crucial aggregate type is in defining the mechanical properties of concrete. Concrete can be made from recycled materials, but their performance impacts must be carefully evaluated to ensure structural integrity and lifetime, especially in applications that need high stiffness and little deformation under load. The data emphasises the need for more research to enhance the use of recycled aggregate without compromising the mechanical performance of concrete.

Roughly speaking, the NASTBC mix exhibits the lowest compressive strength among the tested concretes, even though it is less porous than recycled concretes and performs better in terms of tensile modulus, elasticity, and ultrasonic wave propagation. Several factors help explain this apparent contradiction:

- Nature and Quality of Interfacial Bonding

Compressive strength is highly dependent on the quality of the interface between the cement paste and aggregates. In the NASTBC mix, this interfacial zone may be weaker or contain microcracks, limiting the concrete's ability to withstand high compressive loads—even if the overall porosity is low.

- Effect of Porosity on Mechanical Properties

While porosity is an important factor, it is not the sole determinant of compressive strength. A concrete with lower porosity may have a more homogeneous microstructure, but it can still contain microscopic defects (such as microcracks or weak zones) that significantly impair compressive performance.

- Differences Between Tensile and Compressive Properties

Properties like tensile strength, elastic modulus, and ultrasonic velocity are more sensitive to internal cohesion and the continuity of the matrix. In contrast, compressive strength depends on the material's resistance to crack propagation under high loads. Therefore, a concrete can demonstrate strong tensile and elastic properties without necessarily excelling in compression.

In summary, the NASTBC mix's superior performance in some mechanical aspects does not guarantee high compressive strength, as compressive behaviour is influenced by distinct microstructural and interfacial factors.

IV. 3.2.8. Deformability

The instantaneous elastic deflection's overall evolution, including its longitudinal and transverse components, as well as the concrete's elasticity and deformability modules, are depicted in Figures IV.15 and IV.16. These graphs illustrate the behaviour of the concrete series, NASTBC, NASDC, DASTBC and DASDC, with regard to the relative stress (η).

IV. 3.2.8.1. Constraint Longitudinal Deflection

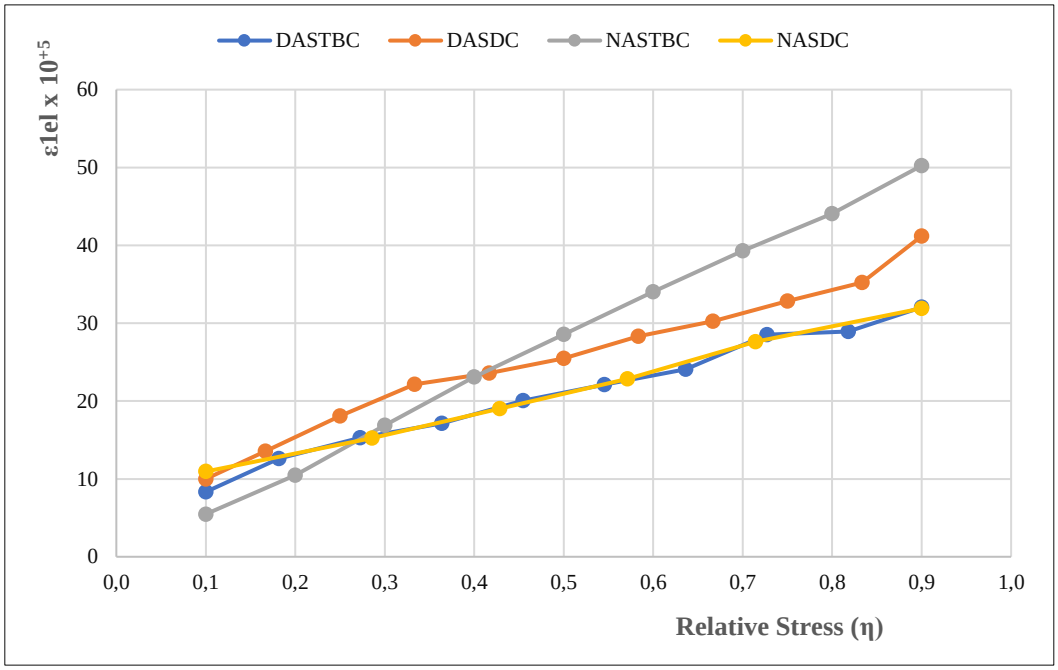

Figure IV. 15 : Elasto-Instantaneous Longitudinal Deflection of Concretes

Figure IV. 15 shows the evolution of elasto-instantaneous longitudinal strain (ε, in $\times 10^{-5}$) as a function of relative stress (η) for four types of concrete. For all concretes, the longitudinal strain increases with relative stress, but the magnitude and progression differ significantly between the mixes. NASTBC (reference concrete) shows the highest deformability, with strain values starting at 5.48×10^{-5} for $\eta \approx 0.1$ and reaching 50.24×10^{-5} at $\eta \approx 0.9$. This indicates a lower stiffness and an earlier transition into the plastic zone. NASDC demonstrates the lowest strains for each relative stress level, starting at 10.95×10^{-5} ($\eta \approx 0.1$) and reaching 31.9×10^{-5} ($\eta = 0.9$). This reflects improved rigidity and delayed onset of plastic deformation, likely due to the optimised

use of dune sand and demolition aggregates. DASTBC exhibits intermediate behaviour, with strains ranging from 8.33×10^{-5} ($\eta \approx 0.1$) to 32.05×10^{-5} ($\eta \approx 0.9$), closely matching NASDC at higher stress levels. DASDC shows higher strains than DASTBC and NASDC, starting at 10×10^{-5} ($\eta \approx 0.1$) and reaching 41.19×10^{-5} ($\eta \approx 0.9$), approaching the deformability of the reference concrete in the plastic range. The elastic zone is observed at lower η values (up to about 0.3–0.4), where the strain increases nearly linearly with stress, and the modulus of elasticity remains relatively constant. Beyond this, the plastic zone begins, characterised by a faster increase in strain for a given increase in stress, indicating permanent (irreversible) deformation. NASDC shows the best mechanical performance, with the lowest strains and the widest elastic zone. DASTBC follows, with good rigidity and moderate plastic deformation. DASDC and especially NASTBC exhibit higher strains and earlier transition to plasticity, indicating lower stiffness and greater susceptibility to permanent deformation. The results confirm that the use of dune sand and demolition coarse aggregates enhances concrete rigidity and delays plastic deformation, while the reference concrete (NASTBC) is the most deformable. DASTBC provides a good compromise, and DASDC performs moderately well but is less rigid than NASDC and DASTBC.

IV. 3.2.8.2. Constraint Transversal Deflection

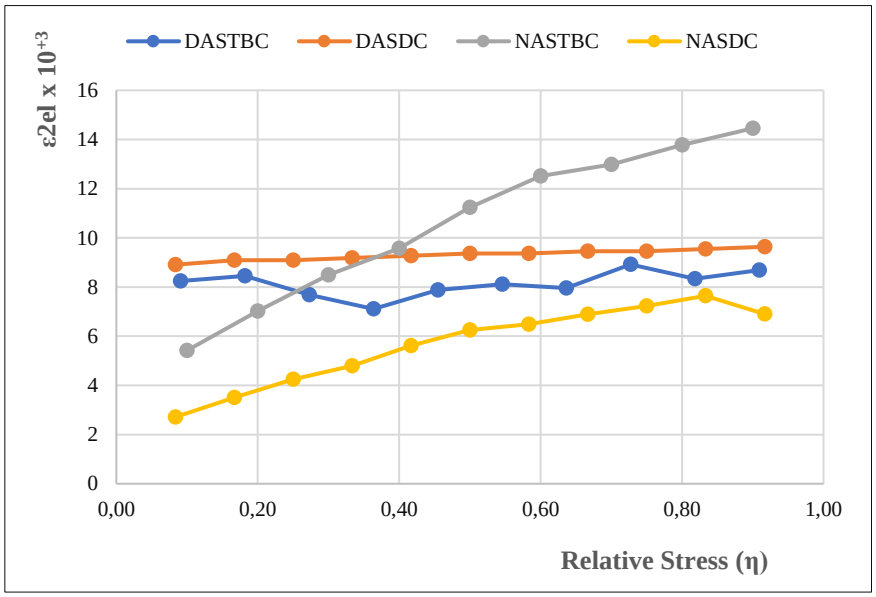

Figure IV. 16 : Elasto-Instantaneous Transveral Deflection of Concretes

Figure IV. 16 presents the evolution of the transversal (lateral) elastic strain ($\varepsilon_2 el \times 10^{-3}$) for four types of concrete as a function of relative stress (η) under compression. NASTBC consistently shows the highest transversal deformation. At η = 0.1, the strain

is 5.42×10^{-3}, increasing steadily to 14.46×10^{-3} at $\eta = 0.9$. This indicates that NASTBC is the most susceptible to lateral expansion under load, reflecting a less compact microstructure and lower resistance to cracking and dimensional instability. NASDC exhibits the lowest transversal deformation at every stress level. For example, at $\eta \approx 0.1$, the strain is 2.71×10^{-3}, and at $\eta \approx 0.9$, it reaches only 6.90×10^{-3}. This performance, nearly half that of NASTBC at maximum stress, highlights the superior dimensional stability and resistance to lateral expansion provided by the use of dune sand and demolition coarse aggregates. DASTBC shows moderate and relatively stable transversal strain values. At $\eta \approx 0.1$, the strain is 8.25×10^{-3}, and at $\eta \approx 0.9$, it is 8.68×10^{-3}. This suggests good resistance to lateral expansion, with values consistently lower than NASTBC and close to NASDC, especially at higher stresses. DASDC displays a gradual increase in transversal strain, from 8.91×10^{-3} at $\eta \approx 0.1$ to 9.64×10^{-3} at $\eta \approx 0.9$. While its performance is better than NASTBC, it is less favourable than DASTBC and NASDC, indicating a somewhat higher tendency for lateral deformation. For all concretes, the relationship between relative stress and transversal strain is nearly linear up to about $\eta = 0.3–0.4$. In this range, deformations are reversible, and the material behaves elastically. Beyond this point, the strain increases more rapidly for a given increase in stress, indicating the onset of irreversible (plastic) deformation and the development of microcracks. NASDC is the best performer, with the lowest transversal deformation and the widest elastic zone, making it the most stable and durable under compression. NASTBC is the most deformable laterally, which could lead to higher risk of cracking and dimensional instability. DASTBC and DASDC offer intermediate performance, with DASTBC closer to NASDC in terms of lower transversal strain.

IV. 3.2.8.3. Deflection Module and Elasticity Module

Figures IV.17 and IV.18 show the evolution of the deflection module and elasticity module in accordance with the relative stress (η) for the NASTBC, NASDC, DASTBC, and DASDC specimens.

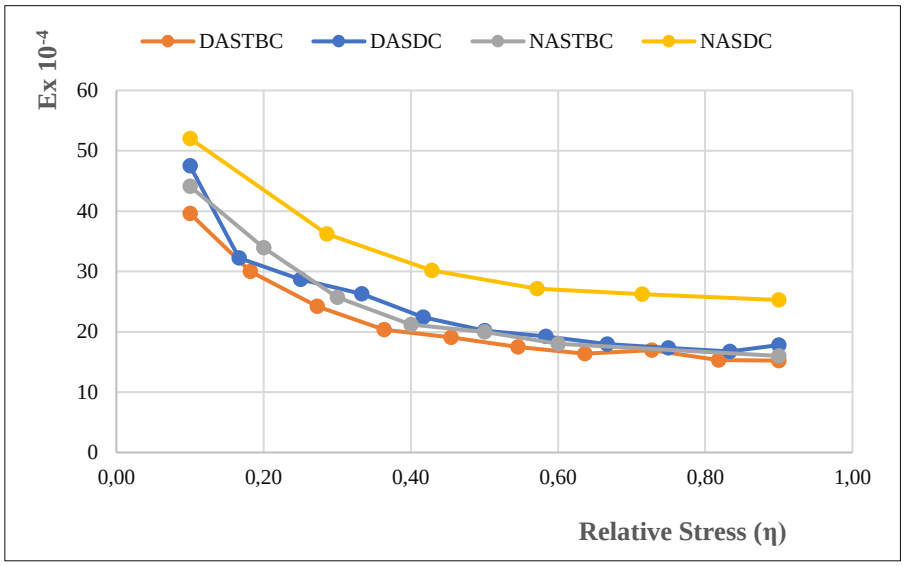

Figure IV. 17 : Deflection Module of Concretes

According to Figure IV. 17, the deflection modulus decreases as the relative stress increases for all concretes, reflecting typical nonlinear behaviour. NASDC consistently shows a higher deflection modulus compared to DASDC, NASTBC, and DASTBC, indicating superior stiffness. This suggests that NASDC's optimised composition better resists elastic deformation. Consequently, NASDC is expected to offer improved durability and structural performance under load.

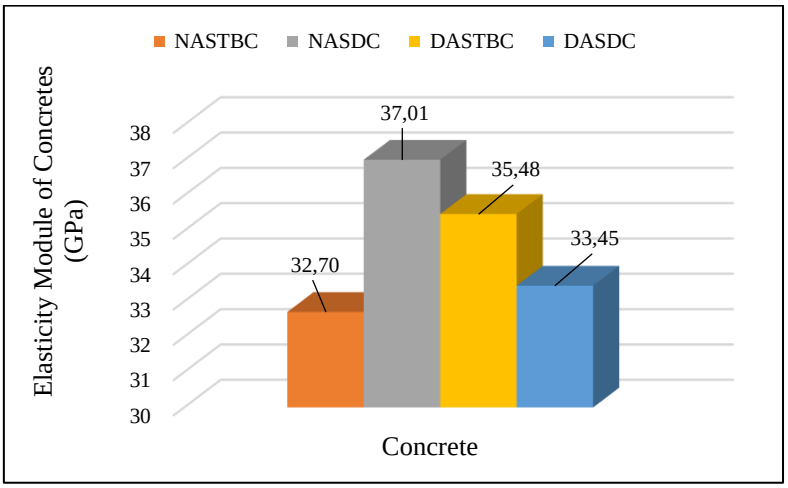

Figure IV. 18 : Elasticity Module of Concretes

The concrete mix NASDC (containing Saharan dune sand and natural aggregates) exhibits the highest modulus of elasticity at 37.01 GPa, followed by DASTBC (35.48 GPa), DASDC (33.45 GPa), and NASTBC (32.70 GPa). Compared to the reference mix NASTBC, the modulus of elasticity increases by 13.18% for NASDC, 8.50% for DASTBC, and 2.29% for DASDC. These results indicate that NASDC significantly outperforms the reference mix in stiffness, while DASTBC and DASDC also show

moderate improvements. The enhanced elasticity of NASDC underscores the beneficial role of Saharan dune sand in optimising concrete performance. Despite the improvements in DASTBC and DASDC, their lower values compared to NASDC suggest that the inclusion of demolition aggregates may slightly reduce stiffness relative to mixes with natural aggregates. These variations highlight the importance of material selection in balancing sustainability and structural integrity. For projects prioritising stiffness, NASDC emerges as the optimal choice, whereas DASTBC and DASDC offer viable alternatives when recycled materials are prioritised.

IV. 3.2.9. Durability Indicators

IV. 3.2.9.1. Absorption by Total Immersion

The total immersion absorption test results, averaged from three measurements per concrete type (Figure IV.19), show porosity values ranging from 4.45% to 5.28%. NASDC exhibits the lowest porosity at 4.45%, followed by NASTBC at 4.65%, DASTBC at 4.86%, and DASDC the highest at 5.28%. The higher porosity in DASDC is mainly due to the coarse demolition aggregates with porous old mortar, which increases overall pore volume. Concretes containing dune sand (SD), such as DASDC and NASDC, tend to have slightly higher absorption than those with traditional sand (STB), explaining why DASDC is more absorbent than DASTBC. Additionally, NASTBC's higher water-to-cement ratio compared to NASDC results in greater absorption. Despite these differences, the porosity values are relatively close, indicating comparable durability among the mixes.

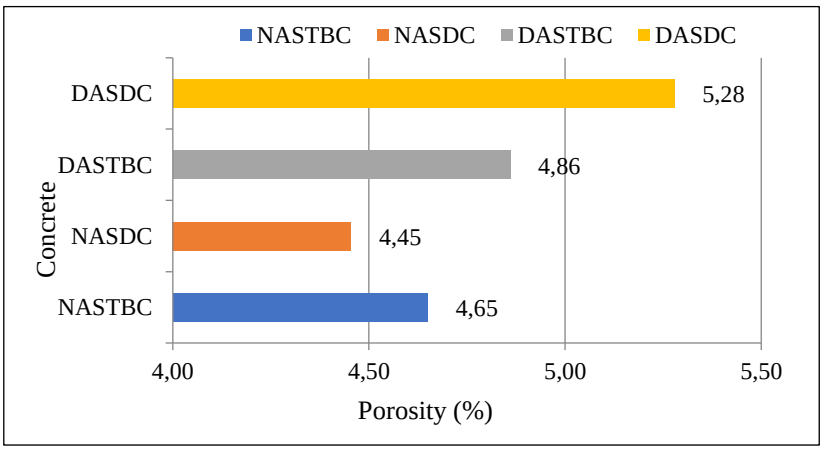

Figure IV. 19 : Porosity of Concretes

IV. 3.2.9.2. Water Permeability

Regarding water permeability (Figure IV.20), the permeability coefficients also show variation: NASDC has the lowest at 0.18 × 10^{-5} m/s, NASTBC at 0.20 × 10^{-5} m/s, DASTBC slightly higher at 0.22 × 10^{-5} m/s, and DASDC significantly higher at 2.27 × 10^{-5} m/s. Although DASDC's permeability is notably greater—about ten times that of NASDC and DASTBC—it still remains within a low range, and all concretes withstand water pressures above 6 bar. This suggests that while DASDC may be more permeable, it maintains sufficient resistance to water ingress for durability. The close permeability values of DASTBC and NASTBC imply similar performance in moist environments, whereas NASDC's lower permeability indicates enhanced durability. Overall, the use of recycled aggregates and dune sand does not substantially compromise the durability of these concretes, though DASDC's higher permeability warrants consideration in highly aggressive conditions. Consequently, the concretes can be considered effective in terms of durability [204].

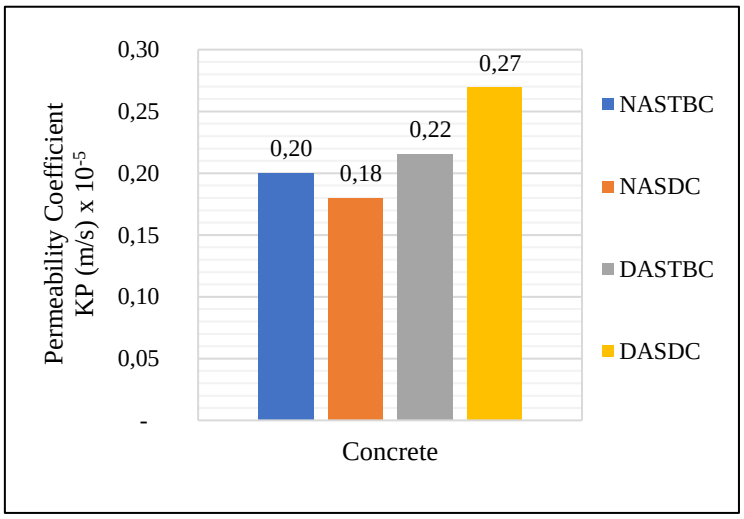

Figure IV. 20 : Permeability Coefficient of Concretes

IV. 3.2.9.3. Absorption by Capillarity

Figure IV.21 displays the capillary absorption test results. Three values are averaged to create each value. The concretes' capillary absorption coefficient (Ca_t) kinetics plot nearly linear curves as a function of the square root of time (√t), showing similarities in the first half-hour, a first regression of the slope for NASDC after half an hour, and a second regression for all concretes after eight hours. Slope regression is typically linked to the presence of many pore families, claims Tahar ALI BOUCETTA [339]. Absorption proceeds in the smallest capillary pores as soon as the capillary rise is

achieved in the larger capillary pores. As a result, these concretes' absorption kinetics slowdown, which accounts for the slope's decline. All concretes have big pores of the same size and/or volume, which explains why the curves during the first half-hour were comparable. Large pores have a low volume and/or size because the absorption coefficient is small (less than 1) during the first half-hour. The regressions of the slopes of the curves for concretes based on natural aggregates (NASDC and NASTBC) produce the offset between the curves, but those for concretes based on demolition aggregates (DASDC and DASTBC) are less significant. When compared to concretes made with natural aggregates (NASDC and NASTBC), this may be explained for two likely reasons: first, the volume of microscopic pores is bigger, and second, the size of those pores is larger. While the old adhering mortar itself is extremely porous, the techniques employed to recover and prepare demolition aggregates cause new microcracks to form [340]. These two elements raise the demolition aggregates' porosity, which in turn raises the aggregates' total porosity in the concrete. After a day, demolition aggregate concretes (DASTBC and DASDC) have a higher capillary action water absorption capacity than NASTBC and particularly NASDC, whose pore volume has been further decreased by the lower W/C ratio. Compared to natural aggregate concretes, aggressive chemicals will have an easier time penetrating demolition aggregate concrete. This aligns with Sasanipour and Aslani's (2020) study [341].

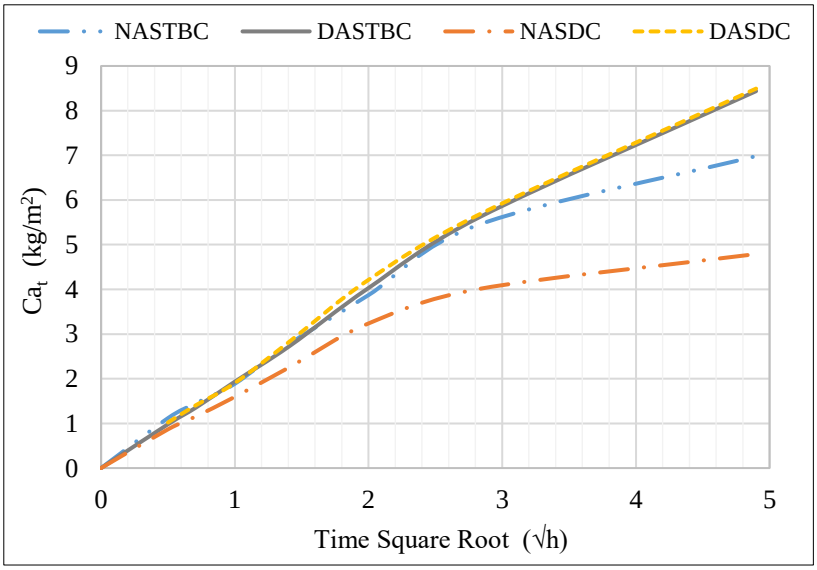

Figure IV. 21 : Kinetics of Capillary Absorption Coefficient (Ca_t) of the Concretes as a Function of the Square Root of Time (√t)

IV. 3.2.10. SEM Observations

Scanning electron microscopy (SEM) analysis of the concrete samples (Figure VI. 22) shows that all four types of concrete have a similar microstructure, with portlandite crystals clearly visible. This structural homogeneity indicates that the basic properties of the concrete matrix are not substantially changed by the addition of Saharan dune sand and demolition coarse aggregates. Indicative of the hydration process, the presence of portlandite crystals enhances the concrete's overall performance and durability. In order to assess how these components interact and impact the concrete's mechanical qualities and endurance in different applications, it is essential to comprehend these microstructural characteristics.

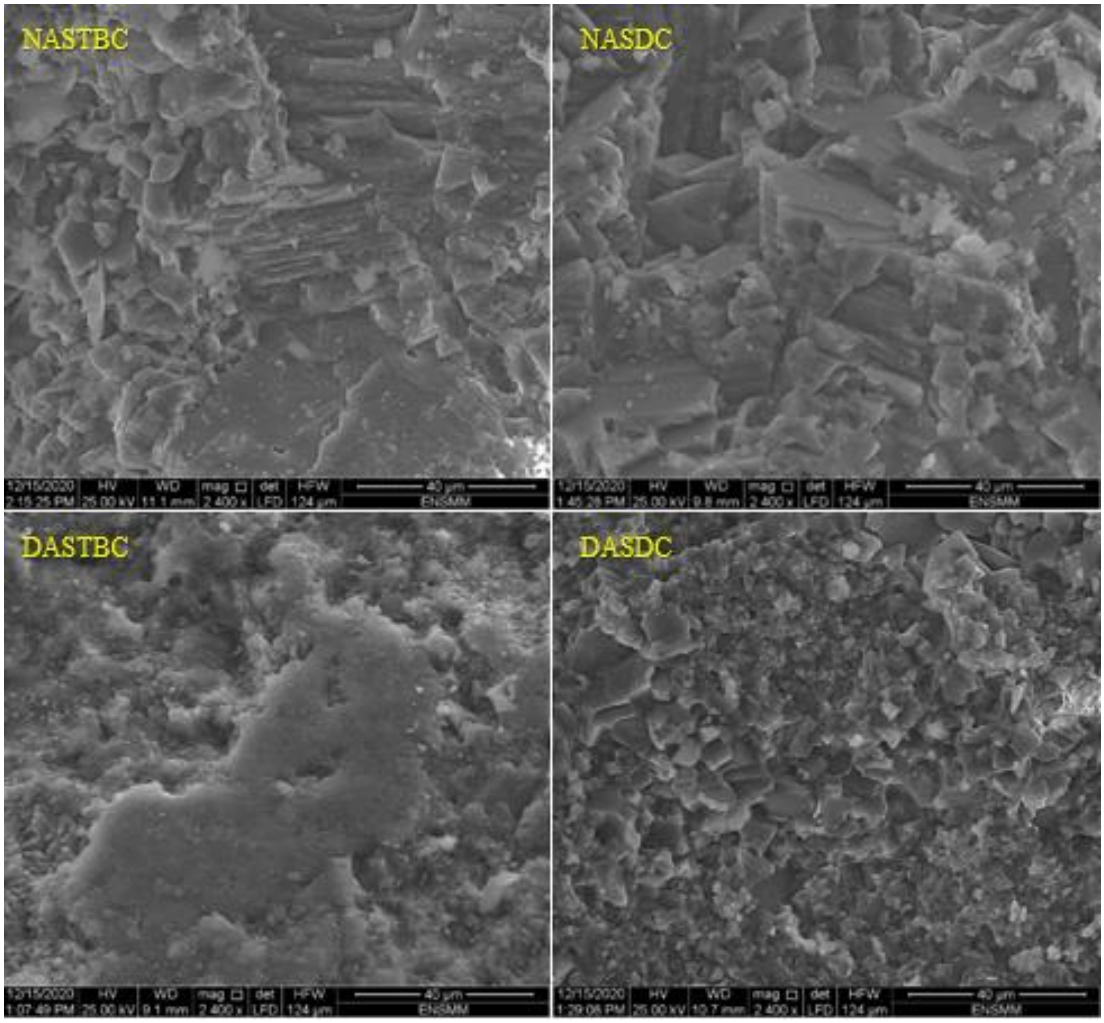

Figure IV. 22 : SEM observation of the concrete samples

IV. 3.2.11. Behaviour in Severe Conditions

IV. 3.2.11.1. Abrasion

❖ Appearance

External examination of the samples after abrasion reveals that they begin to lose their shape and reduce in size (mass and volume) within the first two hours. The harsh angles and edges soften further. Additionally, leaching resulted in the samples losing their outer layer, making the larger aggregates that had previously been obscured by the cement matrix more visible. These particles degrade similarly to the cement matrix as the abrasion time increases. An example concrete specimen following 2, 4, 6, and 8 hours of abrasion is shown in Figure VI. 23.

Figure IV. 23 : Concrete Specimen After 2, 4, 6 and 8 Hours of Abrasion

❖ Mass Evolution

The mass evolution and mass loss ratio of concrete samples as a function of abrasion time are displayed in Figure VI. 24. The results for the NASTBC, NASDC, DASTBC, and DASDC samples show the following mass loss:

The next two hours: 19.37%, 15.09%, 20.59%, and 32.83%

Specifically, 67.43%, 35.86%, 40.00%, and 39.81% four hours later

83.53%, 48.47%, 54.03%, and 58.89% after six hours

93.81%, 57.36%, 67.18%, and 72.97% after eight hours

By demonstrating a steady increase in mass loss over time for every sample, our results highlight linear abrasion-induced degradation. The control sample has a larger weight loss, but all of the concrete types under examination exhibit almost the same degree of degradation. The ratio of paste to aggregate and aggregate quality have a major impact on abrasion resistance. Compared to alluvial and dune sands, the aggregates in the

tested concretes had less wear resistance. Concretes with a higher paste-to-aggregate ratio exhibit improved resistance to abrasion as a result.

The abrasion test findings generally show that concrete made of demolition Coarse aggregates and dune sand is more abrasion resistant than ordinary concrete. More proof that dune sand and demolition aggregates are preferable to traditional sands and aggregates is provided by this discovery.

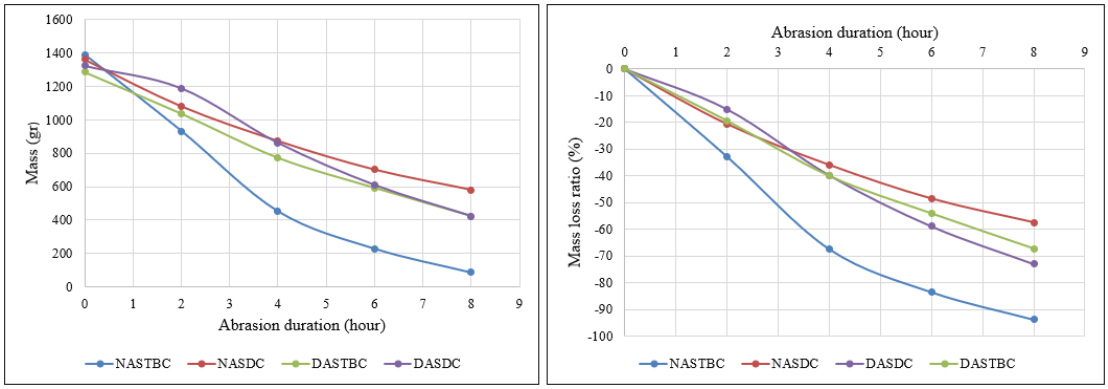

Figure IV. 24 : Mass Evolution (left, in grams) and Mass Loss Ratio (right, %) of Concrete Samples as a Function of Abrasion Duration

IV. 3.2.11.2. Freeze-Thaw Cycles

❖ Appearance

The concrete cubes' skin and edges have somewhat changed after 50 freeze-thaw cycles, but there is no surface flaking or cracking visible when the specimens are visually examined (Figure IV. 25).

Figure IV. 25 : The External Appearance of the Concretes Exposed to 50 Freeze-Thaw Cycles

❖ Mass Evolution

The mass development findings of the concrete exposed to freeze-thaw processes for 90 days, along with their observation concretes, are displayed in Figure IV. 26. After 25 cycles, the mass of all the concretes increased. The cement's anhydrous phases' ongoing hydration provides an explanation for this. The concrete's fissures make it easier for water and CO_2 to enter, which is essential for the hydration processes that

produce solids from the anhydrous phases. Canals for conveyance are found in capillary pores and cracks [342, 343]. This fills the pores and voids, promotes material gain, and repairs fissures. The bulk growth is less intense after 50 rounds. This can be explained by the gradual narrowing of the transportation canals, which gradually limits the supply of humidity and CO_2 required for the reactions to continue. By themselves, the ongoing obstructing of the cracks and filling of the pores and voids will be gradually reduced until it stops. The reduction in NASTBC concrete's compressive strength might be the result of partial healing brought on by blockage of the capillary pores and fissures. In other words, some of the pores, voids, and fissures are either completely or partially unhealed. This is consistent with Argouges and Gagné's (2010) findings [342, 344].

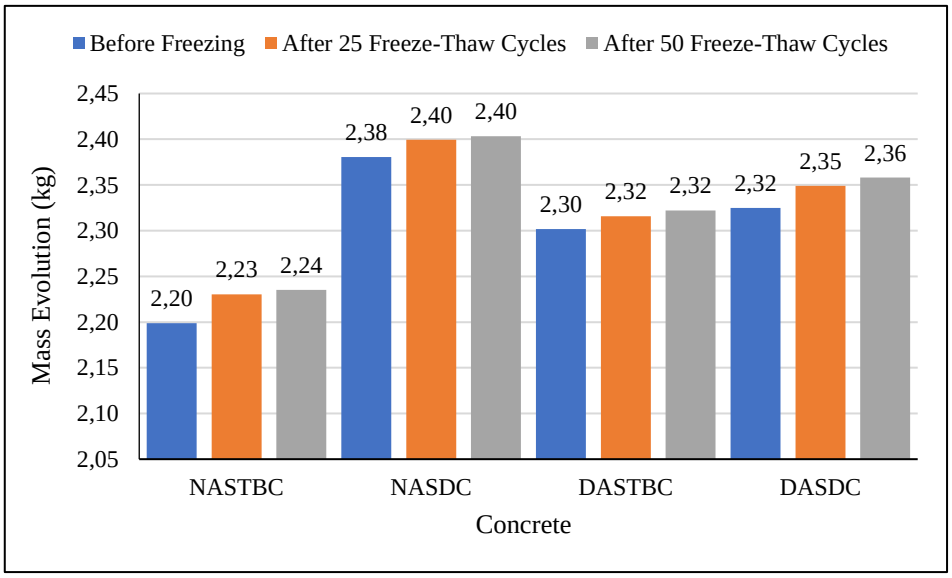

Figure IV. 26 : Mass Evolution After Freeze-Thaw Cycles

❖ Compressive Strength

The results of the 90-day concrete exposure to freeze-thaw cycles and their observation concretes' compressive strength are displayed in Figure IV. 27. For NASTBC, NASDC, and DASTBC, the compressive strength dropped by 16.66%, 14.40%, and 13.51%, respectively. DASDC had a 4.92% growth. Khouadjia and Mezghiche (2019) [345] Claim that concrete with lower porosity and smaller pores performs better. The presence of fine dune sand particles reduces the diameters of the pores, which lowers the demand for water. This is achieved by reducing the effective water-cement ratio (W_{eff} /C), which ensures that the cement is hydrated. As a result, during freeze-thaw cycles, the concrete will sustain less damage. Every concrete under study is frost-resistant based on the Frost Strength Coefficient (FSC) that was computed (Table IV.

16). The analysis of the FSC for the concretes NASTBC, NASDC, DASTBC, and DASDC, with values of 0.83, 1.02, 1.05, and 1.05 respectively, clearly demonstrates the superior performance of mixes incorporating dune sand and demolition aggregates. The reference concrete NASTBC experiences a notable strength loss after freeze-thaw cycling, whereas NASDC shows a modest improvement of about 2%, highlighting the positive influence of dune sand on the concrete's compactness and microstructure. The DASTBC and DASDC mixes exhibit an even greater enhancement, with a 5% increase in strength, reflecting the excellent durability imparted by combining dune sand with low-absorption recycled aggregates. This improvement is attributed primarily to the very fine size of connected pores, which restricts water ingress and limits freeze-thaw damage, as well as to the self-healing of microcracks that helps restore the concrete's microstructure. Additionally, the dune sand's high silica content promotes chemical reactions within the cement matrix, fostering the formation of solid hydration products that further enhance durability. These findings confirm that the use of alternative materials significantly improves freeze-thaw resistance, making these concretes particularly well-suited for environments subject to severe thermal cycling.

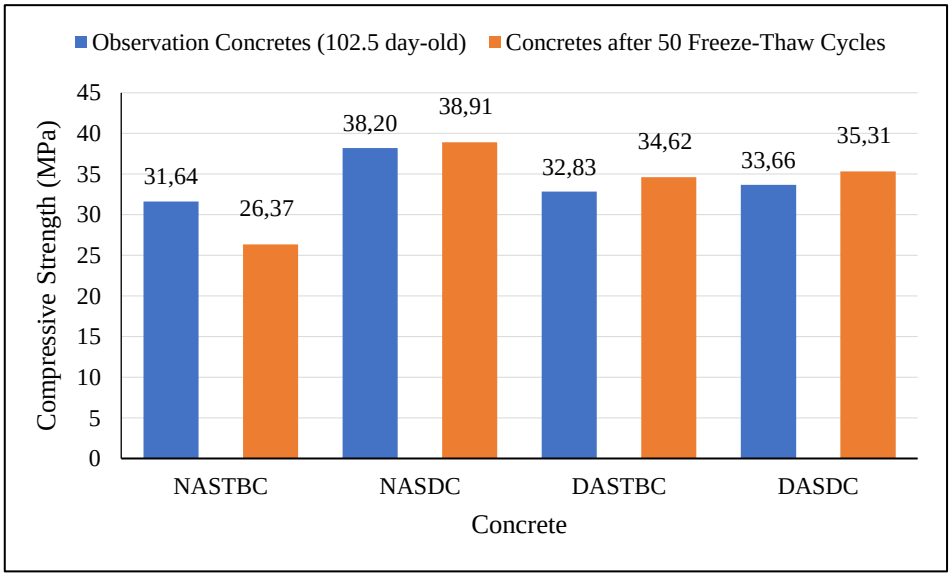

Figure IV. 27 : Compressive Strength After Freeze-Thaw Cycles

Table IV. 16 : Frost Strength Coefficient

Concrete	FSC
NASTBC	0.83
NASDC	1.02
DASTBC	1.05

DASDC	1.05

IV. 3.2.11.3. Chemical Attacks

The type of the chemical and the susceptibility of the concrete determine how aggressive the chemical is towards hydraulic concrete. Important factors influencing aggressiveness include concrete permeability, the extent of cracking, material selection, type and amount of cement utilised, and curing environment. The cement matrix has a PH of about 13, making the PH disparity especially significant because any environment with a lower PH is viewed as unfriendly. This interaction causes a chemical equilibrium through the dissolution of portlandite, which affects the concrete's density and porosity and ultimately its compressive strength. To evaluate resistance, 100x100x100 mm^3 cube samples were cured in tap water for 28 days before being tested monthly in a variety of challenging circumstances. Mass measurements were made every month for two years to assess chemical resistance in compliance with ASTM C 267-96 after samples had been washed to remove modified mortar. Mass loss measurements taken both before and after exposure were used to gauge the extent of assault on the concrete samples. At 28 days of age, 100x100x100 mm^3 cubes of each of the four types of concrete were submerged in demineralised water, a 5% NaOH solution, and saltwater. Control samples, meanwhile, were maintained immersed in tap water. The solutions were changed every month to maintain a pH level different from the concrete's, guaranteeing the liquid habitats' constant aggressiveness. Weight measurements, ultrasonic velocity evaluations, and visual inspections were carried out over the course of the investigation. The samples were subjected to basic compression testing at age two in order to assess their residual strength.

❖ Appearance

Visual inspection of concrete samples subjected to different chemical conditions shows minor surface and edge changes, but no flaking or cracking is seen. According to this finding, the concrete's surface integrity is affected by chemical conditions in a measurable way, which may result in modifications that effect the material's durability and mechanical qualities. Even if these changes are slight, they show how important it is to evaluate the concrete's resistance in various settings in order to acquire a better understanding of how it behaves when confronted with hostile substances. To measure these changes and assess their consequences for the actual usage of concrete in

comparable circumstances, more research could be needed. Figure VI. 28 shows the external appearance of some specimens after two years of immersion in different fluids.

Figure IV. 28 : External Appearance After 2 Years of Immersion in Chemical Media

❖ Mass Evolution

Figure VI. 29 displays the mass variation following two years of immersion. Important details on the durability and environmental resistance of concrete specimens NASTBC, NASDC, DASTBC, and DASDC are provided by the data on the variation in mass of these specimens following two years of immersion in different fluids.

Tap Water: For NASTBC, NASDC, DASTBC, and DASDC, the corresponding mass changes were 0.56%, 0.23%, -0.96%, and -1.21%. Given that concrete may absorb moisture, the positive mass increases in NASTBC and NASDC suggest a minor degree of water absorption. On the other hand, the negative mass changes in DASTBC and DASDC suggest a material loss that might be the consequence of leaching or the gradual deterioration of the concrete matrix.

The corresponding mass variations for NASTBC, NASDC, DASTBC, and DASDC were 0.79%, 0.65%, 0.23%, and 0.36%. Positive results indicate that all of the specimens absorbed water while immersed, with NASTBC showing the highest rate of absorption. This suggests that the porosity of the concrete allows for the absorption of moisture, which may enhance its hydration but may also cause problems with long-term durability if it happens excessively.

For DASTBC, NASDC, NASTBC, and DASDC, the mass fluctuations in sea water were -0.13%, -0.25%, and 0.60%, respectively. The positive readings for NASTBC and NASDC indicate a little absorption, but the negative findings for DASTBC and DASDC suggest material loss. Chemical processes brought on by the salts in seawater may compromise the integrity of certain concrete mixtures.

In the 5% NaOH solution, mass changes of 0.67% for NASTBC, 0.64% for NASDC, -0.56% for DASTBC, and -0.53% for DASDC were noted. Again, the hostile alkaline environment resulted in positive mass increases in N but negative changes in DASTBC and DASDC that indicated deterioration.

General Interpretation: The concrete specimens' varied reactions to various immersion fluids demonstrate their unique durability traits: In comparison to DASTBC and DASDC, NASTBC and NASDC continuously showed superior resistance to absorption and degradation in all mediums. Significant mass loss was seen by DASTBC and DASDC in tap water, sea water, and NaOH solution, suggesting a susceptibility to chemical assault or leaching.

The results imply that the composition of the concrete mixes greatly determines their performance in difficult conditions; consequently, improving mix design might boost durability. These findings demonstrate how important it is to employ the proper materials and formulae to prolong the life of concrete structures exposed to various climatic conditions. More research may be done on changes that would make more vulnerable mixtures—like DASTBC and DASDC—more resilient to chemical attacks and moisture incursion.

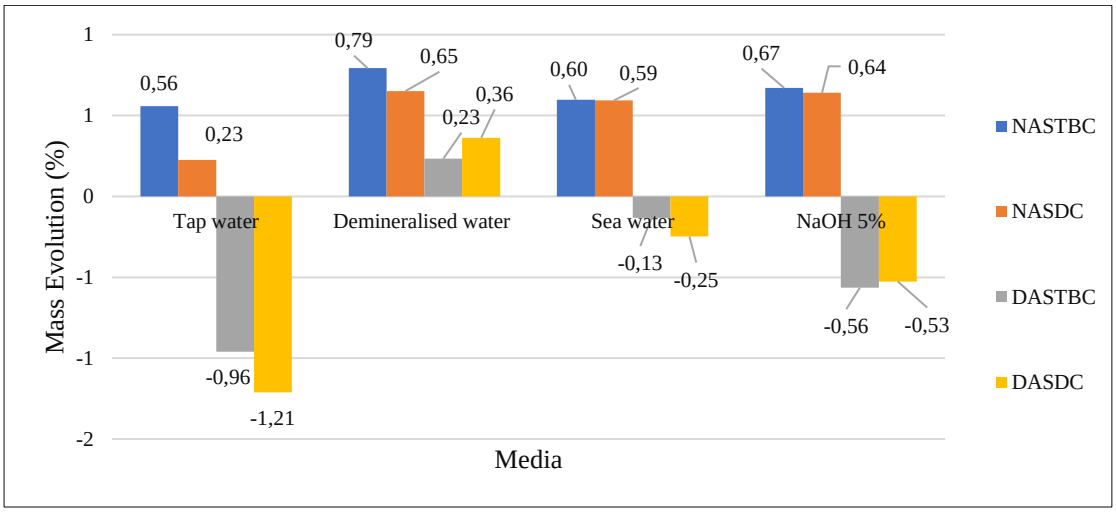

Figure IV. 29 : Mass Evolution After 2 Years of Immersion in Chemical Media

❖ Compressive strength

Comparing the concrete specimens to those kept in an environment with non-renewed tap water, the residual compressive strength shows notable differences, ranging from 35.96 MPa to 54.28 MPa. This range highlights how various exposure circumstances affect the concrete's longevity and overall performance, underscoring the crucial role that environmental elements play in assessing the quality of concrete throughout time.

Figure VI. 30 shows the variations in compressive strength after two years of immersion, providing important information on how resilient the concrete types NASTBC, NASDC, DASTBC, and DASDC are under different circumstances. In tap water, DASTBC unexpectedly improved by 3.56%, whereas NASTBC had a significant drop of -15.94%. DASTBC demonstrated a noteworthy rise of 14.88% in demineralised water, in stark contrast to NASTBC's decline of -13.90%. Exposure to sea water produced a range of results, with DASTBC once more demonstrating a positive alteration of 9.88%. Lastly, DASTBC demonstrated a remarkable 18.01% increase in a 5% NaOH solution, underscoring its improved tolerance to alkaline conditions. When taken as a whole, these findings show how various media may greatly affect concrete's durability and compressive strength, guiding future material use and selection techniques in building operations.

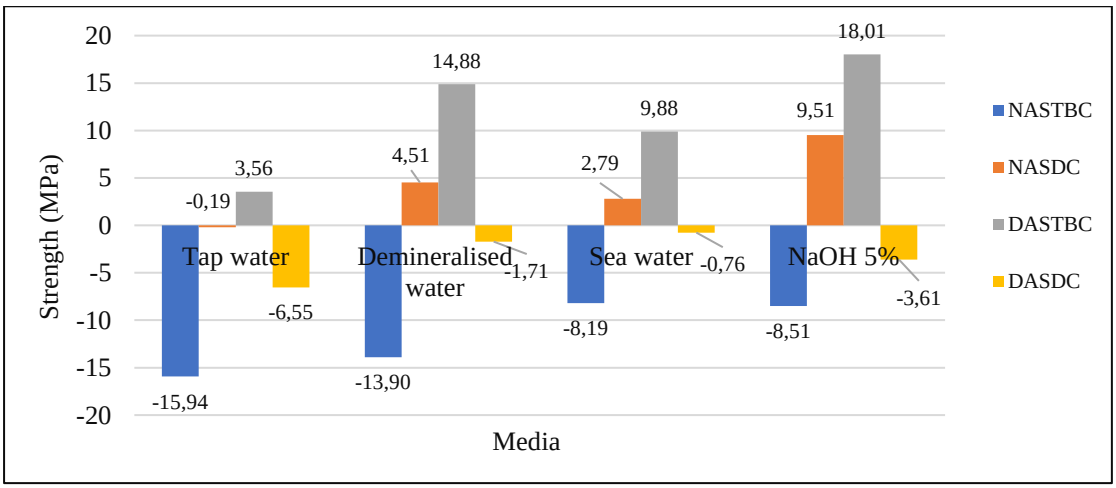

Figure IV. 30 : Compressive Strength Evolution After 2 Years of Immersion in Chemical Media

❖ Ultrasonic velocity Evolution

Figure VI. 31 shows the variations in ultrasonic velocity after two years of immersion. Tap Water: Increases of 7.2% for NASTBC, 5.29% for NASDC, 0.89% for DASTBC, and 2.61% for DASDC were among the positive ultrasonic velocity changes seen in tap water. These findings imply that the concrete specimens kept in tap water improved in density and structural integrity, most likely as a result of ongoing hydration processes and moisture absorption.

Demineralised Water: There were very minor changes in demineralised water, with NASDC, DASTBC, and DASDC all seeing declines of -1.33%, -3.96%, and -1.02%, respectively, and NASTBC experiencing a little gain of 0.15%. The adverse alterations

suggest that these combinations may become more porous or lose some of their material qualities.

Sea Water: For NASTBC, NASDC, DASTBC, and DASDC, the variances in sea water were -0.06%, -7.08%, and -3.30%, respectively. The notable decrease in NASDC's ultrasonic velocity raises the possibility that exposure to salty environments may have compromised its structural integrity through leaching or chloride assault.

Ultrasonic velocity variations in a 5% NaOH solution were 1.63% for NASTBC, -1.24% for NASDC, -2.69% for DASTBC, and -1.13% for DASDC. The negative changes in the other specimens suggest that the alkaline environment may have caused deterioration or decreased bonding within the concrete matrix, even if NASTBC exhibited a minor improvement. All things considered, our results demonstrate how various immersion conditions may have a substantial effect on the ultrasonic velocity of concrete specimens over time, indicating variations in their structural performance and longevity. While the negative variances in sea water and NaOH solution highlight the necessity of taking environmental conditions into account when evaluating concrete lifespan and integrity in real-world applications, the favourable trends in tap water show positive benefits of moisture retention.

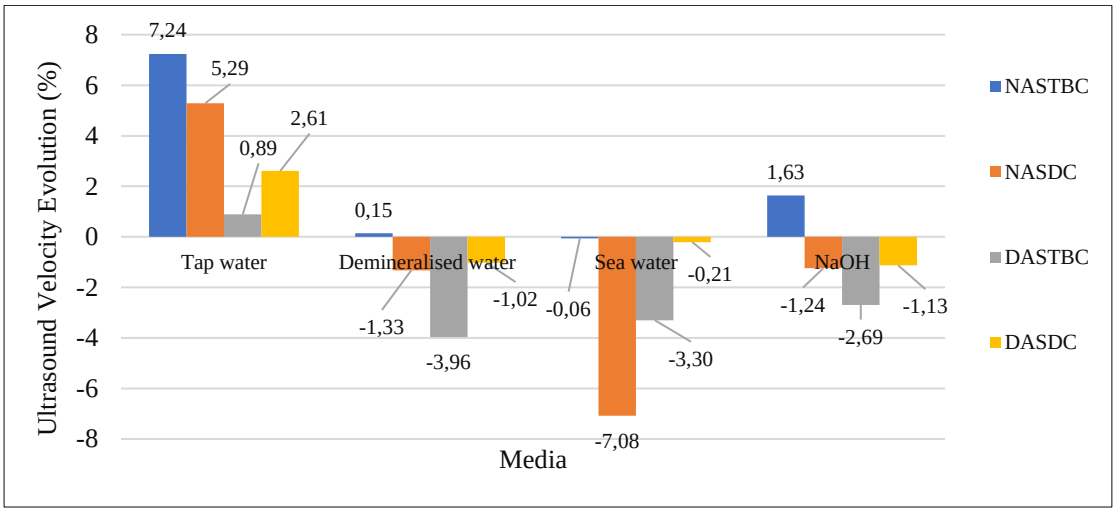

Figure IV. 31 : Ultrasonic Velocity Evolution after 2 Years of Immersion in Chemical Media

❖ Correlation Between Ultrasonic Velocity and Compressive Strength

Polynomial trendlines obtained from experimental data may be used to examine the relationship between ultrasonic velocity and concrete strength (Figure IV. 32). With an R^2 value of 0.8429, the equation $y = -1.8549x^2+16.323x+2.679$ for NASTBC shows a significant connection, indicating that concrete strength rises with ultrasonic velocity, although at higher velocities with decreasing returns. The negative quadratic term

suggests a maximum strength at a specific speed, after which additional increases could not produce much of an improvement. The equation $y=-0.8228x^2+11.962x+5.5237$ for NASDC shows a fair match, however it shows a somewhat weaker association than for NASTBC (R^2 = 0.8113). With $y=-2.0296x^2+17.837x-0.2225$ and $R^2=0.9389$, DASTBC exhibits a greater correlation, indicating a more noticeable strength response in respect to variations in ultrasonic velocity. With an R^2 of 0.9226 and the equation $y=-2.8526x^2+21.804x-2.5146$, DASDC also exhibits significant sensitivity to variations in ultrasonic velocity.

All things considered, these results highlight how crucial it is to optimise the composition and processing of concrete in order to get the required mechanical characteristics, while also using ultrasonic velocity as a trustworthy quality indicator in structural applications.

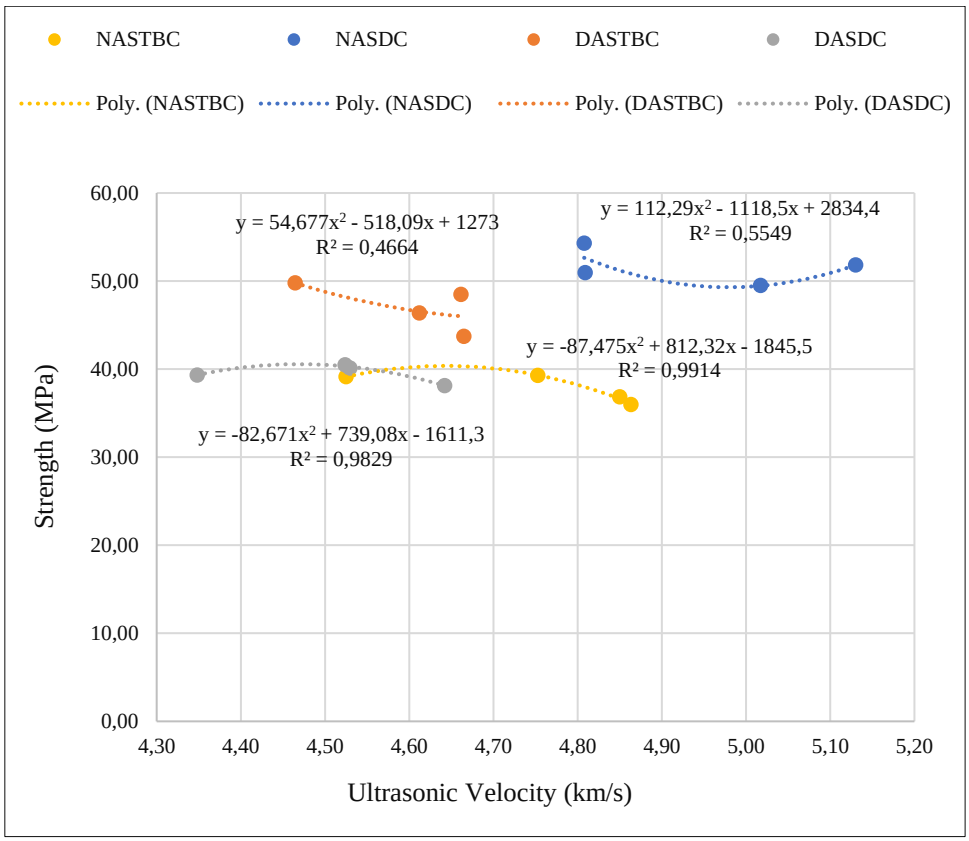

Figure IV. 32 : Correlation Between Ultrasonic Velocity and Compressive Strength after 2 Years of Immersion in Chemical Media

❖ Correlation Between Mass and Compressive Strength

After two years of immersion in chemical media, there are notable differences in the association between mass and compressive strength across the various concrete mixes. With an R^2 value of 0.311 for NASTBC, the equation $y=-1492.9x^2+6992.1x-8138.1$

shows a poor correlation, showing that changes in mass have little effect on compressive strength. However, NASDC has a substantial connection with $y=2835.2x^2-13766x+16760$ and an R^2 value of 0.9281, suggesting that mass has a considerable impact on this mix's compressive strength. Additionally, with an R^2 of 0.868 and a substantial correlation with the equation $y=-2438.6x^2+11295x-13039$, DASTBC indicates that mass is a significant factor in determining strength, albeit a less significant one than NASDC. However, with $y=4343.9x^2-20904x+25184$ and an R^2 of 0.3004, DASDC shows a poor association, suggesting that mass is not a reliable indicator of compressive strength for this combination.

All things considered, our findings demonstrate the variation in the relationship between mass and compressive strength among various concrete formulations, highlighting the necessity of customised material design strategies to maximise performance in chemically harsh situations.

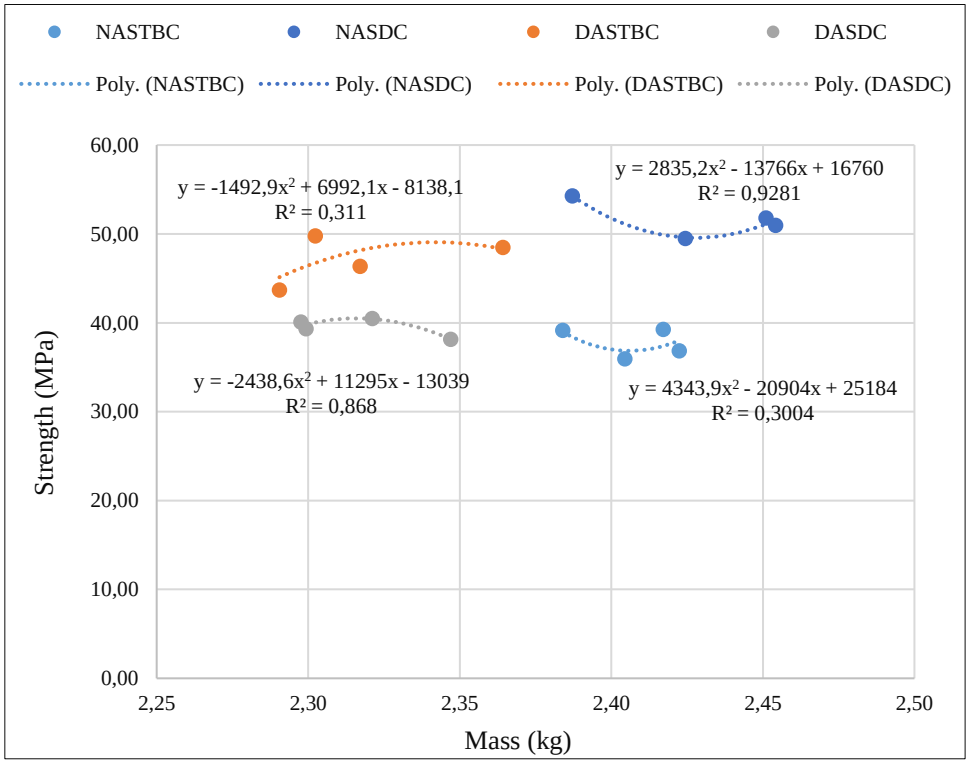

Figure IV. 33 : Correlation Between Mass and Compressive Strength after 2 Years of Immersion in Chemical Media

IV. 3.2.11.4. High Temperature

❖ Appearance

When regular concrete is heated between 150°C and 900°C, it changes significantly in appearance, with cracking and spalling being the main effects (Figure VI. 34).

Concrete's moisture content may quickly evaporate as the temperature rises, creating internal pressure that causes top layers to peel off—a process called spalling. This leads to loss of material integrity and obvious surface degradation. Furthermore, concrete's uneven thermal expansion causes tensile stresses that may be greater than the material's strength, which can result in cracking (Figure VI. 35). The concrete's structural performance may be jeopardised by these cracks, which can range in size from tiny fissures to major fractures. All things considered, exposure to high temperatures has a substantial impact on the strength and look of regular concrete, thus applications requiring fire or intense heat require careful thought.

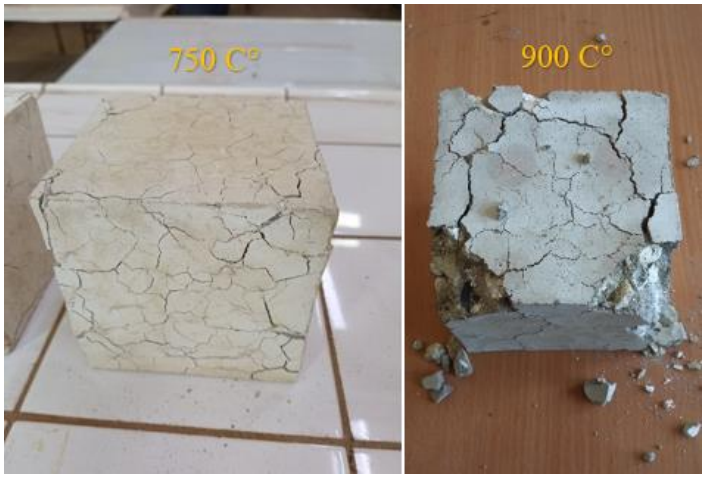

Figure IV. 34 : Spalling of a Concrete Specimen after High Temperature Exposure

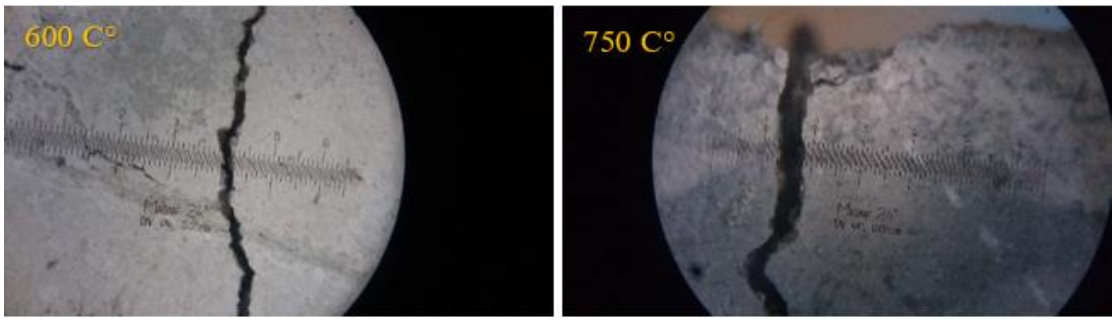

Figure IV. 35 : Concrete Cracking after High Temperature Exposure Seen with a Crack Meter

❖ Mass Evolution

The observed mass changes provide important information about the durability of concrete specimens NASTBC, NASDC, DASTBC, and DASDC after they were heated for two hours at temperatures ranging from 150°C to 900°C (Figure IV.36). While NASDC, DASTBC, and DASDC showed losses of -1.18%, -3.22%, and -1.98%, respectively, at 150°C, NASTBC showed a modest mass gain of 0.46%, suggesting that their capacities for retaining moisture varied. All specimens showed notable mass

losses as temperatures rose to 300°C and higher, but DASTBC and DASDC showed the largest drops, dropping to -9.22% and -9.95% at 300°C, respectively, and getting worse as temperatures rose. NASTBC lost -14.91%, NASDC lost -16.96%, DASTBC lost -20.43%, and DASDC lost the most at -29.48% by the time the specimens were subjected to 900°C. These findings suggest that greater temperatures have a substantial effect on the structural integrity of the concrete by increasing moisture evaporation and perhaps degrading the material.

Overall, the findings highlight how crucial it is to choose the right material for applications involving exposure to high temperatures since some types of concrete are more vulnerable to thermal damage than others.

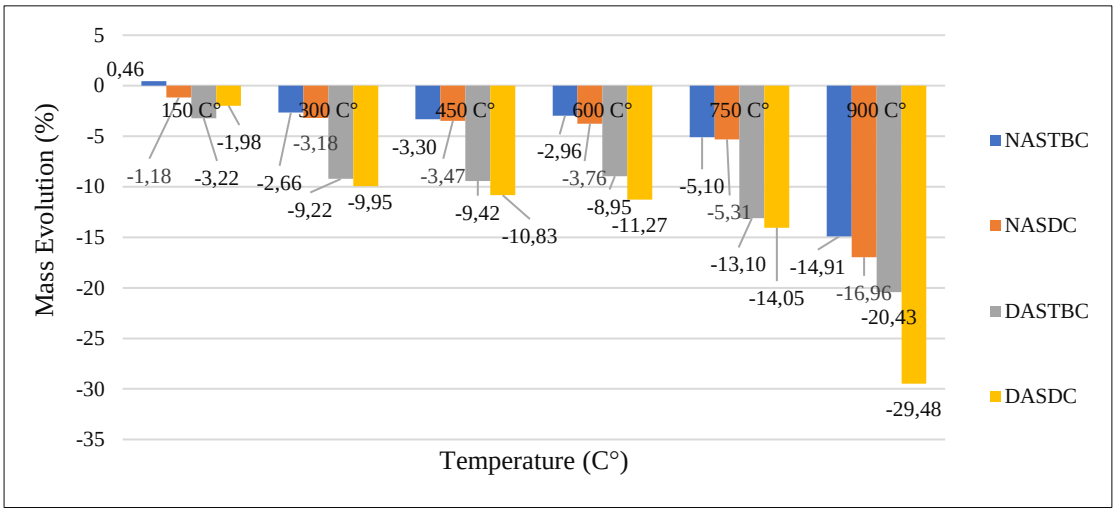

Figure IV. 36 : Mass Evolution after High Temperature Exposure

❖ Compressive strength

The measured strength variations after two hours of heating concrete specimens NASTBC, NASDC, DASTBC, and DASDC at temperatures between 150°C and 900°C offer important information on their durability (Figure IV. 37). All specimens showed significant strength decreases at 150°C, with NASTBC demonstrating a decline of -24.66%, NASDC -19.48%, DASTBC -25.01%, and DASDC -23.67%. NASTBC unexpectedly increased in strength by 3.83% when the temperature rose to 300°C, whereas NASDC and DASTBC continued to decrease, suggesting that different substances react differently to heat exposure. The strength losses were more noticeable at higher temperatures, especially 450°C and above; for example, NASDC drastically decreased by -36.33% at 450°C and -64.16% at 750°C. All samples had considerable strength reductions by the time they reached 900°C, with DASDC seeing the largest drop at -96.78%. These findings demonstrate how high temperatures weaken concrete,

emphasising the significance of material choice and design concerns for applications involving extremely high temperatures.

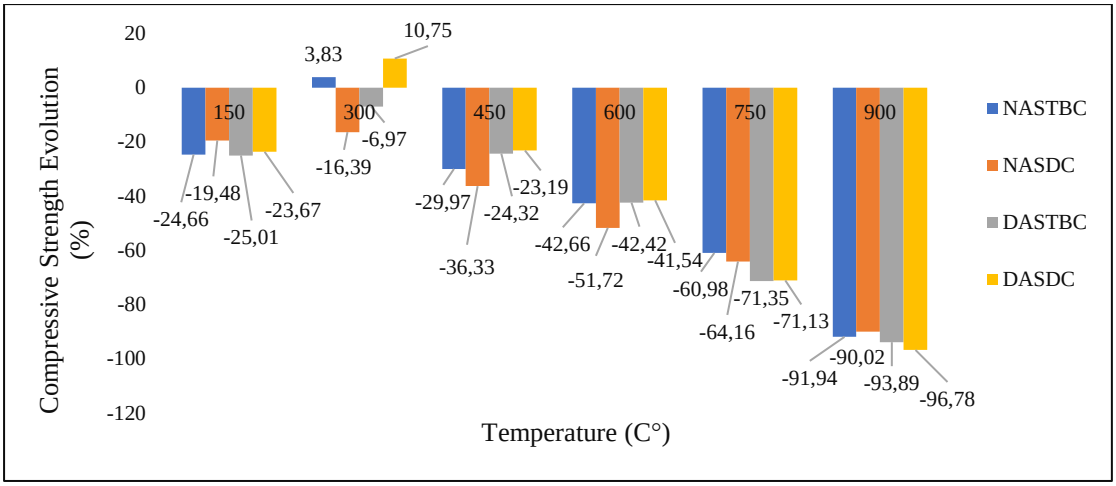

Figure IV. 37 : Compressive Strength Evolution after High Temperature Exposure

❖ Ultrasonic velocity

The observed variations in ultrasonic velocity after two hours of heating concrete specimens NASTBC, NASDC, DASTBC, and DASDC at temperatures between 150°C and 900°C offer crucial information about their durability (Figure IV. 38). Ultrasonic velocity decreases at 150°C were very small, with NASTBC and NASDC exhibiting decreases of -1.38% and -0.93%, respectively, whilst DASTBC and DASDC had more notable dips of -9.59% and -8.40%. All specimens displayed higher losses at temperatures over 300°C, whereas NASTBC and NASDC decreased by -30.10% and -31.82%, respectively. At higher temperatures, the trend persisted; NASTBC and NASDC showed significant deterioration by losing more than half of their ultrasonic velocity by 450°C. The losses were severe at 750°C, with both NASTBC and DASDC surpassing -82%, indicating serious structural integrity deterioration. All mixtures showed sharp drops in ultrasonic velocity by the time the specimens reached 900°C, with NASTBC losing -98.20%. These results highlight how high temperatures shorten the lifespan of concrete, indicating that choosing the right material is essential for applications subjected to intense heat.

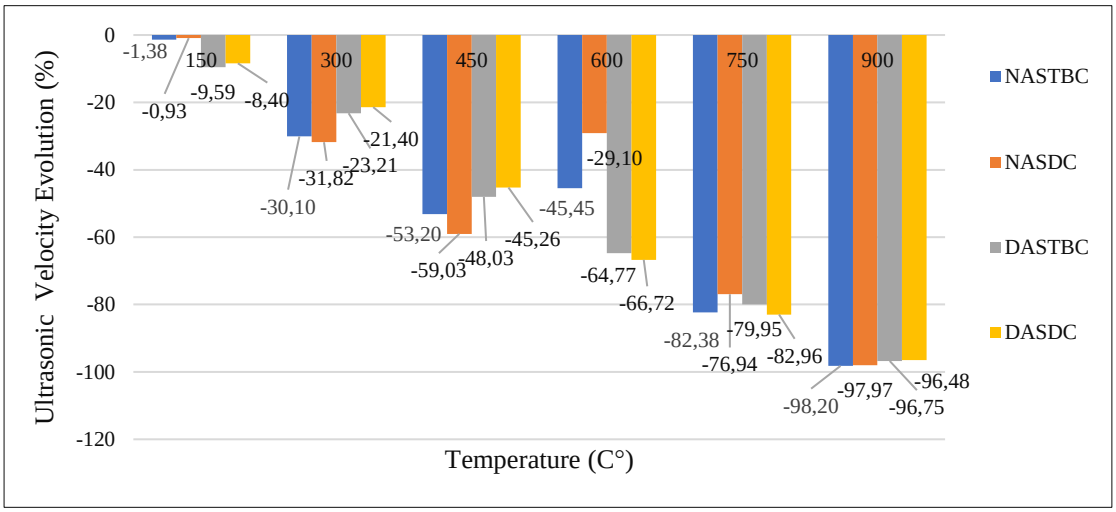

Figure IV. 38 : Ultrasonic Velocity Evolution after High Temperature Exposure

❖ Correlation Between Ultrasonic Velocity and Compressive Strength

Quadratic equations are used to illustrate the relationship between ultrasonic velocity and compressive strength after exposure to high temperatures for the different concrete mixes. The results show that compressive strength tends to increase with ultrasonic velocity, albeit at a decreasing rate (Figure IV. 39). A significant association is indicated by the equation's R^2 value of 0.8429 for NASTBC and a little lower correlation of 0.8113 for NASDC. Conversely, DASTBC and DASDC show even more robust associations, with corresponding R^2 values of 0.9389 and 0.9226. This suggests that these mixtures can accurately forecast compressive strength because they are more sensitive to variations in ultrasonic velocity. Each mix reacts differently to changes in ultrasonic velocity, as indicated by the coefficients in the equations; DASTBC exhibits the strongest rise in strength per unit of velocity. All things considered, these results highlight the potential of ultrasonic testing as a non-destructive technique for evaluating the strength and quality of concrete in a range of applications.

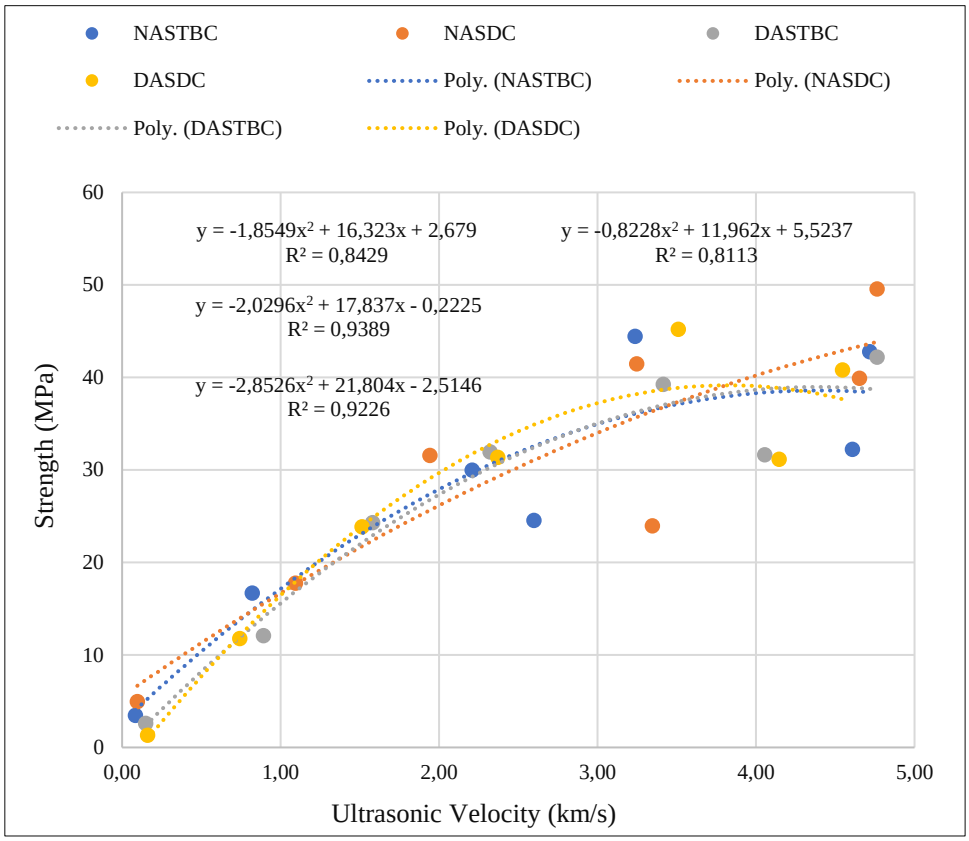

Figure IV. 39 : Correlation Between Ultrasonic Velocity and Compressive Strength Following High-Temperature Exposure

❖ Correlation Between Mass and Compressive Strength

Quadratic equations show the intricate connection between mass and compressive strength after exposure to high temperatures for the various concrete mixtures (Figure IV. 40). An R^2 score of 0.6697 for NASTBC indicates a moderate connection, but an R^2 value of 0.8249 for NASDC indicates a greater association. Conversely, DASTBC and DASDC show comparatively good associations as well, with R^2 values of 0.7301 and 0.7164, respectively. Potential limits in material performance at larger densities are shown in the negative coefficients in the quadratic terms for NASTBC, DASTBC, and DASDC, which imply that the rate of increase in compressive strength decreases as mass rises. On the other hand, a higher positive reaction to increased mass is shown by NASDC's positive coefficient. All things considered, these results demonstrate how mass affects concrete's mechanical qualities, stressing that although greater mass may increase strength, the connection is not linear and differs greatly amongst mixes.

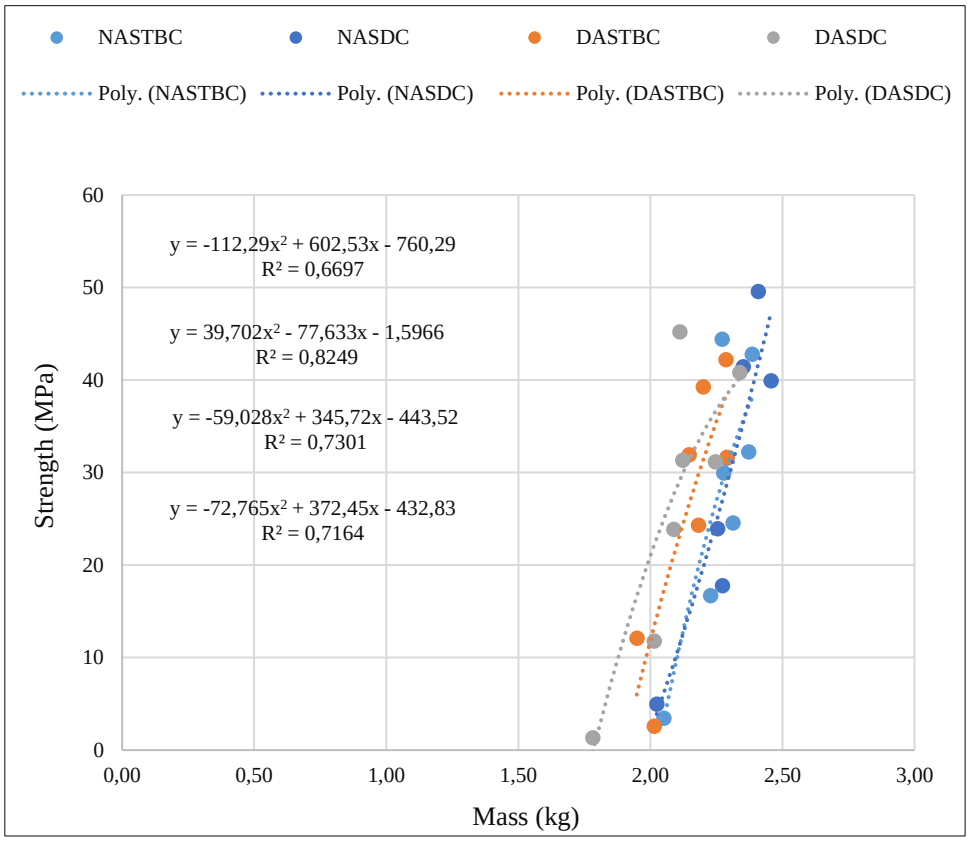

Figure IV. 40 : Correlation Between Mass and Compressive Strength Following High-Temperature Exposure

IV. 4. CONCLUSION

The experimental findings pertaining to the creation of demolition aggregates and their application with Saharan dune sand in concrete compositions have been thoroughly examined in Chapter IV. The objective of this experimental investigation was to minimise production delays and health hazards while effectively and economically lowering the amount of old mortar (OM) in demolition aggregates (DAs). Furthermore, the study assessed how well concrete made with these aggregates and Saharan dune sand performed. In order to improve the mechanical qualities of the final concrete and support sustainable building methods, we concentrated on optimising the aggregate composition. The results highlight the possibility of using recycled resources to produce concrete, which would help Algeria deal with its resource shortage and environmental issues. This study supports the creation of more resilient infrastructure by highlighting creative waste management strategies and encouraging the use of local resources.

- The following are the research's main conclusions:

- Significantly lower water absorption capacity is associated with a ratio threshold of 0.8 for DA sub-fractions, ranging from 12% to 82% below average values and 28% to 89% below maximum values.
- When DA fractions made from the same Parent Concrete (PC) sub-fractions have a threshold ratio of 1, they have a noticeably low water absorption capacity, exhibiting decreases of 21% to 43% from average values and 31% to 58% from maximum values.
- The water absorption capacity is further reduced by 4% to 7% when choosing DA sub-fractions based on water absorption capacity without taking the PC into account.
- The DAD_{max}/NAD_{max} ratio threshold should serve as a reference for determining the minimum size of DA prior to crushing.
- For optimal selection, sub-fractions with a DAD_{max}/NAD_{max} ratio greater than or equal to 0.8 for the current DA are chosen, and the desired DA fractions are then reconstituted from these sub-fractions.
- The size of parent concrete's (PC) NA affects water absorption in the same way as the size of DA does. In conclusion, this study offers a novel strategy to raise the calibre of DAs meant for usage in structural concrete, hence encouraging the sustainability of building projects. The data presented provides helpful recommendations for maximising the production of DAs with lower OM content, which would lower construction-related health hazards and save money.
- Even with a discontinuous granular structure, flexible ordinary concrete may be formed.
- Because of the unique shape and granulometry of its grains, dune sand can alter the workability of regular concrete from hardness to plasticity.
- Microscopic measurements and particle size curve analysis of both types of sand shown that having the same workability does not simply mean that they fall into the same range (fine sand).
- The morphology and form of the grains have a significant impact on how workable regular concrete is.
- Adding dune sand to regular plastic concrete creates more compact concrete and necessitates a mixture with less water.

- When dune sand and natural coarse aggregates are combined, the water-to-cement ratio (W/C) must be decreased in order to maximise compressive strength.
- Wetting is not necessary when combining demolition coarse materials with dune sand.
- Ordinary concretes based on SD and STB sand have a remarkably comparable progression in compressive strength.
- Unlike concretes made from natural resources, alternative resource concretes maintain a respectable level of strength and sustainability despite the fact that aggressive chemicals will find it easier to penetrate them.
- Concrete with smaller pores and less porosity performs better and resists frost better.
- Concrete cracks serve as pathways for the movement of CO_2 and water to anhydrous phases, promoting healing, density growth, and compressive strength.
- One possible method is to include beach sand into fresh concrete together with coarse aggregates from destroyed concrete.

GENERAL CONCLUSION

GENERAL CONCLUSION

This research, structured in four chapters, has thoroughly explored the potential for sustainable innovation in the Algerian and global construction sector by focusing on the use of demolition coarse aggregates and Saharan dune sand in ordinary concrete. The findings provide a solid scientific basis and practical guidance for addressing current and future challenges in construction materials.

The first chapter established the strategic importance of the construction sector for economic development and infrastructure improvement, both in Algeria and worldwide. In Algeria, major investments in housing, transportation, and hydraulic structures illustrate a clear commitment to upgrading living standards and connectivity. These trends reflect a global emphasis on infrastructure as a driver of growth and quality of life, but also highlight the urgent need for new solutions to resource scarcity and environmental impact.

Chapter II offered a comprehensive bibliographic synthesis on aggregates, detailing their types, properties, and roles in concrete. It emphasised the growing interest in alternative aggregates—particularly Saharan dune sand and demolition aggregates—due to their abundance and potential for sustainable use. Methods for improving the quality of recycled aggregates were reviewed, highlighting the importance of the choice of aggregates for obtaining high-performance, long-lasting concrete.

Chapter III rigorously describes the experimental methodology, from the selection and preparation of the materials (cement, mixing water, plasticiser, conventional natural sand and Saharan dune sand, natural coarse aggregates and aggregates from demolition concrete), the physical and mechanical characterisation of the study concretes, to the study of their durability and their behaviour under severe conditions.

Chapter IV presented, firstly, the experimental results of the preparation and selection of demolition aggregates and, secondly, the experimental results of the incorporation of demolition aggregates and dune sand into ordinary concrete. The critical threshold set at a DAD_{max}/NAD_{max} ratio greater than or equal to 0.8 made it possible to reduce the water absorption of the sub-fractions of the demolition aggregates from 12 to 82% compared with the average values, and from 28 to 89% compared with the maxima. For reconstituted fractions, a ratio of 1 resulted in reductions of 21 to 43% (average) and 31 to 58% (maximum). The concrete mixes were designed to achieve a moderate slump of around 7 cm, typical of plastic ordinary concrete, with careful adjustment of the

effective water-to-cement ratio to account for the water demand of the demolition aggregates and dune sand. The DASDC concrete, incorporating demolition aggregates and dune sand, demonstrates overall durability performance that is superior or comparable to the reference NASTBC concrete. Its compressive strength is higher (31.95 MPa compared to 29.86 MPa), confirming better mechanical resistance. Flexural strength values are similar (4.92 MPa for DASDC versus 5.0 MPa for NASTBC), while splitting tensile strength is slightly lower (1.75 MPa versus 2.02 MPa), which remains acceptable. The ultrasonic pulse velocity, an indicator of compactness, is slightly lower for DASDC (4.59 km/s vs. 4.87 km/s), as is the dynamic modulus of elasticity (42.64 GPa compared to 50.76 GPa), whereas the static modulus is marginally higher (33.45 GPa vs. 32.70 GPa). DASDC exhibits a slightly higher porosity (5.28% versus 4.65%), resulting in a marginally increased permeability (0.27×10^{-5} (m/s) vs. 0.2×10^{-5} (m/s)) and a higher capillary absorption coefficient after 24 hours (8.5 $kg/m^2 \cdot s^{1/2}$compared to 7 $kg/m^2 \cdot s^{1/2}$). These factors partly explain the greater mass loss during abrasion testing (72.97% for DASDC versus 93.8% for NASTBC). Regarding freeze-thaw resistance, DASDC shows better compressive strength retention after 50 cycles (35.31 MPa vs. 26.37 MPa), although mass loss is similar. In aggressive chemical environments, DASDC displays improved chemical stability, with significantly reduced strength losses, notably in seawater (-0.76% vs. -8.19%) and 5% NaOH solution (-3.61% vs. -8.51%). Ultrasonic velocity measurements support this enhanced chemical resistance with smaller variations.

However, under high-temperature exposure, DASDC experiences more pronounced degradation, with greater losses in mass and strength at 600 °C and 900 °C, as well as more significant decreases in ultrasonic velocity, indicating a microstructure more affected by heat. In summary, DASDC concrete offers improved durability against common environmental aggressions (freeze-thaw cycles, chemical attacks) while providing better mechanical strength. Nevertheless, it requires careful consideration for applications subjected to elevated temperatures.

Overall, this research demonstrates that by carefully selecting demolition aggregate fractions (with $DAD_{max}/NAD_{max} \geq 1$) and incorporating Saharan dune sand, it is possible to produce ordinary concrete with mechanical and durability properties equal to or exceeding those of traditional mixes. This approach not only valorises local and

recycled resources but also supports circular economy principles and environmental sustainability.

In conclusion, the results provide clear evidence that the combined use of demolition coarse aggregates and Saharan dune sand is a viable, good-performance, and eco-friendly solution for the construction industry in Algeria and similar contexts. The protocols and thresholds established in this study offer practical recommendations for optimising recycled aggregate production and concrete formulation, promoting safer, more sustainable, and cost-effective construction practices. This work paves the way for broader adoption of alternative materials in building codes and infrastructure projects, supporting resilient and sustainable urban development.

PERSPERCTIVES

PERSPECTIVES

Based on the suggested study areas, the following viewpoints for further research are presented:

Impact of Concrete Age: Researching the relationship between concrete age and demolition aggregate quality may help identify the best recycling techniques. Improved processing methods might result from an understanding of the connection between aggregate characteristics and concrete maturity.

Cement Type and Dosage: The best methods for optimising the quality of recycled materials may be found by examining how various cement kinds and doses affect the performance of demolition aggregates. This research might also investigate how these elements affect concrete's overall durability.

Water-Cement Ratio (E/C): Future studies should concentrate on how altering the water-cement ratio impacts the performance of the final concrete as well as the quality of the demolition aggregates. Optimised formulations that improve workability and strength may result from this.

Quality of conventional Aggregates: A more thorough grasp of material interactions may be obtained by looking at how the characteristics of demolition aggregates are influenced by the quality of conventional gravel and sand in parent concrete. Better selection criteria for recycling aggregates might be informed by this.

Saharan Dune Sand with Low-Quality Aggregates: Researching the use of Saharan dune sand with medium- and low-quality demolition aggregates will help clarify how it affects hardened state performance and rheology. This study may provide strategies for enhancing strength and workability in less-than-ideal circumstances.

Combining Techniques: Examining the best ways to blend fine sand, especially when combined with recycled materials, might improve the way concrete is made. This investigation ought to take into account variables including equipment kind, speed, and mixing duration.

Continuous Gradation Aggregates: Research on concrete composed of continuously graded aggregates will be useful in determining how well it performs in comparison to conventional mixes. This study may provide fresh perspectives on how to use recycled materials to achieve desired mechanical qualities.

By exploring these perspectives, future research can contribute significantly to enhancing the quality and sustainability of concrete produced with recycled materials, ultimately promoting more environmentally friendly construction practices.

APPENDIX

APPENDIX 1

المجمع الصناعي لإسمنت الجزائر GICA Groupe Industriel des Ciments d'Algérie	شركة الاسمنت لحجار السود			F03-01/1000
	FICHE TECHNIQUE CIMENT			
	Date : 31/05/ 2009	Version : 05	Page 1 sur 1	

CIMENT PORTLAND COMPOSE CPJ-CEMII/A 42,5

sept-16

CARACTERISTIQUE CHIMIQUE		CARACTERISTIQUE PHYSIQUE			CARACTERISTIQUE MECANIQUE		
ELEMENTS	% EN MASSE	NORME NA			NORME NA	EN MpA	
PAF 975°C	1 - 2	NA230	CONSISTANCE NORMALE	≥ 25	NA 442	COMPRESSION	
CaO	55 - 65	NA230	DEBUT DE PRISE	≥ 60		02 jours	≥ 12.50
SiO2	22 - 28	NA230	FIN DE PRISE	150 - 250		07 jours	25 - 35
Al2O3	5 - 6	NA232	EXPANSION A CHAUD	≤ 10mm		28 jours	42.5 - 52.5
Fe2O3	3 - 3,6	NA231	SSBlaine cm²/g	3300 - 4000	NA 234	FLEXION	
MgO	1 - 2	NA231				02 jours	3,0-4,0
K2O	0,3 - 0,6					07 jours	5,0-6,5
Na2O	0,1 - 0,16	NA440	RETRAIT SUR MORTIER µm/m	≤ 1000		28 jours	6,5-8,5
SO3	1.8 - 2,5	COPOSITION POTENTIELLE EN %			% DES CONSTITUANTS		
CaOL	0,8 -1,8	C3S	55 - 65	CLINKER	≥ 74%		
CL^-	0 - 0,01	C2S	10 - 25	GYPSE	4 - 6%		
NB: le % calcaire + pouzzolaine est de 50% chacun		C3A	8 - 12	CALCAIRE	≤ 12 %		
dans le mélange calcire +tuf le tuf est de l'ordre de 5% Max		C4AF	9 - 13	pouzzolaine+ calcaire	≤ 18%		
				calcaire + TUF	≤ 14%		

DOMAINE D'UTILISATION

Utilisation courante de notre ciment :

- *Fondations (béton de propreté et béton de semelle en milieux non agressifs).*
- *Ouvrage en béton armé (Murs, Linteaux, Poteaux et dalle de compressions).*
- *Dallage en béton , Montage de mure et maçonnerie et Scellements de carrelage (Dalles, pierres et carrelage).*
- *Chape (mortier de ciment) .*

PRECAUTION D'EMPLOI

Ce type de ciment ne convient pas pour :

- *Ouvrages en milieux agressifs (terrains gypseux, sulfates, eaux industrielles) emploi obligatoire de ciment* ES pour travaux en eaux à haute teneur en sulfates.
- *Travaux à la mere (emploi obligatoire de ciment **PM** pour travaux à la mer).*
- *Bétonnage au dessous de 5° C (il est conseillé d'utiliser des ciments de résistance initiale élevée **R**)*

STOCKAGE :

Eviter :

- Un stockage prolongé au-delà de trois (03) mois.
- Un stockage dans des endroits humides.

EMBALLAGE :

- Le ciment est emballé dans des sacs en papier kraft à 02 plis, le système de fermeture garantie l'inviolabilité du sac.

ATTENTION

- Un contact prolongé du ciment avec la peau peut être irritant.

APPENDIX 2

BUILDING TRUST

NOTICE PRODUIT

Sika® ViscoCrete®-3045

Plastifiant/Réducteur d'eau de nouvelle génération pour bétons prêts à l'emploi

INFORMATIONS SUR LE PRODUIT

Sika® ViscoCrete®-3045 est un plastifiant réducteur d'eau non chloré et prêt à l'emploi, à base de polycarboxylates modifiés, qui se présente sous la forme d'un liquide marron.

DOMAINES D'APPLICATION

Sika® ViscoCrete®-3045 permet d'obtenir un long maintien de rhéologie (>1H30). Il est donc parfaitement adapté à l'industrie du BPE et à l'utilisation sur chantier.
Sika® ViscoCrete®-3045 permet la fabrication de :
- bétons plastiques à fluides,
- bétons à faibles rapports E/C avec ou sans fumée de silice,
- bétons pompés sur longues distances.

Dans les bétons fluides, Sika® ViscoCrete®-3045 améliore la stabilité, limite les risques de ségrégation et rend la formule moins sensible aux variations d'eau et des constituants.

CARACTÉRISTIQUES / AVANTAGES

Sika® ViscoCrete®-3045 est un plastifiant réducteur d'eau qui confère au béton les propriétés suivantes :
- haute réduction d'eau,
- maintien prolongé de la rhéologie,
- robustesse vis-à-vis de la ségrégation,
- bel aspect de parement au décoffrage.

AGRÉMENTS / NORMES

Conforme à la Norme NF EN 934-2 Tab. 1 et 2

DESCRIPTION DU PRODUIT

Conditionnement	▪ Fût de 250 kg ▪ Cubi de 1110 l ▪ Vrac
Durée de Conservation	6 mois dans son emballage d'origine intact
Conditions de Stockage	Dans un local fermé, à l'abri de l'ensoleillement direct et du gel, entre 5 et 30 °C. Le produit peut geler, mais, une fois dégelé lentement et réhomogénéisé, il retrouve ses qualités d'origine. En cas de gel prolongé et intense, vérifier qu'il n'a pas été déstabilisé.
Aspect / Couleur	Liquide marron/vert
Densité	1,11 ± 0,02
Valeur pH	5 ± 1

Notice produit
Sika® ViscoCrete®-3045
Juillet 2023, Version 01.03
021301011000000038

1 / 2

Équivalent Oxyde de Sodium	≤ 2,5 %

RENSEIGNEMENTS SUR L'APPLICATION

Dosage	Plage d'utilisation recommandée : 0,25 à 2,5 % du poids de liant selon les performances recherchées. Dosage usuel du Sika® ViscoCrete®-3045 : 0,3 % à 0,8 %.
Distribution	Sika® ViscoCrete®-3045 est ajouté, soit, en même temps que l'eau de gâchage, soit en différé dans le béton préalablement mouillé avec une fraction de l'eau de gâchage.

VALEURS DE BASE

Toutes les valeurs indiquées dans cette Notice Produit sont basées sur des essais effectués en laboratoire. Les valeurs effectives mesurées peuvent varier du fait de circonstances indépendantes de notre contrôle.

ÉCOLOGIE, SANTÉ ET SÉCURITÉ

Pour obtenir des informations et des conseils sur la manipulation, le stockage et l'élimination en toute sécurité des produits chimiques, les utilisateurs doivent consulter la fiche de données de sécurité (FDS) la plus récente contenant les données physiques, écologiques, toxicologiques et autres données relatives à la sécurité.

RESTRICTIONS LOCALES

Veuillez noter que du fait de réglementations locales spécifiques, les données déclarées pour ce produit peuvent varier d'un pays à l'autre. Veuillez consulter la Notice Produit locale pour les données exactes sur le produit.

INFORMATIONS LÉGALES

Les informations, et en particulier les recommandations concernant les modalités d'application et d'utilisation finale des produits Sika sont fournies en toute bonne foi et se fondent sur la connaissance et l'expérience que Sika a acquises à ce jour de ses produits lorsqu'ils ont été convenablement stockés, manipulés et appliqués dans des conditions normales, conformément aux recommandations de Sika. En pratique, les différences entre matériaux, substrats et conditions spécifiques sur site sont telles que ces informations ou recommandations écrites, ou autre conseil donné, n'impliquent aucune garantie de qualité marchande autre que la garantie légale contre les vices cachés, ni aucune garantie de conformité à un usage particulier, ni aucune responsabilité découlant de quelque relation juridique que ce soit. L'utilisateur du produit doit vérifier par un essai sur site l'adaptation du produit à l'application et à l'objectif envisagés. Sika se réserve le droit de modifier les propriétés de ses produits. Notre responsabilité ne saurait d'aucune manière être engagée dans l'hypothèse d'une application non conforme à nos renseignements. Les droits de propriété détenus par des tiers doivent impérativement être respectés. Toutes les commandes sont soumises à nos conditions générales de vente et de livraison en vigueur. Les utilisateurs doivent impérativement consulter la version la plus récente de la Notice Produit correspondant au produit concerné, accessible sur internet ou qui leur sera remise sur demande.

Sika Algerie SPA
09 rue Ziadi Lotfi
16035 Les Eucalyptus
ALGERIE
Tel: 0 23 88 89 92 09
Fax: 0 23 88 89 92 08
dza.sika.com

BIBLIOGRAPHICAL REFERENCES

BIBLIOGRAPHICAL REFERENCES

[1] DJEMACI, B. (2012). La gestion des déchets municipaux en Algérie : Analyse prospective et éléments d ' efficacité. Doctoral thesis, University of Rouen, France.

[2] BOUTARAA, Z. (2013). La gestion du risque sismique dans la ville de Chlef - Algérie-. Mémoire de Projet Professionnel CES Voie d'approfondissement : Génie Civil, Ecole Nationale des Travaux Publics de l'Etat, university of Lyon, France.

[3] Verrhiest-Leblanc, G., Winter, T. (2019). "Séisme de Boumerdès (Algérie) du 21 mai 2003, les conséquences dramatiques de l'effet mille feuilles."

[4] BOUTARAA, Z. (2018). "SEISME D ' EL ASNAM 1980 (ALGERIE): QUELLES REVELATIONS NOUS APPORTENT LES OBSERVATIONS POST-SISMIQUES ?" In 8èmeSymposium International sur la construction en zone sismique (SICZS'2018), Chlef les 10 et 11 Octobre 2018 SEISME (Vol. 1980, pp. 1–9). Retrieved from https://www.researchgate.net/publication/328282818

[5] Québaud, M., Zaharieva, R., Buyle-Bodin, F. (2011). "Le comportement des bétons incluant des granulats recyclés," Vol. 5119, . https://doi.org/10.1080/12795119.1998.9692222.

[6] Québaud, M., Zaharieva, R., Buyle-Bodin, F. (1998). "Le comportement des bétons incluant des granulats recyclés." Revue Française de Génie Civil, Vol. 2, Issue 8, pp. 969–984. https://doi.org/10.1080/12795119.1998.9692222.

[7] Serres, N., Braymand, S., Feugeas, F. (2014). "Evaluation environnementale de bétons de granulats recyclés de béton et de béton de granulats recyclés de terre cuite à partir d'analyses de cycle de vie." In Symposium 01 Ecomaterials Materials 2014, 24-28 November 2014 (pp. 1–10). Montpellier, France.

[8] Curien, R. (2017). "Singapour, modèle de développement urbain (durable ?) en Chine, Regard sur 20 ans de coopération sino-singapourienne." Chinese Perspectives [on line], Vol. 1, Issue 2017, pp. 27–37. Retrieved from https://journals.openedition.org/perspectiveschinoises/7596

[9] MAP. (2018). "Denmark is experiencing a worrying depletion of gravel supplies." Retrieved from http://mapecology.ma/actualites/danemark-connait-epuisement-inquietant-approvisionnements-gravier/.

[10] Sahara and Sahel Observatory. (2017). Atlas of the Water Resources of the Iullemeden, Taoudeni-Tanezrouft Aquifer System Countries (1st ed.).

[11] Bouhnik, B. (2007). Contribution à la valorisation du sable de dune dans la formulation du béton destiné aux ouvrages hydrauliques en milieux sahariens. Magister's thesis, University of Ouargla, Algeria.

[12] Guettala, A., Mezghiche, B., Chebili, S. (2003). "Valorisation d'un déchet industriel pour la confection d'un béton de sable." Construction and Building Materials, pp. 413–21.

[13] Bentata, A. (2004). Etude expérimentale d'un béton avec le sable de dune de la région de Ouargla (Ain Elbaida). University of Ouargla, Algeria.

[14] Zhao, Z., Courard, L., Remond, S., Damidot, D., Fiandaca, T. (2015). "Tentatives de prétraitement des granulats recyclés pour l'amélioration des bétons préfabriqués." In 16e édition des Journées scientifiques du Regroupement francophone pour la recherche et la formation sur le béton (RF)2B (pp. 1–9).

[15] de Juan, M. S., Gutiérrez, P. A. (2009). "Study on the influence of attached mortar content on the properties of recycled concrete aggregate." Construction and Building Materials, Vol. 23, Issue 2, pp. 872–877. https://doi.org/10.1016/j.conbuildmat.2008.04.012.

[16] Hani Mokbel, T. (2014). "Study of The Mechanical Properties of Recycled Aggregate Concrete." Doctoral thesis, University of Damascus, Syria.

[17] Kang, M., Weibin, L. (2018). "Effect of the aggregate size on strength properties of recycled aggregate concrete." Advances in Materials Science and Engineering, Vol. 2018, . https://doi.org/10.1155/2018/2428576.

[18] Théréné, F., Keita, E., Naël-Redolfi, J., Boustingorry, P., Bonafous, L., & Roussel, N. (2020). "Water absorption of recycled aggregates: Measurements, influence of temperature and practical consequences." Cement and Concrete Research, Vol. 137, , pp. 106196. https://doi.org/https://doi.org/10.1016/j.cemconres.2020.106196.

[19] Hemmati Pourghashti, H., Madandous, R., Ranjbar, M. (2022). "Studying Tensile Strength of the Recycled Coarse Aggregate Concrete Using Double-Punch Test." Journal of Rehabilitation in Civil Engineering, Vol. 10, Issue 3, pp. 100–120. https://doi.org/10.22075/JRCE.2021.20395.1413.

[20] Guéguen Minerbe, M., Martinez Hernandez, H., Nour, I., Pechaud, Y., Sedran, T. (2022). "Impact de la biocarbonatation multicouche sur l'absorption d'eau d'un mortier." Academic Journal of Civil Engineering, Vol. 40, Issue 3, pp. 69–81.

[21] Kaddah, F., D, F. K., Ranaivomanana, H., Amiri, O., Rozière, E. (2022). "Accelerated carbonation of recycled concrete aggregates: Investigation on the microstructure and transport properties at cement paste and mortar scales." CO2 Utilization, Vol. 57, Issue 2022, pp. 101885. https://doi.org/doi.org/10.1016/j.jcou.2022.101885.

[22] Fanara, A., Courard, L., Collin, F., & Hubert, J. (2022). "Transfer properties in recycled aggregates concrete: Experimental and numerical approaches." Construction and Building Materials, Vol. 326, , pp. 126778. https://doi.org/https://doi.org/10.1016/j.conbuildmat.2022.126778.

[23] Wu, J., Zhang, Y., Zhu, P. et al. (2018). "Microstructure of Recycled Aggregate Concrete Using Carbonated Recycled Coarse Aggregate." Journal of Wuhan University of Technology-Materials Science Edition, Vol. 33, , pp. 648–653.

[24] Jingyu Yang a b, Yinchuan Guo a, Vivian W.Y. Tam b, Jingjing Tan a, Aiqin Shen a, Chong Zhang a, J. Z. a. (2022). "Feasibility of recycled aggregates

modified with a compound method involving sodium silicate and silane as permeable concrete aggregates." Construction and Building Materials, Vol. 361, , pp. 129747. https://doi.org/10.1016/j.conbuildmat.2022.129747.

[25] Houria, M., Nourredine, A. (2011). "Les granulats recyclés humidifiés : comportements des bétons frais et durcis." In XXIXeRencontres Universitaires de Génie Civil. Tlemcen, 29 au 31 Mai 2011 (pp. 401–410).

[26] Parmentier, V., Michel, F. (2013). "Fixation du CO2 dans les blocs de beton à base de," pp. 1–11.

[27] Thang, L. (2015). Influence de l'humidité des granulats de béton recyclé sur le comportement à l'état frais et durcissant des mortiers. L'ÉCOLE DES MINES DE DOUAI ET L'UNIVERSITE LILLE 1.

[28] Guerzou, T., Mebrouki, A., Castro-Gomes, J. (2018). "Study of concretes properties based on pre-saturated recycled aggregates." Journal of Materials and Engineering Structures, Vol. 5, Issue 3, pp. 279–288.

[29] Sereng, M., Co, D. (2021). "Amélioration des propriétés des granulats recyclés par stockage de CO2 : étude de la faisabilité pré-industrielle." Paris-Est.

[30] Braymand, S., Roux, S., Schlupp, F., & Mendoza, H. M. (2022). "Carbonatation accélérée de granulats de béton recyclé–Évolution des propriétés selon leur classe granulaire." Journal of Civil Engineering, Vol. 40, Issue 1, pp. 76–79.

[31] Djerbi, A., Cazacliu, B. B., Sereng, M., dos Reis, G. S., Metalssi, O. O., Jeong, J., ... & Torrenti, J. M. (2022). "Stockage du CO2 dans les granulats recyclés: développement des procédés de carbonatation accélérée." Academic Journal of Civil Engineering, Vol. 40, Issue 3. https://doi.org/https://doi.org/10.26168/ajce.40.3.2.

[32] Abbas, A.; Fathifazl, G.; Isgor, O.B.; Razaqpur, A.G.; Fournier, B.; Foo, S. (2007). "Proposed method for determining the residual mortar content of recycled concrete aggregates." Journal of ASTM International, Vol. 5, Issue 1, pp. 1–12. https://doi.org/DOI:10.1520/JAI101087.

[33] Forero, J.A.; Brito, J. d. ., Evangelista, L.; Pereira, C., GOST 10060-87, (State Construction Committee of the USSR Moscow). (2022). "Improvement of the Quality of Recycled Concrete Aggregate Subjected to Chemical Treatments: A Review." Materials, Vol. 15, , pp. 2740. https://doi.org/https://doi.org/10.3390/ma15082740.

[34] Tam, V.W.Y.; Tam, C.M.; Le, K. N. (2007). "Removal of cement mortar remains from recycled aggregate using pre-soaking approaches." Resources, Conservation and Recycling, Vol. 50, , pp. 82–101. https://doi.org/https://doi.org/10.1016/j.resconrec.2006.05.012.

[35] Wang, L.; Wang, J.; Qian, X.; Chen, P.; Xu, Y.; Guo, J. (2017). "An environmentally friendly method to improve the quality of recycled concrete aggregates." Construction and Building Materials, Vol. 144, , pp. 432–441. https://doi.org/https://doi.org/10.1016/j.conbuildmat.2017.03.191.

[36] Butler, L.; West, J.; Tighe, S. (2011). “The effect of recycled concrete aggregate properties on the bond strength between RCA concrete and steel reinforcement.” Cement and Concrete Research, Vol. 41, , pp. 1037–1049. https://doi.org/https://doi.org/10.1016/j.cemconres.2011.06.004.

[37] Kim, H.-S.; Kim, B.; Kim, K.-S.; Kim, J.-M. (2017). “Quality improvement of recycled aggregates using the acid treatment method and the strength characteristics of the resulting mortar.” Journal of Material Cycles and Waste Management, Vol. 19, , pp. 968–976. https://doi.org/https://doi.org/10.1007/s10163-016-0497-9.

[38] Javier A. Forero, Jorge de Brito, Luís Evangelista, and C. P. (2022). “Improvement of the Quality of Recycled Concrete Aggregate Subjected to Chemical Treatments: A Review.” Materials, Vol. 15, , pp. 2740. https://doi.org/https://doi.org/10.3390/ ma15082740.

[39] Akbarnezhad, A.; Ong, K.; Zhang, M.; Tam, C. (2013). “Acid treatment technique for determining the mortar content of recycled concrete aggregates.” Journal of Testing and Evaluation, Vol. 41, , pp. 441–450. https://doi.org/https://doi.org/10.1520/JTE20120026.

[40] Al-Bayati, H.K.A.; Das, P.K.; Tighe, S.L.; Baaj, H. (2016). “Evaluation of various treatment methods for enhancing the physical and morphological properties of coarse recycled concrete aggregate.” Construction and Building Materials, Vol. 112, , pp. 284–298. https://doi.org/https://doi.org/10.1016/j.conbuildmat.2016.02.176.

[41] Ismail, S.; Ramli, M. (2013). “Engineering properties of treated recycled concrete aggregate (RCA) for structural applications.” Construction and Building Materials, Vol. 44, , pp. 464–476. https://doi.org/https://doi.org/10.1016/j.conbuildmat.2013.03.014.

[42] Ismail, S.; Ramli, M. (2014). “Mechanical strength and drying shrinkage properties of concrete containing treated coarse recycled concrete aggregates.” Construction and Building Materials, Vol. 68, , pp. 726–739. https://doi.org/https://doi.org/10.1016/j.conbuildmat.2014.06.058.

[43] Kim, Y.; Hanif, A.; Kazmi, S.M.S.; Munir, M.J.; Park, C. (2018). “Properties enhancement of recycled aggregate concrete through pretreatment of coarse aggregates—Comparative assessment of assorted techniques.” Journal of Cleaner Production, Vol. 191, , pp. 339–349. https://doi.org/https://doi.org/10.1016/j.jclepro.2018.04.192.

[44] Pandurangan, K.; Dayanithy, A.; Prakash, S. O. (2016). “Influence of treatment methods on the bond strength of recycled aggregate.” concrete, Construction and Building Materials, Vol. 120, , pp. 212–221. https://doi.org/https://doi.org/10.1016/j.conbuildmat.2016.05.093.

[45] Purushothaman, R.; Amirthavalli, R.R.; Karan, L. (2014). “Influence of treatment methods on the strength and performance characteristics of recycled aggregate.” Journal of Materials in Civil Engineering, Vol. 27, Issue 5, pp. 04014168. https://doi.org/https://doi.org/10.1061/(ASCE)MT.1943-

5533.0001128.

[46] Saravanakumar, P.; Abhiram, K.; Manoj, B. (2016). “Properties of treated recycled aggregates and its influence on concrete strength characteristics.” Construction and Building Materials, Vol. 111, , pp. 611–617. https://doi.org/https://doi.org/10.1016/j.conbuildmat.2016.02.064.

[47] Yin Jinming a b, Kang Aihong a, Xiao Peng a, Kou Changjiang a, Gong Yongfan a, X. C. c. (2023). “Influences of spraying sodium silicate based solution/slurry on recycled coarse aggregate.” Construction and Building Materials, Vol. 377, , pp. 130924. https://doi.org/10.1016/j.conbuildmat.2023.130924.

[48] Braymand, S. (2017). “Separation and Quantification of Attached Mortar in Recycled Concrete Aggregates,” pp. 1393–1407. https://doi.org/10.1007/s12649-016-9771-2.

[49] Jang, H.; Kim, J. . S., A. (2021). “Effect of Aggregate Size on Recycled Aggregate Concrete under Equivalent Mortar Volume Mix Design.” Applied Science, Vol. 11, , pp. 11274. https://doi.org/https://doi.org/10.3390/app112311274.

[50] Zhao, Z., Xiao, J., Damidot, D., Rémond, S., Bulteel, D., Courard, L. (2022). “Quantification of the Hardened Cement Paste Content in Fine Recycled Concrete Aggregates by Means of Salicylic Acid Dissolution.” Materials, Vol. 15, Issue 9, pp. 3384. https://doi.org/doi.org/10.3390/ma15093384.

[51] Martaud, T. (2009). “Evaluation environnementale de la production de granulats en exploitation de carrières - Indicateurs , Modèles et Outils.” https://doi.org/HAL Id : tel-00412080.

[52] TRACHTE, S. (2023). “Vers un «zéro déchet / zéro émission» en construction.” Ressources naturelles et Environnement. Retrieved from https://orbi.uliege.be/bitstream/2268/308450/1/SPW_ZéroDéchets_Vers un zero déchet_zero emission en construction_ STrachte.pdf%0A

[53] Nedjraoui, D., Bédrani, S. (2008). “La désertification dans les steppes algériennes : causes, impacts et actions de lutte.” (Environmental Science Electronic Journal)[VertigO], Vol. 8, Issue 1. https://doi.org/doi.org/10.4000/vertigo.5375.

[54] N. Koull, T. Benzaoui, A. Sebaa, ME. Kherraze, S. B. (2015). “Grain size characteristics of dune sands of the Grand Erg Oriental (Algeria).” Journal Algérien des Régions Arides (JARA), Vol. 13, .

[55] BOUVIER, É., NOURY, A., PELLOUX, P. (2022). “Principales filières des déchets du BTP, quels organisations, valorisations et gisements à venir ?” In Atelier Parisien d’Urbanisme. Retrieved from https://www.apur.org/sites/default/files/principales_filieres_dechets_btp_grand_paris.pdf?token=L1Go6IVs.

[56] Alatshan, Faesal & Altlomate, Abdelmajeed & Rezgui, B. (2015). “Utilisation de déchets locaux pour la production d’un béton écologique.” JSFM-CMC 2015. Retrieved from

https://www.researchgate.net/publication/283214162_Utilisation_de_dechets_locaux_pour_la_production_d'un_beton_ecologique/citation/download

[57] Vrijders, J., De Bock, L. (2019). Utilisation de granulats de béton recyclés dans le béton. (O. Vandooren, Ed.). CSTC, Rue du Lombard 42 Bruxelles, 1000: CENTRE SCIENTIFIQUE ET TECHNIQUE DE LA CONSTRUCTION CSTC.

[58] Statista. (2024). "les principaux pays producteurs de sable et de gravier dans le monde en 2023 (en milliers de tonnes)." Statista. Retrieved from https://fr.statista.com/statistiques/574806/production-industrielle-mondiale-de-sable-et-de-gravier-par-pays/

[59] H., K. (2023). "Algérie : vers la construction d'un million de logements sociaux." dzairdaily.

[60] APS. (n.d.). "Education: nécessité d'une mobilisation totale pour la réussite de la prochaine rentrée." Retrieved from https://www.aps.dz/algerie/142773-education-necessite-d-une-mobilisation-totale-pour-la-reussite-de-la-prochaine-rentree

[61] mhuv.gov.dz. (2021). "Ville Nouvelle de Sidi Abdellah." Retrieved from https://www.mhuv.gov.dz/fr/ville-nouvelle-de-sidi-abdellah/

[62] AICHA RABAH. (2022). HISTORIQUE DE LA ROUTE EN ALGERIE. Retrieved from https://fr.scribd.com/document/460655568/1-Algerie-Aicha-Rabah

[63] Rédaction AE. (2022). "Autoroute Est-Ouest : le dernier tronçon finalisé avant la fin de l'année 2022." ALGERIE ECO. Retrieved from https://www.algerie-eco.com/2022/06/13/autoroute-est-ouest-le-dernier-troncon-finalise-avant-la-fin-de-lannee-2022/

[64] imagesappgoogle. (2024). "Situation du réseau routier en Algérie." imagesappgoogle. Retrieved from https://images.app.goo.gl/biYiouyLFexRp6oZA

[65] lechantier. (2020). "Rseau ferroviaire national 6500 km en 2023 comme objectif." lechantier. Retrieved from https://lechantier.dz/26-Rseau-ferroviaire-national--6-500-km-en-2023--comme-objectif

[66] Gifex. (2022). "Gifex.com." Map of the Algerian Railway Network. Retrieved from Gifex.com

[67] AE, R. (2021). "Métro d'Alger : l'extension vers l'aéroport réceptionnée en 2026." Journal d'information indépendant algerie-eco.com. Retrieved from https://www.algerie-eco.com/2021/10/05/metro-dalger-lextension-vers-laeroport-receptionnee-en-2026/

[68] Rédaction. (2021). "Métro d'Alger : l'extension vers l'aéroport réceptionnée en 2026." algerie-eco.

[69] ebourse. (2017). "El Qantas: le tunnel le plus long d'Algérie." ebourse. Retrieved

from https://ebourse.dz/el-qantas-le-tunnel-le-plus-long-dalgerie/

[70] Wikimedia. (2019). “Viaduc_Salah-Bey.” wikimedia.

[71] pizzarotti. (2007). “AIN TURK VIADUCT.” pizzarotti.

[72] DJOUDI, F. (2023). “Viaduc sur l’oued Ménar.” Linkedin.

[73] Anesrif. (2019). “Viaduc exceptionnel de Tlemcen.” anesrif.

[74] aeroport-alger. (2018). “Nouvel aéroport d’Alger : un projet à 80 milliards DA.” aeroport-alger. Retrieved May 24, 2024, from https://www.aeroport-alger.com/fr/informations_aeroport.php?idnew=794

[75] Infotraficalgerie. (2017). “aeroport ahb new alger.” Retrieved from https://infotraficalgerie.dz/wp-content/uploads/2017/02/aeroport-ahb-new-alger.jpg

[76] PRESSE-ALGÉRIE. (2021). “Port d’El Hamdania : prendre toutes les dispositions nécessaires au lancement des travaux.” dimanche, 28 février 2021.

[77] Lilia, A. (2022). “niveau-actuel-eau-barrages/.” Actualité Algérie dzairdaily. Retrieved from https://www.dzairdaily.com/algerie-voici-niveau-actuel-eau-barrages/

[78] Aps. (2022). “Barrage Béni Haroun de Mila : destination privilégiée des amateurs de la pêche continentale en Algérie.” APS.

[79] Agence France-Presse. (2015). “Algeria builds giant mosque with world’s tallest minaret.” theguardian. Retrieved from https://www.theguardian.com/world/2016/may/06/algeria-builds-giant-mosque-with-worlds-tallest-minaret

[80] algerie-eco. (2022). “Publication des decrets executifs relatifs à la grande mosquée d’Alger.” algerie-eco. Retrieved from https://www.algerie-eco.com/2022/05/06/publication-des-decrets-executifs-relatifs-a-la-grande-mosquee-dalger/

[81] Lafarge. (2024). “Record coulée de béton en continu 8 400 m3 en 51 heures.” lafarge. Retrieved from https://www.lafarge.dz/record_coule_de_bton_en_continu_8_400_m3_en_51_heures

[82] opera d’alger. (2018). “Opera d’alger.” operaalger. Retrieved from https://operaalger.com.dz/galerie/

[83] Cscec. (2024). “Centre International Des Conférences «C.I.C», Alger.” cscec. Retrieved from https://www.cscec.dz/fr/services/projects/d-6.html

[84] Agenceecofin. (2023). “Algérie : le gouvernement dévoile pour 2024 un plan de développement du transport par câble.” agenceecofin. Retrieved from https://www.agenceecofin.com/transports/2211-113929-algerie-le-gouvernement-devoile-pour-2024-un-plan-de-developpement-du-transport-par-cable

[85] Jacques PEKEMSI. (2021). “ALGÉRIE : STADE D’ORAN, TOUT SAVOIR SUR LE JOYAU INAUGURÉ JEUDI.” africatopsports. Retrieved from https://www.https//www.africatopsports.com/wp-content/uploads/2021/06/E3_t_wFWUAI7Tul.jpg.com/wp-content/uploads/2021/06/E3_t_wFWUAI7Tul.jpg

[86] M. Mahfoud. (2023). “La presse visite le stade Nelson Mandela de Baraki: Un joyau architectural digne des grands complexes.” lejourdalgerie. Retrieved from https://lejourdalgerie.com/la-presse-visite-le-stade-nelson-mandela-de-baraki-un-joyau-architectural-digne-des-grands-complexes/

[87] m-culture. (2016). “Opéra d’Alger- Boualam Bessaih.” m-culture. Retrieved from https://www.m-culture.gov.dz/index.php/fr/arts-vivants-et-spectacles/etablissements-sous-tutelletablissements-sous-tutelle/opéra-d’alger

[88] constructioncayola. (2018). “Construction dans le monde : +3,6% de croissance par an jusqu’en 2022.” constructioncayola. Retrieved from https://www.constructioncayola.com/infrastructures/article/2018/10/08/121062/construction-dans-monde-croissance-par-jusqu-2022

[89] Safwan Moubaydeen, Julian Pope, Julie Tuck, M. W. and N. M., Dentons & Co, Q. (2013). “Construction and projects in Qatar: overview.” Practical Law, Construction and projects, Multi-jurisdictional Guide, pp. 1. https://doi.org/5-519-5882.

[90] C21redaction. (2018). “China-Singapore Tianjin Eco-city South District.” construction21.

[91] Designboom. (2024). “neom-line-progress-video-megacity-saudi-arabia.” designboom. Retrieved from https://www.designboom.com/architecture/neom-line-progress-video-megacity-saudi-arabia-02-26-2024/

[92] voyages d’affaires. (2023). “naissance d’une nouvelle capitale futuriste.” voyages-d-affaires. Retrieved from https://www.voyages-d-affaires.com/egypte-nouvelle-capitale-futuriste-20230503.html

[93] ekoatlantic. (2023). “WELCOME TO EKO ATLANTIC INVEST IN THE FUTURE OF LAGOS.” ekoatlantic. Retrieved from https://www.ekoatlantic.com/

[94] Lewis, N. (2024). “A new city is rising in Egypt. But is it what the country needs?” CNN. Retrieved from https://edition.cnn.com/world/egypt-new-administrative-capital-spc-intl/index.html

[95] Tom Ravenscroft. (2024). “Video reveals construction progressing on The Line in Neom.” dezeen.

[96] Qarjouli, A. (2023). “News : Qatar’s Lusail City named ‘Capital of Islamic Culture’ for year 2030.” dohanews.

[97] Ferrovial. (2024). “LBJ Express, TX.” Ferrovial.

[98] Techniques-ingenieur. (2012). “Les grands chantiers en Chine.” techniques-

ingenieur.

[99] Wang Bin. (2019). “Draw the marking lines and put up the signboards! Qingdao ‘Chongqing Elevated Road’ is waiting for work.” skyscrapercity from Peninsula Net.

[100] Lanouvellerepublique. (2017). “La voie se dégage pour le prolongement de la LGV Tours-Bordeaux vers Toulouse et l’Espagne.”

[101] Distriartisan. (2017). “Les plus grands chantiers actuels du monde : entre nécessité et démesure.” Distriartisan.

[102] Web. (2024). “Métro de Riyad – Arabie Saoudite.” egis-group. Retrieved from https://www.egis-group.com/fr/projets/metro-de-riyad

[103] thyssenkrupp-materials. (2023). “thyssenkrupp Materials France, l’ingénierie au service de l’un des plus ambitieux projets du Moyen-Orient.” thyssenkrupp-materials.

[104] LEMONITEUR. (2019). “Vinci Construction livre le Pont de l’Atlantique, au Panama.” LE MONITEUR. Retrieved from https://www.lemoniteur.fr/article/vinci-construction-livre-le-pont-de-l-atlantique-au-panama.2049310

[105] railway-technology. (2021). “Gotthard Base Tunnel, Switzerland The Gotthard Base Tunnel, which runs through the Alps in Switzerland, is the world’s longest railway tunnel.” railway-technology.

[106] ingebime. (2019). “Pékin Daxing : Le plus grand aéroport au monde prêt à ouvrir ses portes….” ingebime. Retrieved from https://ingebime.fr/news/pekin-daxing-le-plus-grand-aeroport-au-monde-pret-a-ouvrir-ses-portes/

[107] WorldAirportAwards. (2024). “The World’s Top 10 Airports of 2024.” WorldAirportAwards. Retrieved from https://www.worldairportawards.com/the-worlds-top-10-airports-of-2024/

[108] Parisaeroport. (2019). “Conception architecturale schématique pour le terminal du nouvel aéroport international Daxing de Pékin.” parisaeroport. Retrieved from https://www.parisaeroport.fr/groupe/strategie/airport-services/realisations/conception-aeroport-daxing

[109] Lepoint. (2019). “Pékin : les secrets de construction du plus grand terminal aéroportuaire au monde.” lepoint. Retrieved from https://www.lepoint.fr/monde/pekin-les-secrets-de-construction-du-plus-grand-terminal-aeroportuaire-au-monde-26-09-2019-2337922_24.php#11

[110] lindependant. (2019). “Le nouveau méga aéroport de Pékin à 12 milliards d’euros a ouvert ses portes.” lindependant. Retrieved from https://www.lindependant.fr/2019/09/25/le-nouveau-mega-aeroport-de-pekin-a-12-milliards-deuros-a-ouvert-ses-portes,8437586.php

[111] sia-partners. (2016). “Croissance du trafic aérien : projets d’infrastructures des aéroports.” sia-partners. Retrieved from https://www.sia-

partners.com/fr/publications/publications-de-nos-experts/croissance-du-trafic-aerien-projets-dinfrastructures-des

[112] Bruno Trévidic. (2018). “Le plus grand aéroport du monde ouvre ses portes à Istanbul.” Lesechos. Retrieved from https://www.lesechos.fr/industrie-services/tourisme-transport/le-plus-grand-aeroport-du-monde-ouvre-ses-portes-a-istanbul-143594

[113] Kamis. (2020). “Bandara Dubai Tersibuk untuk Penumpang Internasional Selama 6 Tahun Berturut-turut.” beritatrans.

[114] Cundall. (2024). “The Hamad Port is the world’s largest greenfield port-development project.” cundall.

[115] Vanhopplinus, P., Rijkswaterstaa, D. (2021). “Building the future.” Nieuwe Sluis Terneuzen and Zandbeek.

[116] Limak. (2024). “Çetin Dam and Hydroelectric Power Plant Started Energy Production.” limak.

[117] L’energeek. (2016). “L’ETHIOPIE INAUGURE LE PLUS HAUT BARRAGE HYDROÉLECTRIQUE D’AFRIQUE.” l’energeek. Retrieved from https://lenergeek.com/2016/12/22/lethiopie-inaugure-le-plus-haut-barrage-hydroelectrique-dafrique/#google_vignette

[118] JEFF OGANGA. (2022). “When Completed, This Hotel Will Be The Largest In The World.” thetravel.

[119] Distriartisan. (2017). “Notre TOP des plus grands chantiers du monde.” Distriartisan. Retrieved from https://www.distriartisan.fr/blog/top-plus-grands-chantiers-monde/

[120] Ben Dreith. (2024). “Super Bowl stadium designed to be ‘fast, angry and intimidating.’” dezeen.

[121] Viessmann. (2024). “Palm Island ‘The Palm Jumeirah’ in Dubai.” viessmann.

[122] Infociments. (2024). “Les constituants des bétons et des mortiers- Les granulats pour béton.” In CT-G10.30-41 (pp. 32–43). Infociments.

[123] Lafarge. (2024). “aggregates_history.” lafarge.

[124] Phongchongthienta. (2022). “AGGREGATES SUPPLY GLOBALLY.” phongchongthienta.

[125] Aggbusiness. (2021). “Growing global aggregates sustainably.” aggbusiness.

[126] Matthieu Combe. (2018). “Nous courrons droit vers une pénurie de sable.” magazine Natura Sciences. Retrieved from https://www.natura-sciences.com/comprendre/penurie-sable.html

[127] Jeanne Merzaux. (2024). “Les enjeux de l’extraction du sable, l’exemple de l’Asie du Sud-Est.” revueconflits. Retrieved from https://www.revueconflits.com/les-enjeux-de-lextraction-du-sable-lexemple-

de-lasie-du-sud-est/

[128] Annabelle Kiéma. (2023). “Le sable, une ressource en voie de disparition.” consoglobe. Retrieved from https://www.consoglobe.com/le-sable-une-ressource-en-voie-de-disparition-cg

[129] le moniteur. (2024). “Une etude internationale : alerte sur la gestion des ressources en granulats.” le moniteur. Retrieved from https://www.lemoniteur.fr/article/une-etude-internationale-alerte-sur-la-gestion-des-ressources-en-granulats.2146389

[130] Tiess, G., Kriz, A. (2011). “Aggregates Resources Policies in Europe Development of IT solutions for the Enhancement of Planning & Permitting Procedures.” International Journal of Environmental Impacts, Vol. 1, Issue 3, pp. 54–61.

[131] Ce.memphis. (2024). “CHAPTER 5 Aggregates for Concrete.” In ce.memphis (pp. 79–103). PCA_manual.

[132] Lafarge. (2024). “Fabrication des granulats.” lafarge. Retrieved from https://www.lafarge.fr/fabrication-des-granulats

[133] KHOUADJIA, M. K. L. (2016). Etudes des propriétés physico-mécaniques et rhéologiques des bétons à base des sables de carrières: expérimentation et modélisation. Mohamed KHIDER- Biskra.

[134] Materialtestingexpert. (2024). “LARGEST LIMESTONE QUARRY IN THE WORLD - KHOR KHUWAIR.” materialtestingexpert.

[135] Futura-sciences. (2019). “Terre mines carrières plus spectaculaires.” futura-sciences.

[136] Stock.adobe. (2024). “Vue aérienne d’une carrière a Bourron Marlotte dans la seine et Marne en France.” stock.adobe.

[137] F. MAUBERT. (1989). mémento roches et minéraux industriel- Les granulats. BRGM.

[138] NF EN 933-2. (1996). “Essais pour déterminer les caractéristiquesgéométriques des granulats, Partie 2 : Détermination de la granularité — Tamis de contrôle,dimensions nominales des ouvertures.” Association Française de Normalisation (AFNOR).

[139] NF P18-554. (1990). “Granulats - Mesures des masses volumiques, de la porosité, du coefficient d’absorption et de la teneur en eau des gravillons et cailloux.” Association Française de Normalisation (AFNOR).

[140] NF P18-555. (1990). “Granulats - Mesures des masses volumiques, coefficient d’absorption et teneur en eau des sables.” Association Française de Normalisation (AFNOR).

[141] NF P18-309. (1982). “Granulats d’argile ou de schiste expansés fabriqués en four rotatif destinés à la confection de bétons.”

[142] Dictionnaire Le Petit Larousse en couleurs. (1980).

[143] mapsofworld. (2024). “Cartes du Monde-Actuel, Cohérentes, Crédibles-Monde Désertique Carte.” Monde Désertique Carte. Retrieved from https://fr.mapsofworld.com/world-desert-map.htm

[144] Geographonic. (2024). “purposegames: Types of Sand Dunes (Advanced).” PurposeGames.

[145] Kate M. (2017). “What are the different types of sand dunes?” socratic.

[146] Omondi, S. (2018). “Types Of Sand Dunes.” Worldatlas-Environment.

[147] Hargitai, H. and K. (2015). “Barchanoid Ridge.” In a of Planetary Landforms. Springer. Springer New York. https://doi.org/10.1007/978-1-4614-3134-3_13.

[148] Parteli, E. J. R. (2021). “Parteli2021.” In Encyclopedia of Planetary Landforms. Springer New York. https://doi.org/10.1007/978-1-4614-9213-9_113-2.

[149] WINANDY Héloïse; Florian WALLAYS. (2023). “actualité : 1ère en Wallonie : le chantier de réhabilitation de l’E411/A4 entre Daussoulx et Thorembais-Saint-Trond accueille une plateforme de recyclage et production de matériaux.” sofico.

[150] Dawood, E. T., Ramli, M. (2011). “High strength characteristics of cement mortar reinforced with hybrid fibres.” Construction and Building Materials, Vol. 25, , pp. 2240–2247.

[151] Bagnold, R. A. (1974). The Physics of Blown Sand and Desert Dunes (1st ed.). Chapman and Hall, London: Springer Dordrecht. https://doi.org/https://doi.org/10.1007/978-94-009-5682-7.

[152] Journal Officiel de la République Algérienne. (1984). “Aticle 2 du décret n° 84-378 du 15 décembre 1984.” Algérie. Retrieved from https://www.joradp.dz/FTP/jo-francais/1984/F1984066.PDF

[153] Juan Marta & Gutiérrez Pilar. (2009). “Study on the influence of attached mortar content on the properties of recycled concrete aggregate.” Construction and Building Materials, Vol. 23, Issue 2, pp. 872–877. https://doi.org/10.1016/j.conbuildmat.2008.04.012.

[154] Abdelgadir Abbas, Gholamreza Fathifazl, O. Burkan Isgor, A. Ghani Razaqpur, Benoit Fournier, S. F. (2009). “Durability of recycled aggregate concrete designed with equivalent mortar volume method.” Cement and Concrete Composites, Vol. 31, Issue 8, pp. 555–563. https://doi.org/https://doi.org/10.1016/j.cemconcomp.2009.02.012.

[155] Padmini, A. K., Ramamurthy, K., & Mathews, M. S. (2009). “Influence of parent concrete on the properties of recycled aggregate concrete.” Construction and building materials, Vol. 23, Issue 2, pp. 829–836. https://doi.org/https://doi.org/10.1016/j.conbuildmat.2008.03.006.

[156]: Purchase, C. K. ., Al Zulayq, D.M.; O’Brien, B. T. ., Kowalewski, M.J.; Berenjian, A. ., Tarighaleslami, A.H.; Seifan, M. (2022). “Circular Economy of Construction and Demolition Waste: A Literature Review on Lessons,

Challenges, and Benefits." Materials, Vol. 15, Issue 76.

[157] Silva Rui Vasco Jorge de Brito. (2015). "Use of recycled aggregates from construction and demolition wastes in the production of structural concrete." In Connecting People and Ideas . Proceedings of EURO ELECS 2015 . Guimarães . Portugal . Guimarães . Portugal . https://doi.org/10.13140/RG.2.1.1750.1526.

[158] National waste agency. (2020). RAPPORT SUR L'ETAT DE LA GESTION DES DECHETS EN ALGERIE (EXERCICE 2020).

[159] Adam Redling. (2018). "Construction debris volume to surge in coming years_Global volume of construction debris to nearly double by 2025, according to report." cdrecycler.

[160] Bishnu Pada Bose. (2022). "State of the art on Recycling of Construction and Demolition Waste in a Circular Economy: An Approach Towards Sustainable Development." International Journal of Earth Sciences Knowledge and Applications, Vol. 4, Issue 3, pp. 516–523. https://doi.org/e-ISSN: 2687-5993.

[161] Ercole-immobilier. (2022). "Les déchets de la construction : un enjeu majeur pour la préservation de l'environnementLe secteur du BTP produit 246 millions de tonnes de déchets par an en France ! Leur valorisation est absolument nécessaire."

[162] Apur. (2022). "Une nouvelle base de données démolition au service des déchets du BTP." Apur.

[163] Nobatek INEF. (2023). "Granulats recyclés : Conditions de Valorisation, Economie circulaire des Déchets de C&D." projet Interreg Poctefa RCDiGreen.

[164] Manseur, N., Ziani, S. (2014). Etude et caractérisation des granulats recyclés de démolition. Abderrahmane Mira-Béjaia, Algeria.

[165] Delvoie, S., Zhao, Z., Michel, F., Courard, L. (2018). "State of the art on recycling techniques for the production of recycled sands and aggregates from construction and demolition wastes." In Circular Concrete - SeRaMCo - Secondary Raw Materials for Concrete Precast Products. Luxembourg, LU: Mid-term conference SeRaMCo.

[166] Oikonomou, N. (2005). "Recycled concrete aggregates." Cement and Concrete Composites, Vol. 27, Issue 2, pp. 315–318.

[167] Omary, S., Ghorbel, E., Wardeh, G. (2016). "Relationships between recycled concrete aggregates characteristics and recycled aggregates concretes properties." Construction and Building Materials, Vol. 108, Issue 10. https://doi.org/10.1016/j.conbuildmat.2016.01.042.

[168] Levacher, D., Bennabi, A., Bouvet, F. (2000). "Valorisation des agrégats issus de bétons de démolition dans la fabrication de nouveaux bétons," pp. 17–22.

[169] PATRICK GUIRAUD. (2018). "Caractéristiques et types de granulats." infociments.

[170] Tam, V. W. Y., Gao, X. F., Tam, C. M. (2005). "Microstructural analysis of

recycled aggregate concrete produced from two-stage mixing approach." Cement and Concrete Research, Vol. 35, Issue 6, pp. 1195–1203. https://doi.org/https://doi.org/10.1016/j.cemconres.2004.10.025.

[171] NF EN 1097-2. (2010). "Tests for mechanical and physical properties of aggregates: methods for the determination of resistance to fragmentation." ASSOCIATION FRANCAISE DE NORMALISATION (AFNOR).

[172] NF EN 1097-1. (2011). "Tests for mechanical and physical properties of aggregates: methods for the determination of the resistance to wear (micro-deval)." ASSOCIATION FRANCAISE DE NORMALISATION (AFNOR).

[173] Francisco Agrela, P Alaejos, and M. S. D. J. P. (2013). "Properties of concrete with recycled aggregates, chapter 12." University of Córdoba, Spain, pp. 304–327. https://doi.org/10.1533/9780857096906.2.304.

[174] Zhao, Z., Rémond, S., Damidot, D., XU, W. (2013). "In uence of hardened cement paste content on the water absorption of ne recycled concrete aggregates." Journal of Sustainable Cement-Based Materials, Vol. 2, , pp. 186–203.

[175] Braymand, S., Roux, S., Fares, H. (2017). Evaluation en laboratoire de techniques destinées à séparer la pate de ciment du gravillon naturel d'origine.

[176] Bru, K., Touzé, S., Bourgeois, F., Lippiatt, N., Ménard, Y. (2014). "Assessment of a microwave-assisted recycling process for the recovery of high-quality aggregates from concrete waste." International Journal of Mineral Processing, Vol. 126, , pp. 90–98.

[177] LinB, E., Mueller, A. (2004). "High-performance sonic impulses_an alternative method for processing of concrete." International Journal of Mineral Processing, Vol. 74, Issue Special Issue Supplement Comminution 2002, pp. S199–S208.

[178] F. Homand-Etienne, Houpert, R. (1989). "Thermally induced microcracking in granites : characterization and analysis." International Journal of Rock Mechanics and Mining Sciences & Geomechanics Abstracts, Vol. 26, Issue 2, pp. 125–134.

[179] Abbas, A., Fathifazl, G., BurkanIsgor, O., Razaqpur, A. G., B., F., Foo, S. (2008). "Proposed method for determining the residual mortar content of recycled concrete aggregates." Journal of ASTM International, Vol. 5, Issue 1.

[180] Heriberto Martinez Hernandez. (2022). Amélioration de granulats de béton recyclé par bioprécipitation. École centrale de Nantes.

[181] Liang, C., Pan, B., Ma, Z., He, Z., Duan, Z. (2020). "Utilization of CO2 curing to enhance the properties of recycled aggregate and prepared concrete : A review." Cement and Concrete Composites, Vol. 105, , pp. 1–14.

[182] Jang, J. G., Kim, G. M., Kim, H. J., Lee, H. K. (2016). "Review on recent advances in CO2 utilization and sequestration technologies in cement-based materials." Construction and Building Materials, Vol. 127, , pp. 762-773.

[183] Poon, C. S., Zhan, B. J., Xuan, D. X., Hossain, M. U. (2019). “Enhancement of properties of recycled aggregate concrete by accelerated CO2 curing.” CO2STO.

[184] Zhan, B. J., Xuan, D. X., Zeng, W., Poon, C. S. (2019). “Carbonation treatment of recycled concrete aggregate : Effect on transport properties and steel corrosion of recycled aggregate concrete.” Cement and Concrete Composites, Vol. 104, , pp. 1–8.

[185] Bravo, M., de Brito, J., Pontes, J., Evangelista, L. (2015). “Mechanical performance of concrete made with aggregates from construction and demolition waste recycling plants.” Journal of Cleaner Production, Vol. 99, , pp. 59–74.

[186] Jiménez, J. R., Ayuso, J., Agrela, F., López, M., Galvín, A. P. (2012). “Utilisation of unbound recycled aggregates from selected CDW in unpaved rural roads.” Resources, Conservation and Recycling, Vol. 58, , pp. 88–97.

[187] Evangelista, L., de Brito, J. (2007). “Mechanical behaviour of concrete made with fine recycled concrete aggregates.” Cement and Concrete Composites, Vol. 29, Issue 5, pp. 397–440.

[188] Güneyisi, E., Gesoğlu, M., Özbay, E. (2009). “Properties of self-compacting concretes made with binary, ternary, and quaternary cementitious blends of fly ash, blast furnace slag, and silica fume.” Construction and Building Materials, Vol. 23, Issue 5, pp. 1847–1854.

[189] Linsel S, S. M. (2009). “Einsatz alternative Baustoffebei der Beton herstellung –Darstellungeinesneuen Verfahrenszur Veredelung von Baumaterialien und Anwendungs potenzialim Straßenbau [Use of alternative materials for the production of concrete. Presentation of a new method for.” Unwelttechnik und Bauwesen. Environ.Technol. Constr.

[190] Berredjem, L., Arabi, N., Molez, L., Jauberthie, R. (2016). “Propriétés mécaniques et durabilité des bétons à base de graviers et sables recyclés issus de béton de démolition.” https://doi.org/hal-01366521.

[191] Berredjem, L., Arabi, N., Molez, L., Berredjem, L., Arabi, N., Contribution, L. M. (2015). “Contribution ` a l ’ ´ etude des indicateurs de durabilit ´ e des b ´ a base des granulats recycl ´ es To cite this version : Contribution à l ’ étude des indicateurs de durabilité des bétons à base des granulats recyclés,” Issue May.

[192] Jean-Claude Souche, Marie Salgues, Philippe Devilliers, G.-D. E. (2015). “INFLUENCE DU DEGRÉ DE SATURATION INITIAL DES GRANULATS RECYCLÉS SUR LES CARACTÉRISTIQUES DE LA PÂTE CIMENTAIRE À L’ÉTAT FRAIS : CONSÉQUENCES SUR LES PROPRIÉTÉS DU BÉTON RECYCLÉ.” In NOMAD 2015, Nov 2015, Douai, France. Douai, France.

[193] GRADT, E.-M. (1998). “Matériaux de construction Le béton est omniprésent dans la construction.” lemoniteur. Retrieved May 18, 2024, from https://www.lemoniteur.fr/article/materiaux-de-construction-le-beton-est-omnipresent-dans-la-construction.1544109

[194] Ramier, S. (2020). “Les différents matériaux de construction.” construction-travaux. Retrieved May 18, 2024, from https://www.construction-

travaux.com/les-differents-materiaux-de-construction/

[195] Dreux, G., Festa, J. (1998). “Nouveau Guide du Béton et de ses Constituants.” (Eyrolles, Ed.) (8th ed.). paris, France: Dreux, G., Festa, J. (1998), Nouveau Guide du Béton et de ses Constituants, 8th edition, Eyrolles, paris, France, ISBN 978-2-212-10231-4.

[196] NF P15-301. (1994). “Liants hydrauliques, Ciments courants, Composition, Spécifications et Critères de Conformité.” French Association for Standardization (AFNOR).

[197] NF EN 1008. (2003). “Eau de gâchage pour bétons - Spécifications d’échantillonnage, d’essais et d’évaluation de l’aptitude à l’emploi, y compris les eaux des processus de l’industrie du béton, telle que l’eau de gâchage pour béton.” Association Française de Normalisation (AFNOR).

[198] NF EN 934-2/A2. (2006). “Adjuvants pour béton, mortier et coulis, Partie 2 : Adjuvants pour béton — Définitions, exigences, conformité, marquage et étiquetage.” Association Française de Normalisation (AFNOR).

[199] Feret, R. (1892). “compacité des mortier.” Annales des Ponts et Chaussées, Vol. 7, Issue 4, pp. 5–164.

[200] Jérôme, B., Lesage, R. (1976). “LA COMPOSITION DU BETON HYDRAULIQUE DU LABORATOIRE AU CHANTIER.” Philosophy. Retrieved from https://www.semanticscholar.org/paper/LA-COMPOSITION-DU-BETON-HYDRAULIQUE-DU-LABORATOIRE-Baron-Lesage/4a3d4c69145923c6bad2286387e251f5c95cf08e

[201] Komar, A. G. (1978). Matériaux et éléments de construction. (Mir, Ed.) (3ème éditi.).

[202] Scramtaiev, N. V. (1951). Concrete Mix Design. (Gosstroiizdat, Ed.).

[203] Neville A.M. (2011). Properties of Concrete. (Pearson Education Limited, Ed.) (5th ed.).

[204] Bouzidi Mezghiche. (2005). Les Essais de Laboratoire des Matériaux de Construction. (Publication Universitaire, Ed.). Université de Biskra.

[205] DREUX, G., FESTA, J. (2007). http://topographi.blogspot.com/. (Eyrolles, Ed.) (Huitième é.).

[206] İlker Bekir Topçu Selim Şengel. (2004). “Properties of concretes produced with waste concrete aggregate.” Cement and Concrete Research, Vol. 34, Issue 8, pp. 1307–1312.

[207] Akash Rao, Kumar N. Jha, S. M. (2007). “Use of aggregates from recycled construction and demolition waste in concrete.” Resources, Conservation and Recycling, Vol. 50, Issue 1, pp. 71–81. https://doi.org/doi.org/10.1016/j.resconrec.2006.05.010.

[208] Houria MEFTAH. (2018). Contribution àl’étude du comportement à haute température des bétons de granulats récycles, renforcés de fibres polypropyléne.

Université BADJI Mokhtar-Annaba.

[209] Oussama, K., Mouret, M., Arabi, N., Cassagnabere, F. (2015). “Adverse Effect of the Mass Substitution of Natural Aggregates by Air-Dried Recycled Concrete Aggregates on the SelfCompacting Ability of Concrete: Evidence and Analysis through an Example.” Journal of Cleaner Production, Vol. 8, , pp. 752–761.

[210] Arabi, N., Berredjem, L. (2011). “Valorisation des déchets de démolition comme granulats pour bétons.” Déchets - revue francophone d’écologie industrielle, pp. 25–30. https://doi.org/DOI:10.4267/dechets-sciences-techniques.2765.

[211] Layachi Berredjem, Nourredine Arabi. (2009). “les matériaux de démolition une source de granulats pour béton : formulation et caractérisation d’un béton a base de ces recycles.” In SBEIDCO – 1st International Conference on Sustainable Built Environement Infrastructures in Developing Countries ENSET Oran (Algeria), October 12-14 (pp. 255–262).

[212] Poon.C.S, Shui.Z.H, Lam.L., Fok.H., Kou.S.C. (2004). “Influence of moisture states of natural and recycled aggregates on the slump and compressive strength of concrete.” Cement and Concrete Research, Vol. 34, Issue 1, pp. 31–36.

[213] Katz, A. (2003). “Properties of concrete made with recycled aggregate from partially hydrated old concrete.” Cement and Concrete Research, Vol. 33, Issue 5, pp. 703–711.

[214] Soutsos, M. N., Tang, K., Millard, S. G. (2011). “Use of recycled demolition aggregate in precast products, phase II: concrete paving blocks.” Construction and Building Materials, Vol. 25, Issue 7, pp. 3131–3143.

[215] Torben, C. H., Narud, H. (1983). “Strength of Recycled Concrete Made From Crushed Concrete Coarse Aggregate.” Concr. Int, Vol. 5, Issue 1, pp. 79–83.

[216] Topçu, İ. B., Şengel, S. (2004). “Properties of concretes produced with waste concrete aggregate.” Cement and Concrete Research, Vol. 34, Issue 8, pp. 1307–1312. https://doi.org/https://doi.org/10.1016/j.cemconres.2003.12.019.

[217] Thomas, J., Thaickavil, N. N., Wilson, P. M. (2018). “Strength and durability of concrete containing recycled concrete aggregates.” Journal of Building Engineering, Vol. 19, , pp. 349–365. https://doi.org/https://doi.org/10.1016/j.jobe.2018.05.007.

[218] Pedro, D., Brito, J. de, Evangelista, L. (2014). “Influence of the use of recycled concrete ag- gregates from different sources on structural concrete.” Constr. Build. Mater., Vol. 71, , pp. 141–151.

[219] McNeil, K., Kang, T. H. K. (2013). “Recycled concrete aggregates: a review.” J. Concr. Struct. Mater., Vol. 7, Issue 1, pp. 61–69.

[220] M.C. Rao, Bhattacharyya, S. K., Barai, S. V. (2011). “Influence of field recycled coarse ag- gregate on properties of concrete.” Mater. Struct., Vol. 44, , pp. 205–220.

[221] Safiuddin, M., Alengaram, U. J., MoshiurRahman, M., AbdusSalam, M.,

Jumaat, M. Z. (2013). "Use of recycled concrete aggregate in concrete: a review." J. Civ. Eng. Manag., Vol. 19, Issue 6, pp. 796–810.

[222] Kisku, N., Joshi, H., Ansari, M., Panda, S. K., Nayak, S., Dutta, S. C. (2017). "A critical review and assessment for usage of recycled aggregate as sustainable construction material." Constr. Build. Mater., Vol. 131, , pp. 721–740.

[223] Silva, R., Brito, J. de. (2015). "Use of recycled aggregates from construction and demolition wastes in the production of structural concrete." In Proceedings of the Euro Elecs, Guimarães, July 2015 (pp. 107–116).

[224] Silva, R. V., Brito, J. de, Dhir, R. K. (2015). "Tensile strength behaviour of recycled aggregate concrete." Constr. Build. Mater., Vol. 83, , pp. 108–118.

[225] Silva, R. V., Brito, J. de, Dhir, R. K. (2016). "Establishing a relationship between modulus of elasticity and compressive strength of recycled aggregate concrete." J. Clean. Prod., Vol. 112, Issue 4, pp. 2171–2186.

[226] Brito, J. de, Saikia, N. (2013). "Recycled aggregate in concrete, Use of industrial construction, and demolition waste, green energy and technology." Springer-Verlag, London.

[227] Silva, R. V., Brito, J. de, Dhir, R. K. (2015). "The influence of the use of recycled aggregates on the compressive strength of concrete: a review." Eur. J. Environ. Civ. Eng., Vol. 19, Issue 7, pp. 825–849.

[228] Brito, J. de, Ferreira, J., Pacheco, J., Soares, D., Guerreiro, M. (2016). "Structural, material, mechanical and durability properties and behaviour of recycled aggregates concrete." J. Build. Eng., Vol. 6, , pp. 1–16.

[229] Verma, S. K., Ashish, D. K. (2017). "Mechanical behavior of concrete comprising successively recycled concrete aggregates." Adv. Conc. Const., Vol. 5, Issue 4, pp. 303–311.

[230] Hamad, B. S., Dawi, A. H. (2017). "Sustainable normal and high strength recycled aggregate concretes using crushed tested cylinders as coarse aggregates." Case Stud. Const. Mater., Vol. 7, , pp. 7 (2017) (2017) 228–239.

[231] Saha, Rajasekaran, C. (2016). "Mechanical properties of recycled aggregate concrete pro_duced with Portland Pozzolana cement." Adv. Concr. Constr., Vol. 4, Issue 1, pp. 201.

[232] Tabsh, S. W., Abdelfatah, A. S. (2009). "Influence of recycled concrete aggregates on strength properties of concrete." Constr. Build. Mater., Vol. 23, , pp. 1163–1167.

[233] Exteberria, M., Vázquez, E., Marí, A., Barra, M. (2007). "Influence of amount of recycled coarse aggregates and production process on properties of recycled aggregate concrete." Cem. Conc. Res., Vol. 37, Issue 5, pp. 735–742.

[234] Rahal, K. (2007). "Mechanical properties of concrete with recycled coarse aggregate." Build Environ., Vol. 42, , pp. 407–415.

[235] Limbachiya, M. C., Dhir, R. K., Leelawat, T. (2000). "Use of recycled concrete

aggregate in high-strength concrete." Materials and Structures, Vol. 33, Issue 9, pp. 574–580.

[236] González-Fonteboa, B., Seara-Paz, S., de Brito, J., González-Taboada, I. Martínez-Abella, F., Vasco-Silva, R. (2018). "Recycled concrete with coarse recycled aggregate, An overview and analysis." Mater. Construcc., Vol. 68, Issue 330, pp. e151.

[237] S Kou, Poon, C. (2008). "Mechanical properties of 5-year-old concrete prepared with recycled aggregates obtained from three different sources." Mag Concr Res, Vol. 60, Issue 1.

[238] Naik, T. R., Malhotra, V. M., Popovics, J. S. (2004). The Ultrasonic Pulse Velocity Method. (C. P. LLC, Ed.) (Handbook o.).

[239] Youcefa, B., Saida, K., Khoudjab, A.-B. (2018). "Prediction of concrete strength by non-destructive testing in old structures: Effect of core number on the reliability of prediction." In 2nd International Congress on Materials & Structural Stability (CMSS-2017) (Vol. 149, p. 5). MATEC Web Conf. https://doi.org/https://doi.org/10.1051/matecconf/201814902007.

[240] R. F. Feidman. (2005). Essais non destructifs du béton.

[241] Khatib J.M. (2005). "Properties of concrete incorporating fine recycled aggregate." Cement and Concrete Research, Vol. 35, Issue 4, pp. 763–769.

[242] Kou, S., Chi-sun, P. (2015). "Effect of the quality of parent concrete on the properties of high performance recycled aggregate concrete." Construction and Building Materials, Vol. 77, , pp. 501–508. https://doi.org/https://doi.org/10.1016/j.conbuildmat.2014.12.035.

[243] Jones, R. (1954). "Testing of concrete by an ultrasonic pulse technique." RILEM Int. Symp. on Nondestructive Testing of Materials and Structures, Vol. 1, .

[244] Khodja ALI BENYAHIA. (2010). Corrélations entre Essais non Destructifs et Essais Destructifs du Béton à Faible Résistance. Université Hassiba Ben Bouali-Chlef- Algérie.

[245] Tegguer, A. D., Saillio, M., Mai-Nhu, J., Schmitt, L., Rougeau, D. (2015). "Propriétés des bétons de granulats recyclés »,." In AFGC. Paris.

[246] Pereira, C. G., Castro-Gomes, J., Oliveira, L. P. de. (2009). "Influence of natural coarse aggregate size, mineralogy and water content on the permeability of structural concrete." Constr. Build. Mater., Vol. 23, , pp. 602–608.

[247] Brito, J. D., Alves, F. (2010). "Concrete with recycled aggregates: The Portuguese experimental research." Mater. Structures, Vol. 43, , pp. 35–51. https://doi.org/doi:10.1617/s11527-010-9595-7.

[248] Evangelista, L., Brito, J. (2010). "Durability performance of concrete made with fine recycled concrete aggregates." Cement and Concrete Composites, Vol. 32, Issue 1, pp. 9–14.

[249] Rasheeduzafar, K. (1984). "Recycled Concrete-A Source of New Aggregates."

Cem. Concr. Aggre, Vol. 69, Issue 1, pp. 17–27.

[250]: Korolev, A.S.; Kopp, A. ., Odnoburcev, D.; Loskov, V. ., Shimanovsky, P.; Koroleva, Y. . V. (2021). “Compressive and Tensile Elastic Properties of Concrete: Empirical Factors in Span Reinforced Structures Design.” Materials, Vol. 14, , pp. 1–15. https://doi.org/https://doi.org/10.3390/ma14247578.

[251] Fib-international. (1973). N° 90. 1973. I - Calcul des Flèches - (Contribution aux travaux de Commission 1971-1973) II - Déformability of concrete structures - Basic assumptions (Preliminary Draft). FIB International. Retrieved from https://www.fib-international.org/publications/ceb-bulletins/i-calcul-des-flèches-detail.html

[252] Dalila Benamara, Bouzidi Mezghiche, Fatma Zohra Mechrouh. (2014). “The Deformability of a High Performance Concrete (HPC).” Physics Procedia, Vol. 55, , pp. 342–347. https://doi.org/https://doi.org/10.1016/j.phpro.2014.07.050.

[253] POPOVICS, S. (1970). “Characteristics of the Elastic Deformations of Concret.” onlinepubs, pp. 1–14. Retrieved from https://onlinepubs.trb.org/Onlinepubs/hrr/1970/324/324-001.pdf

[254] Guettala, S. (2011). Contribution à l’étude de l’influence de l’ajout du sable de dune finement broyé au ciment, sur les performances physico-mécaniques, la déformabilité & la durabilité du béton. université Mohamed Khider–Biskra. Algérie.

[255] F. GABRYSIAK. (n.d.). Matériaux - Les bétons. Cours. Retrieved from https://pdfcoffee.com/chapitre-004-les-betonspdf-pdf-free.html

[256] Nguyen, M.-D., Wardeh, G., Ghorbel, E. (2015). “Etude de l’endommagement des bétons à granulats recyclés.” In Rencontres Universitaires de Génie Civil. Bayonne, France. https://doi.org/ffhal-0116762.

[257] Cikrle, P., Bílek, V. (2010). “Modulus of elasticity of high strength concretes.” Beton TKS, Vol. 5, , pp. 40- 44 (in czech).

[258] Brito, J. De, Saikia, N. (2013). “Recycled Aggregate in Concrete.” London: Springer_Verlag.

[259] PAVLŮ, T., ŠEFFLOVÁ, M. (2014). “The Static and the Dynamic Modulus of Elasticity of Recycled Aggregate Concrete.” Advanced Materials Research, Vol. 1054, , pp. 221–226. https://doi.org/doi:10.4028/www.scientific.net/AMR.1054.221.

[260] Mehta, P. K., Monteiro, P. J. M. (2006). Concrete, MicrostructureProperties and Materials (3rd ed.). McGraw-Hill eBooks. https://doi.org/DOI: 10.1036/0071462899.

[261] Du, T., Wang W., L. Lin H., X. Liu Z., J. Liu. (2010). “Experimental Study on Interfacial Strength of the High Performance Recycled Aggregate Concrete.” Earth, Issue Sp. 2010, pp. 2821–2828.

[262] J. Xiao, Li, W., Sun, Z., Shah, S. P. (2013). “Crack Propagation in Recycled

Aggregate Concrete under Uniaxial Compressive Loading." ACI Mater. J., Vol. 109, , pp. 451–462.

[263] Rasheeduzzafar, Khan, A. (1984). "Recycled Concrete A Source for New Aggregate." Cem. Concr. Aggregates, Vol. 6, , pp. 17–27.

[264] Nagataki, S., Gokce, A., Saeki, T., Hisada, M. (2004). "Assessment of recycling process induced damage sensitivity of recycled concrete aggregates." Cement and concrete research, Vol. 34, Issue 6, pp. 965–971.

[265] V.W.Y. Tam, X.F. Gao, C.M. Tam. (2005). "Microstructure analysis of hardened recycled aggregate concrete produced from two stage mixing approach." Cement and concrete research, Vol. 35, Issue 6, pp. 1195–1203. https://doi.org/https://doi.org/10.1016/j.cemconres.2004.10.025.

[266] Poon, C. S., Shui, Z. H., Lam, L. (2004). "Effect of microstructure of ITZ on compressive strength of concrete prepared with recycled aggregates." Construction and Building Materials, Vol. 18, Issue 6, pp. 461–468.

[267] Brito, J. de. (2010). "Abrasion resistance of concrete made with recycled aggregates." International Journal of Sustainable Engineering, Vol. 3, Issue 1, pp. 58–64. https://doi.org/DOI: 10.1080/19397030903254710.

[268] Dhir, R. K., Hewlett, P. C., Chan, Y. . (1991). "Near surface characteristics of concrete abrasion resistance." Materials and Structures, Vol. 24, Issue 140, pp. 122–128.

[269] Laplante, P., Aitcin, P. C., Vezina, D. (1991). "Abrasion resistance of high performance concrete." Journal of Materials in Civil Engineering, Vol. 3, Issue 1, pp. 19–28.

[270] Olorunsogo, F. . (1999). "Early age properties of recycled aggregate concrete." In Proceedings of the international seminar on exploiting wastes in concrete (pp. 163–170). Scotland: University of Dundee.

[271] Sagoe-Crentsil, K. K., Brown, T., Taylor, A. H. (2001). "Performance of concrete made with commercially produced coarse recycled concrete aggregate." Cement and Concrete Research, Vol. 31, Issue 5, pp. 707–712.

[272] Zaharieva, R., Buyle-Bodin, F., Skoczylas, F., Wirquin, E. (2003). "Assessment of the surface permeation properties of recycled aggregate concrete." Cem. Concr. Compos., Vol. 25, Issue 2, pp. 223–232.

[273] Coquillat, G. (1982). "Recyclage de materiaux de demolition dans la confection de Beton. CEB-Service d'Etude des Materiaux Unite." Technology des Béton.

[274] Malhotra, V. M., Wilson, H. S., Painter, K. E. (1989). "Performance of Gravel stone Concrete Incorporating Silica Fume at Elevated Temperatures." American Concrete Institute, Vol. 114, , pp. 1051–1076.

[275] Buck A. D. (1976). "Recycled concrete as a source of aggregate." In Proc. of Symposium, Energy and Resource Conservation in the Cement and Concrete Industry. Canmet, Ottawa.

[276] Lavado, J., Bogas, J., de Brito, J., Hawreen, A. (2020). “Fresh properties of recycled aggregate concrete.” Construction and Building Materials, Vol. 233, , pp. 117322. https://doi.org/https://doi.org/10.1016/j.conbuildmat.2019.117322.

[277] Pedro, D., Brito, J. de, Evangelista, L. (2015). “Performance of concrete made with aggregates recycled from precasting industry waste: influence of the crushing process.” Mater. Struct., Vol. 48, Issue 12, pp. 3965–3978.

[278] Richardson, A., Coventry, K., Bacon, J. (2011). “Freeze/thaw durability of concrete with recycled demolition aggregate compared to virgin aggregate concrete.” J. Clean. Prod., Vol. 19, , pp. 272– 277.

[279] Hermann, K. (1992). “Dégâts du béton dus à l’agression des ions de sulfate.” Bulletin du ciment, Vol. 60, Issue 4, pp. 1–8.

[280] Hermann, K. (2018). “Substances exerçant une action chimique sur le béton.” Bulletin du ciment, pp. 3–11. Retrieved from http://doi.org/10.5169/seals-146377

[281] Loic Divet. (2001). Les réactions sulfatiques internes au béton: contribution à l’étude des mécanismes de la formation différée de l’ettringite. https://doi.org/1161-028X.

[282] Wu, Q.; Ma, Q.; Huang, X. (2021). “Mechanical Properties and Damage Evolution of Concrete Materials Considering Sulfate Attack.” Materials, Vol. 14, , pp. 2343. https://doi.org/https://doi.org/ 10.3390/ma14092343.

[283] Phan, L. T., & Carino, N. J. (1998). “Review of mechanical properties of HSC at elevated temperature.” Journal of Materials in Civil Engineering, Vol. 10, Issue 1, pp. 58–64.

[284] Kodur, V. K., & Sultan, M. A. (2003). “Effect of temperature on thermal properties of high-strength concrete.” Journal of Materials in Civil Engineering, Vol. 15, Issue 2, pp. 101–107.

[285] Arioz, O. (2007). “Effects of elevated temperatures on properties of concrete.” Fire Safety Journal, Vol. 42, Issue 8, pp. 516–522.

[286] HACHEMI, S. (2015). Etude du Comportement du béton soumis à haute température : Influence du type de béton et de la nature des constituants. Mohamed Khider – Biskra, ALGERIE.

[287] Kanema, M., Noumowe, A., Gallias, J.-L., Cabrillac, R. (2005). “Influence des paramètres de formulation et microstructuraux sur le comportement à haute température des bétons.” In XXIIIièmes Rencontres Universitaires de Génie Civil – Risque & Environnement.

[288] Isabela Gaweska Hager. (2004). Comportement à haute température des bétons à hautes performances-évolution des principales propriétés mécaniques. Ecole Polytechnique de Cracovie.

[289] Bazant., Z., Kaplan.MF. (1996). “Concrete at high temperature: Material properties and mathematical models.” Concrete Design & Construction Series,

pp. 196.

[290] NF P15-301. (1994). “Hydraulic binders, Common cements, Composition, Specifications and Compliance Criteria.” French Association for Standardization (AFNOR).

[291] NF P18-597. (1990). “Granulats - Détermination de la propreté des sables : équivalent de sable à 10 % de fines.” Association Française de Normalisation (AFNOR).

[292] NF P18-598. (1991). “Granulats - Équivalent de sable.” Association Française de Normalisation (AFNOR).

[293] NF EN 933-8. (2012). “Essais pour déterminer les caractéristiques géométriques des granulats - Partie 8 : évaluation des fines - Équivalent de sable.” Association Française de Normalisation (AFNOR).

[294] NF EN 932-1. (1996). “Essais pour déterminer les propriétés générales des granulats - Partie 1 : méthodes d’échantillonnage.” Association Française de Normalisation (AFNOR).

[295] NF EN 932-2. (1999). “Essais pour déterminer les propriétés générales des granulats - Partie 2 : méthodes de réduction d’un échantillon de laboratoire.” Association Française de Normalisation (AFNOR).

[296] NF EN 933-1. (1997). “Essais pour déterminer les caractéristiques géométriques des granulats, Partie 1. Détermination de la granularité, Analyse granulométrique par tamisage.” (Association Française de Normalisation AFNOR).

[297] NF P18-560. (1990). “Granulats, Analyse granulométrique par tamisage.” (Association Française de Normalisation AFNOR).

[298] NF P18-573. (1990). “Granulats - Essai de Los Angeles.” Association Française de Normalisation (AFNOR).

[299] Akroum, K., Derdour, D., Lagaguine, M. (2022). “Influence of the quality of parent concrete on the quality of son concrete: compression strength case.” In ICADET (Ed.), 4th International Conference on Advanced Engineering Technologies 28-30 September 2022.

[300] Kebaili, B., Benzerara, M., Menadi, S., Kouider, N., Belouettar, R. (2022). “Effect of parent concrete strength on recycled concrete performance.” Frattura ed Integrità Strutturale, Vol. 62, Issue 2022, pp. 14–25. https://doi.org/10.3221/IGF-ESIS.62.02.

[301] NF P18-405. (1981). “Concretes, Information tests, preparation and preservation of specimens.” Association Française de Normalisation (AFNOR).

[302] NF P18-404. (1981). “Study, suitability and control tests, Preparation and storage of test specimens.” Association Française de Normalisation (AFNOR).

[303] NF EN 12390-1. (2001). “Testing for hardened concrete, Part 1. Shape, dimensions and other requirements for specimens and molds.” Association Française de Normalisation (AFNOR).

[304] NF EN 12350-2. (1999). “Fresh Concrete Testing, Slump Testing.” Association Française de Normalisation (AFNOR).

[305] EN 12390-3. (2003). “Essai pour béton durci, Partie 3 : Résistance à la compression des éprouvettes.” Association Française de Normalisation (AFNOR).

[306] Xiao, J., Huang, Y., Yang, J., Zhang, C. (2012). “Mechanical properties of confined recycled aggregate concrete under axial compression.” Construction and Building Materials, Vol. 26, , pp. 591–603. https://doi.org/10.1016/j.conbuildmat.2011.06.062.

[307] Duan, Z.; Zhao, W.; Ye, T. ., Zhang, Y.; Zhang, C. (2022). “Measurement of Water Absorption of Recycled Aggregate.” Materials, Vol. 15, , pp. 5141. https://doi.org/https://doi.org/10.3390/ma15155141.

[308] Kun Liang, Yingjie Hou, Jianchun Sun, Xiaoguang Li, Jiahong Bai, Wei Tian, Y. L. (2021). “Theoretical analysis of water absorption kinetics of recycled aggregates immersed in water.” Construction and Building Materials, Vol. 302, , pp. 124156. https://doi.org/10.1016/j.conbuildmat.2021.124156.

[309] Zhenhua Duan a, Qi Deng a, Jianzhuang Xiao a, Hanghua Zhang a b, Ahmed Nasr a, Long Li a b, S. Z. a b. (2023). “Early-stage water-absorbing behavior and mechanism of recycled coarse aggregate.” Construction and Building Materials, Vol. 394, , pp. 132138. https://doi.org/10.1016/j.conbuildmat.2023.132138.

[310] NF EN 1097-6. (2014). “Tests to determine the mechanical and physical properties of aggregates — Part 6: Determination of true density and water absorption coefficient.” Association Française de Normalisation (AFNOR).

[311] NF EN 12350-6. (2019). “Tests for fresh concrete - Part 6: Density.” Association Française de Normalisation (AFNOR).

[312] NF EN 12350-7. (2019). “Tests for fresh concrete — Part 7: Air content — Compressibility method.” Association Française de Normalisation (AFNOR).

[313] Fabbri, A. (2006). “Physico-mécanique des matériaux cimentaires soumis au gel-dégel = Physics and mechanics of cementitious media submitted to frost action,” pp. 282.

[314] NF P18-553. (1990). “Granulats, Préparation d´un échantillon pour essai.” (Association Française de Normalisation AFNOR).

[315] Redjel, B., Khelifi, W., Jauberthie, R. (2014). “Mesure de la résistance à la compression du béton : influence des méthodes destructives (écrasement) et non destructives (ultrason) et des géométries des corps d’épreuve.” Algérie Équipement, Vol. 53, , pp. 56–64.

[316] Talaat, A., Emad, A., Tarek, A., Masbouba, M., Essam, A., Kohail, M. (2020). “Factors affecting the results of concrete compression testing: A review.” Ain Shams Engineering Journal, Vol. 12, . https://doi.org/10.1016/j.asej.2020.07.015.

[317] NF P18-407. (1981). “Bétons_essai de flexion.” Association Française de Normalisation (AFNOR).

[318] NF EN 12390-6. (2001). “Essai pour béton durci, Partie 6. Résistance en traction par fendage d’éprouvettes.” Association Française de Normalisation (AFNOR).

[319] NF P 18-418. (1989). “Béton - Auscultation sonique - Mesure du temps de propagation d’ondes soniques dans le béton.” Association Française de Normalisation (AFNOR).

[320] Mezghiche, B. (1996). “Résistance et déformabilité des béton basiques.” In Actes du premier séminaire national en génie civil (pp. 86–93).

[321] Cuvelier, D. (2013). “Indicateurs de durabilité Essais et seuils.” In Journée technique “ Concevoire, construire et gérer des structures durables en béton Approche performantielle et évolutions normatives.” Lille, France: Centre d’étude techniques de l’équipement de l’Est “CETE”, Nord Picardie Polytech’ Lille.

[322] Wirquin, E., Hadjieva-Zaharieva, R., Buyle-Bodin, F. (2000). “Utilisation de l’absorption d’eau des bétons comme critères de leur durabilité—Application aux bétons de granulats recyclés.” Materials and Structures, Vol. 33, Issue 6, pp. 403. https://doi.org/10.1007/bf02479650.

[323] AFPC-AFREM. (1997). “Durabilité des bétons.” Méthodes recommandées pour la mesure des grandeurs associées à la durabilité des bétons. INSA-LMDC, Toulouse.

[324] ISO 7031. (1998). “Concrete hardened — Determination of the depth of penetration of water under pressure.” International Organization for Standardization (ISO).

[325] Setti.F, Ezziane.K, S. . (2012). “Quantification de la résistance à l’abrasion d’un béton renforcé par des fibres métalliques.” In Séminaire international.

[326] Gost10060-87. (2012). “Concretes, Methods for the determination of Frost-Resistance.” Gosudarstvennyy Standart.

[327] Jeonghyun, K. (2022). “Influence of quality of recycled aggregates on the mechanical properties of recycled aggregate concretes: An overview.” Construction and Building Materials journal, Vol. 328, , pp. 127071. https://doi.org/10.1016/j.conbuildmat.2022.127071.

[328] MONTGOMERY, D. C. (2022). “Design and Analysis of Experiment.” (I. John Wiley & Sons, Ed.) (8th ed.). Arizona State University.

[329] E898-20, A. standard. (2020). “Standard Practice for Calibration of Non-Automatic Weighing Instruments.”

[330] ISO. (2017). “Guidelines for the use of estimates of repeatability, reproducibility and accuracy in assessing measurement uncertainty.”

[331] ISO. (2019). “Accuracy (trueness and precision) of results and measurement methods Part 2: Basic method for determining the repeatability and

reproducibility of a standardized measurement method." International Organization for Standardization (ISO).

[332] S. Yang, J. Zhang, X. An, B. Qi, W. Li, D. Shen, P. Li, M. Lv. (2021). "The Effect of Sand Type on the Rheological Properties of Self-Compacting Mortar." Buildings, Vol. 11, , pp. 441. https://doi.org/https://doi.org/10.3390/buildings11100441.

[333] Pilate, O., Ployaert, C. (2013). "La granulométrie correcte des sables pour une qualité optimale des betons routiers." docplayer. Retrieved from https://webcache.googleusercontent.com/search?q=cache:r4-N_em51fMJ:https://docplayer.fr/14934875-La-granulometrie-correcte-des-sables-pour-une-qualite-optimale-des-betons-routiers.html+&cd=1&hl=fr&ct=clnk&gl=dz&client=firefox-b-d

[334] M. Soltani, R. Moayedfar, P. C. Yi Wen. (2022). "Evaluating the effect of aggregate size, cement content and water-cement ration performance of previous concrete." Road and Bridges, Vol. 21, , pp. 63–79. https://doi.org/10.7409/rabdim.022.004.

[335] NF EN 1992-1-1. (2005). "Eurocode 2 Calcul des structures en béton Partie 1-1 : Règles générales et règles pour les bâtiments." Association Française de Normalisation (AFNOR).

[336] B. E. Koku-Ojumu, A. S. Kehinde, O. P. Faboro, O. O. Omojola. (2021). "Effect of water/cement (W/C) ratio and coconut shell ash (CSA) on some engineering properties." international journal engineering research and technology, Vol. 10, . https://doi.org/10.17577/IJERTV10IS100170.

[337] P. Wang, L. Ke, H. Wu, C. K.Y. Leung. (2022). "Effects of water-to-cement ratio on the performance of concrete and embedded GFRP reinforcement." construction and building materials, Vol. 351, . https://doi.org/https://doi.org/10.1016/j.conbuildmat.2022.128833.

[338] H. Jaromír, P. Zdenek. (2017). "The effect of plasticizer on mechanical properties of the cement paste with fine ground recycled concrete." Acta Polytechnica CTU Proceedings, Vol. 13, , pp. 61–65. https://doi.org/https://doi.org/10.14311/APP.2017.13.0061.

[339] T. Ali-Boucetta. (2014). Contribution of Granulated Slag and Glass Powder on Flow and Durability Properties of Self-Compacting Concrete and High Performance Self-Compacting Concrete. University of Annaba, Algeria.

[340] J. Ahmad, A. Majdi, , A.F. Deifalla, H.J. Qureshi, M.U. Saleem, S.M.A. Qaidi, M.A. El-Shorbagy. (2022). "Concrete Made with Dune Sand: Overview of Fresh, Mechanical and Durability Properties." Materials, Vol. 15, , pp. 6152. https://doi.org/https://doi.org/10.3390/ma15176152.

[341] Sasanipour, H., Aslani, F. (2020). "Durability properties evaluation of self-compacting concrete prepared with waste fine and coarse recycled concrete aggregates." Construction and Building Materials, Vol. 236, , pp. 117540. https://doi.org/10.1016/j.conbuildmat.2019.117540.

[342] Argouges, M., Stiffening, T. (2021). “A study of the natural self-healing of mortars using air-flow measurements A study of the natural self-healing of mortars using air-flow measurements,” Issue November 2012. https://doi.org/10.1617/s11527-012-9861-y.

[343] J. Ollivier, J. T. (2008). “La structure poreuse des bétons et les propriétés de transfert, La durabilité des bétons.” In sous la direction de J.P. Ollivier et A. Vichot (Ed.), (Vol. 1, pp. 51–134). Presses de l’école nationale des ponts et chaussées.

[344] Molez, L., Bian, H., Prince-Agbodjan, W. (2012). “Freeze/thaw resistance of UHPFRCs: competition between damage and healing.” In 30th AUGC-IBPSA Meeting. Chambery, Savoy, France.

[345] Khouadjia, M. L. K., Mezghiche, B. (2019). “Analyse de la Résistance à la Compression des Bétons à Base des Sables Locaux Algériens Soumis à des Cycles de Gel Dégel.” In 3ème Conférence internationale sur la Mécanique des Matériaux et des Structures 13, 14 et 15 Novembre 2019 (Marrakech, MAROC).

PUBLICATIONS AND COMMUNICATIONS FROM THE THESIS

PUBLICATIONS AND COMMUNICATIONS FROM THE THESIS

A. PUBLICATION OF ARTICLES

- Akroum, K., & Mezghiche, B. (2024). DAD_{max}/NAD_{max} Ratio: Criterion for the Production and Selection of Demolition Aggregates with Low-Water Absorption. *Journal of Rehabilitation in Civil Engineering*, 12(4), pp. 1-19. https://doi.org/10.22075/jrce.2024.31002.1870

B. INTERNATIONAL COMMUNICATIONS

- Kamel Akroum et Bouzidi Mezghiche. Résistance à l'abrasion des bétons à base d'agrégats de démolition et sable de dune. The 1st International Congress on Advances in Geotechnical Engineering and Construction Management (ICAGECM'19), december10th -11th, 2019 Skikda-Algeria-.

- Kamel Akroum, Dounia Derdour, Maroua Lagaguine. Influence of the quality of parent concrete on the quality of son concrete: compression strength case. 4th International Conference on Advanced Engineering Technologies. September 28-30, 2022. Bayburt, Türkiye.